Hydrological and Suspended Sediment Modeling in the Lake Tana Basin, Ethiopia

Agizew Nigussie Engida

UNIVERSITÉ DE GRENOBLE

THÈSE

Pour obtenir le grade de

DOCTEUR DE L'UNIVERSITÉ DE GRENOBLE

Spécialité «TERRE, UNIVERS, ENVIRONNEMENT»

Arrêté ministériel : 7 août 2006

Présentée et soutenue publiquement par

AGIZEW NIGUSSIE ENGIDA

le 15 NOVEMBRE 2010

MODELISATION HYDROSEDIMENTAIRE DANS LE BASSIN VERSANT DU LAC TANA EN ETHIOPIE

Hydrological and Suspended Sediment Modeling in the Lake Tana Basin, Ethiopia

---

Thèse dirigée par MICHEL ESTEVES

JURY

M. Etienne Jaillard	Directeur de Recherche	IRD, LGCA Grenoble	Président
M^{me} Isabelle Braud	Directeur de Recherche	CEMAGREF, HH Lyon	Rapporteur
M. Philippe Ackerer	Directeur de Recherche	CNRS, LHyGeS Strasbourg	Rapporteur
M. Jean Albergel	Directeur de Recherche	IRD, IRD Nairobi	Examinateur
M. Michel Esteves	Directeur de Recherche	IRD, LTHE Grenoble	Directeur de thèse

Thèse préparée au sein de l'équipe RIVER du Laboratoire d'études des Transferts en Hydrologie et Environnement (LTHE)

Water is needed in all aspects of life. The general objective is to make certain that adequate supplies of water of good quality are maintained for the entire population of this planet, while preserving the hydrological, biological and chemical functions of ecosystems, adapting human activities within the capacity limits of nature and combating vectors of water-related diseases.

Agenda 21: 18.2

UN Conference on Environment & Development, 1992

ብርታቴ ሆይ፤ ውዳሴ አቀርብልሃለሁ፤
አግዚአብሔር ሆይ፤ አንተ መጠጊያዬ፣
የምትወደኝም አምላኬ ነህና። መዝ ፶፱፥፲፯

Acknowledgements

This dissertation would not have come to fruition without the support and encouragement of different individuals and organizations. First and foremost, I would like to extend my deepest gratitude to my advisor, Michel Esteves. His interest to the study, serious follow-up, proper guidance, constant encouragement, and insightful and timely comments have been invaluable in shaping and enriching the dissertation. His valuable assistances in other matters are also gratefully acknowledged. I have learned many other qualities from him which would be important for my career as a researcher and academician.

I am thankful to Dr. Hadush Seged, Dr. Yonas Michael, Dr. Semu Moges, Dr Yilma Seleshi, Dr. Dagnachew Legesse, Ato Yohannes Daniel and Ato Essayas Kaba for providing me with valuable data and/or documents. I am also grateful to Pierre Viallet for his supports in relation to the application of the distributed hydrological model, DHSVM.

My acknowledgements are also extended to the Ministry of Water Resources and the National Meteorological Agency of Ethiopia for their cooperation in providing relevant hydro-meteorological data. I am indebted to different staffs of Addis Ababa University, Faculty of Technology and Civil Engineering Department for having facilitated various administrative matters. My appreciation also goes to staffs of the RIVER research group, LTHE, TUE and CROUS de Grenoble, who in one way or the other facilitated my study and stay in France.

I appreciate the sandwich scholarship of the French Ministry of Foreign Affairs that enabled me pursue the PhD study. Moreover, I acknowledge the financial assistances of the French Embassy in Addis Ababa and the French Institute of Research and Development (IRD) which allowed me to visit the study area and collect primary and secondary data.

I thank all the jury members for having devoted their precious time to evaluate this work and particularly, Mme Isabelle Braud and M. Philippe Ackerer for their constructive comments and suggestions.

I am grateful to my relatives and friends for their encouragement and wishes of successful accomplishment. Many thanks are due to my father, mother, brothers, sisters and all other members of my family for their prayers, unconditional love and support. My heartfelt gratitude goes to my lovely wife, Alaynesh Goshime, for her constant encouragement, patience and strength in shouldering diverse responsibilities during my absence. Special thanks to my little daughter, Ruth, whose birth has filled our home with immeasurable joy. I was struggling to finalize this dissertation while others were around her singing her very first *happy birthday to you*. I hope I will be around in the coming birthdays.

Abstract

This study is conducted in Lake Tana basin located in the Upper Blue Nile Basin in Ethiopia where water resources issues are critical and availability of relevant data is poor. The study is divided into three major components that include evaluation and analysis of the existing data, evaluation of the applicability of a physically-based distributed hydrological model and water and suspended sediment balance modeling for Lake Tana. The temporal and spatial coverage of various hydro-meteorological variables was assessed in light of recommended practices in the literature. Analyses of the hydro-meteorological datasets comprised data quality control, and determination of their characteristics in space and time. The applicability of the fully distributed physically-based hydrological model was assessed on selected catchments. The modeling exercise revealed the importance of weather data disaggregation models in generating meteorological forcings at finer time scales. Considering the quality and resolution of the inputs used, the performance of the distributed model could be judged satisfactory in two of the selected mesoscale catchments. The water balance modeling of Lake Tana was done at a monthly time step and involved estimation of the major inflow and outflow components. A dynamic conceptual model was used to estimate the contribution of catchments for which data could not be obtained. The results of the water balance model at monthly and annual time scales was generally good and the observed lake levels could be reproduced satisfactorily. Estimation of the suspended sediment balance of the lake involved development and use of rating curves and a regional area-specific model. The results of the study are useful for planning and management of water resources in the study area.

Keywords: *hydrological modeling, DHSVM, weather data disaggregation, suspended sediment, Lake Tana basin, Ethiopia*

Résumé

Cette étude a été menée dans le bassin versant du lac Tana situé dans le haut bassin du Nil Bleu en Ethiopie, où les enjeux liés à l'exploitation des ressources en eau sont critiques et la disponibilité de données pertinentes est faible. L'étude est divisée en trois parties principales qui comprennent l'évaluation de la qualité et l'analyse des données existantes, l'évaluation de l'applicabilité d'un modèle hydrologique à base physique et le calcul des bilans en eau et des matières en suspension du lac Tana. Les couvertures spatiales et temporelles des variables hydro-météorologiques ont été évaluées à partir des méthodes recommandées dans la littérature. L'analyse des jeux de données hydro-météorologiques comprend le contrôle de la qualité des données, et la détermination de leurs caractéristiques spatiales et temporelles. L'applicabilité du modèle hydrologique à base physique a été évaluée sur deux bassins versants. Cet exercice de modélisation a montré l'intérêt des méthodes de désagrégation temporelle pour générer des données météorologiques à des échelles de temps plus courtes. Compte tenu de la qualité des données utilisées, la performance du modèle dans deux des bassins versants a été jugée satisfaisante. Le bilan en eau du lac Tana a été calculé au pas temps mensuel ce qui a impliqué l'estimation des différents termes. Un modèle dynamique et conceptuel a été utilisé pour estimer les contributions des bassins versants pour lesquels les données hydrométriques sont manquantes. Les résultats du calcul sont généralement bons et les niveaux observés du lac sont reproduits de manière satisfaisante. L'estimation du bilan des matières en suspension pour le lac a nécessité le développement et l'utilisation des courbes débit-concentration et un modèle régional. Les résultats présentés dans ce travail sont utiles pour la planification et la gestion des ressources en eau dans cette région d'Ethiopie.

Mots-clés: *modélisation hydrologique, DHSVM, désagrégation des données météorologiques, matières en suspension, lac Tana, Ethiopie*

Table of Contents

Acknowledgements iii

Abstract v

Table of Contents vii

List of Figures xii

List of Tables xiv

Résumé étendu en français xv

Introduction 1

Research questions and objectives 1

Methodological framework 3

Outline of the thesis 4

1 Water Resources Issues 7

1.1 Water resource issues in developing countries 7

1.1.1 Water quantity issues 7

1.1.2 Water quality issues 9

1.1.3 Hydrological extremes 10

1.1.4 Soil erosion and reservoir sedimentation 12

1.1.5 Concluding remarks on water resources issues 14

1.2 Role of hydrology, and erosion and sediment transfer in watershed management 15

1.3 Hydrological modeling 17

1.4 Conclusion 19

2 Description of the Study Area 21

2.1 Location 21

2.2 Topography 22

2.3 Geology and soil 23

2.4 Land use and land cover 24

2.5 Climate 25
2.6 Hydrology and hydrogeology 28
2.7 Water resources development 30
3 Data availability and analysis 33
3.1 Meteorological data availability 33
3.1.1 Rainfall 34
3.1.1 Temperature 36
3.1.2 Wind speed, relative humidity and sunshine hour 37
3.2 Hydrological data availability 38
3.2.1 Streamflow and lake level 38
3.2.2 Suspended sediment 40
3.2.3 Lake Tana bathymetry 41
3.3 Spatial data availability 41
3.3.1 Soil types and properties 41
3.3.2 Vegetation 41
3.3.3 Digital elevation model 42
3.4 Data analysis 42
3.4.1 Analysis of meteorological data 42
3.4.2 Hydrological data analysis 59
3.4.3 Suspended sediment yield 67
3.4.4 Soil and land cover data analysis 70
3.5 Concluding remarks 73
4 Sensitivity analysis of Distributed Hydrology, Soil, Vegetation Model Parameters 75
4.1 Introduction 75
4.2 Materials and methods 77
4.2.1 Description of the model 77
4.2.2 The sensitivity analysis method 78

4.2.3 Virtual catchments 79
4.3 Results and discussion 83
4.3.1 Sensitivity to terrain slope 84
4.3.2 Sensitivity to soil depth 85
4.3.3 Sensitivity to soil parameters 88
4.3.4 Sensitivity to vegetation parameters 91
4.4 Conclusions 97
5 DHSVM Input Data Creation for Lake Tana Basin 99
5.1 Introduction 99
5.2 Weather data disaggregation 100
5.2.1 Rainfall 100
5.2.2 Temperature 105
5.2.3 Wind speed 107
5.2.4 Relative humidity 108
5.2.5 Solar radiation 109
5.2.6 Downward longwave radiation 111
5.3 Spatialization of meteorological data 113
5.4 Creation of spatial datasets 114
5.4.1 Soil and land cover maps 114
5.4.2 Soil depth 114
5.4.3 Binary maps 115
5.4.4 Stream files 116
5.5 Creation of initial model state files 116
5.6 Parameterization of soil and vegetation properties 117
5.7 Creation of configuration file 118
5.8 Concluding remarks 118

6 Application of DHSVM to Selected Catchments in the Lake Tana Basin 121
6.1 Introduction 121
6.2 Calibration and validation of models: Literature review 121
6.2.1 Calibration 121
6.2.2 Validation 122
6.2.3 Model performance measures 123
6.3 Selected catchments 125
6.4 Calibration and validation of the model 127
6.5 Results and discussion 128
6.5.1 Performance of the model at daily time step 128
6.5.2 Performance of the model at monthly time step 133
6.6 Conclusion 135
7 Water and Suspended Sediment Balances of Lake Tana 137
7.1 Introduction 137
7.2 Lake water balance model 138
7.3 Computation of the water balance components of Lake Tana 139
7.3.1 Rainfall 139
7.3.2 Inflow from contributing catchments 141
7.3.3 Evaporation 148
7.3.4 Interaction with groundwater 150
7.3.5 River outflow 150
7.3.6 Floodplain evaporation 151
7.3.7 Change in lake water storage 151
7.3.8 Summary of the major water balance components of Lake Tana 152
7.3.9 Simulation of lake level fluctuation 154
7.4 Suspended sediment balance of Lake Tana 156
7.4.1 Suspended sediment discharge from gauged catchments 157

7.4.2 Suspended sediment discharge from streams with no data 158
7.4.3 Total suspended sediment inflow 159
7.4.4 Suspended sediment outflow 160
7.4.5 Suspended sediment deposition 160
7.5 Concluding remark 161
General conclusion and perspectives 163
Summary and conclusion 163
Perspectives 165
Uncertainty and sensitivity analysis 165
Meteorological data disaggregation 165
Testing DHSVM on other catchments 166
Further study on suspended sediment 166
References 167
Annex A: Paper submitted for journal publication 185
Annex B: Information on hydro-meteorological and spatial characteristics of Lake Tana basin 207
Annex C: Main processes of DHSVM and typical input files 216
Annex D: Equations used to calculate the various terms in the Penman equation 234

List of Figures

Figure 1-1 Classification of hydrological models. 18
Figure 2-1 The study area 22
Figure 2-2 Topography of Lake Tana basin 23
Figure 2-3 Geology and soil types of Lake Tana basin 24
Figure 2-4 Land cover/use types in the Lake Tana Basin 25
Figure 2-5 The ITCZ over Africa . 26
Figure 2-6 Mean annual climatic variables over Ethiopia 28
Figure 2-7 Rainfall regimes of Ethiopia 28
Figure 2-8 Major hydrological systems of Lake Tana Basin 30
Figure 3-1 Meteorological stations in the Lake Tana basin 34
Figure 3-2 Rainfall data availability in the Lake Tana Basin 35
Figure 3-3 Spatial coverage of rainfall gauges in the Lake Tana basin according to WMO standard 36
Figure 3-4: Temperature data availability for lake Tana Basin 37
Figure 3-5 Availability of wind speed, relative humidity and sunshine hour data, Lake Tana basin 38
Figure 3-6 Major streamflow and lake level gauging stations in the Lake Tana basin 39
Figure 3-7: Streamflow and lake level data availability in the Lake Tana Basin 39
Figure 3-8 Availability of suspended sediment concentration/load data in the Lake Tana basin 40
Figure 3-9 Boxplot of annual rainfall of stations located within and around Lake Tana basin. 46
Figure 3-10 Monthly rainfall pattern of Class 1 stations within Lake Tana basin 47
Figure 3-11 Spatial pattern of rainfall in the Lake Tana basin 48
Figure 3-12 Median annual rainfall-latitude relationship in the Lake Tana basin 49
Figure 3-13 Characteristics of annual temperature in the Lake Tana basin. 52
Figure 3-14 Monthly minimum and maximum temperature pattern in the Lake Tana basin 53
Figure 3-15 Temperature-Altitude relationship in the Lake Tana basin 53
Figure 3-16 Wind speed in the Lake Tana basin 55
Figure 3-17 Relative humidity in the Lake Tana basin 57
Figure 3-18 Mean monthly sunshine hour at Bahir Dar 58
Figure 3-19 Mean monthly potential evapotranspiration in the Lake Tana basin 59
Figure 3-20 Boxplot of annual runoff of gauged catchments in the Lake Tana basin 62
Figure 3-21 Monthly runoff and lake level pattern in the Lake Tana basin 62
Figure 3-22 Effect of Chara Chara weir on the outflow and level of Lake Tana 62
Figure 3-23 Log-normal probability plot of annual maximum daily streamflow, Lake Tana basin 65
Figure 3-24 Rainfall-runoff relationship in the Lake Tana basin catchments 66
Figure 3-25 Bathymetry of Lake Tana based on data collected in 2006 67
Figure 3-26 Suspended sediment rating curves for four gauged catchments, Lake Tana basin 69
Figure 4-1 The virtual catchment 79
Figure 4-2 Sensitivity of DHSVM mass balance outputs to terrain slope 86
Figure 4-3 Sensitivity of DHSVM mass balance outputs to soil depth 87
Figure 4-4 Sensitivity of DHSVM outputs to soil parameters 93
Figure 4-5 Sensitivity of DHSVM mass balance outputs to vegetation parameters 95
Figure 4-6 Sensitivity of DHSVM hydrograph simulations to vegetation parameters 96
Figure 5-1 Required input files for DHSVM 99
Figure 5-2 Rainfall process as assumed in the MBLRPM 101

Figure 5-3 Comparison between observed and disaggregated mean hourly rainfall of Bahir Dar station for the wet months 103
Figure 5-4 Typical distribution of rain start hour for Bahir Dar station 104
Figure 5-5 Comparison between observed and disaggregated hourly rainfall after adjustment. Bahir Dar, for the main rainy season. 105
Figure 5-6 Average diurnal temperature pattern of four Class 1 stations in the Lake Tana basin 106
Figure 5-7 Diurnal wind speed pattern on a typical day at Gonder 107
Figure 5-8 Mean diurnal pattern of relative humidity in the Lake Tana basin..... 109
Figure 5-9 Comparison of daily solar radiation values computed by the A-P and Hargreaves equations at Bahir Dar meteorological station for the period 1992-2005. 110
Figure 5-10 Average diurnal pattern of solar radiation in the Lake Tana basin..... 111
Figure 5-11 Mean diurnal pattern of downward longwave radiation in the Lake Tana basin..... 113
Figure 5-12 Soil depth map of Lake Tana basin derived from topographic attributes 115
Figure 6-1 Catchments on which DHSVM was evaluated 126
Figure 6-2 Distribution of soil types in Megech and Rib catchments..... 127
Figure 6-3 Measured and simulated hydrographs for Megech catchment 130
Figure 6-4 Measured and simulated hydrographs for Rib catchment 132
Figure 6-5 Measured and simulated monthly discharges in Megch and Rib catchments 134
Figure 7-1 Components of Lake water balance..... 138
Figure 7-2 Stations used for spatial rainfall interpolation..... 140
Figure 7-3 Methods used to estimate inflow contributions 141
Figure 7-4 The model Equations 143
Figure 7-5 Calibration and validation results of the conceptual rainfall-runoff model 145
Figure 7-6 Comparison of observed and simulated levels of Lake Tana..... 155
Figure 7-7 Catchments to which rating curves or regional models were applied to estimate suspended sediment discharges..... 156

List of Tables

Table 3-1 Recommended minimum precipitation network density 36
Table 3-2 WMO minimum recommendation for hydrometric network density 40
Table 3-3 Some examples of soil surveys within Lake Tana basin 41
Table 3-4 Weibull distribution parameters for wind speed in the Lake Tana basin 55
Table 3-5 Characteristics of gauged catchments in the Lake Tana basin 60
Table 3-6 Baseflow indices for major gauged catchments of Lake Tana basin 63
Table 3-7 Distribution of major soil types in the gauged catchments of Lake Tana basin (%) 71
Table 3-8 Distribution of land cover types in the gauged catchments of Lake Tana basin (%) 72
Table 4-1 Description of virtual catchments used for the sensitivity analysis 80
Table 4-2 Soil parameters and corresponding base values 80
Table 4-3 Vegetation parameters and corresponding base values 81
Table 4-4 Sensitivity criteria for the mass balance outputs 83
Table 4-5 Sensitivity criteria for the outputs per simulation time step 83
Table 5-1 Meteorological stations used for simulation catchments in the Lake Tana basin 113
Table 6-1 Characteristics of the simulation catchments 126
Table 6-2 DHSVM performance at daily time step on Megech catchment 129
Table 6-3 DHSVM performance at daily time step on Rib catchment when all nearby meteorological stations were used 131
Table 6-4 DHSVM performance at daily time step on Rib catchment when Debre Tabor meteorological station was used 131
Table 6-5 DHSVM performance at monthly time step on Megech and Rib catchments 133
Table 7-1 Reported magnitudes of major Lake Tana water balance components 138
Table 7-2 Estimated mean annual on-lake precipitation for Lake Tana 140
Table 7-3 Mean monthly on-lake precipitation on Lake Tana 140
Table 7-4 Contributions of major gauged catchments to surface inflow to Lake Tana 142
Table 7-5 Recommended model performance ratings for monthly streamflow 144
Table 7-6 Optimum model parameter values for the gauged catchments 144
Table 7-7 Goodness-of-fit of the conceptual model during the calibration and validation periods .. 144
Table 7-8 Regression coefficients used to estimate the regional model parameters 146
Table 7-9 Validation results of the regional model parameters equations 147
Table 7-10 Runoff contribution of catchments without streamflow data 147
Table 7-11 Mean monthly and annual evaporation from Lake Tana using the Penman method 150
Table 7-12 Mean monthly and annual outflow from Lake Tana 151
Table 7-13 Estimated evaporation from the floodplains that surround Lake Tana 151
Table 7-14 Mean changes in Lake Tana water storage 152
Table 7-15 Mean monthly and annual water balance of Lake Tana 153
Table 7-16 Suspended sediment rating curve equations of four gauged catchments in the Lake Tana basin 157
Table 7-17 Suspended sediment discharges from four gauged catchments in the Lake Tana basin . 158
Table 7-18 Estimated mean annual suspended sediment discharges from catchments without rating curves 159

Résumé étendu en français

Introduction

Contexte

De nombreux pays dans le monde sont confrontés à des problèmes en relation avec l'utilisation des ressources en eau comme la pénurie d'eau, la pollution de l'eau et les catastrophes liées à l'eau. Ces problèmes sont plus graves dans les pays en développement en raison de leurs importants impacts socio-économiques négatifs, des faibles capacités financières et de l'absence de mécanismes d'adaptation dans ces pays.

Cette étude a été conduite dans le bassin versant du lac Tana en Ethiopie, où le potentiel actuel des ressources en eau est peu exploité, l'érosion des sols par l'eau est un problème grave, la sécheresse et les inondations sont des phénomènes récurrents. La gestion non durable des bassins versants provoque de sérieux impacts négatifs socio-économiques et écologiques depuis l'échelle locale jusqu'à celle de la région. Ce bassin correspond au bassin versant amont du Nil Bleu qui est le principal contributeur au débit du Nil. Le lac Tana, le plus grand lac d'Ethiopie, est situé au centre de la zone d'étude. Ce lac présente une grande diversité de valeurs socio-économiques et écologiques. De nombreux projets de développement des infrastructures pour l'utilisation des ressources en eau sont également en cours de réalisation. Dans ce contexte les études hydrologiques et sur le transfert des sédiments associés sont des composantes essentielles de la gestion intégrée de ces bassins versants et constituent l'objet principal de la recherche présentée dans ce mémoire. L'étude est organisée en trois volets principaux qui sont : l'évaluation et l'analyse des données spatiales et hydrométéorologiques existantes, l'évaluation d'un modèle hydrologique distribué à base physique, et l'estimation des bilans hydrologique et des sédiments en suspension du lac Tana.

Les questions de recherche et les objectifs

Les recherches dans les domaines de l'hydrologie et des bilans des sédiments en suspension sont indispensables pour proposer des scénarios de gestion durable des bassins versants. Leur rôle est particulièrement important dans les régions comme celle du lac Tana où l'utilisation des ressources en eau est critique, la disponibilité et la qualité des données hydrométéorologiques sont pauvres. Certaines questions de recherche prioritaires dans les domaines biophysique, de la gestion et sur les aspects socio-économiques du bassin du Nil ont déjà été abordées dans une étude récente (Mohamed et Loulseged, 2008).

Cette thèse tente d'apporter une contribution à certains des besoins de recherche évoqués ci-dessous en répondant aux questions suivantes.

La première question abordée est liée à la disponibilité des données et à leur qualité. Un inventaire critique des types, de la qualité et des caractéristiques spatiales et temporelles des données existantes est fondamental avant de réaliser les études hydrologiques. Il met en évidence les lacunes et les erreurs dans les jeux de données existants et permet d'identifier les stratégies pertinentes pour résoudre ces problèmes. Selon les objectifs de l'analyse, la nature des données et la disponibilité de moyens financiers, différentes

stratégies peuvent être utilisées. Ces stratégies peuvent comprendre l'utilisation directe des données existantes, l'estimation des données manquantes à partir de méthodologies appropriées (modèles de désagrégation temporelle pour les séries de données météorologiques, les fonctions de pédotransfert pour les propriétés du sol, l'interpolation spatiale, etc.), ou la réalisation de nouvelles campagnes de collecte de données. Cette étude a évalué les caractéristiques des jeux de données existants pour le bassin du lac Tana en soulevant quelques questions clés liées à la nature, la couverture spatiale, la qualité et la cohérence des séries de données hydrométéorologiques. Les données géographiques décrivant les bassins versants ont également été étudiées.

Dans la région étudiée il y a de nombreux bassins versants non jaugés (environ 40% de la superficie). Les problèmes d'érosion et de transfert de sédiments sont critiques à cause de leurs impacts négatifs localement (pertes en terre) mais également en aval du site d'étude (envasement des retenues). L'importance de ces impacts, dans la zone d'étude, pourrait être élevée du fait des projets de développement des infrastructures hydrauliques et de la présence de systèmes naturels ayant de grandes valeurs socio-économiques et écologiques. Les projets de développement de l'irrigation, en cours de réalisation ou prévus (plus de 100 000 hectares) ainsi que les centrales hydroélectriques d'une puissance supérieure à 500 MW pourraient être directement affectés.

Dans cette perspective, les recherches qui visent à améliorer les estimations des écoulements de surface provenant des bassins versants non jaugés et des apports de sédiments sont nécessaires pour assurer la durabilité de l'usage des ressources en eau. À cet égard, l'utilisation de modèles hydrologiques distribués à base physique peut se révéler très utile. La deuxième question abordée dans cette étude concerne donc l'évaluation d'un modèle hydrologique distribué en utilisant les données hydrométéorologiques et géographiques existantes.

La disponibilité de données météorologiques à un pas de temps horaire est généralement médiocre. Les données météorologiques à des échelles de temps plus fines que la journée sont nécessaires pour de nombreuses applications comme les études sur l'érosion des sols et le transport des sédiments et l'analyse des crues. Dans le cadre de l'application du modèle distribué à base physique des méthodes pertinentes et originales de désagrégation des séries de données météorologiques journalières ont été appliquées pour produire des séries horaires.

Le bilan hydrologique du lac Tana a été étudié par différents auteurs dans le passé qui ont abouti à des estimations différentes des principaux termes du bilan. Les causes de ces différences sont dues à la prise en compte de périodes de référence et à l'utilisation de méthodes d'estimation des écoulements de surface des bassins non jaugés différentes. Par exemple, Kebede et al. (2006) estiment la précipitation directe sur le lac en utilisant les données d'une seule station. De plus, ils font l'hypothèse que la contribution des bassins versants non jaugés est négligeable. Dans une région où la variabilité spatiale des précipitations est élevée, le calcul du terme précipitation à partir d'une seule station est critiquable et l'incertitude associée importante. Les composantes du bilan hydrologique du lac doivent être estimées aussi précisément que possible à partir de données représentatives. C'est un élément important dans le choix des options retenues pour la gestion durable du lac. Dans cette thèse un effort important a été consenti pour calculer le

bilan hydrologique du lac en utilisant un jeux de données issu d'un contrôle de qualité et représentatif des conditions hydrométéorologiques de la période 1992 à 2005.

Comme l'érosion des sols est un problème critique dans le bassin du lac Tana son impact sur le lac ne doit pas être sous-estimé. Les études existantes sont limitées à la bathymétrie du lac et à l'estimation de la production de sédiments sur quelques bassins. Aucune étude globale du bilan hydro-sédimentaire n'existe dans la littérature. Une étude conduite dans le cadre de cette thèse propose une première estimation du bilan hydro-sédimentaire du lac.

Les objectifs spécifiques de cette thèse sont les suivants :

- Inventaire, collecte, critique et analyse des données hydrométéorologiques et géographiques disponibles dans le bassin du lac Tana
- Evaluation et application de modèles désagrégation des données météorologiques
- Évaluation d'un modèle hydrologique distribué à base physique « Distributed Hydrology Soil Vegetation Model » (DHSVM)
- Calcul du bilan hydrologique du lac Tana
- Calcul du bilan sédimentaire du lac Tana

En abordant les questions de recherche présentées ci-dessus, cette thèse apporte une contribution notable à la gestion durable des ressources en eau dans la région du lac Tana. Les outils et méthodes utilisés ou développés pour ce travail de recherche peuvent être utilisés pour réaliser des études similaires sur d'autres bassins versants.

Chapitre 1 Questions relatives aux ressources en eau

Ce chapitre présente le cadre général de cette thèse. Un inventaire des principaux problèmes liés à l'utilisation des ressources en eau dans les pays en développement et dans la zone d'étude est présenté dans la première partie. Elle est suivie par une brève note sur le rôle des études de bilan hydrologique et des sédiments pour résoudre les questions relatives à la gestion des bassins versants. Comme l'utilisation de modèles hydrologiques est un point important de cette étude, la dernière partie du chapitre est consacrée à une présentation des différents types de modèles et de leur application.

Les principaux problèmes de ressources en eau auxquels sont confrontés les pays en développement et la zone d'étude sont présentées en quatre catégories principales : quantité d'eau disponible, qualité de l'eau, phénomènes hydrologiques extrêmes et érosion et sédimentation. La pénurie d'eau dans la zone d'étude est un problème crucial en raison de la pression démographique croissante, la forte variabilité hydrologique dans l'espace et le temps, et de la nature transfrontalière de la plupart des cours d'eau. La dégradation de la qualité de l'eau à partir de sources ponctuelles ou non de polluants est également un sujet de préoccupation en raison du niveau médiocre des infrastructures de gestion des déchets. Ces dernières années, les inondations sont devenues un problème sérieux avec ses effets néfastes sur les terres agricoles, les zones habitées et les infrastructures. Pendant des années, l'Ethiopie a été frappée par des sécheresses dévastatrices qui affectent des millions de personnes. L'érosion des sols par l'eau et ses effets néfastes sur place et les

conséquences hors site ont des impacts environnementaux et économiques importants et depuis longtemps.

L'analyse et la solution des problèmes relatifs à l'eau sont encore plus difficiles du fait de la faiblesse des mécanismes institutionnels et de l'insuffisance des capacités humaines, financières et techniques. Le manque de données hydrométéorologiques et géographiques représentatives et fiables constitue un autre enjeu scientifique majeur qui participe à la formulation inadéquate des questions et l'évaluation biaisée des options de gestion. Dans la région étudiée, il y a de nombreux bassins versants non jaugés ou mal mesurés. Les principaux problèmes spécifiques aux données sont la présence de lacunes et des erreurs dans les observations existantes, le manque de données hydrométéorologiques à des pas de temps courts, la représentation des éléments naturellement hétérogènes de la surface comme les sols et les types de végétation par des informations ayant une faible résolution spatiale. Ces problèmes rendent l'analyse hydrologique difficile alors qu'elle constitue un élément fondamental pour la gestion durable des bassins versants. Une combinaison de stratégies pertinentes doit être utilisée pour résoudre les problèmes liés aux données et rendre l'analyse hydrologique possible.

Chapitre 2 Description de la zone d'étude

Ce chapitre décrit la zone d'étude en présentant le milieu physique et les ressources en eau. La localisation géographique du bassin versant du lac Tana ainsi que ses principales caractéristiques, qui comprennent le relief, la géologie, les types de sol, l'usage du sol et le couvert végétal, sont décrites. La climatologie de la zone d'étude, les principaux systèmes hydrologiques et l'état des ressources en eau sont également présentés.

Le bassin du lac Tana correspond à un plateau situé au nord-ouest de l'Ethiopie. Il représente la source du Nil Bleu, qui est le principal contributeur en débit du Nil. Le Nil est partagé par dix pays riverains qui sont confrontés aux mêmes problèmes pour l'utilisation des ressources en eu.

La superficie du bassin du lac Tana est de 15 120 km² avec une altitude moyenne de 2025 m. Le relief est constitué de zones plates autours du lac, de collines ondulées dans la partie médiane et des zones de montagne dans la partie amont. La géologie du bassin est dominée par des séries de roches volcaniques du Quaternaire dans la partie sud et du Tertiaire dans les autres régions. Le lac Tana est situé dans un fossé d'effondrement qui contrôle la circulation des eaux souterraines. Environ 70% de la superficie du bassin est couverte par quatre types de sols principaux qui sont les luvisols, les leptosols, les vertisols et les fluvisols (suivant la classification FAO/Unesco). Le bassin est majoritairement cultivé avec deux grands centres urbains, ayant chacun plus de 200 000 habitants. Le climat de cette région est contrôlé par la position et les mouvements de la Zone de convergence intertropicale (ZCIT). Les précipitations moyennes annuelles et la température moyennes sont respectivement de 1345 mm et 19 °C. La pluviométrie est très concentrée avec plus de 70% de la pluie annuelle qui tombe en quatre mois, entre les mois de juin et de septembre.

Le lac Tana, avec une superficie moyenne de 3012 km², représente un important système hydrologique dans le bassin du Nil. Il est alimenté par plusieurs cours d'eau et possède un

seul exutoire naturel, le Nil Bleu. L'écoulement des eaux souterraines à l'intérieur et autour du bassin du lac Tana est drainé par les cours d'eau de surface. L'état de développement des ressources en eau dans le bassin du lac Tana est faible. Mais, il se développe avec la réalisation d'importants projets d'infrastructures hydrauliques.

Chapitre 3 Inventaire des données disponibles et analyse

La disponibilité, la qualité et les caractéristiques des jeux de données hydrométéorologiques et géographiques existants dans le bassin du lac Tana ont été évaluées. Les données disponibles sont constituées de série de données journalières. Les autres données sont des chroniques de débits journaliers, des mesures de la concentration des sédiments en suspension et des propriétés physiques des différents types de sol ou de végétation.

L'analyse des données hydrométéorologiques a été effectuée sur la période 1992-2005 car la couverture spatiale et temporelle sur cette période a été jugée satisfaisante. Les analyses des données hydrométéorologiques ont consisté à vérifier la qualité des données, combler les lacunes et caractériser leurs distributions spatiales et temporelles. Des séries continues de précipitations journalières ont été construites suivant les méthodes présentées dans Romero et al. (1998) et Federico et al. (2009). L'estimation des données de température manquantes a été obtenue en utilisant une méthode d'interpolation basée sur l'inverse de la distance entre les stations avec des observations. Les données journalières de vitesse du vent ont été complétées par une méthode stochastique basée sur une distribution de Weibull. Le contrôle de la qualité des données s'est appuyé sur des procédures de détection d'erreurs, de valeurs « horsains », et de recherche d'incohérences spatiales et temporelles. Les caractéristiques des distributions spatiales et temporelles des différentes variables hydrométéorologiques ont ensuite été déterminées à partir des jeux de données dont la qualité avait été contrôlée.

Les résultats de ce contrôle de qualité montrent que la majorité des stations ont des données de bonne qualité. Bien que de nombreuses stations météorologiques ne présentent pas de séries continues d'observations des précipitations sur de longues périodes, la distribution temporelle peut être considérée comme adéquate étant donné l'absence de tendance forte dans l'évolution des cumuls de pluies dans la région étudiée. Environ 34% de la superficie du bassin du lac Tana n'est pas mesurée par les stations pluviométriques conformément aux recommandations de l'Organisation Météorologique Mondiale (OMM, 1994). La disponibilité de données pluviographiques (pas de temps inférieur à la journée) est très limitée, les séries sont très fragmentées et de mauvaise qualité. L'utilisation de techniques de désagrégation temporelle des observations de pluies journalières est considérée comme une bonne stratégie dans les applications qui nécessitent le recours à des données à pas de temps court. La distributions des observations de la température est considérée comme suffisante compte tenu des faibles variabilités interannuelle et saisonnière. En outre, compte tenu de la relation linéaire entre la température et l'altitude, la distribution spatiale est suffisante. Bien que les données d'humidité relative soient disponibles uniquement dans un nombre limité de stations, sa distribution spatiale peut être amélioré en raison de sa forte relation avec la température dont la mesure présente une meilleure distribution spatiale.

Considérant la longueur et la continuité des séries de débits journaliers sur les principaux cours d'eau, la distribution temporelle de ces observations peut être considérée comme suffisante. En ce qui concerne les observations sur les sédiments en suspension les données disponibles sont très insuffisantes. Il est préférable de limiter l'utilisation des relations débits-concentrations obtenues à partir de ces observations en nombre limité à des applications dans la phase de planification. Acquérir des données fiables sur les concentrations de sédiments en suspension est indispensable pour la conception et la gestion des infrastructures hydrauliques dans la région. Les données sur les propriétés physiques du sol ne sont pas suffisantes pour caractériser la grande hétérogénéité des propriétés hydrodynamiques des sols.

Chapitre 4 Analyse de sensibilité des paramètres du modèle DHSVM

Le modèle « Distributed Hydrology-Soil-Vegetation Model » (DHSVM) est un modèle à base physique complètement distribué qui a déjà été appliqué dans de nombreux bassins versants. La sensibilité des principaux processus hydrologiques représentés par ce modèle aux valeurs des quarante-six paramètres représentant les propriétés des sols et de la végétation a été évaluée. Les effets de la profondeur du sol et des changements de la valeur de la pente des versants ont également été inclus dans cette évaluation. Les processus étudiés sur une période de simulation d'une année sont la dynamique de l'humidité du sol, l'évapotranspiration, le ruissellement et les débits à l'exutoire. Les simulations ont été réalisées sur un petit bassin versant virtuel caractérisé par des combinaisons de différentes textures de sol (argileuse, limoneuse, sableuse), de couverture végétale (sol nu, arbustes, forêt) et deux pentes des versants. Les simulations ont été réalisées avec un pas de temps de 1 heure pour une période d'un an représentative d'un climat tempéré. L'analyse de sensibilité a été réalisée en appliquant la méthode de « changement d'un paramètre à la fois ». Deux critères ont été utilisés pour évaluer la sensibilité relative de chaque paramètre. Pour le bilan de masse on a utilisé un pourcentage pondéré de déviation part rapport à la simulation de référence. Le coefficient d'efficacité adimensionnel de Nash-Sutcliffe a été utilisé pour juger des différences entre les hydrogrammes à l'exutoire.

Les résultats sont en accord avec ceux rapportés dans la littérature pour les études à l'échelle du versant. Cette étude a permis d'identifier l'influence relative des paramètres du modèle sur les principaux processus. Elle a mis en évidence les paramètres les plus sensibles pour la calibration du modèle. Ce dernier résultat sera très utile pour guider la calibration des paramètres de bassins versants réels. Enfin, cette analyse constitue la première étape d'une analyse plus approfondie utilisant une méthode globale d'analyse de sensibilité.

Les conclusions de cette étude sont particulièrement utiles pour limiter la calibration aux paramètres les plus influents. La profondeur du sol est un paramètre important pour la calibration des faibles débits. La porosité et la conductivité hydraulique latérale saturée peuvent être utilisés comme paramètres de calibration des sols à texture moyenne et grossière et à texture fine sous couvert forestier. Les paramètres de végétation ne sont influents que dans le cas de bassins couverts de forêts. Le pourcentage de couverture, l'atténuation du rayonnement et l'indice de surface foliaire sont ceux qui ont le plus

d'influence quelque soit le type de sol. L'ajustement de paramètres supplémentaires de sol et de végétation peut être nécessaires pour les sols à texture grossière.

Chapitre 5 Création des fichiers de données pour le modèle DHSVM : application au bassin du lac Tana

Ce chapitre présente les méthodologies utilisées pour la création des jeux de données d'entrée et le paramétrage du modèle hydrologique distribué appliqué à des bassins versants du lac Tana. Les données de forçages météorologiques à une résolution temporelle d'une heure ont été créées par désagrégation des séries de données journalières. Les jeux de données spatiales et les fichiers des conditions initiales ont été créés dans le format requis à l'aide d'outils SIG et des programmes exécutables fournis avec le code source DHSVM. Les fichiers décrivant le réseau hydrographique ont été créés à partir du modèle numérique de terrain en utilisant un programme développé par la société Hydrowide. Des valeurs des paramètres de sol et de la végétation ont été définies à priori à partir d'informations trouvées dans la littérature du fait du nombre limité d'observations disponibles pour cette région.

Les observations de pluie journalières ont été désagrégées en données horaires en utilisant une version modifiée du modèle à impulsion rectangulaire de Bartlett-Lewis (MBLRPM). L'application directe de ce modèle n'a pas donné de résultats satisfaisants pour la distribution horaire des pluies. Pour tenir compte de la nature à dominante convective des pluies dans cette région, le modèle a été amélioré en utilisant une distribution statistique de type loi Bêta. Les chroniques horaires de température ont été calculées en utilisant un modèle sinusoïdal et les observations de température minimale et maximale journalière. La température minimale journalière a aussi été utilisée pour représenter la valeur du point de rosée dans l'estimation des valeurs horaires d'humidité relative. La désagrégation de la vitesse du vent en données horaires a été effectuée à l'aide d'un simple modèle de distribution aléatoire. Les données horaires de rayonnement solaire et atmosphérique ont été estimées à partir de relations empiriques basées sur les données de température. Enfin, la profondeur du sol a été obtenue à l'aide d'une régression linéaire multi variables dérivées du modèle numérique d'altitude (pente, altitude et surface drainée).

La création de fichiers d'entrée de bonne qualité est une étape importante de la modélisation hydrologique. Dans cette optique les techniques de désagrégation ont été largement utilisées. L'utilisation de méthodes de désagrégation des données météorologiques peut être considérée comme une stratégie efficace pour obtenir des jeux de données à haute résolution. Cela est particulièrement vrai dans les pays en développement où la plupart des données existantes se trouvent à faible résolution et le potentiel pour faire des observations à des échelles plus fines est limitée en raison de contraintes financières fortes. Il est souvent difficile d'obtenir des jeux de données spatiales, comme les types de sol et leurs propriétés hydriques à la résolution des grilles des modèles hydrologiques distribués. Les données provenant de différentes sources, y compris les mesures de terrain, l'utilisation des données de télédétection et de fonctions de pédotransfert constituent de bonnes alternatives pour combler ce déficit. Dans cette étude un effort important a été consenti pour produire les données spatiales nécessaires à la modélisation hydrologique distribuée à partir d'observations limitées et d'informations pertinentes issues de la littérature. Au final les

données nécessaires pour l'application de DHSVM à 4 bassins versants du lac Tana ont été mises en forme.

Chapitre 6 Application de DHSVM à quatre bassins versants du bassin du lac Tana

Il y a eu au cours de ces dernières années un important développement de l'utilisation de modèles hydrologiques distribués à base physique en dépit des difficultés dans leur paramétrage et leur calibration (Beven, 2001). Les raisons scientifiques et pratiques de cet accroissement sont la nécessité de mieux prédire l'érosion et le transport des sédiments dans un bassin versant, et l'évaluation des impacts hydrologiques des changements dans l'utilisation des terres et des caractéristiques des bassins versants.

Ce chapitre évalue les performances du modèle distribué DHSVM pour la simulation des débits sur les 4 bassins versants sélectionnés dans la zone d'étude. Une brève revue de la littérature sur la calibration et la validation des modèles hydrologiques distribués est présentée en première partie. Elle est suivie par une présentation détaillée de la calibration et de la validation du modèle sur les bassins versants sélectionnés. Les jeux de données hydrométéorologiques, géographiques et dérivés ont été traités pour créer les fichiers d'entrée du modèle (cf. chapitre 5).

Les critères qui ont été retenus pour choisir les bassins versants tests incluaient la disponibilité en données météorologiques, la pertinence des données de débit journalier et leur représentativité spatiale. Les bassins sélectionnés sont ceux de Rib (1 448 km²), de Megech (514 km²), de Gumara (1 279 km²) et de Gilgel Abay (1 641 km²). Les simulations ont été réalisées sur la période 1992-2005 avec une résolution temporelle de 1 heure pour les petits bassins et 3 heures pour les bassins plus grands. La résolution spatiale est de 90 m. Les deux premières années ont été utilisées comme une période d'initialisation du modèle pour minimiser les effets du choix de mauvaises conditions initiales. Le modèle a été calibré sur chaque bassin sur la période 1994-2000 en utilisant une procédure de calibration manuelle. Les principaux paramètres de calibration (cf. chapitre 5) sont la porosité, la conductivité hydraulique latérale à saturation et son taux de décroissance exponentielle, et les profondeurs du sol et d'enracinement de la végétation. Une seconde période a été utilisée pour valider le modèle (2001-2005). La qualité de la calibration du modèle a été évaluée aux pas de temps journalier et mensuel, en utilisant les tracés graphiques et des critères numériques.

Les performances du modèle sont très mauvaises pour les bassins versants de Gumara et Gilgel Abay avec une sous-estimation systématique des débits. La cause de ces mauvais résultats n'a pas été identifiée. Les résultats pour les bassins de Megech et Rib sont relativement meilleurs. Pour le bassin de Megech, la valeur du coefficient d'efficacité de Nash-Sutcliffe au pas de temps journalier au cours de la calibration est de 0.46 et de 0.35 pour la période de validation. Pour Rib on obtient 0.59 et 0.69 respectivement. Au pas de temps mensuel les valeurs du coefficient sont meilleures.

Chapitre 7 Bilans hydrologique et sédimentaire du lac Tana

Les bilans hydrologique et sédimentaire des lacs fournissent des informations de base qui contribuent à la gestion durable de ces importantes ressources. Des études antérieures sur le bilan hydrologique du lac Tana présentent des résultats contradictoires qui pourraient être attribuables à des différences dans les périodes de référence et les méthodes utilisées pour estimer les différentes composantes. Aucune étude antérieure sur le bilan sédimentaire du lac n'a été trouvée dans la littérature.

Les objectifs de cette étude sont de deux ordres: (i) affiner et actualiser le bilan hydrologique du lac Tana en s'appuyant sur des jeux de données hydrométéorologiques représentatives et fiables et (ii) fournir une estimation du bilan des sédiments en suspension qui sera utile pour la planification de la gestion du lac. La modélisation du bilan hydrologique au pas de temps mensuel du lac nécessite l'estimation des différentes composantes du bilan. Cette dernière a été réalisée à partir de données existantes de bonne qualité et par l'application d'un modèle conceptuel dynamique dérivé du modèle de Budyko. Le calcul du bilan des sédiments en suspension est basé sur l'utilisation de courbes débits-concentrations et l'application d'un modèle régional empirique de production de sédiments.

Les principales composantes du bilan hydrologique du lac Tana sont les précipitations directes sur le lac, les débits liquides en provenance de bassins jaugés et non jaugés, l'évaporation de l'eau du lac, l'évaporation de l'eau des plaines inondables, les débits à l'exutoire du lac et les variation de volume du lac. Des études antérieures ont montré que la contribution des eaux souterraines au bilan est faible. Les précipitations directes sur le lac ont été estimées à partir des relevés journaliers des stations situées autours du lac et en utilisant une technique d'interpolation spatiale. Elles correspondent à une contribution moyenne annuelle de 1225 mm. Les apports des bassins jaugés ont été calculés à partir des chroniques historiques de débit. Le modèle conceptuel dynamique a été utilisé pour estimer les débits provenant des bassins versants non jaugés et pour combler les périodes de lacunes sur les bassins jaugés. Le lac Tana est entouré de plaines inondables, où une quantité importante des écoulements de surface en provenance des bassins amont est perdue par évaporation. L'évaporation des plaines inondables a été estimée à partir de données satellites sur l'étendue des zones inondées et le taux d'évaporation. Le flux net en provenance des bassins versants a été calculé en soustrayant l'évaporation des plaine d'inondation de l'écoulement total apporté par les bassins jaugés et non jaugés. La moyenne annuelle de ce flux est de 2344 mm. L'évaporation du lac a été déterminée par la méthode de Penman avec une estimation moyenne annuelle de 1687 mm. Le débit sortant du lac a été estimé à partir des chroniques de débits journaliers à l'exutoire, soit un débit moyen annuel de 1403 mm. La variation du stockage de l'eau dans le lac a été estimée à partir des données observées du niveau du lac. La variation du stock est d'environ 30 mm par an. La fermeture du bilan se traduit par un écart relatif de 12,6% qui s'est avéré être inférieure à l'écart admissible théorique. La validité et la précision du bilan hydrologique ont été évaluées en comparant les niveaux d'eau simulés et observés sur le lac.

Les apports liquides en provenance des bassins versants représentent 66% de l'apport total moyen annuel. En outre, la contribution des parties non jaugés a été jugée significative ce qui est en contradiction avec les résultats de certaines études antérieures. Il est donc

important de veiller à limiter les perturbations sur les régimes hydrologiques des quelques bassins versants qui contribuent le plus aux apports d'eau de surface.

Les apports en sédiments de quatre bassins jaugés ont été estimés sur la base de relations débits-concentrations établies à partir d'un nombre limité d'observations. On a fait l'hypothèse que 30% des apports en sédiments en provenance des hauts bassins se déposent dans les plaines inondables qui entourent le lac Tana. Un modèle empirique régional d'estimation de la production de sédiments développé par Nyssen et al. (2004) a été utilisé pour évaluer les flux de sédiments en suspension provenant des bassins versants non mesurés. L'apport moyen annuel de sédiments en suspension au lac est de $6,6 \times 10^6$ tonnes. Les exportations à partir du lac ont été estimées à l'aide d'une relation débits-concentrations, elles correspondent à une charge annuelle moyenne de $1,3 \times 10^6$ tonnes. La sédimentation annuelle dans le lac représente donc $5,3 \times 10^6$ tonnes ce qui correspond à un piégeage de 80% des sédiments en provenance des bassins versants. Ces résultats doivent être considéré comme une première estimation grossière mais utile pour les études préliminaires de la phase de planification.

Conclusions générales et perspectives

Les bassins versants du bassin du lac Tana sont confrontés à un certain nombre de questions essentielles pour leur développement telles que l'érosion des sols et la sédimentation, la disponibilité en eau, les inondations et la pollution diffuse. La recherche d'options de gestion durable et efficaces pour répondre à ces questions nécessite des bases de données hydrométéorologiques et géographiques de qualité, avec une bonne résolution temporelle et spatiale ainsi que des outils d'analyse adaptés.

Au cours de cette thèse, un important travail de collecte, de critique et d'analyse a été réalisé pour évaluer les données hydrométéorologiques existantes et construire un jeu de données de base continu au pas de temps journalier et de bonne qualité. Suivant les critères de l'Organisation Météorologique Mondiale, 34% de la superficie du bassin du lac Tana a été jugée insuffisamment couverte par les stations pluviométriques existantes. Comme les données sur les précipitations sont des données essentielles pour les études hydrologiques, il est important de renforcer la densité du réseau existant.

Cette thèse a aussi été l'occasion de développer une méthodologie pour palier le faible nombre de données disponibles qui pourra être appliquée dans d'autres régions où le faible nombre d'observations est un frein à l'analyse hydrologique des ressources en eau. Cette approche a permis de créer un jeu de données continu au pas de temps journalier critiqué et homogénéisé sur la période 1992-2005.

La disponibilité et la qualité des données horaires de précipitations sont très faibles. Ainsi, une amélioration de la collecte et de la qualité de ces données est recommandée. Des données de précipitations fiables, pour des pas de temps courts, sont indispensables pour mener les études scientifiques sur certaines des questions clés qui se posent sur ce bassin. L'utilisation de techniques de désagrégation temporelle doit être considérée comme une stratégie alternative pour générer des données météorologiques à des pas de temps inférieur à la journée. Dans le cadre de cette thèse un modèle classique de désagrégation

des pluies (MBLRPM) a été adapté de manière originale pour tenir compte du caractère convectif dominant de la distribution des averses sur la journée. Ce modèle est applicable dans d'autres régions tropicales présentant les mêmes caractéristiques de pluie.

Les données disponibles sur les concentrations des sédiments en suspension sont limitées et discontinues. Compte tenu de la sévérité de l'érosion des sols et des problèmes de sédimentation dans les retenues et de la construction d'infrastructures hydrauliques, un effort important doit être consenti pour l'acquisition, l'analyse et l'archivage des données sur les sédiments en suspension.

L'analyse de sensibilité des paramètres des sols et de la végétation du modèle hydrologique distribué (DHSVM) a permis d'identifier quelques paramètres influents comme la porosité, la conductivité hydraulique latérale à saturation et son taux de décroissance, les profondeurs du sol et d'enracinement. Les résultats de l'analyse de sensibilité peuvent être utilisés comme un guide pour appliquer et calibrer le modèle sur d'autres bassins versants y compris dans des contextes climatiques et géographiques différents.

L'évaluation du modèle hydrologique à base physique a été conduite sur une sélection de bassins versants de méso échelle. Cette tâche a exigé la préparation de jeux de données d'entrée, de calage et de validation des paramètres du modèle. Comme le modèle a été utilisé avec un pas de temps inférieur à la journée, les données météorologiques ont été désagrégées en utilisant des techniques adaptées. La calibration du modèle a été conduite suivant une procédure manuelle en suivant une exploration systématique qui s'est appuyée sur une analyse de sensibilité pour déterminer les paramètres les plus influents. Le modèle a été validé en comparant les valeurs des écoulements simulés aux valeurs observées d'un échantillon indépendant. Au vue de la résolution grossière des jeux de données hydrométéorologiques et géographiques, le modèle hydrologique DHSVM a montré une performance prometteuse pour les bassins versants de Megech et de Rib. Du fait de l'importance de l'utilisation de ce type de modèle pour répondre aux questions scientifiques posées par l'étude de l'érosion des sols et des impacts hydrologiques des changements de l'utilisation des terres et climatiques, il serait utile de poursuivre cette évaluation dans le contexte éthiopien.

La préservation des valeurs socio-économiques et écologiques du lac Tana, par une gestion raisonnée de ses ressources, nécessite de connaître le bilan hydrologique. Celui-ci a été calculé en utilisant les observations disponibles et un modèle conceptuel. La majorité du flux d'eau vers le lac provient des principaux bassins versants jaugés. Les bassins non jaugés contribuent également pour une part non négligeable. Ces dernières années la réalisation de barrages, dont certains sont déjà construits, s'est développée sur le bassin du lac. Ces ouvrages auront pour effet de modifier les entrées en provenance des principaux bassins versants. De plus une prise d'eau dérive une partie des eaux du lac vers un bassin situé en aval (Beles). Compte tenu de ces évolutions majeures il sera important d'actualiser le bilan hydrologique du lac.

Le lac Tana est un important puits de sédiments fins avec un taux de piégeage de 80%. Ces premiers résultats sont utiles pour la phase de planification des aménagements.

Il est souhaitable de développer un réseau de mesure des flux de sédiments en suspension sur plusieurs sites représentatifs à la fois des zones de production dans la partie amont et

des zones de dépôt en aval. Cela contribuerait à mieux comprendre les processus d'exportation des sédiments et le rôle des plaines d'inondation dans le transfert des sédiments fins.

L’établissement de bilans a été l’occasion de produire des connaissances sur les variabilités spatiales et temporelles des processus hydrologiques et des variables de forçage météorologique et de permettre de mieux comprendre le fonctionnement de cet hydrosystème tropical d’altitude. Les outils et méthodes utilisés ou développés pour ce travail de recherche peuvent être utilisés pour réaliser des études similaires sur d’autres bassins versants. Enfin, cette thèse apporte une contribution notable pour l’aide à la gestion durable des ressources en eau dans la région du lac Tana.

Introduction

Many countries in the world are faced with diverse water and water-related issues that include water scarcity, water pollution and water-related disasters. The problems are more serious in the developing world due to their huge adverse socioeconomic impacts and the countries' weak capacity and coping-up mechanisms to deal with the issues.

This study is conducted in the Lake Tana basin in Ethiopia where the current level of water resources development is low, soil erosion by water is a serious problem, flooding is a recurrent phenomenon, and unsustainable watershed management could have major adverse socioeconomic and ecological impacts at local and regional scales. The basin represents the headwater catchment of the Blue Nile River that makes the largest contribution to the main Nile flow. Lake Tana, the largest lake in Ethiopia with diverse socioeconomic and ecological values, is located in the middle of the study basin. Major water resource development projects are also going on in the basin. Hydrological and sediment-related studies are essential components of watershed management and are the focus of this research. The study has three major components that include evaluation and analysis of the existing hydro-meteorological and spatial datasets, evaluation of the applicability of a physically-based distributed hydrological model, and determination of the water and suspended sediment balances of Lake Tana. The specific issues addressed, the overall methodological framework followed and the outline of the thesis are presented below.

Research questions and objectives

Researches in the areas of hydrology and sediment budget are indispensable for sustainable watershed management. Their role is particularly crucial in regions like Lake Tana Basin where water resources issues are critical, and availability and quality of hydro-meteorological data is poor. Some priority research areas that address biophysical, management and socio-economic aspects of the Nile Basin have already been outlined in a recent study (Mohamed and Loulseged, 2008). This study tried to make a contribution to some of the research needs by addressing the following issues:

- The first issue addressed in this research is related to data availability and quality. Knowledge of the type, quality and spatial and temporal characteristics of existing data is fundamental for hydrological studies. It illuminates gaps and problems in the existing

datasets and helps to identify relevant strategies to address the problem. Depending on the objectives of the analysis, nature of the data and availability of resources, different strategies may be used to resolve the problem. The strategies may include direct use of existing data, generation of the required type of data from existing datasets using appropriate methodologies (e.g. disaggregation models for weather data series, pedotransfer functions for soil properties, spatial interpolation, etc.), or conducting a new data collection campaign. This study tried to assess the characteristics of the existing datasets for Lake Tana basin by raising some key questions related to the type, coverage, quality and consistency of the hydro-meteorological data series. The type and coverage of datasets that pertain to watershed characteristics were also investigated.

- In Ethiopia in general, and the study region in particular, there are several ungauged catchments. For instance, about 40 % of Lake Tana basin is ungauged. Moreover, the problems of erosion and sediment transfer are critical due to their onsite and offsite adverse consequences. The significance of this problem in the study area could be high as water resource development schemes and natural systems with great socioeconomic and ecological values are found. Ongoing and planned irrigation schemes to develop more than 100 000 hectares of land, and operating hydropower systems having a capacity in excess of 500 MW could be directly affected. Researches that aim at improving estimates of runoff contributions from ungauged catchments and sediment yields would be important to ensure the sustainability of water resource systems. In this regard, use of physically-based hydrological models may prove to be valuable. The second issue addressed in this study is, therefore, evaluation of the applicability of a distributed hydrological model using existing/derived hydro-meteorological and spatial data.
- Availability of meteorological data at hourly time scales is generally poor. Meteorological data at finer time scales are, however, required for several applications like erosion and sediment transport studies, flood analysis, etc. In connection with the application of the physically-based distributed hydrological model, this study would explore and apply relevant weather data disaggregation methods for generating hourly meteorological time series from existing daily data.
- The water balance of Lake Tana has been studied by different authors in the past with noticeable variations in estimates. Reasons for these variations include differences in the meteorological datasets and simulation periods used, and methods used to estimate contributions of ungauged catchments. For instance, Kebede *et al*. (2006) estimated direct precipitation on the lake by taking data of a single station and assumed the contribution of

ungauged catchments to be insignificant. In a region where the spatial variability of rainfall is high, the accuracy of the water balance estimates obtained from a single station is questionable. The water balance components of the lake should be estimated as accurately as possible based on representative datasets. This is an important element in identifying options for sustainable management of the lake. In this study effort has been exerted to model the water balance of the lake using quality-controlled and representative hydro-meteorological datasets from 1992-2005.

- As erosion is a critical problem in the Lake Tana Basin its impact on the lake and its various socio-economic and ecological values could not be underestimated. Limited studies on the bathymetry of the lake and sediment yields of some of its contributing catchments could be found. It was not possible to find a full-fledged study on the suspended sediment balance of the lake. This study tried to indicate the longterm mean annual suspended sediment balance of Lake Tana based on comprehensive analysis.

By addressing the research issues presented above, the study will make a contribution to sustainable management of the lake and its watershed. The various tools and techniques used would be useful for making similar studies on other catchments. The specific objectives of this study are the following:

- Evaluation and analysis of existing hydro-meteorological and spatial data in the Lake Tana Basin
- Application and/or evaluation of weather data disaggregation models
- Evaluation of the applicability of a physically-based distributed hydrology-soil-vegetation model (DHSVM)
- Refinement and updating of Lake Tana's water balance
- Estimation of the suspended sediment balance of Lake Tana

Methodological framework

The study employed diverse methodologies to fulfill the stated objectives. Analyses of hydro-meteorological data involved checking of data quality, gap filling and their characterization in space and time. The specific techniques for each of these activities are presented in the relevant sections.

Evaluation of the applicability of the physically-based distributed hydrological model was conducted on selected mesoscale catchments. The task required preparation of input datasets, and calibration and validation of the model parameters. As the model was run at subdaily time steps, disaggregation of observed daily weather data series was carried out. Depending on the type of meteorological variable, different disaggregation techniques were used. A calibration period of seven years (1994-2000) was used to obtain good parameter values for runoff simulation. The calibration was done manually following a systematic approach that involved identification of few influential parameters based on sensitivity analysis. The model was further validated by comparing the simulated runoff against observed discharges using the standard split approach.

Water balance study of Lake Tana considered direct rainfall, inflow from gauged and ungauged basins, evaporation and outflow from the lake as major components of the model. Direct rainfall on the lake was estimated from observed daily records of stations using a spatial interpolation technique that is considered to be good. The Penman approach was used to estimate evaporation from the free water surface. Inflow contributions of gauged basins were estimated from historical runoff records. A dynamic conceptual model developed based on Boudyko framework was used to estimate runoff from ungauged catchments and to fill missing records of gauged basins. The accuracy of the water balance model was evaluated by comparing the simulated and observed water levels of the lake. The study on suspended sediment balance involved estimation of sediment influxes from contributing catchments, sediment outflows and deposition in the lake and surrounding floodplains. Suspended sediment rating curves and area-specific regional sediment yield model were employed.

Outline of the thesis

Chapter 1: The whole purpose of this chapter is to provide a wider context for the research by highlighting some of the critical water resources issues of developing countries and Ethiopia. Existing and anticipated water resource concerns of the study basin are also briefly stated. The importance of scientific researches in the areas of hydrology, soil erosion and sediment transfer in addressing the various water resources issues is presented. In line with the objectives of this study, an overall presentation on the types of hydrological models and their applications in water resources management is made.

Chapter 2: This chapter describes the environmental settings of the study area and region. It begins with the presentation of the whereabouts of the study area in terms of its geographic, local and regional settings. This is followed by sections on geology, soil and land cover types of Lake Tana basin. An overview of the climate and hydrological systems of the study area is also included. The status of water resources development in Ethiopia in general, and Lake Tana basin in particular, is briefly presented in the last part of the chapter.

Chapter 3: This is an important part of the research which addresses the first objective on data availability and analysis. Availabilities of relevant hydro-meteorological and spatial datasets are explored and assessment of their temporal and spatial coverage is made. Analysis of the hydro-meteorological data involved checks on data quality and consistency, gap filling, and temporal and spatial characterizations. The annual and seasonal characteristics of the hydro-meteorological variables are given in terms of relevant statistical descriptors. Spatial patterns of annual rainfall and temperature and their relation with altitude/latitude is also indicated. In the analysis of the hydrological data, efforts were exerted to estimate annual areal rainfall and baseflow contributions of the major catchments. Suspended sediment rating curve equations of streams are also presented. Both historical records and the limited data collected during the field campaign of this study were used in the development of the suspended sediment rating curve equations. The spatial datasets covered in the analysis include distribution of soil and land cover types and soil hydraulic properties.

Chapter 4: This chapter is dedicated to the physically-based distributed hydrological model (DHSVM) used in the study. The different hydrological processes, input requirements and outputs of the model are described. Moreover, some examples of the model application from around the world are included. As the model comprises several parameters, identification of few influential parameters is important to facilitate the calibration task. To this end sensitivity analysis of the model parameters using virtual catchments was made and the results are presented.

Chapter 5: Creation of the different hydro-meteorological and spatial datasets for the physically-based distributed hydrological model is presented in this chapter. A section on weather data disaggregation, from daily to hourly time scale, constitutes this chapter. The model was run at time step of one or three hours on selected catchments. Other inputs required by the model include soil and vegetation types, soil depth, basin mask file, digital elevation model, and initial state files. The methods employed in creating these inputs from the existing data are also presented.

Chapter 6: Application of the physically-based distributed hydrological model to selected catchments is presented in this chapter. An overview of methods used for calibration and validation of hydrological models is included in the first part. This is followed by the procedures used in calibrating and validating the model on the selected catchments. The modeling results and their implications are finally discussed.

Chapter 7: Determination of the water and suspended sediment balance of Lake Tana is one of the drivers of this study. The major water balance components of Lake Tana include direct rainfall, evaporation, inflow from gauged and ungauged catchments, and surface outflow. Computations of the different hydrological fluxes and the water balance of the lake are presented and discussed. In addition, a section on suspended sediment balance of the lake is included. The suspended sediment rating curve equations developed in Chapter 3 were used in the estimation of the sediment influxes.

Finally, summary of the main results, overall conclusion and perspectives are presented. Key contributions of the study and brief notes on identified areas for further researches are included.

Chapter 1

1 Water Resources Issues

This chapter sets a general context to the research by making concise presentations on relevant topics. An overview of major water resource problems faced in developing countries and the study area is presented in the first part. This is followed by a brief note on the role of hydrology and sediment budget studies in addressing watershed issues. As application of hydrological models is an important aspect of this study, an overall presentation on the types and applications of hydrological models is included.

1.1 Water resource issues in developing countries

A concise presentation of pertinent water resource issues, with particular emphasis on developing countries and Ethiopia, is made. The various water resources issues are grouped into four classes: water quantity issues, water quality issues, hydrological extremes, and soil erosion and reservoir sedimentation.

1.1.1 Water quantity issues

Water is required to meet various consumptive and non-consumptive uses. Consumptive uses comprise water for irrigation, domestic and industrial supplies. Non-consumptive uses include water required for hydropower generation, waste disposal, fish and wildlife habitat, inland transport and recreation. Meeting these needs for water is becoming increasingly difficult worldwide due to rapid population growth, improving living standards, urbanization and expansion of agricultural and industrial activities (Jones, 1997). A comprehensive study on water resources vulnerability indicated that about 60% of the world population would live in moderately to extremely vulnerable regions by year 2025 (Kulshreshtha, 1998). The spatial and temporal variability of water availability together with impacts of land use and climate changes would exacerbate the problem.

Water scarcity is serious in the developing world where most of the population growth takes place and the coping-up capacities are weak. Half of the population of developing countries lives in water poverty, having difficulty of getting a minimum per capita share of 1700 m^3/year (WWAP, 2009). In Asia and Africa water is said to be a major constraint for agriculture in the coming decades (Rijsberman, 2006). In Africa, only one-seventh of the continent has surplus runoff, making water shortage a critical problem (Jones, 1997). The transboundary nature of many rivers complicates and politicizes the issue of water supply-demand issues. Large parts of Africa (60%) and Asia (65%) are located within transboundary river basins where, in most cases, binding water use agreements are lacking (Jones, 1997).

The problem could also be an issue of major concern in Ethiopia as the various factors that could lead to water scarcity do exist. An average per capita water share of 1700 m^3/year could be obtained based on the recent population census data and total freshwater potential of the country. Water resources vulnerability is found to be high in Ethiopia according to a recent study conducted for Eastern Nile Basin countries (Hamouda *et al.,* 2009). Moreover, the high spatial and temporal variability of water resources in Ethiopia makes the issue more serious. Eighty three percent of the country has drier climate (moisture index ranging from -60 to 0) with limited surplus water during the rainy season (Gonfa, 1996). The lowlands are water deficit regions with unreliable annual rainfall of 200-600 mm. Most of the highlands receive annual rainfall in excess of 1000 mm, but it is highly seasonal with most of it occurring between June and September (Korecha and Barnston, 2006). The highlands are also regions where population concentration, urbanization, and increasing agricultural and industrial activities are seen. The water scarcity problem may also be aggravated by climate change. For instance, predictions of hydrological impacts of climate change indicated decreases in runoff in catchments located in the south central and eastern parts of the country (Hailemariam, 1999; Legesse *et al.,* 2003). The transboundary nature of most rivers of Ethiopia is a serious challenge (World Bank, 2006). It is particularly serious in the Blue Nile Basin which contributes about 60% of the Nile flow. The Nile basin is shared by 10 riparian countries whose major source of livelihood is agricultural production. Equitable water allocation has been and continued to be a serious issue among the basin countries.

The pressure on the freshwater resources of Lake Tana Basin would mount, as the various factors that are responsible for water demand increase do exist. According to the recent census data, a total population of about 7 million lives in and around the basin (CSA, 2008). Two major cities of the country, Bahir Dar and Gonder, with more than 200000 residents each are located within the basin. Moreover, the Lake Tana region has been identified as one of the

economic growth corridors of the country (MoFED, 2006). To this end implementation of water resources development projects that are identified in the Abay Basin Master Plan study (BCEOM, 1999a) has been going on. The Tana-Beles multipurpose project that relies on water transfer from Lake Tana was recently completed. Major dam projects for irrigation agriculture are going in different parts of the basin. A simulation study on the impact of the different development scenarios indicated a decrease in the level and area of the lake with anticipated socio-economic and environmental impacts (Alemayehu *et al.,* 2009). Water resources of Lake Tana basin are said to be susceptible to climate change with predicted reduction in streamflows (Hassan, 2006; Abdo *et al.,* 2009).

1.1.2 Water quality issues

Freshwater quality impairment has been a major issue of concern worldwide. The sources of water pollution can be point or diffuse sources. Point sources of pollution include municipal and industrial wastewaters for which specific points of entry to a receiving water body can be identified. Diffuse sources of pollution include general land runoff from urban and agricultural areas and other sources that do not have specific discharge points. Unlike point sources, diffuse sources of pollution are difficult to manage (Novotony and Olem, 1994). Due to the extensive damages that could be caused by diffuse sources of water pollution, the need for addressing the issue as an international priority of concern was already heralded long ago (Duda, 1996). Diffuse pollution is considered to be the dominant cause of water quality impairment in many developing countries due to poor waste management and environmentally unfriendly agricultural methods (Novotony, 1995). For instance, a study in Uganda indicated pollution from diffuse sources to be higher than point sources (Banadda *et al.,* 2009). Water quality impairment in general, and diffuse pollution in particular, can be a serious problem in Ethiopia for reasons related to widespread sources of pollution, favoring hydrologic factors and lack of environmental services. The favorable hydro-meteorological factors are related to the nature of the rainfall climate and watershed characteristics. Many catchments in Ethiopia receive intense seasonal rainfall on steep slopes that have scarce vegetation cover. These factors enhance high surface runoff and transport of sediments and associated contaminants.

Though a general and systematic water quality assessment program is lacking, isolated studies indicated existence of water pollution problems (MoWR *et al.*, 2004). Major urban centers and industrial establishments are sources of water pollution due to inadequate waste

management services. For instance, pollution of streams that drain Addis Ababa due to poor waste management practices is considered to be a major problem with adverse public health and ecological impacts (Nigussie, 1999; Gebre and Rooijen, 2009). Various Water quality studies on rift valley lakes indicated problems of pollution that include eutrophication, heavy metals, salinity, and other pollutants (Zinabu *et al.,*2002, 2003; Teklemariam and Wenclawiak, 2005; Ayenew, 2007). The causes of these problems are related mainly to improper utilization of land and water resources in the lakes catchment (Legesse and Tenalem, 2006). In another study high salinity level is noted in the middle Awash River Basin due to intensive irrigation and upstream pollution sources (Tadesse *et al.*, 2007).

Water quality studies in the Lake Tana Basin are limited. But, considering the extensive agricultural activities using chemical fertilizers, the growing urban settlement with poor waste management services, as well as the favorable hydrological factors of erosion, the problem of water pollution could be high. Indications of pollution of Lake Tana, with adverse socio-economic and ecological impacts have already been reported (Teshale *et al.,* 2001). Assessment of the impact of Bahir Dar city on pollution of Lake Tana and groundwater resources indicated high levels of nutrient and suspended sediment loads (Wondie, 2009).

1.1.3 Hydrological extremes

Two common and devastating hydrological extremes, floods and droughts, are discussed. These disasters continue to affect generations, bringing suffering, death, and immense material losses worldwide.

1.1.3.1 Flooding

A flood is an unusual high-water period in which water overflows its natural or artificial banks onto normally dry land. Flood can cause great damage to land and water-related infrastructure and it can have disastrous short and long-term consequences on people and economies. Flooding problem is a critical issue in developing nations due to the magnitude of the problem and lack of adequate coping-up mechanisms. A storm surge flood in 1991, for instance killed 140 000 persons in Bangladesh (Kundzewicz and Kaczmarek, 2000). In Africa, Mozambique was hit by a devastating flood that caused huge socio-economic disruptions (Christie and Hanlon, 2001). Since the mid 1990s Africa has become the second most flood-affected continent in the world following Asia (Yoganath and Junichi, 2009).

In Ethiopia flooding affects mainly riverine and lowland areas with adverse consequences on agricultural land, settlements and infrastructure. Areas commonly flooded in Ethiopia include the Gambela Plain in the Baro-Akobo Basin, floodplains and irrigation areas along the Awash River, the lower parts of Wabi-Shebele Basin and the downstream reaches of major catchments in Lake Tana Basin (Woube, 1999; Achamyeleh, 2003). The socio-economic impacts of flooding could be huge as exemplified by the year 2006 incident which covered almost the entire country with affected population of about 700 000 (EWD, 2007).

Flooding is a recurrent problem in the Lake Tana basin (SMEC, 2008a). Flood risk areas include floodplains located in the downstream reaches of Megech, Rib, Gumara and Gilgel Abay rivers. Flooding is caused by combination of factors that include bank overflow, sedimentation, poor drainage, lake level rise, and changes in the watershed characteristics. The impacts of past flood incidents were serious with displacements of several inhabitants and inundation of croplands (Riverside *et al.,* 2009).

1.1.3.2 Drought

In the literature different types of drought are recognized- meteorological, hydrological, agricultural and socio-economic drought (Kundzewicz *et al.,* 2002). Meteorological drought is generally taken as shortage of rainfall. A meteorological drought can develop into agricultural drought which is described by soil moisture deficit and low crop productivity. Hydrological droughts are characterized by a reduction in lake storage, lowering of groundwater levels and decrease of streamflow discharge. A socio-economic drought occurs when the demand for water and water-related economic goods and services (e.g., fish, hydropower, irrigated agriculture and horticulture) exceed supply. Hydrological droughts usually lag the occurrence of meteorological and agricultural droughts. Although climate is a primary contributor to hydrological drought, other factors such as changes in land use (e.g., deforestation), land degradation, and construction of dams all can affect the hydrological characteristics of a basin. Because regions are interconnected by hydrologic systems, the impact of hydrological drought may extend well beyond the borders of precipitation-deficient area.

Drought is an issue of great concern in several countries, particularly, in the developing world. The African continent suffered an extraordinary drought without precedence in the records due to a significant drop in precipitation and decreasing streamflows (Kundzewicz and Kaczmarek, 2000). Global analysis of water related disasters between 1980 and 2006

indicated that 99% of the total drought fatalities were in Africa (Yoganath et Junichi, 2009). In sub-Saharan Africa, where rain-fed agriculture is the predominant economic sector, drought poses a great challenge to the overall performance of their economies (Gautam, 2006).

Drought is a recurring phenomenon in Ethiopia, with increased frequency of occurrence in recent years (MoWR *et al.,* 2004). According to the international disaster database, drought has been top in the list of natural disasters affecting millions in the country for long (CRED, 2010). Combinations of the various types of drought could be the cause of the problem (MoWR *et al.,* 2004). Drought analysis in the Awash River indicated an average lag period of 7 months between hydrological and meteorological droughts (Edossa and Babel, 2010). The adverse socio-economic impacts of drought are huge as most of the population depends on agriculture and hydropower is the major source of electricity. For instance during the 1984/85 drought GDP declined by 9.7 percent, agricultural output declined by 21 percent, and gross domestic savings declined by 58.6 percent (World Bank, 2006). Lower water level in reservoirs has also been a major cause for extensive power rationing in recent years.

1.1.4 Soil erosion and reservoir sedimentation

Soil erosion by water and subsequent sediment transfer are global issues of great concern because of their multiple adverse onsite and offsite consequences. The onsite effects include soil degradation and reduction in crop productivity which would lead to food insecurity (Lal, 2001; Blanco and Lal, 2008). The offsite consequences are diverse and include changes in channel morphology and habitat, reservoir sedimentation, transport of sediment-adsorbed nutrients and contaminants such as particulate phosphorus, heavy metals, and pesticides (Owens, 2005; Owens and Collins, 2006). Because of its diverse negative effects, soil erosion is considered to be the single most environmental degradation problem in developing countries (Ananda and Herath, 2003). Soil erosion contributes to chronic malnutrition and rural poverty in these countries because of farmers' weak capacity to establish mitigation measures (Blanco and Lal, 2008).

Sedimentation in reservoirs and river beds could be an issue of major concern due to its multiple effects. Some of the adverse effects include loss of storage capacity, damage of hydraulic structures, modification of river morphology, and disruption of aquatic habitat (Morris, 1998). Reservoir sedimentation is considered to be one of the most economically crippling problems because of large investments in dams for generation of hydroelectric

power and irrigation development (Nagle *et al.,* 1999). For example, a drastic reduction in hydropower generation and inefficiency of irrigation schemes due to large sediment loads coming from Ethiopian highlands are noted to be serious problems encountered at Roseires Dam in Sudan (Elsheikh *et al* ., 1991). Siltation in Lake Victoria is one of the critical factors that is affecting the fishing industry (Ntiba *et al.,* 2001).

Soil erosion by water has been a longstanding environmental problem in Ethiopia and is considered to be a critical economic problem (Hurni, 1993; Bewket and Sterk, 2003). The annual rate of soil loss in the country is greater than the annual rate of soil formation (Tamene and Vlek, 2008). The rate of soil erosion is high due to a number of favoring factors that include erosive rains, steep gradients, cultivation on steep terrain, deforestation, overgrazing, and poor agricultural techniques (REDECO and HSD, 2002; Nyssen *et al*., 2004). The most important soil erosion processes are sheet and rill erosion, and water-induced soil movements by gullying and landsliding, particularly in the highlands (Oldeman *et al.,* 1991; Nyssen *et al*., 2004). The mean annual soil loss rate by sheet and rill erosion in the highlands is estimated to be 12 t/ha (Hurni, 1990). The soil loss rate from croplands by sheet and rill erosion is 42 t ha^{-1} $year^{-1}$. Assessment of gully erosion rates is limited in which soil loss rates of 26 t $ha^{-1}year^{-1}$ and 6.2 t ha^{-1} $year^{-1}$ are noted, respectively, in the eastern and northern highlands (Shibru *et al.*, 2003; Nyssen *et al*., 2006).

Different studies indicated siltation of water systems in different parts of the country as a major problem in Ethiopia. Assessment of siltation of water harvesting schemes in the northern highlands indicated that most of them will be filled with sediment within less than 50% of their intended service time (Tamene *et al* ., 2006). Land degradation due to soil erosion and reduction of storage capacity of Lake Alemaya, in the eastern highlands of Ethiopia, is dubbed as a serious problem (Muleta *et al.,* 2006). Siltation and nutrient enrichment are found to be the major problems of Gilgel Gibe hydropower dam which is located in the southwestern part of the country (Devi *et al*., 2008).

Soil erosion and sedimentation could be a major threat in the Lake Tana basin. Agriculture is the mainstay of most of the population in the basin and hence land degradation by soil erosion would directly affect the lives of millions. Sedimentation could adversely affect the storage capacity, socioeconomic values and ecological health of Lake Tana. Moreover, the capacity and efficiency of the existing and ongoing dam projects in the basin could be endangered. Factors that contribute to accelerated soil erosion are evident in the basin and include extensive cultivation (even on steep slopes), overgrazing, scarce vegetation cover on hillslopes, and high rainfall intensity. Some relevant studies indicated high rates of soil

erosion and adverse impacts of siltation. A recent study by Tebebu *et al.* (2009) on hydrological controls of gully formation in the southern part of the basin indicated an average gully erosion rate of 24.8 t ha^{-1} $year^{-1}$. A modeling study found 18.4% of the basin highly susceptible to erosion with estimated sediment yield of 30 t ha^{-1} $year^{-1}$ (Setegn *et al*., 2009). Siltation in the downstream reaches of the major rivers is one of the causes of overbank flow and flooding (SMEC, 2008a).

1.1.5 Concluding remarks on water resources issues

The notes made in the previous sections did indicate how diverse and critical are watershed problems in the developing world and the study area. The analysis and management of the issues is even more challenging for various reasons. Some of the key constraints include weak institutional arrangements and inadequate human, financial and technical capacities. Lack of adequate and reliable hydro-meteorological and spatial data is the other major scientific challenge that contributes to the improper formulation of problems and evaluation of management options. Many catchments are ungauged or poorly gauged in many parts of the world and the problem is worse in developing countries (Sivapalan, 2003). In Ethiopia in general, and the study region in particular, there are several ungauged or poorly gauged watersheds. Examples of specific problems associated with data availability include lack of hydro-meteorological data at shorter time scales, representation of the naturally heterogeneous land surface elements such as soil and vegetation types by very coarse-resolution. Such problems make applications of hydrological models difficult, resulting in high prediction uncertainties. As a response to this critical issue, the International Association of Hydrological Sciences (IAHS) launched an international initiative called Predictions in Ungauged Basins (PUB) and declared the period 2003-2012 as the decade of PUB (Sivapalan *et al*., 2003). So far diverse promising outputs of the initiative have been noted (e.g. Sivapalan *et al*., 2006). Different strategies can be used to bridge data paucity and make hydrological predictions possible. Some of the strategies may include use of data from diverse sources, disaggregation of existing meteorological data to finer time scales, application of pedotransfer functions to derive soil hydraulic properties, and estimation of values of model parameters from watershed physical characteristics through regionalization techniques. Such strategies have been used in this study to make it more scientific.

1.2 Role of hydrology, and erosion and sediment transfer in watershed management

Watershed management is concerned with the protection and maintenance of land and water resources. It is multidisciplinary and requires the involvement of various actors (Diplas, 2002). Watershed management is an effective tool in dealing with one or more of the issues discussed in Section 1.1. It is a process that involves the following planning-stage activities (Brooks *et al*., 2003):

- Formulation of the problem
- Identification of alternative plans
- Appraisal and evaluation of impacts of alternative plans
- Prioritization of alternatives to deal with the problem(s)
- Implementation of selected plans

The roles of hydrological and sediment-related studies are explicit and direct in the problem formulation and evaluation of alternative plans. The problem formulation is a key step in the process and should indicate among others, the magnitude and frequency of the problem, priority problem areas, and causative factors. Appraisal and evaluation of impacts of alternative plans require information on the socio-economic and environmental burdens of proposed interventions.

Hydrological inputs and analysis make important contribution in addressing problems of water quantity by providing basic information on water balance in space and time. Knowledge of the relative magnitudes of the various water balance components such as evapotranspiration, direct runoff, subsurface flow, soil moisture, etc. are essential in assessing adequacy of water for current and planned developments. It also helps decision makers to weigh the advantages of each proposed intervention on the hydrologic cycle against the disadvantages (Ward and Trimble, 2004). Decisions made in the absence of basic hydrological inputs would entail immense socio-economic and ecological costs. Hydrology also allows assessment of land use and climate change impacts on water balance. The fact that the hydrological literature is filled with several water balance related studies, from catchment to global scale, is an indication of its importance in water management.

Watershed managers are interested in the magnitude and frequency of hydrological extremes for several purposes, from planning of water supply systems to protection against natural disasters. Hydrological analysis allows estimation of the scale of devastating floods under existing and predicted conditions. The results of the analysis can be used to identify flood prone areas and optimal flood protection levels (Plate, 2002; Morita, 2008). Similarly, hydrological studies on the magnitude and variability of low flows are important for integrated and environmentally sensitive catchment management (Smakhtin, 2001). Outputs of hydrological analysis are also required for the design and operation of flood control structures and water supply systems.

Hydrological information such as low discharge, flow velocity, etc. are also required in water quality management. Water quality management involves activities that include identification of critical pollution source areas and pathways, estimation of pollutant loading, and evaluation and selection of water quality management plans. Identification of critical source area is important in order to utilize the limited available resources effectively. Several articles that deal with these different aspects of water quality management could be found in the literature (e.g. Cugier *et al.,* 2005; Zhang and Jørgensen, 2005; Ouyang *et al.,* 2008; Pandey *et al.,* 2008).

Soil erosion and sediment transport is a critical environmental issue because of its adverse socio-economic and environmental impacts such as loss of soil productivity, reservoir sedimentation and associated effects, and water quality impairment (Owens and Collins, 2006). Studies on soil erosion and sediment transfer contribute to effective management of the problem by providing basic information that include sediment source areas, pathways, sediment yield, and other controlling factors (Owens, 2005). Such information, for instance, could be used to identify and prioritize critical areas for soil conservation measures (Tripathi *et al.,* 2003).

In summary, watershed management should be scientifically valid, economically viable and socially acceptable (Freehafer, 2008). Understanding the hydrologic response of watersheds to land use and management is paramount if we are to sustain land and water resources for future generations (Gregersen *et al.,* 2007). Hydrological and sediment related studies contribute to the scientific bases of sustainable watershed management. Suffice to mention recent international level efforts to highlight the importance of hydrology and sediment budget studies to the society (Walling and Horowitz 2005; Oki *et al.,* 2006; Liebscher *et al.,* 2009).

1.3 Hydrological modeling

Watershed models play a fundamental role in addressing a range of water resources, environmental and social problems (Singh and Frevert, 2006). Hydrological models of different levels of complexity are invaluable tools in the planning, design, operation and management of water resources. The use of modeling studies in water management decisions is in fact increasing (Refsgaard *et al*., 2005). This can be evidenced by the plethora of simple to complex models that simulate various processes like rainfall-runoff, nonpoint source pollution, stormwater management, groundwater flow, erosion and sediment transport, etc.

Hydrological models may be divided into deterministic and stochastic models which are further subdivided depending on the level of process description and spatial discretization as presented in Figure 1-1. A deterministic model is one in which given inputs in a certain physical environment produce same outputs. It could be a simple, data-driven "black-box" model derived from past data such as the SCS curve number method (USDA-NRCS, 1986) and the modern day artificial neural network (ANN) models (Govindaraju, 2000). It could be a conceptual model in which processes are represented in a simplified manner like TOPMODEL (Franchini *et al*., 1996) and HBV (Bergström, 1976). It could be a true physically based model, in which processes are modeled according to fundamental scientific laws like SHE (Abbott *et al*., 1986) and SHETRAN (Ewen *et al.,* 2000). Stochastic models allow for some randomness or uncertainty in the possible outcomes due to uncertainty in input variables, boundary conditions or model parameters (Beven, 2001). They also consider the natural variability that may occur in some model input parameters. The recognition that hydrological processes contain both deterministic and stochastic elements leads to the identification of another category called coupled deterministic-stochastic models.

The development and application of physically based distributed hydrological models is getting wider as can be seen in the literature (Abbott, *et al*. 1986; Wigmosta, *et al*. 1994; Ewen *et al.*, 2000; Liu and Todini 2002). Such models require a large number of input factors that vary in space and time.

Although this has been a bottleneck in their use, increasing availabilities of distributed meteorological and spatial data have facilitated the development and application of physically based models (Todini, 2007). Physically based models have two important advantages (Jones, 1997):

- They can be applied in different watersheds with minimum adjustments of parameter values. This makes them suitable for applications in ungauged catchments.
- They enable to conduct more realistic assessment of hydrological consequences of different scenarios like land use and climate changes.

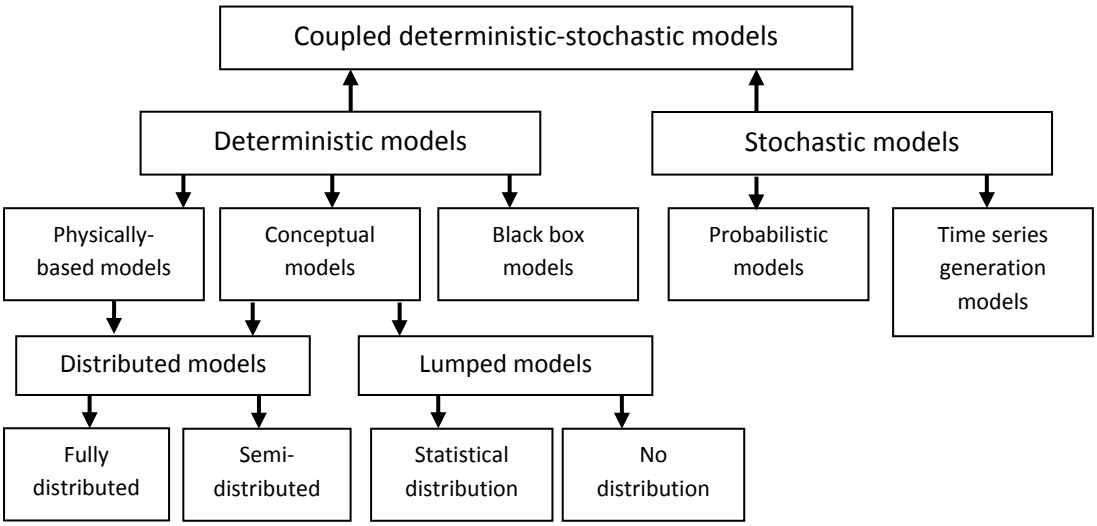

Figure 1-1 Classification of hydrological models. Based on Becker and Serban (1990)

Applications of physically-based hydrological models involve key steps that include parameterization, calibration and validation (Refsgaard, 1997). The parameterization step involves assignment of representative values to the model parameters based on data obtained from field measurements and other sources. The use of data from other sources is necessary because of the high heterogeneity of basin characteristics and lack of field data at the same grid scale (Moreda *et al*., 2006). Model calibration is a process of adjustment of parameter values of a model to reproduce the response of reality within the range of accuracy specified in the performance. Model validation is substantiation that a model within its domain of applicability possesses a satisfactory range of accuracy (Refsgaard and Henriksen, 2004).

Physically based distributed models have been successfully used to conduct water quantity and quality analyses under existing and envisaged future conditions. Examples include simulation of runoff and groundwater processes (Grayson *et al*., 1992; Giertz *et al*., 2006) evaluation of effects of climate and land-use changes on water resources and hydrological regimes (Thanapakpawin *et al*., 2006; Guo *et al*., 2009), nutrient load scenario analysis and sediment yield modeling (Pandey *et al*., 2008; Yoshimura *et al*., 2009), water balance simulation in ungauged catchments (Wanger *et al*., 2009), prioritization of watershed

management options (Mishra *et al*., 2007; Prochnow *et al*., 2008), identification of priority areas for soil and water management (Kaur *et al*., 2004), assessment of flood contributing areas (Fiorentino *et al*., 2007).

A limited number of studies using distributed hydrological models are also available for Ethiopia and neighboring countries. Examples include a study on agricultural nonpoint source pollution (Mohammed *et al*., 2004), modeling effects of soil and water conservation practices (Hengsdij *et al*., 2005), climate and land use change impacts on catchment response (Legesse *et al*., 2003), prediction of runoff and soil erosion in East African highland catchments (Hessel *et al*., 2006).

1.4 Conclusion

The study region in general, and Lake Tana basin in particular, are faced with diverse watershed issues. Hydrology plays a central role in clarifying the nature of these problems and selecting scientifically valid watershed management options. To this end availability of relevant and quality datasets as well as use of appropriate hydrological models and methods are crucial. Creation of a sound knowledge base of the spatial and temporal coverage of the existing hydro-meteorological datasets, their quality and characteristics based on a systematic and critical approach is fundamental. Moreover, in areas where lack of meteorological data at finer temporal resolution constrains application of hydrological models, the use of relevant weather data disaggregation techniques could be an important strategy. In this study utmost efforts have been exerted to evaluate and analyze the existing hydro-meteorological datasets in the basin and construct quality-controlled continuous daily database following a systematic approach. Physically-based, conceptual and empirical models have been used for different purposes. The performances of a physically-based hydrological model have been evaluated on selected catchments by using hourly meteorological forcings disaggregated from daily data. Sustainable management of Lake Tana and its diverse socio-economic and ecological values requires basic information on its water and suspended sediment balances. Generation of this basic information has involved use of representative and quality-controlled datasets, a dynamic conceptual model to estimate runoff from ungauged parts and empirical models to quantify suspended sediment discharges.

Chapter 2

2 Description of the Study Area

This chapter describes the study area in terms of relevant aspects of the physical environment and water resources development. The geographic and regional location of the basin as well as major watershed characteristics that include topography, geology, soil and land cover are described. The climatology of Ethiopia and the study area, the major hydrological systems and the state of water resources development are also presented.

2.1 Location

Lake Tana basin is located in the northwestern plateau of Ethiopia. Geographically, it extends from 10.9^{o}N to 12.8^{o}N latitude and from 36.7^{o}E to 38.2^{o}E longitude. In terms of the universal transverse mecator (UTM) coordinate system it is located in zone N-37 extending between 253277E-416717E and 1211053N-1410403N.

The basin is located in an area where water resources issues are critical for sustainable development, locally and regionally. It constitutes the upper catchment of the Blue Nile River (locally called *Abay*) that has about 60% contribution to the main Nile River flow (Sutcliffe and Parks, 1999). The Nile River is shared by ten riparian countries with an estimated current and projected 2025 population of 420 and 600 million inhabitants, respectively[1]. Critical issues in the basin include food insecurity, water scarcity, flooding, drought, soil erosion, sedimentation, and lack of adequate and reliable hydro-meteorological data (Mohamed and Loulseged, 2008).

In Ethiopia, the basin is located in an area where water resources development for various purposes is identified to be a key element for achieving local and national development goals (MoFED, 2006). Figure 2-1 illustrates the location of the study area.

[1]http://esa.un.org/unpp/

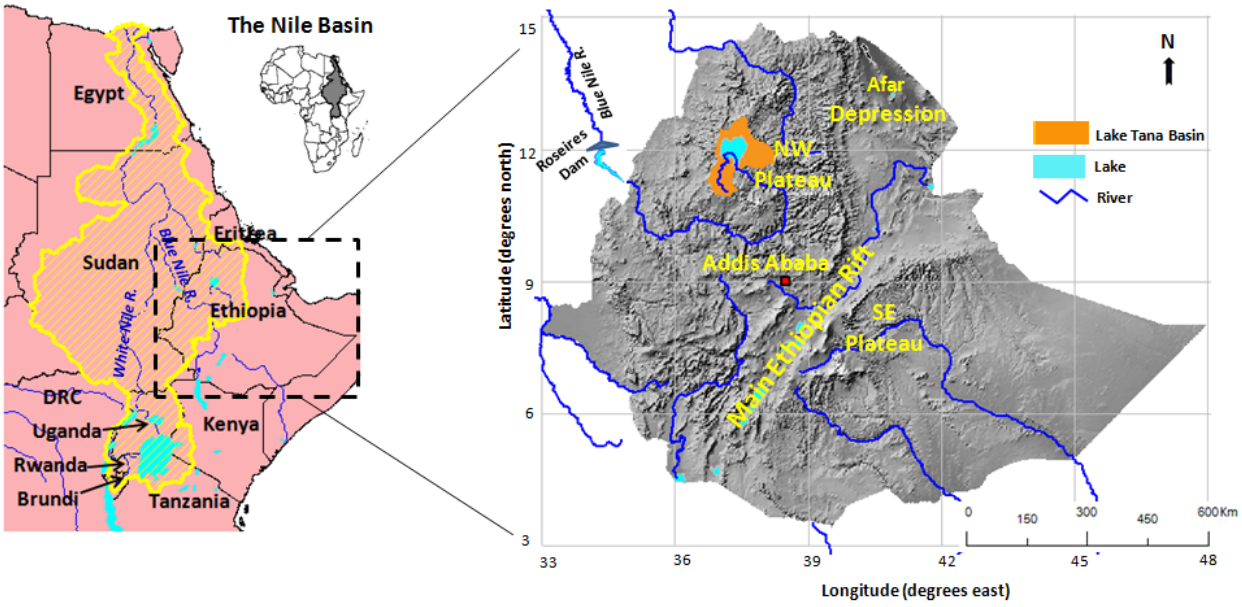

Figure 2-1 The study area

2.2 Topography

The total catchment area of Lake Tana Basin is in excess of 15 000 square kilometer[2] of which 20% is occupied by the lake's water surface. It constitutes several streams and catchments that all drain into Lake Tana. The basin is surrounded by lowlands to its west and mountainous areas otherwise (Figure 2-2a). The mean altitude of the basin is 2025 m.a.s.l. with about 90% having elevation in the range 1780-2500 m.a.s.l. Some areas close to the watershed divide have altitude of 2500-4100 m.a.s.l. Following the topographic classification indicated in REDECO and HSD (2002), the basin can be grouped into five relief types (Figure 2-2b)

- Flat areas with slopes between 0-2%
- Undulating terrain with slopes between 2-10%
- Rolling land with 10-15% slope
- Hilly areas having slopes of 15-30% and
- Steeply dissected and mountainous lands of slope > 30%

Most of the downstream part of the basin is either flat or gently undulating rendering a large tract of floodplain around Lake Tana. The middle part of the basin has mainly rolling or hilly relief. The upper part is dominantly hilly with limited mountainous and dissected land close to

[2] Various estimates of catchment areas that vary from 15030-15340 km^2 are reported in different studies. This variation could be attributed to the method used in delineating the basin. In this study the catchment area of Lake Tana Basin was found to be 15120 km^2 by delineating the basin using the Wang and Liu (2006) algorithm.

the watershed divide. Mount Guna, one of the highest mountains in Ethiopia, is located at extreme east of the basin.

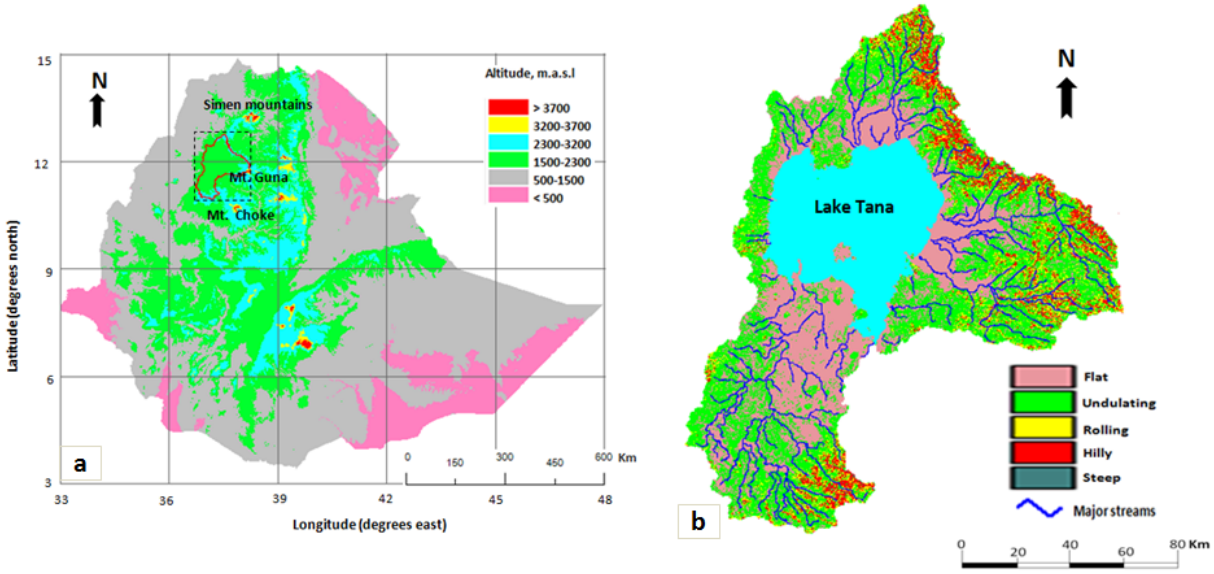

Figure 2-2 Topography of Lake Tana basin (a) Elevation relative to other regions in Ethiopia. Altitude ranges correspond to classes used for traditional climate classification (b) Relief types based on terrain slope.

2.3 Geology and soil

The geology of the study region is dominated by thick Cenozoic volcanic sequence (Pik *et al.,* 1998). The volcanic sequence is underlain by 1.5-2 km thick sedimentary series that could have been deposited from early Mesozoic to Tertiary (Hautot *et al.,* 2006). Precambrian metamorphic rocks constitute the basement complex.

Most of the southern part of the basin is covered by Quaternary Volcanics overlying older Tertiary flood basalts (Mohr, 1962). They consist of blocky and fractured vesicular basalt, some basaltic breccias and tuff. The Quaternary Volcanics become less blocky with deeply developed soils further to the south (SMEC, 2008b). The remaining part of the basin is covered mainly by Tarmaber Basalts that overlie Ashangi Basalts (WWDSE and TAHAL, 2007a,b). The Ashangi Basalts are characterized by deep weathering and comprise basaltic flows with scarce tuffs. The Tarmaber Basalt series is thick and consists of basaltic rocks interbedded with tuffs, scoraceous lava and paleosoils. Alluvial sediments composed of fine and coarse grained materials are found in the lower reaches of the main rivers and the floodplains. Lacustrine deposits are observed in the eastern and northwestern parts of the basin. Stiff and compacted sediment deposits with at least 50 m depth are also noted beneath Lake Tana floor (Lamb *et al.,* 2007). The geology of the basin is indicated in Figure 2-3a.

A prominent structure that plays an important role in controlling groundwater flow path is the Lake Tana graben (Kebede *et al.,* 2005). It is a tectonically deformed circular depression characterized by faulted blocks that dip towards the lake from all directions. Other structures noted in the basin include joints and lineaments (WWDSE and TAHAL, 2007a,b; WWDSE and TAHAL, 2008). Dikes and pipe feeders are also features that are commonly observed in the Tana region (Chorowitcz, 1998).

The soils of the study area are derived from weathered volcanic rocks. Based on the FAO soil classification system, ten types of soils are identified. The spatial distribution of the various soil types is indicated in Figure 2-3b. About 70 % of the basin is covered by four major soil groups: Luvisols, Leptosols, Vertisols and Fluvisols. The majority of the study area has deep to very deep soil depth (BCEOM, 1999c) with hillslopes having thin soil layer.

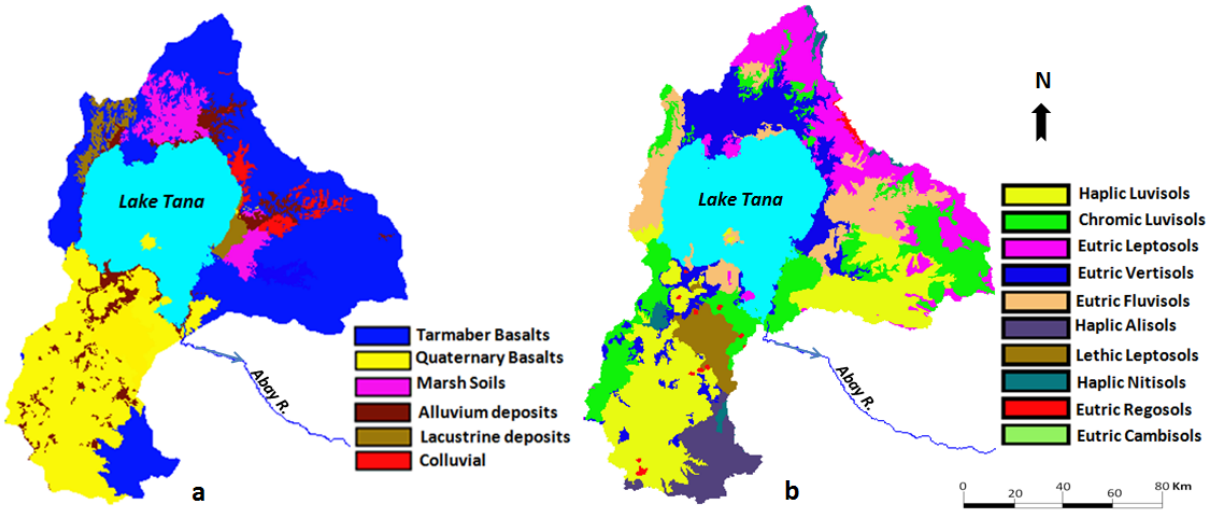

Figure 2-3 (a) Geology and (b) soil types of Lake Tana basin
[Source: Ministry of Water Resources, Ethiopia]

2.4 Land use and land cover

Significant part of the basin is designated for crop production using rain-fed agriculture making it vulnerable to drought and flooding. Dominantly cultivated crop types include barley, maize and *teff*. Because of the growing population pressure, cultivation is also practiced on marginal lands with a resulting increase in upstream soil erosion and sedimentation in downstream areas (SMEC, 2008c). The low-lying parts of the basin bordering Lake Tana are extensive floodplains where recession cultivation is practiced.

Valuable wetlands are also found all around Lake Tana but they have been drained for agricultural purposes (Kindie, 2001). Two major urban centers of the country, Bahir Dar and

Gonder, with more than 200 000 inhabitants each are also found in the basin. Other land cover types include grasslands, open shrublands and plantation, mainly eucalyptus. A major road network traverses the study area from south to north. Figure 2-4 shows the land cover/use types of the study area.

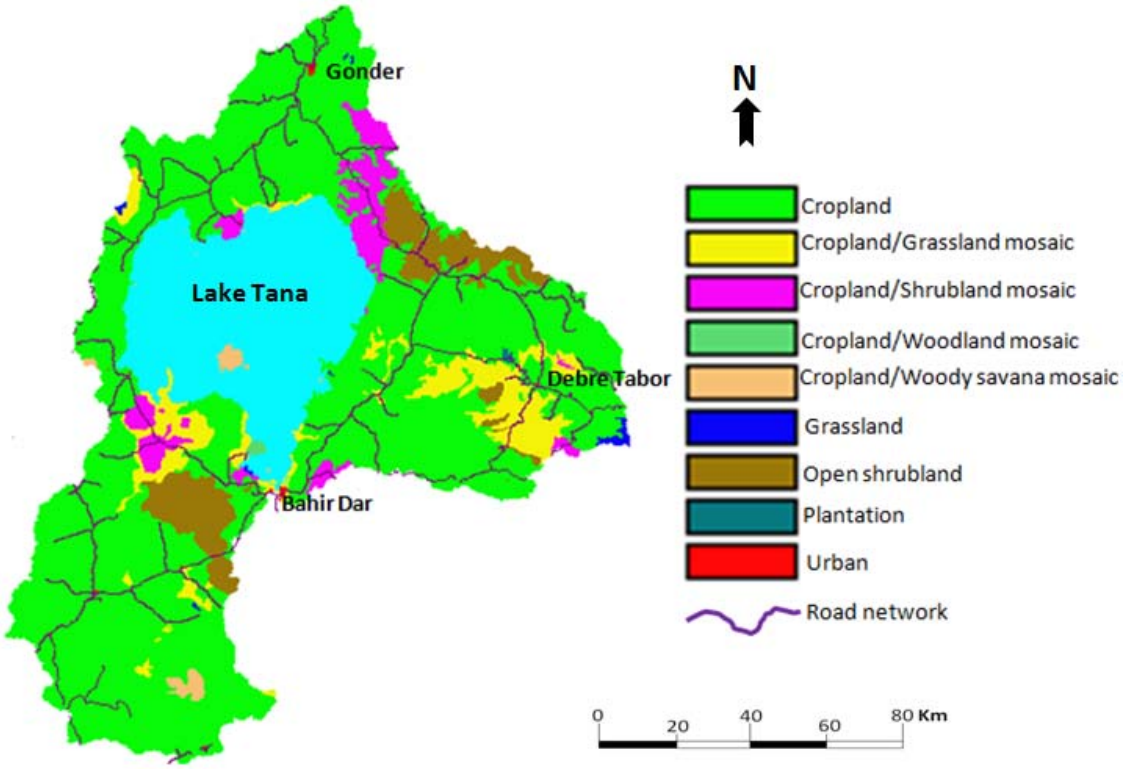

Figure 2-4 Land cover/use types in the Lake Tana Basin
[Source: Ministry of Water Resources, Ethiopia]

2.5 Climate

Ethiopia is located in East Africa where the common climatic feature is relatively low rainfall with complicated distribution pattern showing a general increase from north to south (McGregor and Nieuwolt, 1998). Rainfall in most of Africa and Ethiopia is highly seasonal as it is dominantly controlled by the migrating inter-tropical convergence zone (ITCZ) (Hulme, 1996). The monthly march of the ITCZ together with typical surface winds and mean sea level pressure over Africa are presented in Figure 2-5.

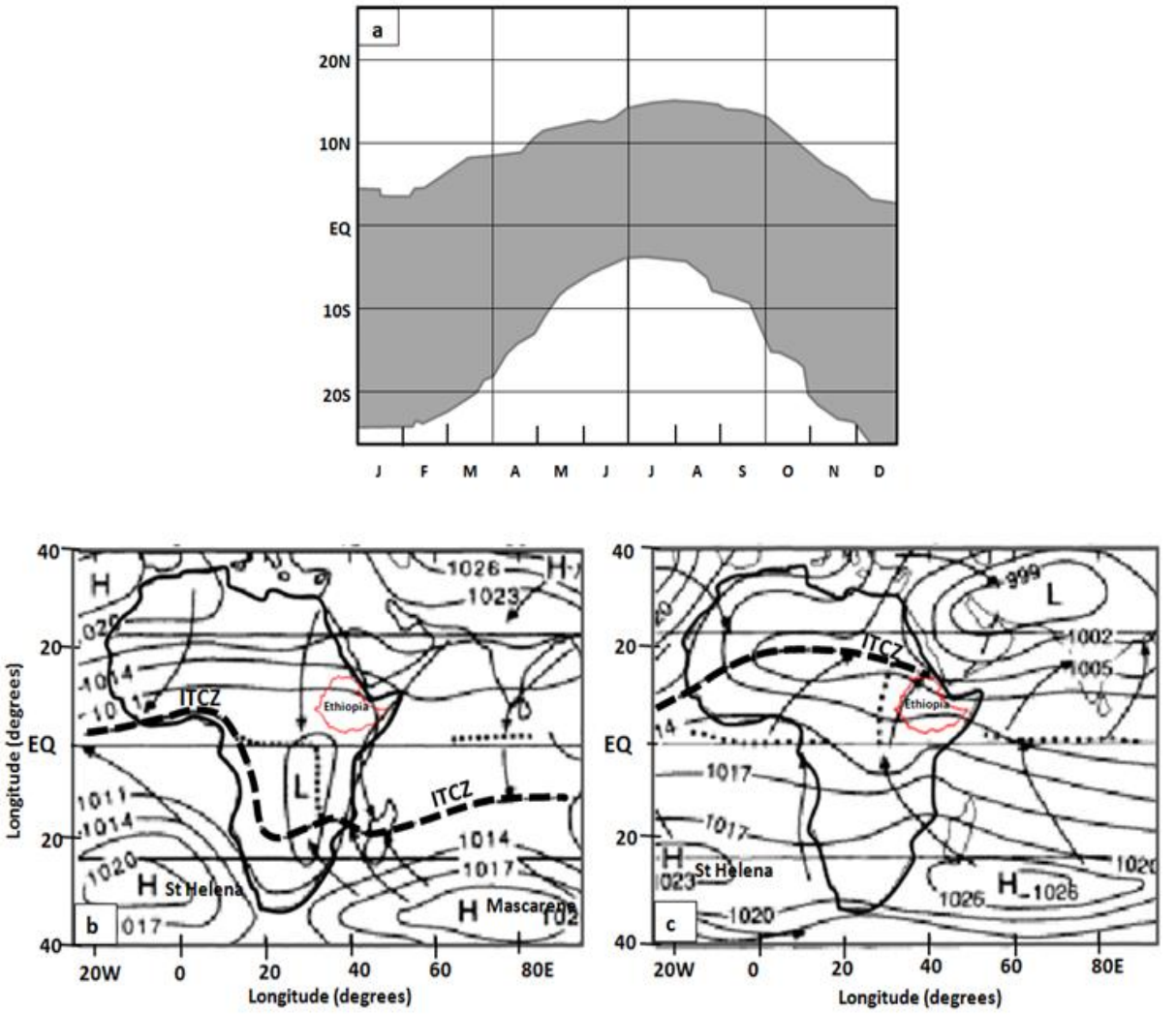

Figure 2-5 The ITCZ over Africa (a) shows the monthly movement in the African ITCZ region, i.e., 10°E-40E° longitude (b) and (c) shows the ITCZ position, mean sea level pressure and surface winds, respectively, for January and July.
[Source: McGregor and Nieuwolt, 1998].

Depending on the amount of rainfall, three seasons are recognized in Ethiopia and they are locally called *Kiremt* (June-September), *Bega* (October-January) and *Belg* (February-May). Different regional and global weather systems control the climate of each season (NMSA, 1996). Moreover, orographic and convective factors shape the spatial and temporal patterns of rainfall in Ethiopian highlands (Korecha and Barnston, 2006).

Kiremt is Ethiopia's principal monsoon rain season. It is characterized by different large-scale atmospheric circulation features that include northward migration of the ITCZ, development of quasi-permanent high pressure systems over South Atlantic Ocean (St Helena) and South Indian Ocean (Mascarene), development and persistence of the Arabian and Sudan cyclones along 20 °N latitude, and generation of Tropical Easterly Jet and Somali low-level Jet (NMSA, 1996). *Kiremt* season starts in March over southwestern regions, progresses

northward to cover the western half of the country by mid-June and reaches northeastern regions in mid-to-late July (Segele *et al.,* 2005). In early September the *Kiremt* rains begin retreating southwestward in the extreme northeast, and progresses gradually and uniformly across the entire *Kiremt* region, and reaches far southwest in November. A large part of the country is covered by the *Kiremt* rainfall, except some areas in the south and southeastern parts (Seleshi and Zanke, 2004).

The *Belg* season is the short rainy season caused mainly by the development of thermal low center over south Sudan and high pressure over the Arabian Sea. Winds from the Gulf of Aden and the Indian Ocean highs are drawn towards this centre and blow across central and southern Ethiopia. These moist, easterly and southeasterly winds produce the main rains in southern and southeastern Ethiopia and the *Belg* rains to the east-central part of the northwestern highlands (Seleshi and Zanke, 2004).

The *Bega* season is the dry, windy and sunny season of Ethiopia due to the influence of the dry northeast monsoons that originate in the Saharan and/or Siberian anticyclones. However, a low pressure air that moves from western to eastern Europe, very occasionally, passes over Ethiopia and interacts with warm and humid air from the tropics creating unseasonal rainfall in Ethiopia during this season (Kassahun, 1999). Moreover, occasional development of the Red-Sea Convergence Zone (RSCZ) affects coastal areas. In *Bega*, most of the country is generally dry except some areas in southern and southeastern parts of the country that receive their second important seasonal rainfall associated with the southward retreat of the ITCZ (NMSA, 1996).

Lake Tana Basin is located in a region where the annual rainfall is more than 900 mm with unimodal pattern, and mean temperature is mainly in the range of 16-20 °C (Figure 2-6 and Figure 2-7). Based on the Köppen climate classification system, the basin has a warm temperate climate with dry summer (Cw). According to the traditional climate classification of Ethiopia, most of the study area falls in Woina-Dega zone (1500-2300 m altitude with mean annual temperature of 16-20°C).

The rainfall climate is highly seasonal with more than 70% of the rainfall occurring in the *Kiremt* season. Based on rainfall data of stations located within and around the basin, the mean annual rainfall of Lake Tana basin was estimated to be 1345 mm. Rainfall is convective with most of it occurring in the afternoon and evening hours. The mean annual temperature is 19 °C with a corresponding coefficient of variation of 0.08. Temperature decreases with altitude at an average lapse rate of 5 °C in 1000 m.

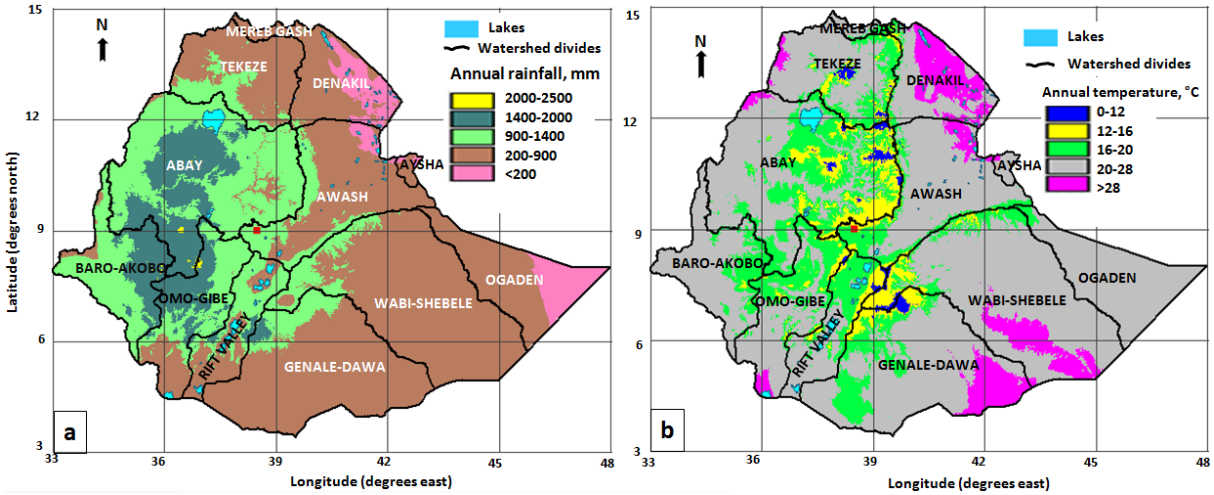

Figure 2-6 Mean annual climatic variables over Ethiopia (a) rainfall (b) temperature.
Based on world climate data, 3o arc-seconds resolution. [http://www.worldclim.org/current]

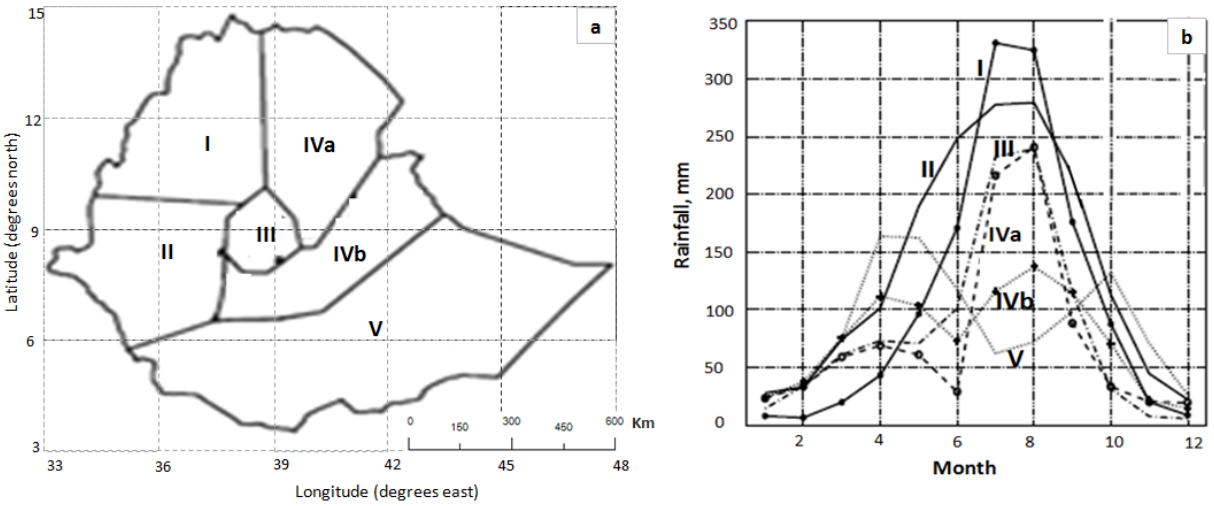

Figure 2-7 Rainfall regimes of Ethiopia (a) homogenous zones (b) monthly distribution
[Source: Diro *et al.,* 2009]

2.6 Hydrology and hydrogeology

Lake Tana basin comprises different catchments that all discharge into the lake (Figure 2-8). About forty percent of the basin, mainly located in the western and lower parts of the various catchments, is yet ungauged. The meteorological network coverage of the southwestern part is also inadequate. More than ninety per cent of the runoff is contributed by four catchments: Megech, Rib, Gumara and Gilgel Abay (Kebede *et al.,* 2006). Analysis of the streamflow data from the gauged catchments indicated that runoff is highly seasonal with more than 75 percent of the annual volume concentrated in the *Kiremt* season. Flooding of low-lying areas

due to overflow of the major rivers and the rising lake level is a frequent problem in the wet season (SMEC, 2008a). Lake Tana discharges into the *Abay* River with a long-term mean annual runoff volume of 3.7 km^3, which is about 8% of the Blue Nile flow at Roseires Dam in Sudan (Conway, 2000).

Lake Tana represents a major hydrological system in the basin. Its formation is believed to be associated with volcanic activity that created a barrier to the south during the Pleiocene (Mohr, 1962). It is the largest lake in Ethiopia with a surface area of 3012 km^2 and volume of 28 km^3 at its longterm mean elevation of 1786 m.a.s.l. It is a shallow meso-oligotrophic lake that is well mixed with no thermal stratification (Dejen, *et al*. 2004). It has an average and maximum depth of 9 m and 14 m, respectively (Ayenew, 2009). Water balance study of the lake indicated a water residence time of 3 years. The lake level has been monitored at three stations for years. Based on the longterm lake level data at Bahir Dar station, the average annual lake level fluctuation was found to be 1.7 m. Lake Tana, together with its surrounding wetlands, provides various services of ecological, social, economic and hydraulic significance for the local and regional inhabitants. The lake is a habitat for diverse fish species, birds and large aquatic animals, some of which are near extinction (Wudneh, 1998; BCEOM, 1999a). The lake is dotted with several islands most of which shelter fascinating monasteries and churches. Lake Tana is one of the major sources of income in the region through fishing and tourism-related activities.

Relevant information on the characteristics of the aquifers and groundwater flow systems of the basin could be extracted from limited hydrogeological studies (SMEC, 2008b; Ayenew *et al.,* 2008; Kebede *et al.*, 2005). In view of the geology of the region, three aquifer types are identified- Tertiary basalt, Quaternary basalt, and Quaternary alluvial aquifers. The Tertiary and Quaternary basalt aquifers are fractured rock systems in which groundwater flow rate is largely determined by the intensity of fracturing in the rock mass. The transmissivity of the basaltic aquifers is variable and their productivity is rated as low to moderate. The Tertiary basalt aquifers generally have poor transmissivity. Most wells drilled in Tarmaber basalt series show transmissivity in the range of <1-11 m^2/d. The Quaternary basalt aquifers have a relatively better transmissivity with reported values in the range of <10-590 m^2/d. The transmissivity of Quaternary alluvial sediments is the highest with reported values greater than 700 m^2/d. In the study area shallow groundwater flow systems controlled by local topography are important. This is evident from the abundance of springs and a geochemical and isotope study by Kebede *et al.* (2005). The existence of Lake Tana graben also favours regional and probably deeper groundwater flows. Based on recorded piezometric levels, the

groundwater flow direction is found to be consistent with the surface water drainage (SMEC, 2008b). In the downstream reaches of the major river systems, where the floodplains are located, the hydraulic gradient is too low and the watertable is close to the ground surface.

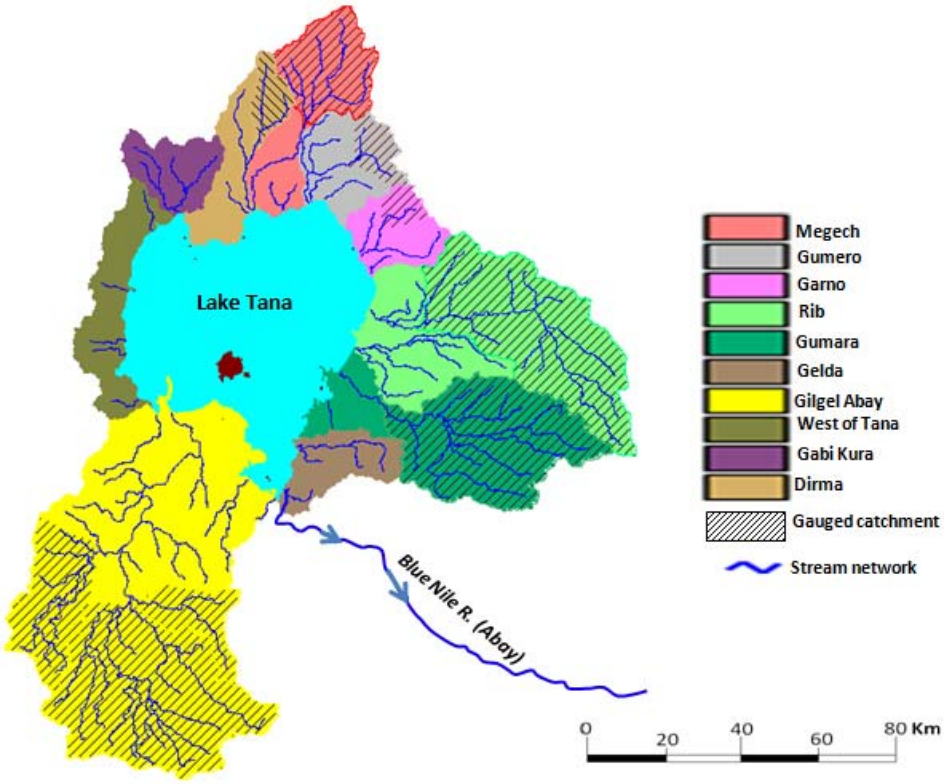

Figure 2-8 Major hydrological systems of Lake Tana Basin

2.7 Water resources development

Ethiopia has 12 river basins with estimated surface and groundwater resources potential of 122 BMC and 2.6 BMC, respectively (MoWR, 2002). The level of water resources development in the country in general, and Lake Tana basin in particular, is low in comparison to the potential. Based on different sources Awulachew *et al.* (2007) indicated the potential to develop 155 TWh/year of hydropower and 3.8 millions hectares of irrigated land. Until recently, only about 8% of the irrigation and 2% of the hydropower potentials were developed and the clean water supply coverage was as low as 34% (MoWR *et al.*, 2004). There have been major water resource development efforts going on in the last five years and there will be some improvements to the figures presented earlier.

One major existing hydraulic structure in the Lake Tana basin is the low-height Chara Chara weir which regulates the outflow of the lake for downstream electricity generation at Tis-Abay hydropower stations. The Abay Basin Master Plan study has identified medium scale

irrigation schemes that have a total capacity to develop 85 375 hectares of land in the Lake Tana basin (BCEOM, 1999a). Notable progresses have been achieved so far towards implementation of these projects. Another recently completed major scheme is the Tana-Beles project that combines generation of 460 MW of hydropower and irrigation development. The project relies on water transfer from Lake Tana through a 12 km tunnel. Various studies indicated the potential impacts of the development projects on the downstream environmental and hydrological systems (SMEC, 2008c; Alemayehu *et al.,* 2009; McCartney *et al.,* 2009).

Chapter 3

3 Data availability and analysis

This study involved the use of a distributed hydrological model that requires extensive hydro-meteorological and spatial data at finer temporal and spatial resolutions. They include:

- Meteorological data: precipitation, temperature, relative humidity, wind speed, short wave solar radiation and long wave solar radiation
- Hydrological data: streamflow, stream network and channel properties
- Sediment data: sediment concentration, particle size distribution
- Spatial data: soil types and their hydraulic properties, vegetation types and properties, and digital elevation model

The chapter presents the availability and characteristics of the major datasets that could be obtained from different sources.

3.1 Meteorological data availability

The major source of meteorological data is the National Meteorological Agency of Ethiopia (NMA) which recognizes four station classes based on the type of observations made (NMA, 2009).

Class 1: These are principal stations where meteorological observations are made for climatological purposes every three hours from 03:00 to 15:00 GMT hours. There are more than 150 principal stations in Ethiopia. Observed climatological variables include rainfall, maximum and minimum temperatures, sunshine hour, relative humidity, wind speed at 2m and 10m heights, pitch evaporation and soil temperature.

Class 2: These are synoptic stations at which meteorological observations are made for synoptic meteorology purpose every hour for 24 hours a day at full GMT hours. There are 22 Synoptic stations in Ethiopia.

Class 3: These are ordinary stations at which only minimum and maximum air temperatures of the day and total rainfall amount in 24 hours are observed. Minimum temperature observation is taken at 06:00 and maximum temperature is observed at 15:00 hours.

Class 4: These are stations at which only total daily rainfall is observed.

The distribution of the meteorological stations in the study area is indicated in Figure 3-1. Detailed information on the stations is presented in Annex B-1.

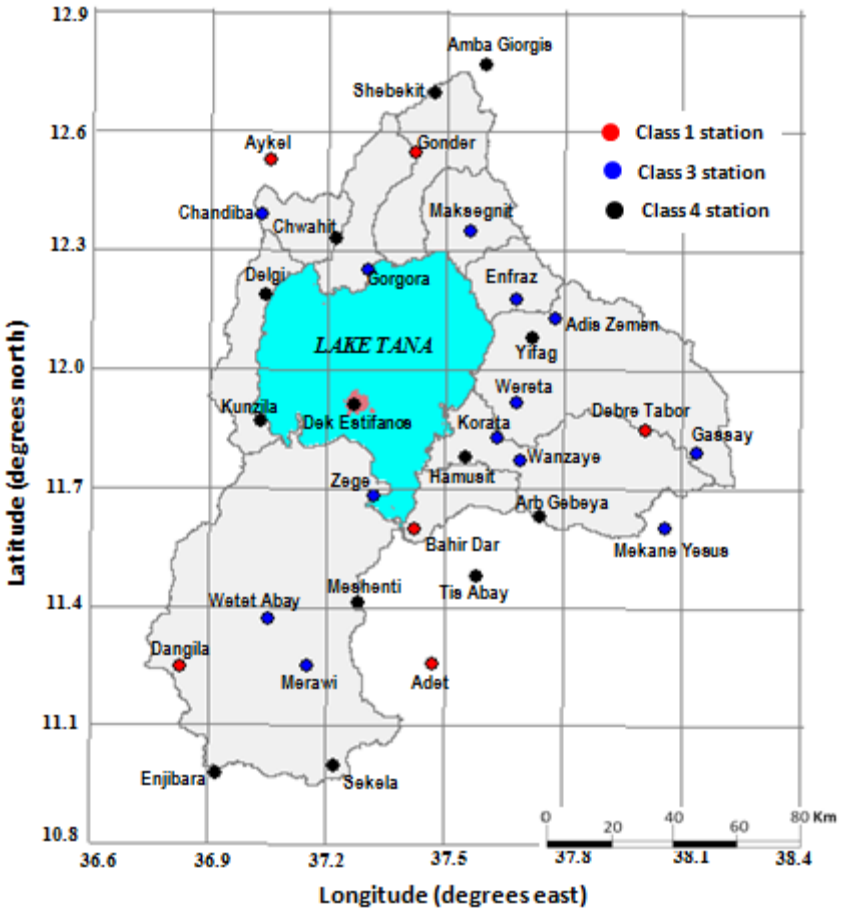

Figure 3-1 Meteorological stations in the Lake Tana basin

Data availability and coverage of the different meteorological elements was assessed based on daily records of stations for which data could be obtained. The results of the assessment are presented in the following sections.

3.1.1 Rainfall

Measurement of daily rainfall in the study area started in 1952 at Gonder station and presently there are more than thirty observation stations fitted with non-recording gauges. Few stations like Bahir Dar and Gonder are also equipped with floating-type recording gauges for rainfall measurements at shorter time scales. Metadata with information about data acquisition and the history of each station could not be found. Stations metadata are very useful in data quality assessment and adjustment.

The rainfall data availability was assessed based on daily records obtained from twenty six stations. Considerations that take into account the rainfall climate of the study region were made in deciding whether data is available or not. Rainfall is highly seasonal with more than 70 % of the annual rainfall occurring in the *kiremt* season, 20% in the *belg* season and 2 % in the *bega* season. Accordingly, rainfall data in a year was considered unavailable if the percentage of missing daily rainfall data was greater than 30 % in *kiremt* or 80% in *belg* or 90% in *bega* season. Application of these criteria to the observations resulted in the rainfall data availability chart presented in Figure 3-2. Data availability in most stations prior to 1982 is by and large poor and fragmented. A major data gap is obvious in 1991 for reasons related to security problems during that period. Overall, the temporal data coverage starting from 1992 appeared to be good.

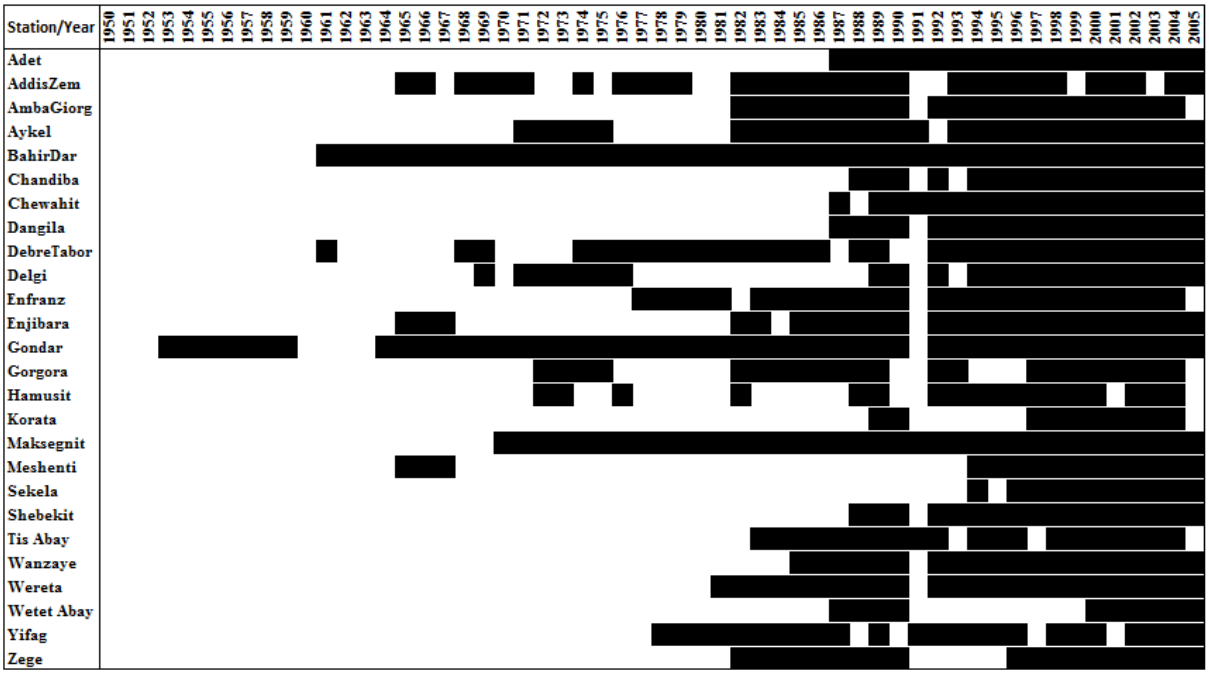

Figure 3-2 Rainfall data availability in the Lake Tana Basin

The spatial coverage of the rainfall data in the basin was evaluated in light of recommended minimum precipitation network density by the World Meteorological Organization (WMO) indicated in Table 3-1. Adequacy of network coverage was analyzed by drawing circles with centers corresponding to each station and radius that give the recommended minimum area in the GIS environment. This has resulted in the spatial coverage of the rainfall stations shown in Figure 3-3. The rain gauges covered 66% of the basin area. Notable areas in Gilgel Abay,

Rib and Gumara catchments as well as the lake surface appeared to be poorly covered by the stations.

Table 3-1 Recommended minimum precipitation network density (WMO, 1994)

Physiographic unit	*Minimum density per station (area in km^2 per station)*	
	Non-recording	*Recording*
Mountainous	250	2500
Interior plains	575	5750
Hilly/undulating	575	5750

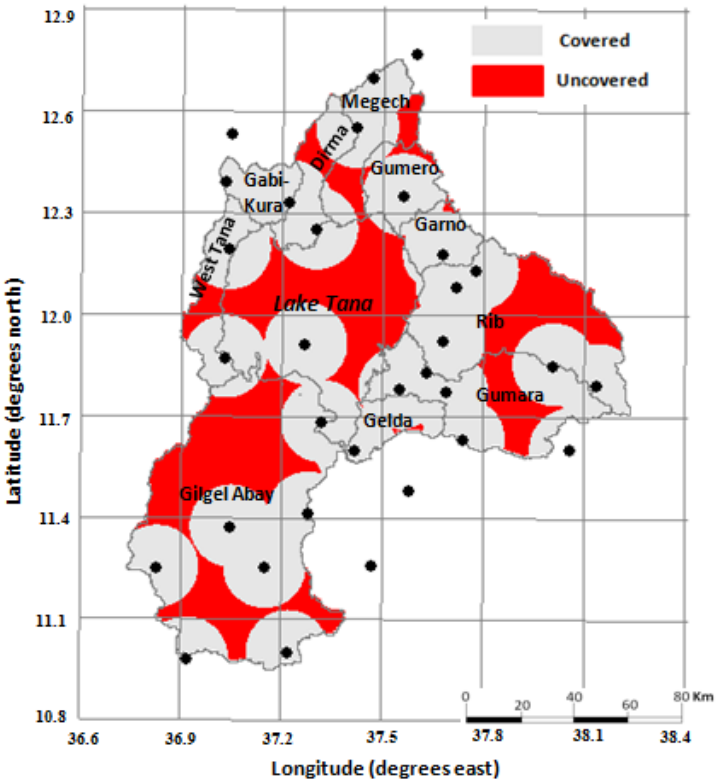

Figure 3-3 Spatial coverage of rainfall gauges in the Lake Tana basin according to WMO standard

3.1.1 Temperature

Availability of minimum and maximum temperature data was assessed based on daily observations taken at 12 stations starting from 1982. In the construction of the data availability chart (Figure 3-4), the low temporal variability of temperature in the tropics (McGregor and Nieuwolt, 1998) was taken into account for setting the criteria. Accordingly, temperature data was considered unavailable if more than 3 months in a year have missing

data. The temperature data availability is relatively poor and fragmented in the period 1988-1996 with a significant breakdown in 1991.

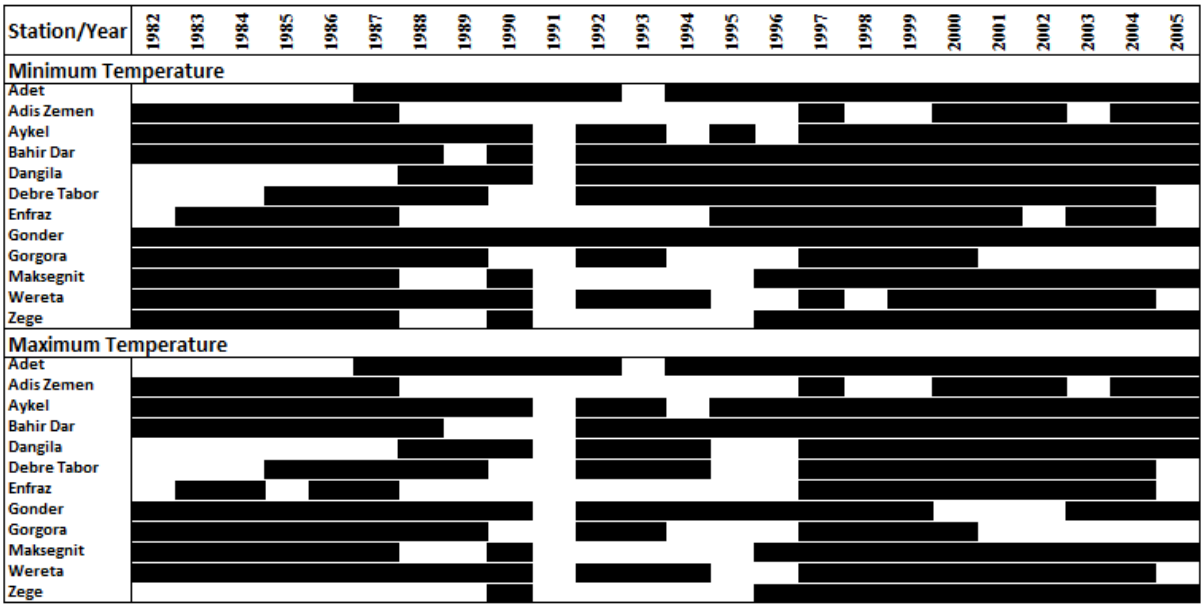

Figure 3-4: Temperature data availability for Lake Tana Basin, Ethiopia

Spatial variation of temperature is mainly related to change in altitude in which temperature decreases linearly with increase in altitude. This rate of decrease in temperature is called lapse rate and it can be estimated from observed records. In light of this note and the spatial distribution of Class 1 and 3 stations, the areal coverage of minimum and maximum temperature measurements could be considered as adequate.

3.1.2 Wind speed, relative humidity and sunshine hour

Wind speed, relative humidity and sunshine hour data at five Class 1 stations could be obtained. Wind speed is measured using standard anemometer at 2 m height. Measurements of relative humidity are taken three times a day at 06:00, 12:00 and 18:00 hours. The data availability charts of these meteorological variables were constructed following the same procedure used for temperature (see Figure 3-5). Wind speed data is available starting from 1992. Most of the stations have a good temporal coverage of relative humidity data since 1985. The sunshine hour data for most of the stations is fragmented and the coverage is poor.

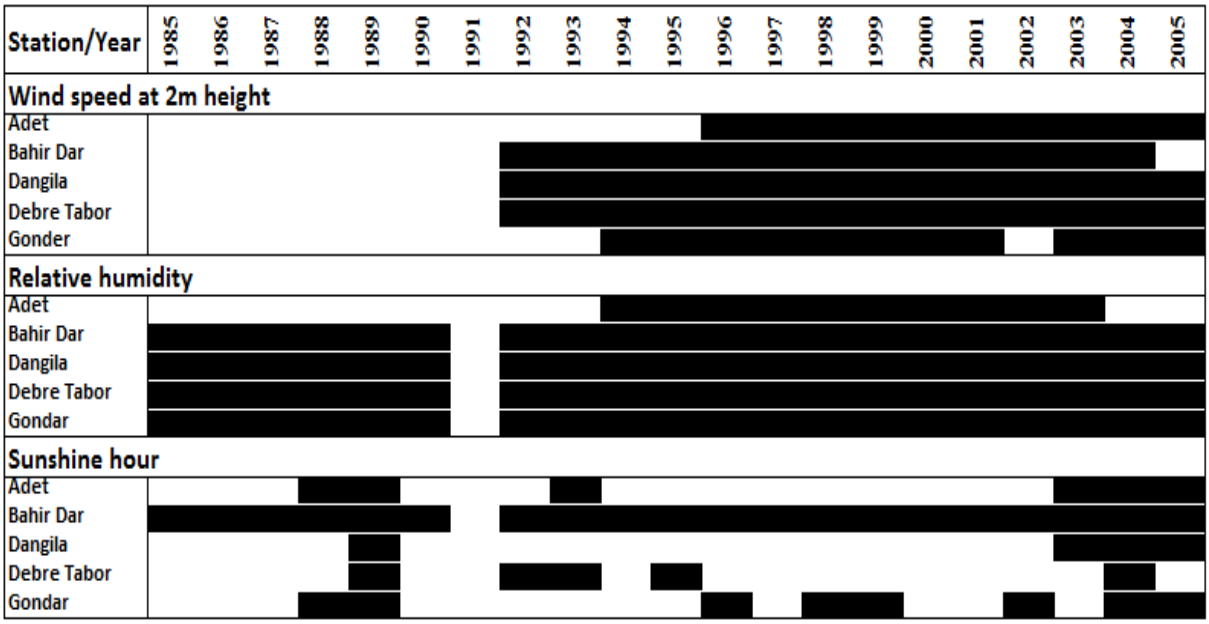

Figure 3-5 Availability of wind speed, relative humidity and sunshine hour data in the Lake Tana basin

3.2 Hydrological data availability

3.2.1 Streamflow and lake level

Data on daily streamflow and lake level were obtained from the Ministry of Water Resources of Ethiopia. Data availability at the major streamflow gauging stations and one of the three limnimetric stations was evaluated (Figure 3-6). Streamflow measurements are done twice a day using manual staff gauges. Some stations appeared to have automatic stage recorders but their use ceased two decades ago (SMEC, 2008a). Although hydrological measurements in the basin started around 1959 in connection with the first Abay Master Plan Study (USBR, 1964), this assessment was based on daily data for the period 1975-2005. As streamflow is highly seasonal, the decision on data availability was made following the approach used for rainfall data. The temporal coverage of the hydrological observations is shown in Figure 3-7. Overall, the streamflow data coverage appeared to be adequate with few missing years at limited hydrometric stations.

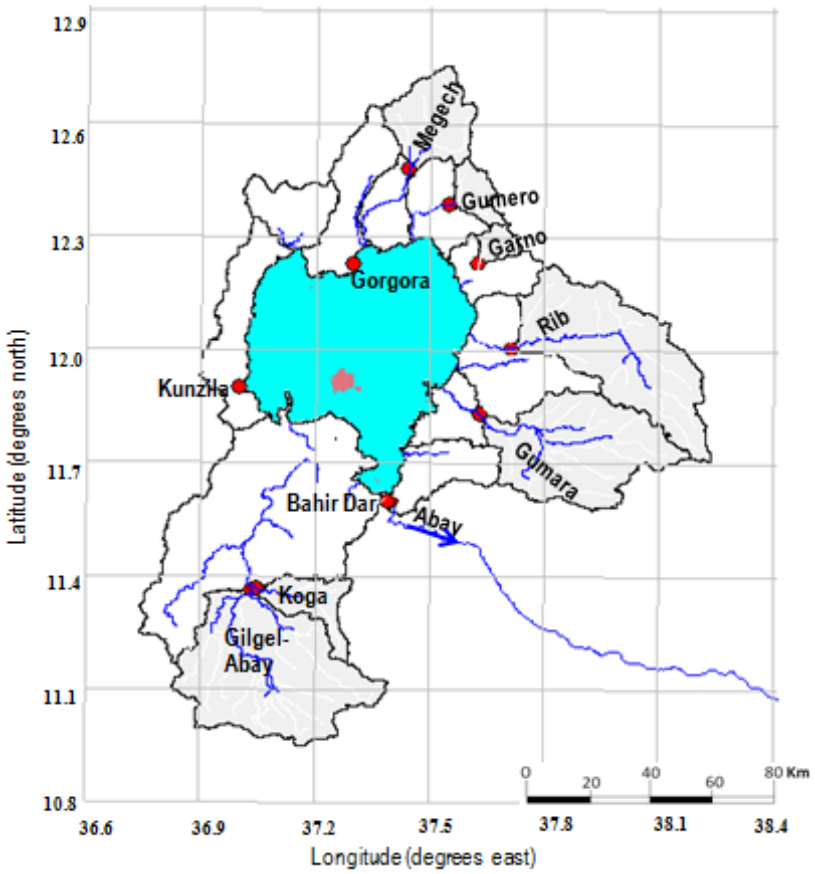

Figure 3-6 Major streamflow and lake level gauging stations in the Lake Tana basin

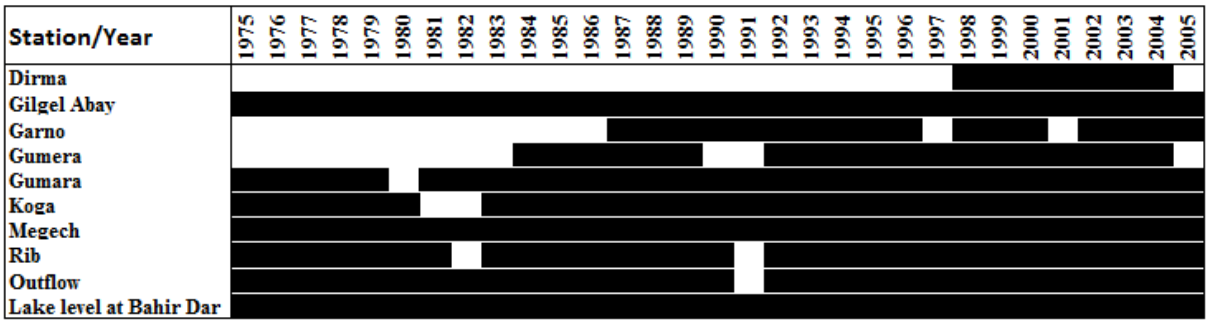

Figure 3-7: Streamflow and lake level data availability in the Lake Tana Basin (1975-2005)

The spatial location and distribution of the streamflow gauging stations were assessed in light of recommended practices. WMO (1994) listed several factors that need to be considered in locating hydrometric stations so that accurate stage-discharge relationship could be established. Some of the important considerations include geometric (e.g. channel should be straight for about 100m upstream and downstream of the gauge), hydraulic (e.g. maintenance of stable stage-discharge relationship), and accessibility at all times and stages of flow. The hydrometric stations of the study area appeared to be located by considering mainly accessibility as most of them are located along or near the main roads. Previous studies

reported problems associated with some of the existing gauging stations that include siltation, bank overflow, variable backwater effect of Lake Tana, and unstable channel bank (BCEOM 1999b, SMEC 2008a). The spatial coverage of the gauging stations could be considered acceptable with reference to the minimum recommendation of WMO (Table 3-2). A large area downstream of the gauging stations and in the western part of the basin, however, remains ungauged.

Table 3-2 WMO minimum recommendation for hydrometric network density (WMO, 1994)

Physiographic unit	*Minimum density per station (area in km^2 per station)*
Mountainous	1000
Interior plains	1875
Hilly/undulating	1875

3.2.2 Suspended sediment

Historical data on suspended sediment concentrations/loads could be obtained for four gauging stations- Gilgel Abay, Gumara, Koga and Megech. Data from Rib and Abay stations could not be obtained. Data availability is limited to very few days in a year and it is highly fragmented as indicated in Figure 3-8. Most of the data corresponds to the main rainy season where erosion rate is high. There is no clear information on the methods of sampling used in the early years (BCEOM, 1999b). A discussion with technicians working at the hydrological unit of the MoWR at Bahir Dar revealed the use of depth integrated suspended sediment samplers in recent years. In addition to the historical data, limited suspended sediment samples were collected at three gauging stations (Gilgel Abay, Koga and Abay close to the lake outlet) as part of the field campaign of this study. Suspended sediment concentration was determined by filtration method and a laser technique using MS-2000 was used to determine the grain size distribution.

Station:Year	Number of days with suspended sediment data in a year																																					
	1968	1969	1970	1971	1972	1973	1974	1975	1976	1977	1978	1979	1980	1981	1982	1983	1984	1985	1986	1987	1988	1989	1990	1991	1992	1993	1994	1995	1996	1997	1998	1999	2000	2001	2002	2003	2004	2005	2006
Gilgel Abay	4															1		1	2	2	3		1			1		1	1								3	1	
Gumara	6												2			1		1	2	2	4	1	2		2	1	1	2	6								2	3	3
Koga	5												2			1		1	3	2	5	1	2		3	2	1	1	3										
Megech	11															1	1	2	2	1	4	1	2			1	1	1	3									4	

Figure 3-8 Availability of suspended sediment concentration/load data in the Lake Tana basin. Based on river stations for which data could be obtained

3.2.3 Lake Tana bathymetry

Bathymetric data of lakes and reservoirs can be used for various purposes that include establishment of relationships between water level-area-volume of a lake or reservoir, estimation of sedimentation rates, prediction of design life of reservoirs, etc. It could be learned that bathymetric surveys of Lake Tana were conducted at three different times in 1940, 1987 and 2006 (Ayana, 2007). Data could be found only for the recent year from the researcher who conducted the bathymetric survey using a GIS-coupled dual frequency echo sounder along traverse routes spaced 5 km apart in north-south direction (Ayana, 2007).

3.3 Spatial data availability

3.3.1 Soil types and properties

Soil types of the study area based on the revised FAO/UNESCO soil map legend (FAO, 1988) could be acquired from MoWR. Soil types are defined by the major soil groups and lower soil units. Data on hydrologic properties of soils was mainly obtained from the Abay Master Plan study (BCEOM, 1999c) and other catchment-specific project studies. Soil physical properties for which data could be found include saturated hydraulic conductibility, field capacity, permanent wilting point, infiltration capacity, bulk density, and soil texture. These properties were determined from soil samples collected at different points in the basin (For instance, see Table 3-3).

Table 3-3 Some examples of soil surveys within Lake Tana basin

Catchment	*Area, km²*	*Number of sample pits*	*No. of sites where infiltration & hydraulic conductivity tests are made*
Gilgel Abay	285	91	14
Koga†	289	46	8
Megech	133	33	7
Northeast Tana	85	28	11
Rib	346	94	24

†**Source: Acres & Shawel, 1995 and for others: BCEOM, 1999c**

3.3.2 Vegetation

Vegetation map of the study area was obtained from MoWR. It contains information on percentage coverage of different land cover types in various parts of the study area. This data

was used as a base for preparing land cover maps based on standard classifications like the IGBP-DISCover legend. Global MODIS black and white sky albedo values at quarter degree spatial resolution and 16 days temporal resolution could be downloaded for the full 2002 year from the ISLSCP II website[3]. The actual blue sky albedo of each month could be determined by linearly combining the black sky and white sky albedos. Albedo data is required to determine net solar radiation which is one of the drivers of evapotranspiration.

3.3.3 Digital elevation model

Downloadable digital elevation data at a spatial resolution of 90 m could be obtained from the Shuttle Radar Topography Mission (SRTM)[4]. SRTM is an international project that obtained a near-global scale elevation data during an 11-day mission in February 2000. The data so acquired enabled to generate the most complete high-resolution digital topographic database of the Earth. The overall quality of SRTM datasets is considered to be sufficient for hydrological modeling applications (Ludwing and Schneider, 2006).

Digital elevation data was used to extract the altitude of the meteorological stations, and to derive basic watershed morphometric properties that include catchment boundaries, slope, stream networks, etc. Moreover, DEM is one of the basic inputs required by the distributed hydrological model used in the study.

3.4 Data analysis

In this section, analysis of the hydro-meteorological and spatial data of the study area is presented. The analysis period for the hydro-meteorological data was set to be 1992-2005 as the spatial and temporal coverage of the rainfall data is relatively better. As availability of suspended sediment data is very limited, all data that could be accessed was used in the analysis.

3.4.1 Analysis of meteorological data

Rainfall is a key meteorological variable that most affects the hydrological regime of the study area. The analysis involved data quality assessment, filling of data gaps, and

[3] http://islscp2.sesda.com/ISLSCP2_1/html_pages/groups/veg/modis_albedo_2002_xdeg.html

[4] http ://srtm.csi.cgiar.org

characterization of the meteorological elements. The methodologies employed for each of the meteorological variables are discussed in the respective sections.

3.4.1.1 Rainfall

Daily rainfall data of twenty five stations for which data could be obtained and have less than 25 % missing data in the analysis period were used. Data of Korata and Wetet Abay meteorological stations were not directly used in the spatial and temporal rainfall characterization as they have long missing records. Their data, however, was used to fill missing observations of nearby stations.

3.4.1.1.1 Filling of missing data

All of the stations have missing data in their daily rainfall series, with lower gaps observed in Class 1 stations. Creation of continuous time series for each station by filling the gaps, therefore, preceded the analysis. Data gaps of a target station may be filled by using available records of the station itself or observed values of nearby stations. Examples from the first approach include use of mean of the data series and linear interpolation. The use of these methods is not recommended in areas where the temporal variability of rainfall is high (Ramos-Calzado, 2008). Patching of rainfall data using observations at neighboring stations has got wider applications (Xia *et al*., 1999; Eischeid *et al*., 2000; Teegavarapu and Chandramouli, 2005). Specific methods in this category include nearest neighbor, inverse distance, normal ratio, kriging, and regression. In this study an approach similar to the inverse distance method was used in which the weighing factor was calculated by considering both distance and correlation between daily rainfall of the target and surrounding stations (Equation 3-1). This kind of weighting factor calculation is recommended for orographically complex regions and the approach has been used to develop long years of continuous rainfall database (Romero *et al*., 1998; Federico *et al*., 2009). All neighboring stations that are within 0.5 degree distance and have at least 1000 raindays in common with the target station were used in the interpolation. A rainday is defined as a day with at least 1 mm of rainfall, following Seleshi and Zanke (2004).

$$p_i^{*n} = \frac{\sum_{j=1}^{J} \alpha_{ij} q_{ij}^{n}}{\sum_{j=1}^{J} \alpha_{ij}} \qquad \textbf{Equation 3-1}$$

Where,

p_i^{*n} = estimated missing rainfall for target station i at day n from J neighboring stations
α_{ij} = weighting factor between target station i and neighboring station j
q_{ij}^{n} = estimated precipitation at the target station i from station j for day n
The weighting factor was calculated using Equation 3-2:

$$\alpha_{ij} = \frac{r_{ij}^2}{d_{ij}^2} \qquad \textbf{Equation 3-2}$$

Where,

r_{ij} = correlation between rainfall amounts at target station i and neighboring station j

d_{ij} = horizontal distance between stations i and j

The contribution of a nearby station j to precipitation at the target station i for day n (q_{ij}^{n}) was computed using Equation 3-3. Interpolating normal ratio precipitations rather than absolute values has the advantage of eliminating the influence of orographically enhanced precipitation (Federico *et al.,* 2009).

$$q_{ij}^{n} = p_j^{n} \frac{\sum_{k=1}^{K} p_i^{k}}{\sum_{k=1}^{K} p_j^{k}} \qquad \textbf{Equation 3-3}$$

Where, p_j^{n} is the observed precipitation at a nearby station j for day n; the other term represents the ratio between total precipitations at the target and nearby stations for a common period of K days which is set to be greater than or equal to 1000.
The gap filling resulted in a continuous daily rainfall series for twenty five stations for the period 1992-2005.

3.4.1.1.2 Data quality and consistency

The continuous daily rainfall series of each station was subjected to quality control to detect outliers caused by instrumental and/or human errors. Methods for outlier identification include use of a fixed threshold derived from statistical properties of the series (Gonzàlez-Rouco *et al.,* 2001), or statistical tests like Grubbs test (Grubb, 1969). In this study the Grubbs test was used to detect the presence of outliers. Grubbs test is used for normally or log-normally distributed data and has got some applications in hydro-meteorological areas (Chow *et al*., 1988; Tang *et al.,* 1996). The daily rainfall data of the stations was found to be log-

normally distributed. Results of the test indicated absence of outliers in the data series of all stations.

Spatially homogeneous historical records are required for various hydrological applications. However, several non-climatic factors could affect the spatial consistency of records at a given station. They may include damage and replacement of a rain gauge, change in the gauge location, growth of high vegetation or construction of a building around the station, change in measurement procedure, or human and instrumental errors in taking readings. Commonly used data consistency checking methods include the graphical double mass analysis and the statistical SNHT methods (Peterson *et al.,* 1998). In this study the double mass analysis was used to check the spatial consistency of the rainfall data as it has got wider applications in hydrological areas and is considered to be reliable (Dingman, 1994; ASCE, 1996). The method assumes that stations have regional consistency over long time period. Inconsistency is detected by plotting accumulated annual rainfall of reference stations against accumulated annual rainfall of the evaluation station and inspecting for abrupt changes in slope. Slope changes are considered to be significant if they persist for at least five years (Dingman, 1994). In using the method, observations of Class 1 stations were taken as reference stations.

The double mass curve plots are presented in Annex B-2. Visual inspection of the double mass curves indicated no significant inconsistency in most of the stations. Inspection of the double mass curves of three meteorological stations, i.e. Dek Estifanos (1992-1996), Hamusit (1992-1998) and Maksegnit (1995-2001) suggested inconsistencies that are not related to the regional climate. Corrections to the observed values of these stations were made following the adjustment procedure of the method (Dingman, 1994).

3.4.1.1.3 Annual rainfall characteristics

Annual rainfall computed from a minimum of 30 years of data is generally accepted as an indicator of the rainfall conditions of a region (McGregor and Nieuwolt, 1998). As most of the stations in the study area have missing or no data in the years before 1992 with a major gap in 1991, it was not possible to characterize the rainfall based on a minimum of thirty years of data. Considering the insignificant annual rainfall trend in the region (Seleshi and Zanke, 2004; Bewket and Coway, 2007; Cheung *et al.,* 2008), however, the annual rainfall calculated based on data of 1992-2005 could be taken as a good approximation to the climate of the study area. To further support this argument, mean annual rainfall amounts of Bahir Dar and Gonder meteorological stations computed from long years of data (1965-2005) were

compared against those obtained from 1992-2005. The difference between the mean annual rainfall amounts of the two periods was only 30 mm.

The annual rainfall characteristic of each station was determined based on the quality-controlled continuous daily rainfall series. The results of the analysis are summarized in a boxplot (Figure 3-9) which contains important information on the median, variability, skewness and outliers of the data. The use of graphical methods like boxplots to summarize hydro-meteorological datasets, which are usually characterized by skewness and outliers, are considered to be better than the classical measures such as mean and standard deviation (Helsel and Hirsch, 2002). It could be seen that stations located at lower latitudes have generally higher median rainfall. This corresponds to the general climatology of East Africa and Ethiopia where rainfall increases from north to south. Most of the stations exhibited interquartile range of 200-330 mm and no well defined relationship between rainfall amount and interannual variability could be detected. Six stations (Amba-Giorgis, Shebekit, Wereta, Dek-Estfanos, Hamusit, and Tis Abay) showed outliers, which could be real or erroneous values. It should be noted that the years that corresponded to these outliers did have observed rainfall data for all or most of the days of the year. Generally, the stations exhibited a non-normal annual rainfall distribution with positive or negative skewness.

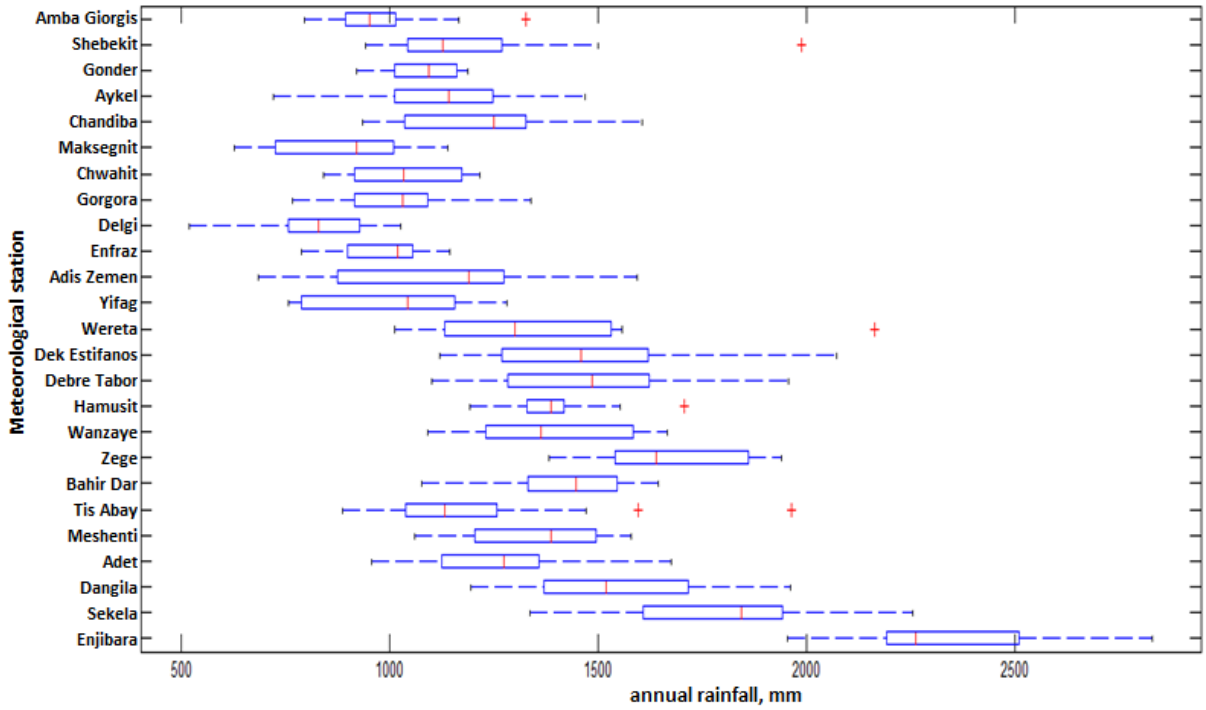

Figure 3-9 Boxplot of annual rainfall of stations located within and around Lake Tana basin (based on 1992-2005 data). The stations are arranged according to their latitude which increases upward.

3.4.1.1.4 Seasonal and monthly rainfall

Knowledge of seasonal rainfall distribution is important in tropical regions as it is a major controlling factor of agricultural activities and forms the basis for classification of climates (McGregor and Nieuwolt, 1998). The seasonal pattern of rainfall was assessed by computing the monthly rainfall contribution and the Precipitation Concentration Index (PCI). PCI is a statistical rainfall variability descriptor calculated using Equation 3-4 (Oliver, 1980). PCI values of less than 10 indicate uniform monthly distribution of rainfall, values between 11 and 20 indicate high concentration, and values above 21 indicate very high concentration. The monthly rainfall distribution of representative Class 1 stations is presented in Figure 3-10.

$$PCI = \frac{\sum P_i^2}{(\sum P_i)^2} \times 100 \qquad \text{Equation 3-4}$$

Where P_i is the rainfall amount of the i^{th} month and the summation is over the 12 months.

Rainfall in the study area was found to be monomodal with the *kiremt* season receiving more than 70 % of the annual rainfall. The computed PCI values varied from 15 to 23, indicating the high or very high seasonality of rainfall. Similar results were reported by Bewket and Conway (2007) who analyzed the rainfall variability of Amhara region based on data of twelve meteorological stations for the period 1975-2003. The seasonality of the rainfall is consistent with the movement of the ITCZ.

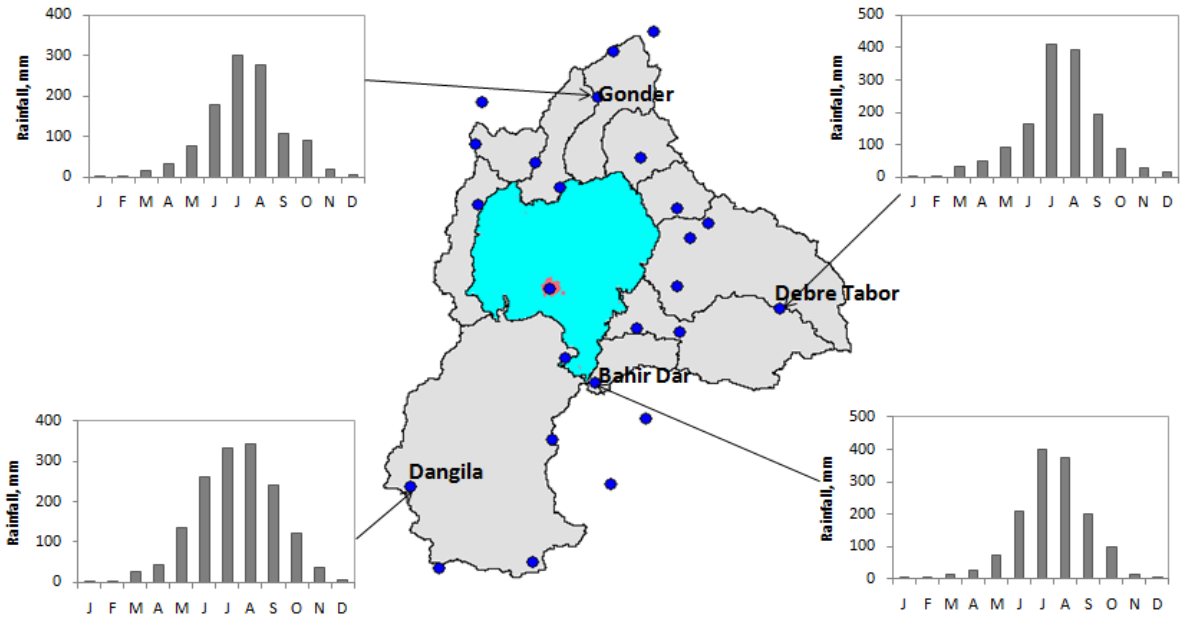

Figure 3-10 Monthly rainfall pattern of Class 1 stations within Lake Tana basin

3.4.1.1.5 Areal rainfall

The median annual rainfalls of the stations were used to draw the isohyetal map of the basin using spatial interpolation. Spatial rainfall interpolation methods are of two broad types: direct average and surface fitting methods (Dingman, 1994). The direct average approaches have low computational complexity and commonly used methods are the arithmetic average and Thiessen polygon. Several types of surface fitting methods with moderate to high computational complexity are available and methods in common use include inverse distance weighting, multiquadric interpolation, spline surface fitting and kriging. Comparison of the different areal rainfall estimation methods indicates the superiority of kriging and multiquadric methods (Tabios and Salas, 1985). The performances of Thiessen polygon and inverse distance weighing methods are also considered to be acceptable.

The isohyetal map developed from the interpolated annual rainfalls and the corresponding interquartile ranges are shown in Figure 3-11. The median annual rainfall of the whole basin was found to be 1330 mm by the multiquadric method with a coefficient of variation of 0.2. The wider Lake Tana region is considered to be homogenous influenced by similar rainfall patterns (Cheung *et al.,* 2008).

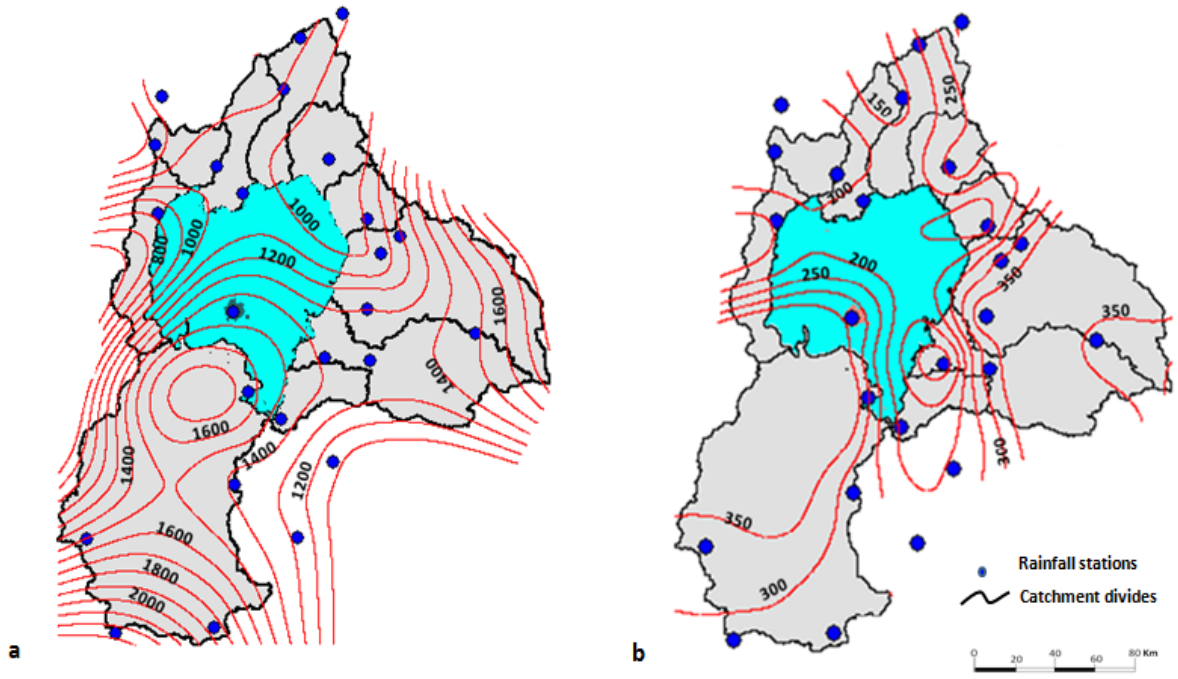

Figure 3-11 Spatial pattern of rainfall in the Lake Tana basin (a) median annual rainfall (b) interquartile range. The units are in mm

3.4.1.1.6 Elevation/Latitude-annual rainfall relationship

Knowledge of rainfall variation with elevation could be used in distributed rainfall-runoff modeling. The distributed hydrological model used in this study, for instance, requires precipitation lapse rate as an input. In most regions of the world, long-term annual rainfall increases with elevation (Dingman, 1994). This assumption, however, breaks down in the tropics where rainfall increases up to 1000-1500 mm and decreases beyond this altitude (McGregor and Nieuwolt, 1998). Effort was exerted to identify the relationship between elevation and annual rainfall in the study area. The results of the analysis indicated no distinct relationship between the two variables. Instead, a general decrease in annual rainfall amount with increase in latitude could be detected as shown in Figure 3-12. This could be related to the south-north-south movement of the ITCZ, which is the main rain producing mechanism in the region during the wet season (NMSA, 1996).

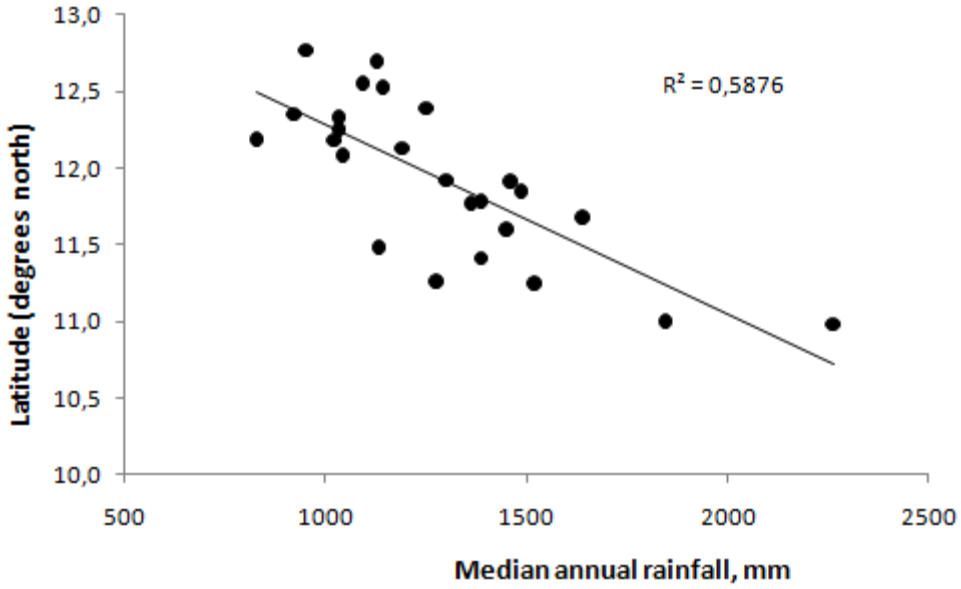

Figure 3-12 Median annual rainfall-latitude relationship in the Lake Tana basin

3.4.1.1.7 Daily and hourly rainfall characteristics

A detailed analysis of the temporal characteristics of daily and hourly rainfall was made for Bahir Dar and Gonder stations based on long years of data. A paper submitted for journal publication is attached in Annex A. The mean daily rainfall intensity varied from about 4 mm in the dry season to 17 mm in the wet season with corresponding variation in raindays of 0.4-

26 days per month. The observed maximum daily rainfall varied from 13 mm in the dry month to 200 mm in the wet month. The average wet/dry spell length varied from 1/21 days in the dry season to 6/1 days in the rainy season.

The hourly rainfall data appeared to be of poor quality as in most cases the hourly totals in a day did not match the daily observation. For instance, investigation of wet season hourly rainfall data of Bahir Dar station showed more than 25% difference between hourly totals and daily observed values for 60% of the records. For Gonder similar difference was obtained in 40% of the records. Most of the hours in the data sheets are blank with notes indicating the malfunctioning of the recorder. The limited good quality hourly rainfall data indicated that most of the rainfall occurs in the afternoon and evening periods of the day with mean duration of 1.5 hours in the dry season and 3.3 hours in the wet season.

3.4.1.2 Temperature

The minimum and maximum temperatures of the study area were assessed using observed data of nine Class 1 and Class 3 stations with less than 25 % data gaps in the analysis period. The analysis involved check for validity and homogeneity of the datasets, spatiotemporal characterization of the annual and seasonal temperature and creation of continuous temperature series by filling missing data.

3.4.1.2.1 Data quality and homogeneity

Temperature records could have errors emanating from instrumental, human and environmental sources. The observed daily minimum and maximum temperature data were subjected to quality control to identify invalid and temporally inconsistent records. The invalid and inconsistent data were considered as missing. Identification of incorrect data was done following the method discussed in Leung *et al* (2007). The first step involved quality control checks to ensure that data is within valid ranges and no strange values are entered. This was done through the following procedure:

- Checking whether the data is within valid ranges: both the minimum and maximum temperature data were checked if they are within valid ranges. Considering the general climate of the study area, the minimum temperature was considered to vary from -2°C to 14°C. For maximum temperature a range of 10 °C to 30 °C was taken.

- Checking whether the minimum temperature is less than the maximum: this check was performed to ensure that the maximum temperature is always greater than the minimum.
- Checking for suspicious data: it may happen that the difference between the maximum and minimum temperature in a day is very large which could not be explained by normal climatic conditions. In this case one or both of the records could be erroneous and they would be flagged as suspicious data.
- Checking existence of constant temperatures for ten successive days, which is unrealistic.

The second data quality control was performed to ascertain that data record at any time is not significantly different from the other records in the series. For each data of a station the standardized Z-score was computed using Equation 3-5. The Z-score values represent the number of standard deviations a data is away from the mean. For a station, those temperature values that are more than 3 standard deviations away from the mean were considered to be temporally inconsistent.

$$Z = \left| \frac{T_t - \overline{T}}{\sigma_T} \right| \qquad \textbf{Equation 3-5}$$

Where, T_t is temperature at any time t; $\overline{T}$ is mean temperature of a station and σ_T represents standard deviation.

The temperature data quality control resulted in 79 records that are temporally inconsistent. Both the minimum and maximum temperature values were found to be within the valid range and there were no unusual big differences between the maximum and minimum data records.
Spatial consistency of observed temperature data was checked using the double mass analysis by taking observations of Class 1 stations as reference. The results are presented in Annex B 3-4. The result showed no significant inconsistency in the observed minimum and maximum temperatures.

3.4.1.2.2 Annual and seasonal temperature characteristics

A boxplot was used to summarize the annual characteristics of the minimum and maximum temperatures (Figure 3-13). The mean monthly temperature of each station together with its coefficient of variation was also computed to depict the seasonal pattern. Results for Class 1

stations are given in Figure 3-14. Moreover, the mean annual temperature of the whole basin and its relationship with altitude were determined.

Stations that are located at higher altitude generally exhibited lower temperature. The majority of the stations showed skewed annual minimum and maximum temperature distributions. The interannual variability of temperature was found to be generally low with most stations showing less than 1°C interquartile range. The apparent outliers and absence of whiskers in the boxplots of some stations could be considered as manifestation of this low variability. The outliers could not be real as they are not far from the median temperature.

During wet months the diurnal range of temperature appeared to be low which could be related to the effects of cloud cover which lowers the daytime temperature. The dry season, with clear day and night skies produced higher diurnal range of temperature. This is a characteristic of tropical climatology (McGregor and Nieuwolt, 1998).

The mean annual temperature of Lake Tana basin was found to be 19 °C with a corresponding coefficient of variation of 0.08. An assessment on the relationship between average temperature and elevation was made. The result indicated a general decrease in temperature with increase in elevation as shown in Figure 3-15. The lapse rate was found to be -0.005 °C per 1 m increase in elevation.

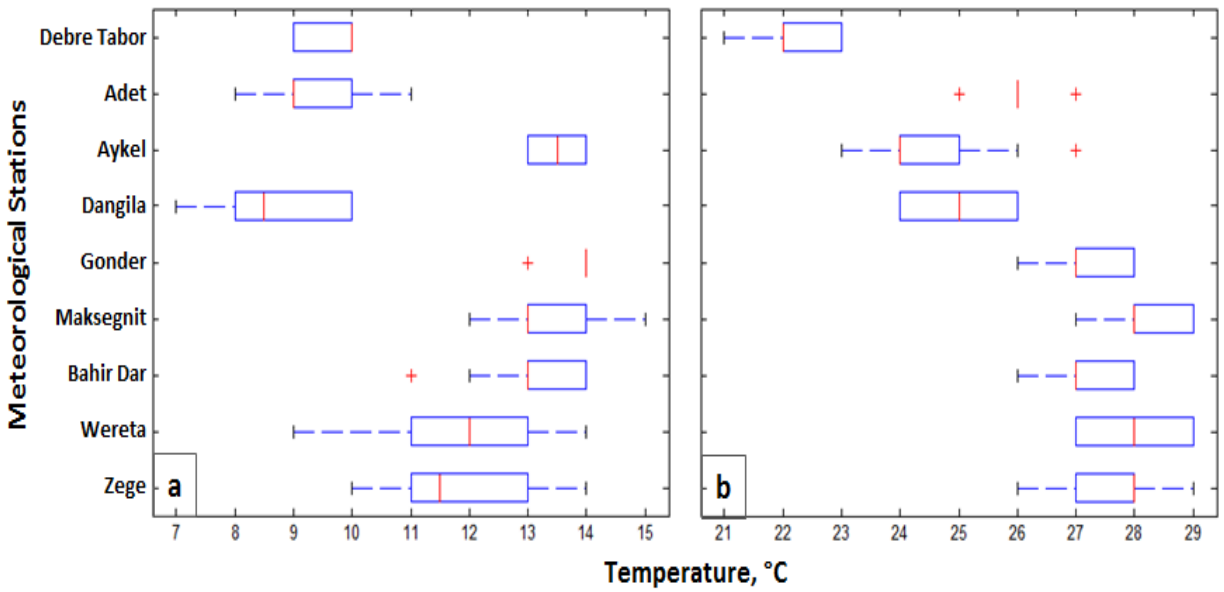

Figure 3-13 Characteristics of annual temperature in the Lake Tana basin (a) minimum temperature (b) maximum temperature. Stations are arranged according to their altitude which increases upward.

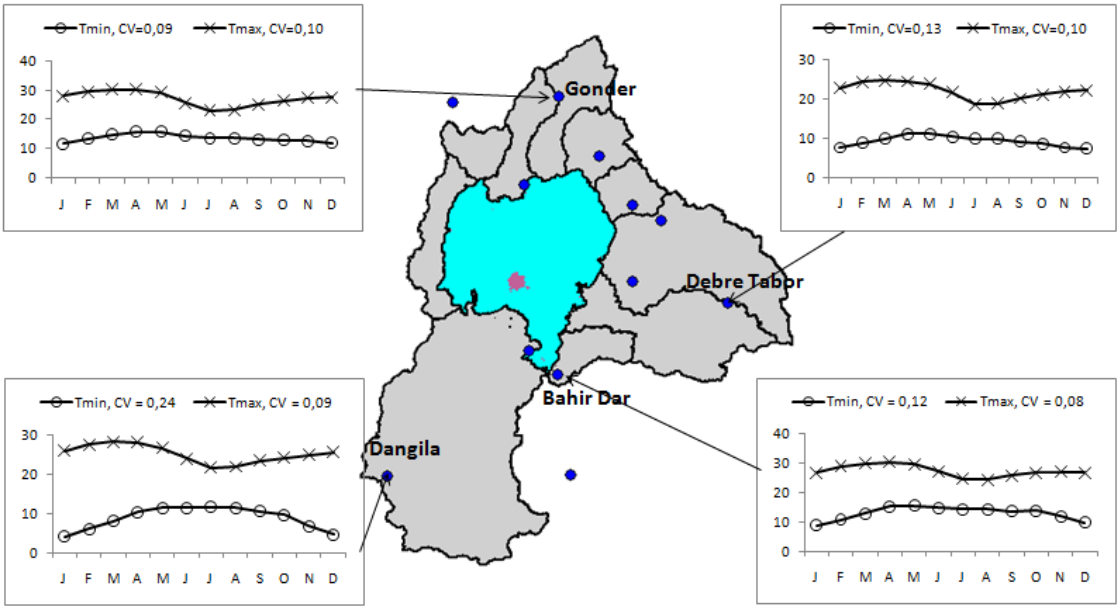

Figure 3-14 Monthly minimum and maximum temperature pattern in the Lake Tana basin

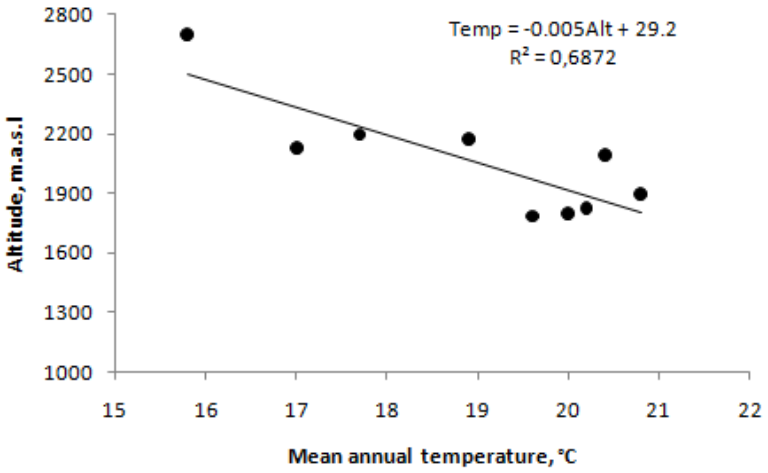

Figure 3-15 Temperature-Altitude relationship in the Lake Tana basin

3.4.1.2.3 Filling of data gaps

If temperature time series is used in hydrological simulations, all data gaps should be filled by appropriate methods. In this study filling of missing daily minimum and maximum temperatures was done using the inverse distance method with adjustment for elevation difference (Equation 3-6). The temperature lapse rate computed in Section 3.4.1.2.2 was used to compute the elevation adjustment factor. The use of similar spatial interpolation method for

filling gaps in temperature data series could be found in the literature (Stahl *et al.,* 2006; Snell *et al.,* 2000).

$$T_m = \frac{\sum_{i=1}^{n}(T_i + LPR(y_i - y_m))d_{im}^2}{\sum_{i=1}^{n} d_{im}^2} \qquad \textbf{Equation 3-6}$$

Where, T_m = estimated temperature at station m with missing data, °C; T_i = observed temperature at surrounding station i, °C; y_i = altitude of station i in meters; y_m = altitude of the station with missing data in meters; d_{im} = horizontal distance between stations with known and missing data in meters; LPR = temperature lapse rate, °C/m; n = number of surrounding stations with observed temperature data.

3.4.1.3 Wind speed

Wind speed data was involved in the computation of potential evaporation from Lake Tana and catchment evapotranspiration using the Penman-Monteith approach. Analysis was based on daily/monthly data obtained from six Class 1 stations for the period 1992-2005.

3.4.1.3.1 Data quality and characteristics

The wind speed data was first visually inspected for obvious errors using graphical plots. This was followed by temporal characterization of the wind speed pattern. No obvious deviations in wind speed could be detected. Graphical presentation of the annual and monthly wind speed pattern in the basin is given in Figure 3-16. The median annual wind speed varied from 0.6 m/s for Bahir Dar to 2.5 m/s for Aykel. After having compared data from different sources, SMEC (2008a) questioned the quality of wind speed data of Bahir Dar station which appeared to be very low. Overall, wind speed showed an increasing trend from south to north. Mulugeta and Drake (1996) noted a general south-north and west-east increase in wind energy distribution for Ethiopia. Right or left skewed distribution of wind speed is obvious from the boxplot. A slight seasonal variation in wind speed could be noted with the *kiremt* season exhibiting relatively calmer conditions. Monthly wind speed showed an increasing pattern starting from October/November and attaining its peak in May/June when the monsoon climate approaches the basin. Mulugeta and Drake (1996) characterize wind speeds as

stronger and weaker, respectively, during dry and wet seasons in the highland regions of Ethiopia.

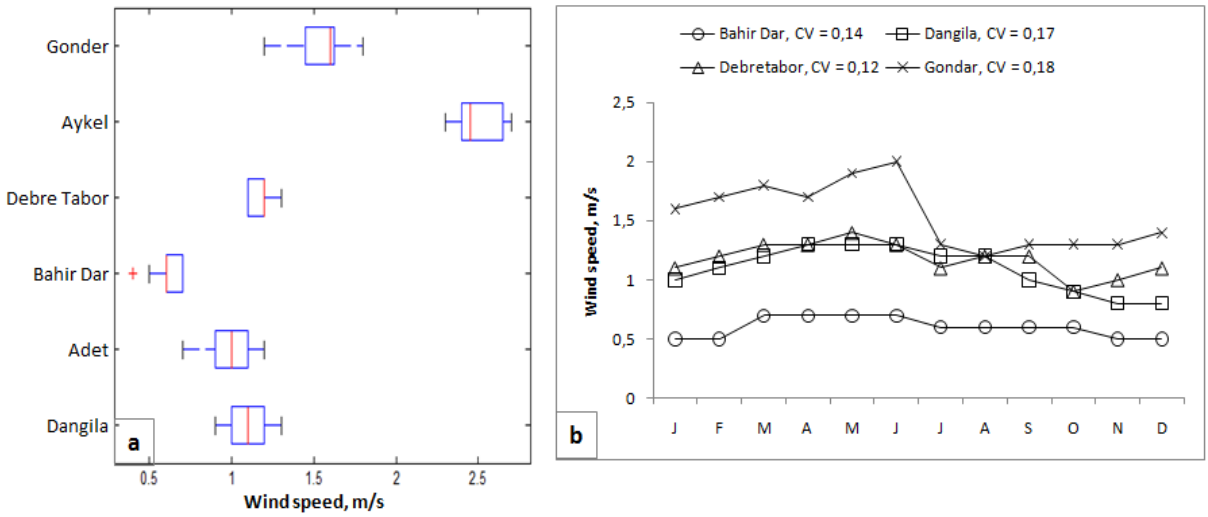

Figure 3-16 Wind speed in the Lake Tana basin (a) annual wind speed (b) mean monthly wind speed. Stations in the boxplot are arranged according to their latitude which increases upward.

3.4.1.3.2 Filling of missing wind speed data

The missing daily wind speed data were filled stochastically using Weibull probability density function (Equation 3-7). The Weibull function is the most widely used and accepted distribution for wind speed (Carta *et al.,* 2009). It is also assumed to be a good model for representing the wind speed pattern in Ethiopia (Mulugeta and Drake, 1996; Bekele and Palm, 2009). The parameters of the model were derived from the observed daily wind speed data and are given in Table 3-4. The continuous daily wind speed series was used in the distributed hydrological modeling.

$$f(x|\alpha,\beta) = \alpha\beta^{-\alpha}x^{\alpha-1}e^{-\left(x/\beta\right)^{\alpha}} \qquad \textbf{Equation 3-7}$$

Where, x is the random wind speed; α (shape parameter) and β (scale parameter) are positive real numbers.

Table 3-4 Weibull distribution parameters for wind speed in the Lake Tana basin

Station	Shape parameter, α	Scale parameter, β
Bahir Dar	0.68	2.56
Dangila	1.19	3.48
Debre Tabor	1.31	3.02
Gonder	1.72	3.07

3.4.1.4 Relative humidity

Relative humidity values are involved in the computation of the convective part of the Penman-Monteith evapotranspiration equation. Data from four Class 1 stations that have three measurements in a day were used in the analysis.

3.4.1.4.1 Data quality

Two simple checks were made to ascertain the quality of the relative humidity data. The first check was done to ensure whether the recorded data is within a valid range. In many places, the air's total vapor content varies only slightly during the entire day, and it is the changing air temperature that primarily regulates the daily variation in relative humidity (Ahrens, 1991). Considering the general climatology of the study region, the valid range for relative humidity was assumed to be 5-100 %. Those relative humidity records that are less than 5% and greater than 100% were treated as missing data. The second check was conducted to make sure that the relative humidity value at sunrise is greater than that recorded at noon. At most tropical stations, the daily maximum relative humidity is recorded shortly before sunrise (McGregor and Nieuwolt, 1998). All of the observed data were found to be within the specified minimum and maximum limits but each station had few records that did not meet the second requirement.

3.4.1.4.2 Characteristics of the relative humidity data

The daily relative humidity was computed as the average of the three observations of the day. This computed average daily data was then used to calculate the annual and monthly relative humidity of the study area. The spatiotemporal behavior of relative humidity was characterized based on the calculated annual and monthly values. Results of the analysis are indicated in Figure 3-17.

The annual relative humidity appeared to have a strong correlation with annual rainfall amount and altitude. Stations with high altitude and rainfall amount showed higher relative humidity. High altitudes are characterized by lower temperature which results in higher relative humidity. Larger amount of annual rainfall is associated with high moisture in the atmosphere which leads to higher relative humidity. Relative humidity is highly seasonal with wet months showing greater values due to the influx of larger amount of moist air. As

expected the relative humidity exhibited high values early in the morning and lower values in the day hours.

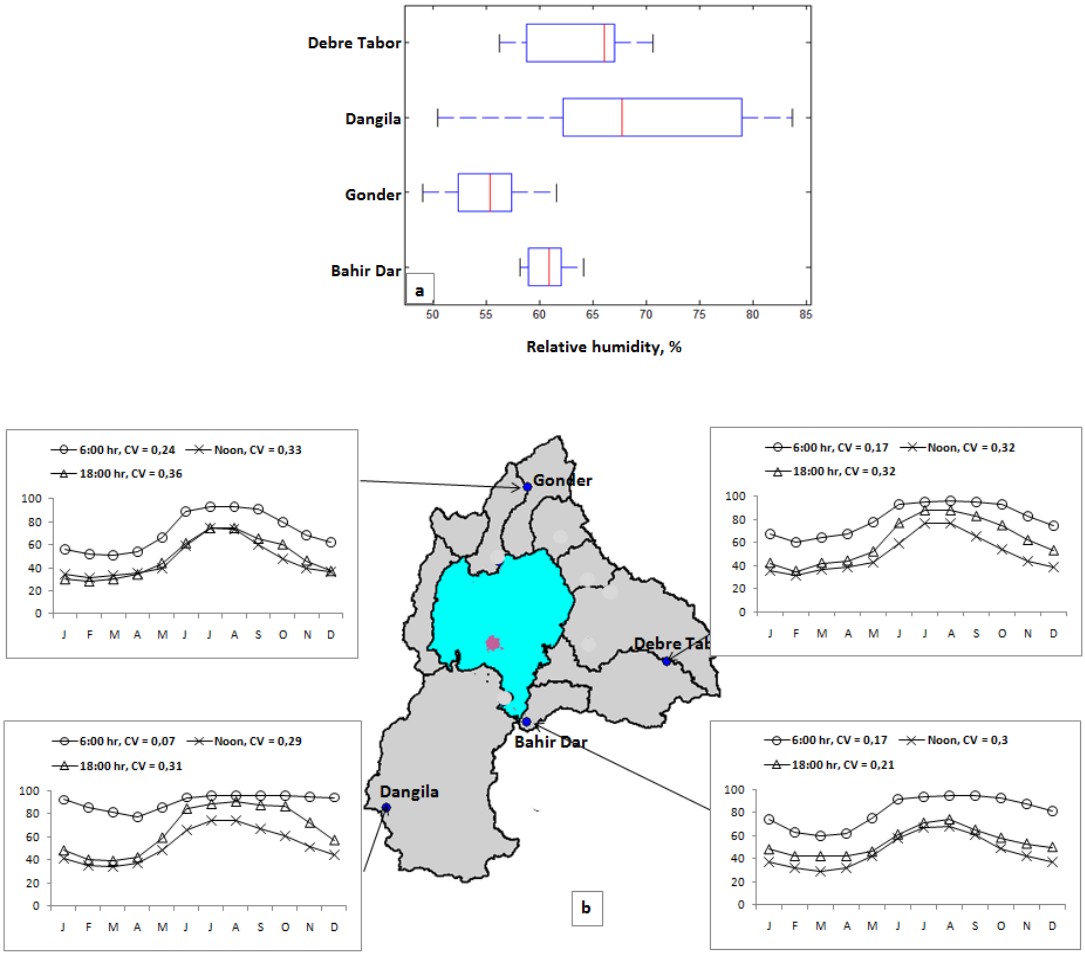

Figure 3-17 Relative humidity in the Lake Tana basin in percent (a) annual (b) monthly. Stations in the boxplot are arranged according to their altitude which increases upward.

As complete relative humidity data series is required for the hydrological simulation, gaps in the records were filled using the inverse distance square method. All stations with recorded relative humidity data were used in the interpolation without setting a limit to distance.

3.4.1.5 Sunshine hour

Sunshine hour data analysis was limited to Bahir Dar station as it is the only station that has adequate data coverage. For the other stations the data gap in the analysis period was found to be more than 60 %.

The daily sunshine hour data was checked graphically for obvious errors and this was followed by another step to verify whether the recorded data is within a valid range. The

lower sunshine hour limit corresponds to a day with cloud cover throughout the day. The upper limit corresponds to the maximum day length that can be experienced in the study area which is a function of latitude and day of the year. The valid sunshine hour range for the study area was set to vary from 0 to 13 hours. Any data with obvious error or outside this valid range was considered missing. No data quality problem could be detected.

The mean monthly sunshine hour distribution is indicated in Figure 3-18. The average sunshine hour length varied from 5.6 hours during the *kiremt* season to 9.3 hours during the dry season. The sunshine hour length during the wet season appeared to be in accordance with the diurnal rainfall pattern where formation of clouds and rainfall generally occurs in the afternoon and evening hours. The temporal variability of sunshine hour is relatively high with a standard deviation of about 2 hours.

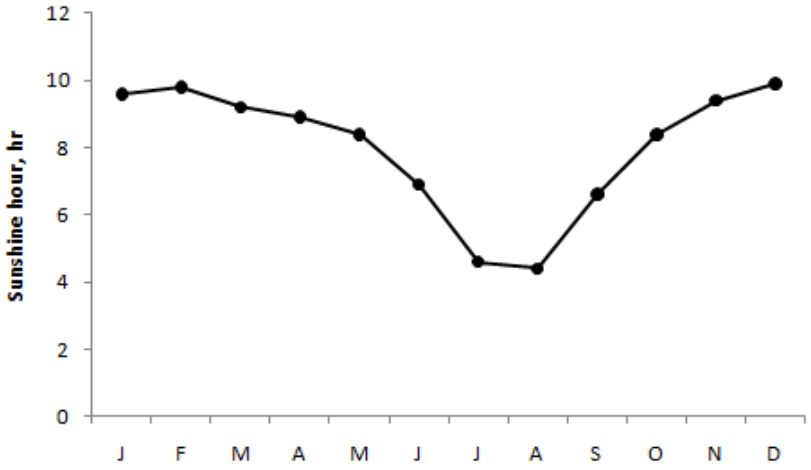

Figure 3-18 Mean monthly sunshine hour at Bahir Dar

3.4.1.6 Potential evapotranspiration

Potential evapotranspiration represents the maximum amount of water that would be lost to the atmosphere if there were no limit to water availability. Due to its geographic location Africa has a positive radiation balance, making evapotranspiration an important water balance component (Shahin, 2003). An estimation of the potential evapotranspiration of the study area was made based on the Penman combination method which requires different meteorological data including temperature, wind speed, relative humidity and shortwave and longwave radiations. The mean annual potential evapotranspiration in Lake Tana basin was found to be 1585 mm. The mean monthly potential evapotranspiration pattern of Class 1 stations is indicated in Figure 3-19. The ratio of mean annual precipitation to that of potential evapotranspiration resulted in 0.85, indicating a humid climate.

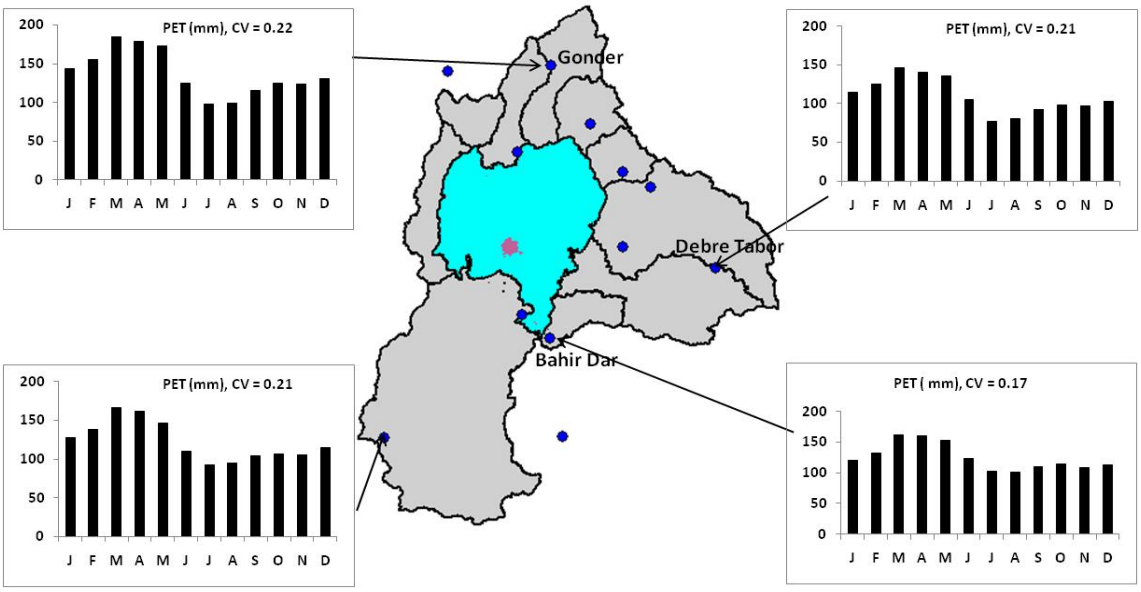

Figure 3-19 Mean monthly potential evapotranspiration in the Lake Tana basin

3.4.2 Hydrological data analysis

The section begins with presentation of the streamflow and lake level data analyses. This is followed by estimation of baseflow from the daily streamflow series. Furthermore, notes on flooding and rainfall-runoff relationships are made. Analysis of the bathymetry of Lake Tana based on data obtained in a recent year is also included. The section concludes with the analysis of the limited suspended sediment data obtained from four gauging stations.

3.4.2.1 Streamflow data

The annual and monthly characteristics of streamflows of eight gauging stations and the lake level were analyzed for the period 1992-2005. The analysis involved description of the watershed characteristics, data quality assessment, and temporal and spatial characterization of the runoff.

3.4.2.1.1 Watershed characteristics

The various catchments of Lake Tana basin were basically delineated from the 90m DEM obtained from SRTM. The DEM was preprocessed using the efficient Wang and Liu (2006) algorithm which can simultaneously remove sinks and determine watersheds and flow paths.

Each catchment was characterized in terms of median annual rainfall/runoff and physiographic variables that included area, average altitude and slope. Areal rainfall was determined from point observations using the multiquadric interpolation method. The average altitude and slope of each catchment was calculated as mean of all cell values contained in the catchment. The spatial distributions of soil and land cover types in each catchment are given in Section 3.4.4. Summary of the characteristics of the gauged catchments in the Lake Tana basin is presented in Table 3-5 and see Annex B-5 for all catchments.

Table 3-5 Characteristics of gauged catchments in the Lake Tana basin

Catchment	Gauged area km^2	Median annual rainfall†, mm	Median annual runoff†, mm	Altitude, m.a.s.l	Slope %
Garno	103	1031	246	2354	23.6
Gilgel Abay	1641	1750	1030	2298	10.7
Gumara	1279	1392	815	2271	13.8
Gumero	169	951	273	2278	20.3
Koga	297	1477	600	2108	6.5
Megech	514	1048	418	2348	19.7
Rib	1448	1486	325	2274	15.5
Whole basin	15120	1330	287	2025	9.3

†**Median annual rainfall and runoff were computed from daily observed data of year 1992-2005**

3.4.2.1.2 Data quality

The streamflow data quality was first checked for unrealistic records such as negative flows and constant observations for successive days following notable rain events. The observed data was treated as erroneous if a constant high runoff was encountered for three or more successive days. This check was followed by Grubbs test to detect outliers in the daily runoff records. The streamflow data was found to be log-normally distributed. The first check enabled to identify few unrealistically constant records for successive days in the streamflow series of Gilgel Abay and Rib rivers. No outlier could be detected with the Grubbs test.

3.4.2.1.3 Characteristics of runoff and lake level

The annual and monthly streamflow characteristics of the study area were described based on observed data of the major gauged catchments. The lake level records at Bahir Dar were used to characterize its fluctuation. The annual and monthly streamflow values were determined from the quality-controlled observed daily data. The runoff in units of millimeter (streamflow in m^3/s divided by the catchment area) was used in the analysis to facilitate comparison

between stations. Boxplots were used to summarize the annual runoff characteristics (Figure 3-20). The monthly runoff and lake level pattern were described by their mean value (Figure 3-21).

The median unit runoff production varied from 283 mm for Garno to 1030 mm for Gilgel Abay and has shown a general increase with rainfall. But an apparent decrease in runoff with increase in rainfall could be seen at Rib and Koga relative to that at Gumara. Possible explanations for this obvious discrepancy may include flooding and deep percolation in the Rib catchment, more baseflow contribution to Gumara catchment from outside its limit, particularly from areas where Mount Guna is situated or the actual rainfall amounts may be very different from the estimated. Detailed studies with good quality datasets may provide sound explanations. The storage effect of the lake is reflected in the outflow which showed a lesser runoff depth than that observed at Megech with lower rainfall. The high runoff generation rate together with its large size makes Gilgel Abay the greatest streamflow contributor to Lake Tana. The interannual rainfall variability was found to be higher at those gauging stations with lower runoff amount.

An obvious outlier could be observed in the streamflow records of Koga which corresponded to data of year 1995. Closer investigation of the daily streamflow data of this year indicated high successive observations in the months of August and September. This was not detected in Section 3.4.2.1.2 where data quality assessment was done based on the daily data. This signifies the importance of making data quality assessment at different temporal scales.

Streamflows in the study area are highly seasonal as illustrated in Figure 3-21 and this is a characteristic feature of regions dominated by monsoonal climate. More than 70% of the runoff occurs during the main rainy season, from June to September. The lake level and outflow attain their maximum in September/October and their minimum in May/June. The mean annual lake level fluctuation in the analysis period was found to be 1.5 m.

Construction of the Chara Chara weir at the outlet of the lake has affected the lake level and its outflow regime as seen in Figure 3-22. The weir was constructed in two stages to regulate the water surface elevation between 1984 and 1987 m.a.s.l. for generation of hydropower at Tis-Abay I and II stations. In the first stage two weirs, each having a capacity of $70m^3/s$, were completed in May 1996. Additional five weirs each also with $70m^3/s$ capacity became operational during the second stage in January 2001 (McCartney *et al*. 2009). A clear reduction in the seasonality of the outflow and the lake level could be seen after all the seven gates have become operational.

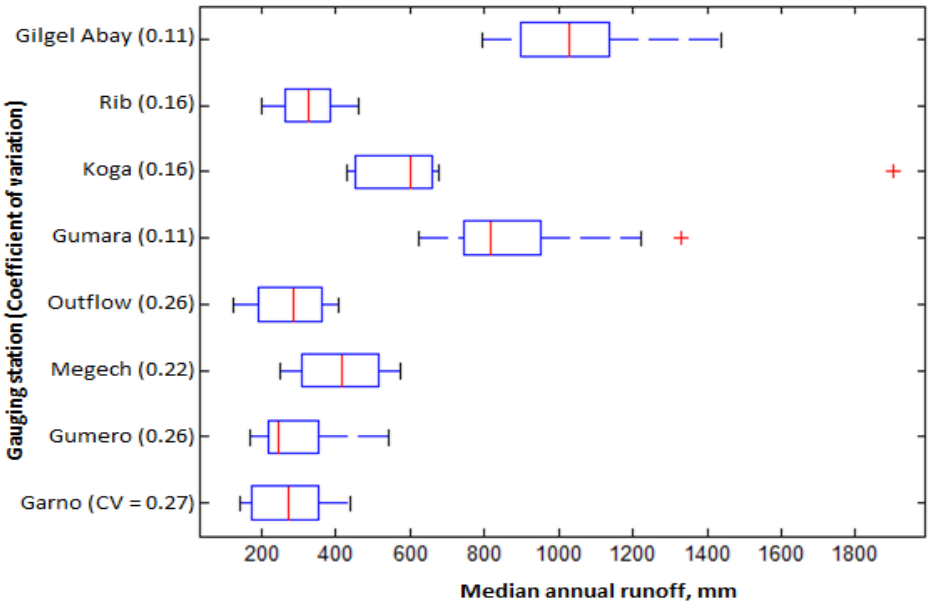

Figure 3-20 Boxplot of annual runoff of gauged catchments in the Lake Tana basin. Stations are arranged according to basin's median annual rainfall which increases upward

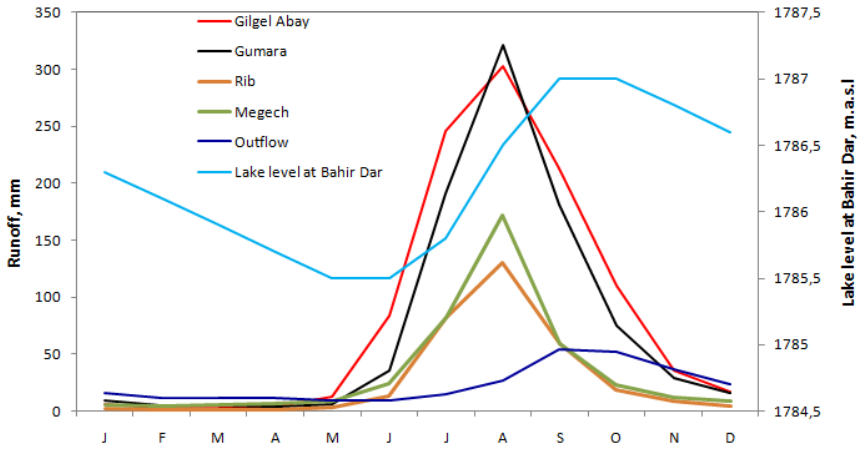

Figure 3-21 Monthly runoff and lake level pattern in the Lake Tana basin

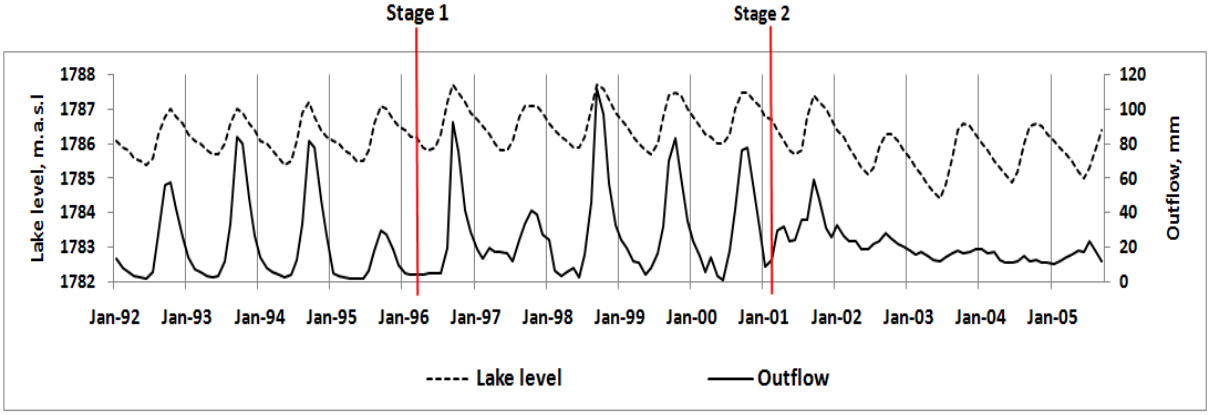

Figure 3-22 Effect of Chara Chara weir on the outflow and level of Lake Tana. Stage 1: two gates of the weir became operational; Stage 2: additional five gates of the weir became operational.

3.4.2.2 Baseflow

Studies on baseflow characteristics of the study area are scant. In this study an attempt was made to estimate the contribution of baseflow following a method originally proposed by the United Kingdom Institute of Hydrology (UKIH) and that has got applications in different studies (Piggott *et al.,* 2005, Aksoy *et al.,* 2008). The method requires daily discharge series and baseflow separation is done through the following summarized procedure:

- Divide the daily flow data into non-overlapping blocks of n days.
- Mark the local minima of each of these blocks, and call them $Q_1, Q_2, \ldots, Q_i$.
- Compare three successive local minima (Q_{i-1}, Q_i, Q_{i+1}) to identify turning points. If $0.9Q_i \leq \min(Q_i - 1, Q_{i+1})$, then the central value is the change point for the baseflow line. Do this for the whole time series.
- Make linear interpolation between successive turning points to estimate the baseflow of each day. If, on any day, the baseflow estimated by this line exceeds the total flow on that day, the base flow is set equal to the total flow.
- Calculate the baseflow index (BFI) as the ratio of mean baseflow to mean total discharge of the whole period.

In the original UKIH method the length of the non-overlapping blocks (n) is 5 days. In this study we used 7 days after having considered the maximum mean wet spell lengths of the study area. Daily rainfall analysis of Bahir Dar and Gonder stations gave a maximum wet spell length of 5-6 days. The baseflow determination was done using continuous daily discharges obtained after having filled missing records by the longterm average flows. Longterm average flows were computed for each month.

Summary results of the baseflow analysis for the major catchments are presented in Table 3-6. Baseflow appeared to be a major flow pathway in all catchments with relatively higher contributions in Gilgel Abay and Gumara watersheds. The calculated baseflow indices are within ranges reported in different studies (Eckhardt, 2008; Aksoy *et al.,* 2008; Chapman, 1999).

Table 3-6 Baseflow indices for major gauged catchments of Lake Tana basin

Catchment	BFI
Gilgel Abay	0.57
Gumara	0.51
Megech	0.44
Rib	0.45

3.4.2.3 Flooding

Flooding is a recurrent problem in the downstream reaches of Megech, Rib, Gumara and Gilgel Abay rivers. A combination of factors that include bank overflow, sedimentation, poor drainage, lake level rise, and changes in the watershed characteristics are the causes of the problem. Annual flood frequency analysis was carried out using time series of maximum daily discharges for the period 1977-2006. Instantaneous peak discharges could not be found. Figure 3-23 shows the results of the analysis for the four major rivers together with the theoretical lognormal distribution. Overall, the lognormal distribution appeared to be a good fit to the observed maximum daily streamflow series. The maximum daily discharges for 50 year recurrence interval (exceedance probability = 0.02) were found to be 488 m^3/s for Gilgel Abay, 400 m^3/s for Gumara, 532 m^3/s for Megech and 171 m^3/s for Rib rivers.

3.4.2.4 Rainfall-runoff relationships

Streamflow is commonly subdivided into two parts- direct runoff and baseflow. Direct runoff is produced by either infiltration excess (Horton) or saturation overland flow (Kinghton, 1998). Infiltration excess overland flow often occurs in semi-arid and arid areas with sparse vegetation and thin soils. Saturated overland flow is produced by precipitation that falls directly on saturated areas and/or return flow from a rising watertable. It usually occurs at the base of slopes (particularly those with concave profile), thin soils and topographic hollows where both surface and subsurface flow converge. In deeper soils with good permeability, baseflow (subsurface flow) is the dominant streamflow mechanism. It may be generated by Darcian flow through microspores of the soil matrix or preferential flows through large voids such as macrospores or pipes.

To get an insight on the possible runoff generating mechanisms of the study area, the observed rainfall and runoff of four catchments were investigated. A scatter plot of weekly rainfall against runoff data for the period 2001-2005 was used for this purpose. For the main rain season a subdivision into three classes was made based on the antecedent rainfall amount. A similar approach is found in Awulachew *et al*. (2008). The results of the analysis are indicated in Figure 3-24. A stronger linear relationship between rainfall and runoff could be seen for Megech, Rib and Gumara catchments when the cumulative rainfall was greater than a certain threshold (500 mm for Megech, 650 mm for Rib and 750 mm for Gumara). This may be related to the dominance of saturated excess overland flow above these thresholds. For

Gilgel Abay catchment such distinct relationship between rainfall and runoff could not be seen even for higher thresholds. This could be explained by the dominance of subsurface flow. A higher baseflow index was also found for Gilgel Abay and Gumara in Section 3.4.2.2.

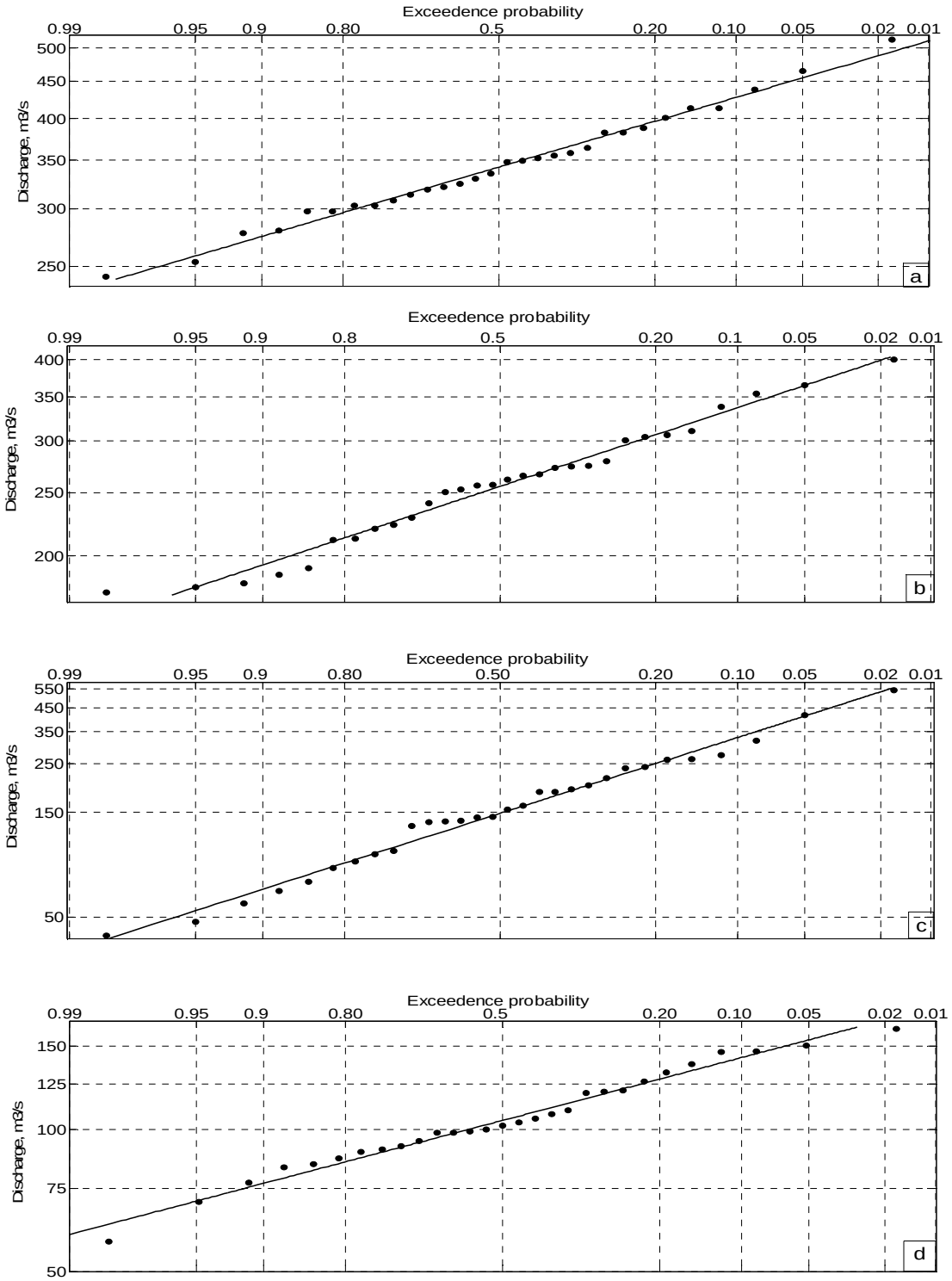

Figure 3-23 Log-normal probability plot of annual maximum daily streamflow in the Lake Tana basin (a) Gilgel Abay (b) Gumara (c) Megech (d) Rib

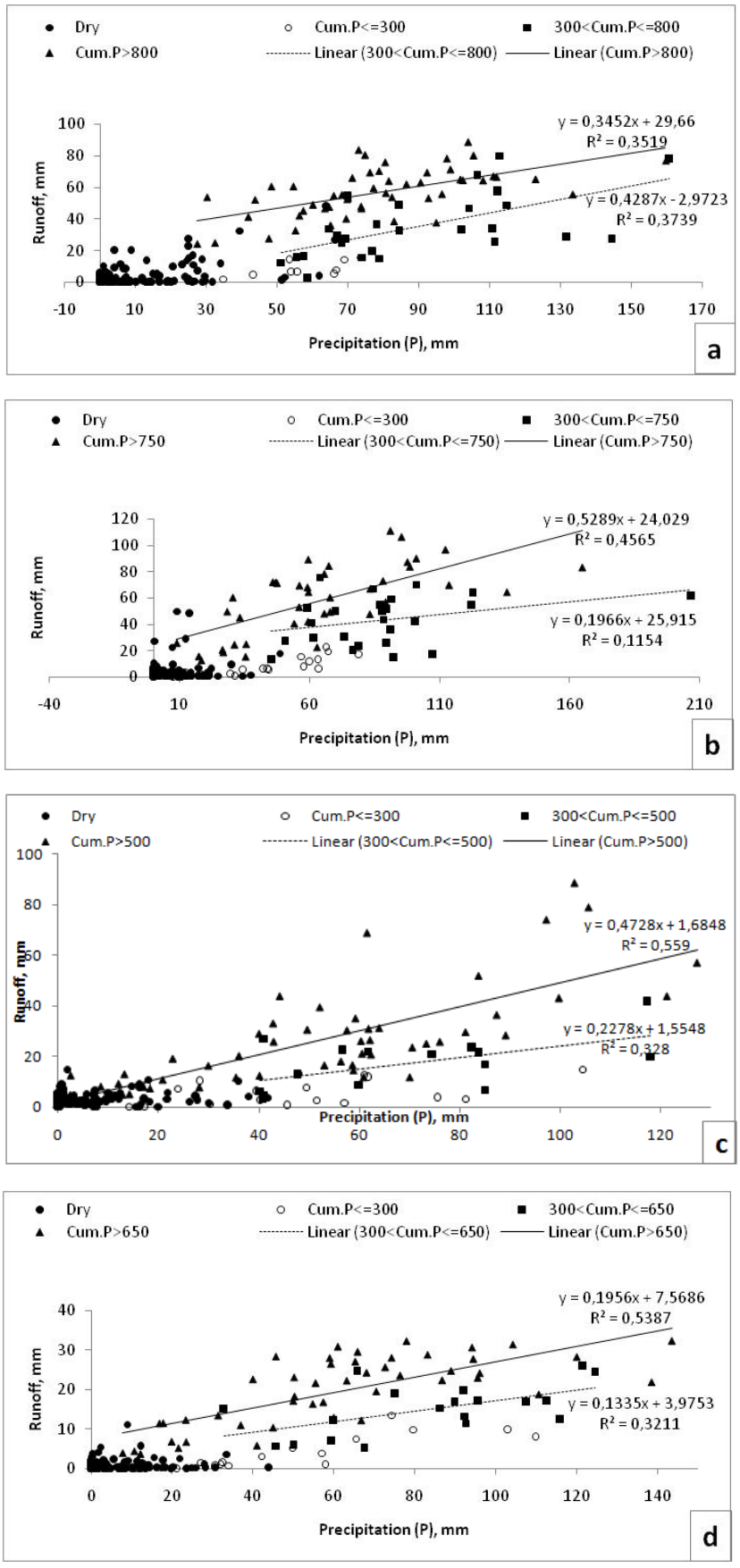

Figure 3-24 Rainfall-runoff relationship in the Lake Tana basin catchments (a) Gilgel Abay (b) Gumara (c) Megech (d) Rib.

3.4.2.5 Lake Tana bathymetry

Analyses were limited to drawing of bathymetric map, establishment of lake level-area-volume relationships and determination of the average and maximum lake depths based on data obtained for year 2006. An estimate on the rate of sediment deposit in the lake could not be made due to lack of bathymetric data of the other two previous years. The average and maximum depths of the lake were found to be, respectively, 8.7 m and 14 m with respect to the longterm mean lake level (1786 m.a.s.l). The lake area and volume corresponding to the mean water level were calculated to be 3012 km^2 and 28 km^3, respectively.

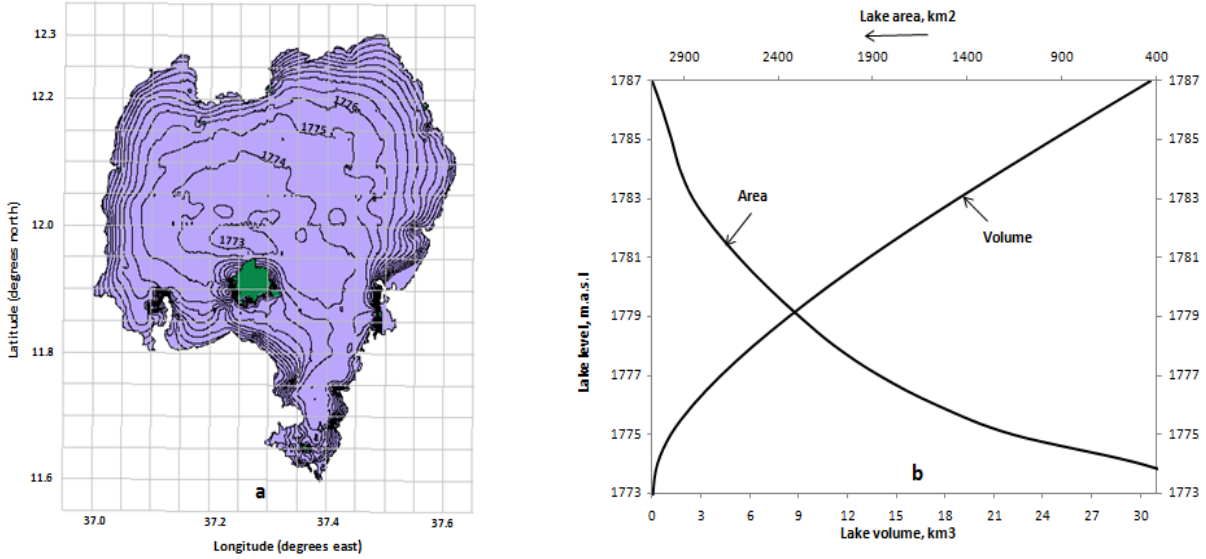

Figure 3-25 Bathymetry of Lake Tana based on data collected in 2006 (a) lake bottom contour map (b) lake level-area-volume relationship.

3.4.3 Suspended sediment yield

Accurate estimates of suspended sediment yields of catchments rely on availability of long and reliable records of suspended sediment concentrations, particularly during peak flow seasons. But when these records are unavailable, estimates are often derived from empirical relations between river discharges and corresponding suspended sediment concentrations/loads (Horowitz, 2003; Ulke *et al.,* 2009). The relationship can be expressed in different forms with the power function shown in Equation 3-8 being the most commonly used one (Asselman, 2000).

$$SS = aQ^b \quad \textbf{Equation 3-8}$$

Where, SS is suspended sediment concentration/load, Q is streamflow rate, a and b are constants to be determined from observed discharges and suspended sediment concentrations/loads.

This type of rating curve, however, has the weakness of underestimating the longterm suspended sediment load by 10-50% due to bias introduced when transformation from a logarithmic to arithmetic scale is made (Asselman, 2000). A better unbiased estimate of the suspended load could be obtained by introducing a correction factor (Equation 3-9).

$$SScorr = \left[aQ^b\right] \times CF \quad \textbf{Equation 3-9}$$

Where, *CF* is the bias correction factor.

Different methods are suggested to calculate the bias correction factor (Ferguson, 1986; Duan, 1983). The smearing estimate suggested by Duan (1983) has got wider acceptance with several applications (Rovira and Batalla, 2006; Horowitz, 2003; Jansson, 1995). The correction factor is calculated by Equation 3-10:

$$CF = \frac{\sum_{i=1}^{n} \exp(\varepsilon_i)}{n} \quad \textbf{Equation 3-10}$$

Where, n is the number of observations and ε_i is the residual at each observation time step which is calculated by Equation 3-11:

$$\varepsilon_i = \ln(SS_{obs}) - \ln(aQ^b) \quad \textbf{Equation 3-11}$$

Availability of suspended sediment data in the study area is very limited and fragmented. Most of the existing data corresponds to the wet season, with few observations during the dry months. Use of rating curve equations to estimate suspended sediment loads can be found in several project-specific study reports (e.g. BCEOM, 1999b; WWDSE and TAHAL, 2008). The suspended sediment loads, however, might have been underestimated as no correction for bias has been applied.

In this study, effort has been exerted to develop suspended sediment rating curve equations at four gauging stations (Gilgel Abay, Gumara, Koga and Megech) where data could be obtained for at least thirty days. All historical data that could be accessed were used. Moreover, the limited suspended sediment data collected during the field campaign of this study was included for Gilgel Abay and Koga stations. Correction factors calculated based on the smearing method were also used. The performance of the rating curves with and without correction factor was measured by the Nash-Sutcliffe efficiency.

The suspended sediment rating curves obtained for both with and without correction factors are shown in Figure 3-26. The calculated Nash-Sutcliffe performance measure is indicated in the legend. Overall, the performance of the rating curves appeared to be good with a slightly better fit when bias corrections were applied.

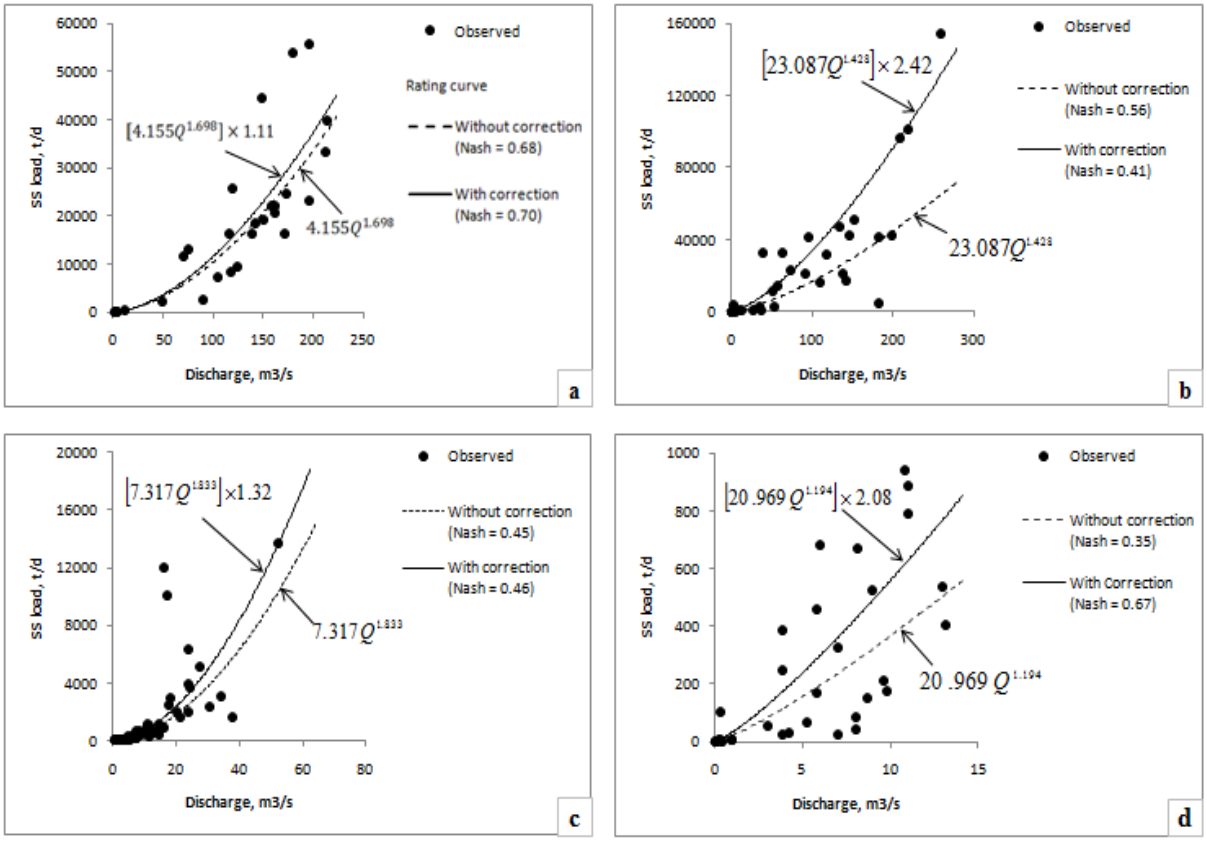

Figure 3-26 Suspended sediment rating curves for four gauged catchments in the Lake Tana basin (a) Gilgel Abay (b) Gumara (c) Koga (d) Megech.

3.4.4 Soil and land cover data analysis

3.4.4.1 Soil

Information on the type and physical properties of the study area soils could be extracted from the Abay Master Plan (BCEOM, 1999c) and other catchment specific studies (Acres and Shawel, 1995). These data and relevant notes from literatures were used to determine the average characteristics of the soil types. Information on soil texture and soil hydraulic properties were used to parameterize the physically based hydrological model used in this study.

Soil types

Lake Tana basin is covered by eight major FAO/UNESCO soil groups: Luvisols (LV), Leptosols (LP), Vertisols (VR), Fluvisols (FL), Alisols (AL), Nitosols (NT), Regosols (RG) and Cambisols (CM). The basin is dominantly covered by the first three soil groups. A brief presentation on the general characteristics of each soil group is given below (Driessen *et al.,* 2001).

Luvisols: represent soils having an argic subsurface horizon. They are most common in flat or gently sloping land and have granular surface soils that are porous and well aerated. The available moisture storage capacity is highest in the argic horizon.

Leptosols: these are shallow soils mostly located at medium-high altitude and strongly dissected topography. The very shallow soils (less than 10 cm thick) are called Lithic Leptosols. They are found in all climatic zones, in particular in strongly eroding areas. By and large, they are free draining and have low water holding capacity.

Vertisols: are deep clayey soils that expand upon wetting and shrink upon drying. They are found in level to undulating terrain with distinct wet and dry periods. They are poorly drained and largely have good water holding capacity.

Fluvisols: These are soils developed in fluvial, alluvial, lacustrine or marine deposits and are common along rivers and lakes, in floodplains and deltaic areas. Fluvisols in upstream parts of river systems are normally confined to narrow strips of land adjacent to the actual riverbed. In the middle and lower stretches, the flood plain is wider and has the classical arrangement of levees and basins, with coarsely textured Fluvisols on the levees and more finely textured soils in basin areas further away from the river. Fluvisols on river levees are porous and better drained than those in low landscape positions.

Alisols: They are strongly acid soils with subsurface accumulation of high activity clays. They are most common in old land surfaces with a hilly or undulating topography, in humid (sub) tropical and monsoon climates.

Nitosols: are deep and well-drained tropical soils with a clayey subsurface horizon. They are found on level to hilly topography.

Regosols: are soils in unconsolidated material without significant evidence of soil formation. They are particularly common in mountainous regions associated with Leptosols. They are well-drained and medium-textured soils with lower water holding capacity.

Cambisols: are soils at an early stage of soil formation. They exhibit different characteristics depending on the environmental setting in which they are developed. However, most Cambisols are medium-textured soils with high porosity, good water holding capacity and internal drainage.

The distribution of each soil group is indicated in Table 3-7 for the gauged catchments and in Annex B-6 for all catchments of the basin. It could be seen that those catchments that are steeper and rugged (Garno, Gumero and Megech) are dominated by Leptosols. The more erodible Luvisols represent a major part in the catchments that exhibited higher runoff generation.

Table 3-7 Distribution of major soil types in the gauged catchments of Lake Tana basin (%)

Catchment	LV	LP	VR	FL	AL	NT	RG
Garno		71	9				20
Gilgel Abay	56		2		40	1	1
Gumara	88	9	3				
Gumero	6	68	16			4	6
Koga	47	10	12		24	7	
Megech	5	81	3			11	
Rib	35	40		24		1	
Whole basin	47	20	13	12	6	1	1

LV: Luvisols; LP: Leptosols; VR: Vertisols; FL: Fluvisols; AL: Alisols; NT: Nitosols; RG: Regosols

Soil physical properties

Relevant soil analysis results reported in the Abay Master Plan study and other catchment-specific documents were used to estimate the average texture and hydraulic properties of each soil type. The estimated soil hydraulic properties included bulk density, porosity, field capacity, permanent wilting point, saturated hydraulic conductivity and infiltration capacity. As measured data on porosity could not be found, it was estimated from bulk density. Because

field capacity and permanent wilting point measurements are limited, pedotransfer functions that relate these parameters to percentages of clay, silt and sand were developed and used. The use of pedotransfer functions to estimate missing soil hydraulic characteristics is considered to be a good strategy where measured data are lacking (Wösten *et al.,* 2001). A good relationship between soil texture and saturated hydraulic conductivity could not be established. The physical characteristic of each soil type is presented in Annex B-7.

3.4.4.2 Land cover

The data obtained from the MoWR is limited to indicating the percentage distribution of land cover types in different parts of the basin. This information was used to identify a set of land cover classes based on the IGBP-DISCover land cover classification legend which was found to be suitable for the modeling aspect of this study. The legend comprises 17 classes and has been used in global-scale modeling of climate, biogeochemistry and other Earth system processes (FAO, 2000; ISLSCP, 2010). Eleven types of land cover classes could be identified for the study basin. They included croplands, cropland/grassland mosaic, cropland/shrubland mosaic, cropland/woodland mosaic, cropland/woody savana mosaic, grassland, open shrubland, plantation, afro-alpine forest, urban area and water. The distribution of the land cover types is indicated in Table 3-8 for the gauged parts of the basin and in Annex B-8 for all catchments. It could be seen that most of the gauged catchment is dominantly cultivated except the two smaller catchments, Garno and Gumero, which are located close to the basin's divide where the topography is mountainous and dissected.

Table 3-8 Distribution of land cover types in the gauged catchments of Lake Tana basin (%)

Catchment	LC1	LC2	LC3	LC4	LC5	LC6	LC7	LC8	LC9	LC10
Garno	33.2		11.2				55.4		0.2	
Gilgel Abay	95.8	1.2			2.9				0.1	
Gumara	65.9	28.1	1.7			0.4	3.9		0.1	
Gumero	29.8		70.2							
Koga	80.5	10.3				0.6	8.5		0.1	
Megech	97.1		1.2			0.5			1.2	
Rib	78.6	4.9	0.3			1.5	14.5	0.1		
Whole basin	63.0	6.5	3.9	0.1	0.5	0.2	5.6	0.1	0.1	20

LC1: cropland; LC2: cropland/grassland mosaic; LC3: cropland/shrubland mosaic; LC5: cropland/woodland mosaic; LC5: cropland/woody savana mosaic; LC6: grassland; LC7: open shrubland; LC8: plantation; LC9: urban; LC10: water.

3.5 Concluding remarks

In this chapter assessments of the availability, quality and characteristics of the existing hydro-meteorological and spatial data in the Lake Tana basin were conducted. Based on the data quality assessment results, the daily hydro-meteorological observations of most stations could be considered as good. Though most of the meteorological stations do not have continuous daily rainfall observations for long years, the temporal coverage could be taken as adequate considering the absence of significant annual rainfall trends in the study region. About 34% of the basin is not covered by the rainfall stations according to the minimum recommendation of WMO. Improving the network coverage by installing more standard rain gauges would be useful. Availability of rainfall data at sub-daily time scale is by far inadequate with existing hourly rainfall records only at Bahir Dar and Gonder stations, but which are highly fragmented and of poor quality. Use of daily rainfall disaggregation techniques could be considered as a good strategy in applications that require shorter time scale data. The temporal coverage of temperature measurements could be taken as adequate in light of its low interannual and seasonal variability. In addition, considering the general linear relationship that temperature has with altitude, the spatial coverage of the observations could be considered as adequate. Though relative humidity data is available only at limited stations, its spatial coverage could be considered as fair due to its stronger relationship with temperature that has a better coverage.

Considering, the long and continuous daily discharge measurements at the major rivers, the temporal coverage could be treated as adequate. The lower reaches of the various feeding rivers and the western and southwestern parts of the basin, however, need improved coverage. In light of the seriousness of erosion and sedimentation problems and the very limited observations, the suspended sediment data coverage could be considered as highly inadequate. It would be better to limit the use of the rating curve equations developed based on this limited data to planning level applications. Acquiring more and reliable suspended sediment data would be crucial for the design and management of water resources systems in the region. The available data on soil physical properties could not adequately characterize the highly heterogeneous soil material. In hydrological modeling the influential soil hydraulic properties should be identified and used as calibration parameters.

Chapter 4

4 Sensitivity analysis of Distributed Hydrology, Soil, Vegetation Model Parameters

4.1 Introduction

Watershed models, which vary from simple empirical to complex physically based models, play a fundamental role in addressing a range of water resources, environmental and social problems. The development and application of physically based distributed hydrological models is getting wider as can be seen in the literature (e.g. Abbot *et al*., 1986; Wigmosta *et al.,* 1994; Ewen *et al*., 2000; Liu and Todini, 2002). Such models require a large number input factors that vary in space and time. This makes parameterization and calibration of these models difficult and demanding (Refsgaard, 1997; Moreda *et al*., 2006; Francés *et al*., 2007). Refsgaard (1997) thus stresses on the significance of rigorous parameterization and identification of few calibration parameters.

The dimensionality of a parameter space can be reduced by different techniques, of which sensitivity analysis is the one that is commonly used (Saltelli *et al.,* 2006). The use of sensitivity analysis is also common in hydrological modeling (Muleta and Nicklow, 2005; Griensven *et al*., 2006; Kannan *et al*., 2007). Model sensitivity analysis is performed to rank factors based on their influence on model outputs. The factors may include parameters, forcings, initial conditions, boundary conditions, etc. By enabling modelers identify factors that contribute most to output variability, sensitivity analysis facilitates model calibration (Hamby, 1994; Kannan *et al.,* 2007; Werkhoven *et al*., 2008). Sensitivity analysis methods are classified into two broad categories: local and global sensitivity analysis (Saltelli *et al*., 1999).

Local sensitivity analysis uses the one-factor-at-time (OFAT) method where one factor is changed at a time keeping the others at their base value. The method enables to unambiguously determine the effect caused by changing a single factor. Implementation of the method is straightforward and its computational requirement is modest (Griensven *et al*., 2006; Cloke *et al.,* 2008). One major drawback of the method is that it does not address interactions among factors which are the case in non-linear models. Two kinds of local sensitivity analysis techniques exist- the nominal range and differential analysis techniques

(Tang *et al*., 2007). In the nominal range technique, the percent change in model output caused by perturbation of a factor relative to its base value is used to measure the sensitivity. The partial derivative of model output with respect to factor perturbation is used in the differential analysis method. In most sensitivity analysis the OFAT approach is used (Wainwright and Mulligan, 2004). The use of OFAT in its different forms is also common in hydrological and environmental modelling applications (De Roo *et al*., 1996; Xevi *et al*., 1997; Lenhart *et al.,* 2002; Dubus *et al.,* 2003; Holvoet *et al*., 2005; Kannan *et al*., 2007; Nishat *et al*., 2007; Bahremand and De Smedt, 2008).

Global sensitivity analysis is multivariate in its approach where model output's sensitivity is evaluated by changing multiple factors simultaneously. The method enables to consider interactions among factors, which is the case in nonlinear models. Global sensitivity analysis is computationally expensive, making its application difficult for models having a large number of factors (Cariboni *et al*., 2007; Cloke *et al*., 2008). To circumvent this disadvantage of the method, global sensitivity analysis using OFAT with different random base values are recommended (Campologo *et al*., 2007).

In this study sensitivity analysis of the Distributed Hydrology-Soil-Vegetation Model (DHSVM) parameters was done using OFAT method. DHSVM is a grid based distributed hydrological model with a number of input factors. The model was originally developed for applications in mountainous forested watershed (Wigmosta *et al*., 1994) and has been applied in different environmental settings. It also incorporates soil erosion and sediment transport module (Doten and Lettenmaier, 2004).

Examples of applications of DHSVM include assessment of impacts of climate and land use changes on streamflows and municipal water supply (Leung and Wigmosta, 1999; Cuo *et al*., 2006; Thanapakpawin *et al*., 2006; Wiley and Palmer, 2008; Cuo *et al*., 2009); real-time streamflow forecasting (Westrick *et al*., 2002) and prediction of soil erosion and sediment transport (Doten *et al*., 2006). The use of the model, with some modifications, in urban watersheds is also noted (Cuo *et al*., 2008).

The number and diversity of applications of DHSVM is increasing. With its large number of soil and vegetation parameters, the task of calibration remains a real challenge. Which of the parameters should be changed so that the simulated and observed quantities closely match? For which of the parameters can we adapt values from literature? Where should we focus our efforts during the data collection campaign? Answering such questions require ranking of the parameters in terms of their contribution to output variability.

This study aims at identifying those soil and vegetation parameters of DHSVM that have relatively greater influence on outputs of the model. Sensitivity analysis using the OFAT approach on small virtual catchments was used for this purpose. The virtual catchments represent different land surface characteristics. The analysis enabled to screen out important soil and vegetation parameters that had greater contribution to output variability. This outcome can be used as a guide for calibration of the model.

4.2 Materials and methods

4.2.1 Description of the model

DHSVM is a grid-based distributed hydrological model that simultaneously solves water and energy balance equations at each pixel per simulation time step (Wigmosta *et al.,* 1994). It provides a dynamic representation of watershed processes at spatial resolution described by Digital Elevation Model (DEM) data. This kind of representation of the watershed enables to model topographic controls on absorbed shortwave radiation, precipitation, air temperature, and downslope water movement. Each grid cell may be covered by bare soil, understory and/ or overstory vegetation. If present, understory vegetation is assumed to fully cover a grid cell. For overstory vegetation, the coverage is limited to a predefined fraction. Individual grid cells are hydrologically linked through surface and subsurface flow routing. The model has been applied from plot to watershed scale at subdaily or daily temporal resolution.

The major hydrological processes represented in the model include interception, evapotranspiration, unsaturated flow, saturated flow, and snow accumulation and melt. Below is a brief presentation of how each process is represented in the model. A detailed account is found in Wigmosta *et al*. (1994, 2002). The main processes and equations of the model are presented in Annex C-1. The overstory and understory vegetation canopies are assumed to intercept precipitation until their maximum storage capacity, which is a function of leaf area index (LAI), is reached. Evapotranspiration from vegetation canopies is calculated in a stepwise fashion where firstly the potential evaporation rate is calculated for the overstory. This represents the maximum moisture that the atmosphere can absorb. Then evaporation of water intercepted by the overstory (wet fraction), is computed as the minimum of the intercepted water or the potential evaporation rate. Transpiration from the dry vegetation surface (dry fraction) is modeled by the Penman-Monteith equation. The total evapotranspiration from the overstory (both dry and wet fractions) is then subtracted from the

potential evaporation of the overstory. The difference is then considered as a modified potential evaporation rate for the understory. The approach ensures that the total evapotranspiration from both canopy layers does not exceed the potential evaporation for the overstory. Evaporation from the upper soil layer is simulated for only bare soil surfaces and the process may be climate- or soil-controlled depending on the soil moisture content.

The snow accumulation and melt module comprises energy and mass balance components. The energy balance component is used to simulate snowmelt, refreezing, and changes in the snowpack heat content. The mass balance component computes snow accumulation/ablation, changes in snow water equivalent, and water yield from the snowpack.

A soil surface may receive water from throughfall, snowmelt or surface runoff from adjacent cells. Water in excess of infiltration capacity becomes overland flow and the remaining infiltrates into the soil. The downward unsaturated moisture movement is simulated using two-layer soil depth model in which discharge is computed by Darcy's law. Saturated flow is modeled by a quasi-three dimensional method with transient conditions approximated by series of steady state solutions. The hydraulic gradient may be approximated by the local terrain slope on steep slopes with shallow soils, and the watertable slope must be used otherwise.

The model involves several factors that include soil and vegetation parameters, initial model states, state variables, constants, and spatial and meteorological forcings. The required input forcings to run the model include DEM, soil types and properties, soil depth, vegetation types and properties, stream networks and characteristics, and meteorological variables. The meteorological forcings comprise precipitation, temperature, wind speed, relative humidity, solar radiation and long wave radiation per simulation time step.

4.2.2 The sensitivity analysis method

Evaluations of sensitivity of different mass balance outputs and flow regimes to terrain slope, soil depth, and soil and vegetation parameters of DHSVM were made. The simulation was done on catchments that represent different land surface characteristics for a period of one year at one hour time step and spatial resolution of 10m. This meant a large number of simulations and consequently, small virtual catchments representing twenty four different land surface characteristics were used. The OFAT sensitivity analysis method was used to determine the relative importance of the soil and vegetation parameters of the model.

4.2.3 Virtual catchments

The size of the virtual catchment was 50m by 170m (Figure 4-1) with different land surface characteristics defined by slope, soil and vegetation types, and soil thickness. Two types of uniform slopes were considered- flat slope (2°) and steep terrain (30°). Bare soil, shrubland, and mixed forest were used to represent land covers. Three types of soils representing fine, medium and coarse-textured soils were considered. Soil thicknesses of 0.1m and 1m for bare soil and 1m for shrubland and mixed forest were used. Combinations of the various land surface characteristics resulted in twenty-four virtual catchments. The characteristics of the different virtual catchments are summarized in Table 4-1.

A one year meteorological data that included precipitation, temperature, relative humidity as well as short and long-wave radiation at a temporal resolution of one hour was also used. The values of the meteorological variables corresponded to data of Fish Lake meteorological station given with the model tutorial data set for Rainy Creek catchment, which is a tributary to Wenatchee River in USA[5]. The model initial state files comprising soil moisture, interception storage, and snow and channel states were created using relevant executable programs provided with the model.

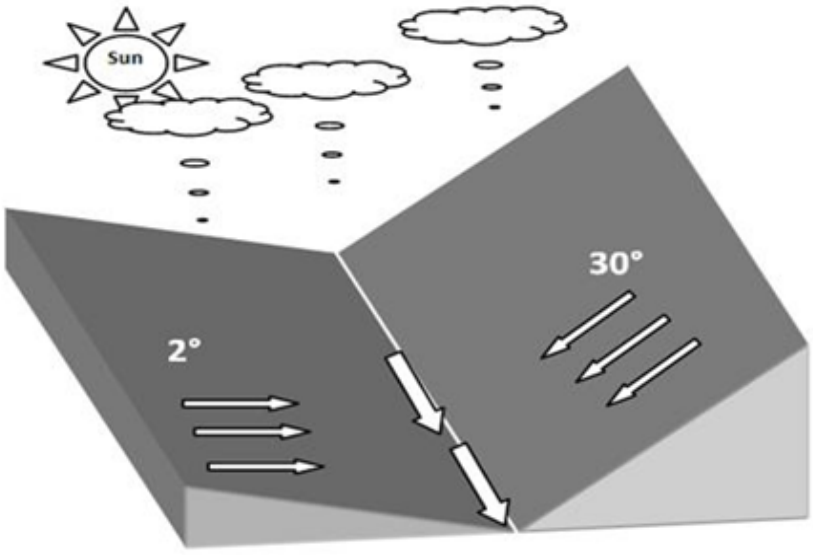

Figure 4-1 The virtual catchment

[5] http://www.hydro.washington.edu/Lettenmaier/Models/DHSVM/documentation.shtml

Table 4-1 Description of virtual catchments used for the sensitivity analysis

Soil type	Vegetation type	Surface slope	Soil thickness (m) †	Land surface type code††
Clay	Bare	2°	0.1/1	1/2
		30°	0.1/1	3/4
	Shrubland	2°	1	5
		30°	1	6
	Mixed forest	2°	1	7
		30°	1	8
Loam	Bare	2°	0.1/1	9/10
		30°	0.1/1	11/12
	Shrubland	2°	1	13
		30°	1	14
	Mixed forest	2°	1	15
		30°	1	16
Sand	Bare	2°	0.1/1	17/18
		30°	0.1/1	19/20
	Shrubland	2°	1	21
		30°	1	22
	Mixed forest	2°	1	23
		30°	1	24

† For bare soil two different thicknesses were used- 0.1 m and 1 m and the corresponding land surface codes are 1 and 2.
††These codes were used in the presentation of the results (Figure 4.4-6)

4.2.3.1 Parameters and reference values

Fifteen soil and thirty-one vegetation parameters were considered for the sensitivity analysis. Base values for each of these parameters were derived from relevant literatures. The list of the parameters and their corresponding base values are presented in Table 4-2 and Table 4-3.

Table 4-2 Soil parameters and corresponding base values

Parameter	**Clay**	**Loam**	**Sand**
Lateral saturated hydraulic conductivity, m/s	1.67×10^{-7}	3.61×10^{-6}	5.83×10^{-5}
Exponential decrease for lateral hydraulic conductivity	1	1	1
Maximum infiltration, m/s	2.80×10^{-7}	5.56×10^{-6}	6.94×10^{-5}
Surface albedo	0.17	0.14	0.2
Porosity	0.48	0.46	0.44
Pore size distribution	0.165	0.22	0.59
Bubbling pressure, m	0.373	0.112	0.073
Field capacity	0.4	0.27	0.09
Wilting point	0.27	0.12	0.035
Bulk density, Kg/m^3	1350	1450	1550
Vertical conductivity, m/s	1.67×10^{-7}	3.61×10^{-6}	5.83×10^{-5}
Thermal conductivity, W/m-°C	0.5	0.6	1.2
Thermal capacity, J/m^3-°C	2.25×10^{-7}	2.19×10^{6}	2.12×10^{6}
Capillary drive	0.41	0.11	0.05
Manning's coefficient	0.225	0.225	0.13

Table 4-3 Vegetation parameters and corresponding base values

Parameter	Bare	Shrubland	Mixed forest
Fractional coverage			0.5
Trunk space (fraction of height)			0.45
Aerodynamic attenuation			1.2
Radiation attenuation			0.15
Max snow interception capacity, m of equivalent water			0.003
Mass release drip ratio			0.4
Snow interception efficiency			0.6
Height of overstory, m			25
Height of understory, m		2	2.5
Maximum resistance of overstory, s/m			4500
Maximum resistance of understory, s/m		600	2300
Minimum resistance of overstory, s/m			300
Minimum resistance of understory, s/m		200	150
Moisture threshold of overstory			0.33
Moisture threshold of understory		0.33	0.13
Vapor Pressure deficit of overstory, Pa			4000
Vapor Pressure deficit of understory, Pa		4000	4000
Fraction of photosynthetically active radiation for overstory			0.5
Fraction of photosynthetically active radiation for understory		0.108	0.5
Depth of root zone layer 1, m	0.02	0.15	0.15
Depth of root zone layer 2, m	0.03	0.4	0.4
Depth of root zone layer 3, m	0.04	0.4	0.4
Overstory root fraction in layer 1			0.2
Overstory root fraction in layer 2			0.4
Overstory root fraction in layer 3			0.4
Understory root fraction in layer 1		0.4	0.5
Understory root fraction in layer 2		0.6	0.5
Understory root fraction in layer 3		0.0	0.0
Overstory monthly LAI†			0.75-10.13
Understory monthly LAI †		0.36-1.12	0.4-4.5
Overstory monthly albedo†			0.2
Understory monthly albedo†		0.2	0.2

†values are given for each month of a year: for LAI a range of values is indicated; for monthly albedo constant value of 0.2 is used; empty cells represent parameters that are not applicable for the specified land cover.

4.2.3.2 Sensitivity analysis

The sensitivities of various processes of the model, i.e., global outputs per simulation period (1 year) and runoff per simulation time step (1 hour), to changed parameter values were assessed. The global outputs included evapotranspiration, runoff and final soil moisture within the catchment. For outputs per simulation time step, different streamflow regimes representing low, medium, high and all flows were considered.

The classification of flow regimes into low, medium and high flows was made based on flow duration curves of reference outputs. In the literature different exceedance probabilities are used to classify flows as low (Q70-Q99), median (Q50) and high (Q5-Q10) (Smakhtin, 2001; Davie, 2003). In this study, flows having exceedance probability greater than 70% (Q70) represented low flows; high flows were flows with less than 10% exceedance probability (Q10) and those between Q10 and Q70 were taken as medium flows.

Each of the soil and vegetation parameters were changed one-at-a-time from -100% to 100% of the base value at a step of 25%. The changed parameter values were made to be physically meaningful.

4.2.3.3 Metrics for sensitivity evaluation

Based on their contribution to output variability, parameters were labeled as insensitive, low, average or high using relevant criteria. In the literature the sensitivity criteria used include sensitivity index, root mean square error, coefficient of variation, percent of output deviation, and Nash-Sutcliffe efficiency (Xevi *et al*., 1997; Anderton *et al*., 2002; Griensven *et al*., 2006; Zoras *et al*., 2007; Bahremand and De Smedt, 2008).

In this study two different sensitivity criteria were used depending on the model output. For mass balance outputs, the criterion used was a weighted percentage of departure from the base output. In this method, first the absolute percentage of departure was calculated for each percentage change in parameter value. In order to represent the overall effect of a parameter on the model output by a single number, the concept of weighted departure was introduced. This was based on the fact that a departure of, say 5 % obtained when a parameter value is increased by 25% is greater than a departure of 5% obtained when the parameter value is increased by 75%. This was accounted in the analysis by assigning weights that vary from 1 to 4 according to the percentage changes of parameter values. A larger weight was given for the smallest percentage of change in parameter value. Accordingly, a weight of 4 was assigned for departures that corresponded to a 25% change in parameter value. Two absolute weighted departures that corresponded to decreasing (-25% to -100%) and increasing (+25% to +100%) parameter values were calculated. The larger of the two absolute weighted departures was used as a measure of the relative importance of the parameter.

The weighted departure was calculated using Equation 4-1.

$$Weigheted\ departure = \frac{\sum_{i=25\%}^{100\%} Weight_i \times Departure_i}{\sum_{i=25\%}^{100\%} Weight_i} \qquad \textbf{Equation 4-1}$$

Decision on the relative importance of a parameter to a mass balance output was made based on the criteria presented in Table 4-4.

Table 4-4 Sensitivity criteria for the mass balance outputs

Weighted departure, %	Level of sensitivity
0	Insensitive
0-5	Low
5-30	Average
>30	High

For outputs per simulation time step, the Nash-Sutcliffe Efficiency (NSE) was used as a measure of sensitivity. The method is commonly used in the performance assessment of hydrological models (Krause *et al*., 2005; Schaefli and Gupta, 2007). The method of calculation is presented in Chapter 6. NSE can have values that vary from $-\infty$ to 1. Lower NSE values indicate greater departure from the base output. If a change in parameter value does not affect the output, then NSE becomes 1 and the parameter is considered to be insensitive. In this study outputs that corresponded to ±50% change in parameter value were used to calculate the NSE values. This was done for each of the flow regimes. The sensitivity ranking was done based on the criteria presented in Table 4-5.

Table 4-5 Sensitivity criteria for the outputs per simulation time step

NSE	Level of sensitivity
1.0	Insensitive
0.9-1.0	Low
0.5-0.9	Average
<0.5	High

4.3 Results and discussion

The level of influence of changes in slope, soil depth, and soil and vegetation parameters on the major outputs of DHSVM are presented in this section. The relative importance of soil and vegetation parameters was assessed by considering virtual catchments that represented different land surface characteristics. The effects of slope and soil depth changes were assessed by comparing outputs obtained with reference parameter values. The simulation

period was representative of the different seasons of temperate climate. A total of 8856 simulations were performed at hourly time step.

4.3.1 Sensitivity to terrain slope

Various studies consider slope as one of the major topographic controls of soil moisture variability (e.g. Moore *et al.,* 1993; Famiglietti *et al.,* 1998). It controls streamflow generating mechanisms, and surface and subsurface flow rates. It is considered to be one of the most important controls of laminar subsurface flow which is assumed to be directly proportional to slope gradient (Whipkey and Kirkby, 1978). In the model slope is used in overland flow routing and computation of saturated subsurface flow.

4.3.1.1 Effect on soil moisture

The effect of terrain slope change on soil moisture in different soil types is presented in Figure 4-2b. Soil moisture decreased with increasing slope. The level of sensitivity was much more pronounced in coarse-grained soil due to its higher hydraulic conductivity. In fine textured soil, slope change appeared to have insignificant effect on soil moisture and this is due to its poor hydraulic conductivity. The model result indicated slope as having influence on soil moisture both in wet and dry periods. This is partially in contrast to the results of Ridolfi *et al* (2003) who noted negligible influence of topography in the dry period. But the model result agrees with findings of Meerveld and McDonnel (2006) who observed topography-related soil moisture pattern in dry period.

4.3.1.2 Effect on evapotranspiration

The difference in evapotranspiration obtained from flatter and steeper slopes is presented in Figure 4-2c. Positive difference signifies greater evapotranspiration on the flatter slope. Slope gradient affects evapotranspiration through its effect on soil moisture availability. Evapotranspiration is moisture controlled when the soil gets drier (Brustaert, 2005). The sensitivity of evapotranspiration to slope change was negligible during the winter period. This period is characterized by very low temperature and evapotranspiration is climate controlled. A general decrease in evapotranspiration with increase in slope could be obtained in the dry period. This could be due to a decrease in soil moisture with slope as noted in Section 4.3.1.1.

The relative effect of slope change is minimal in fine textured soils due to low variability of soil moisture.

4.3.1.3 Effect on runoff

The influence of terrain slope on runoff volume is indicated in Figure 4-2d. During low flow periods, runoff volume was generally greater on the steeper slope. An exception to this is the observed runoff decrease on steeper sand soil during the dry period which could be due to depletion of soil moisture in the previous dry days. During peak flow periods, runoff did not show significant variation with slope in fine textured soil as the dominant flow pathway is overland flow. On small areas, like the virtual catchment used here, the variation of overland flow response time with slope is negligible (Burt, 1992). In loam and sand soils, flatter slopes generated more runoff and this could be due to the enhancement of saturation excess overland flow. Flatter slopes tend to retard flow rate and hence enhance saturation excess overland flow (Jones, 1997).

4.3.2 Sensitivity to soil depth

Soil depth is one of the most important controls of water storage capacity and streamflow generating mechanisms (Dunne, 1978). It is also considered important to understand the relationships between soil moisture and transpiration (Meerveld and McDonnell, 2006). In the model, soil depth is involved in the determination of soil moisture dynamics and saturated subsurface flow.

4.3.2.1 Effect on soil moisture

Increase in soil moisture storage could be seen with increasing depth in both wet and dry periods (Figure 4-3b). The effect was considerable in fine and medium-textured soils. These soils have greater moisture holding capacity and slower drainage. Coarse textured soils have lesser water storage capacity and it is highly variable due to its high hydraulic conductivity. Results of the simulation are similar to findings of Meerveld and McDonnel (2006) who noted depth as a major factor that controls variations in soil moisture storage.

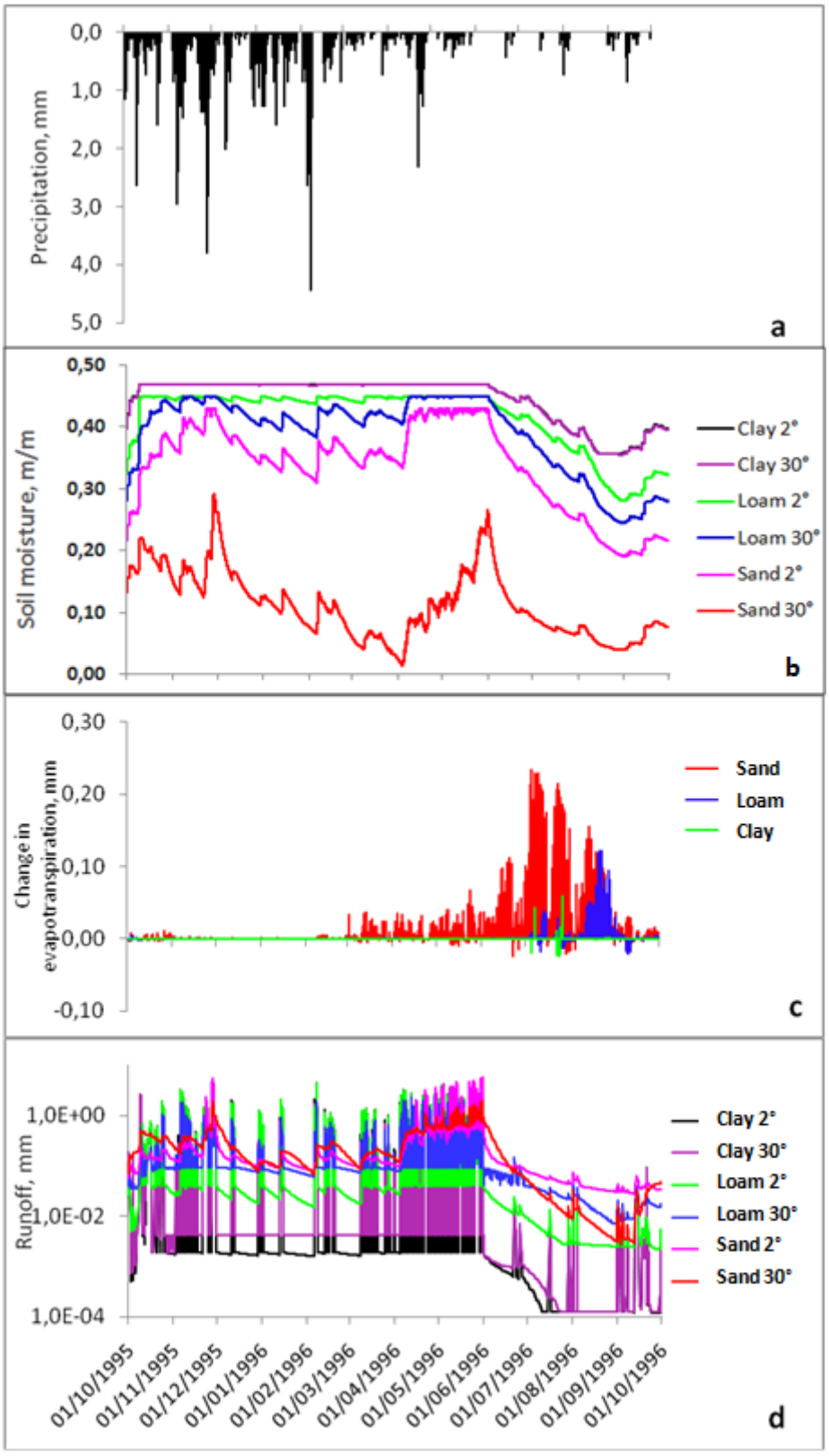

Figure 4-2 Sensitivity of DHSVM mass balance outputs to terrain slope (a) precipitation (b) soil moisture (c) evapotranspiration (d) runoff

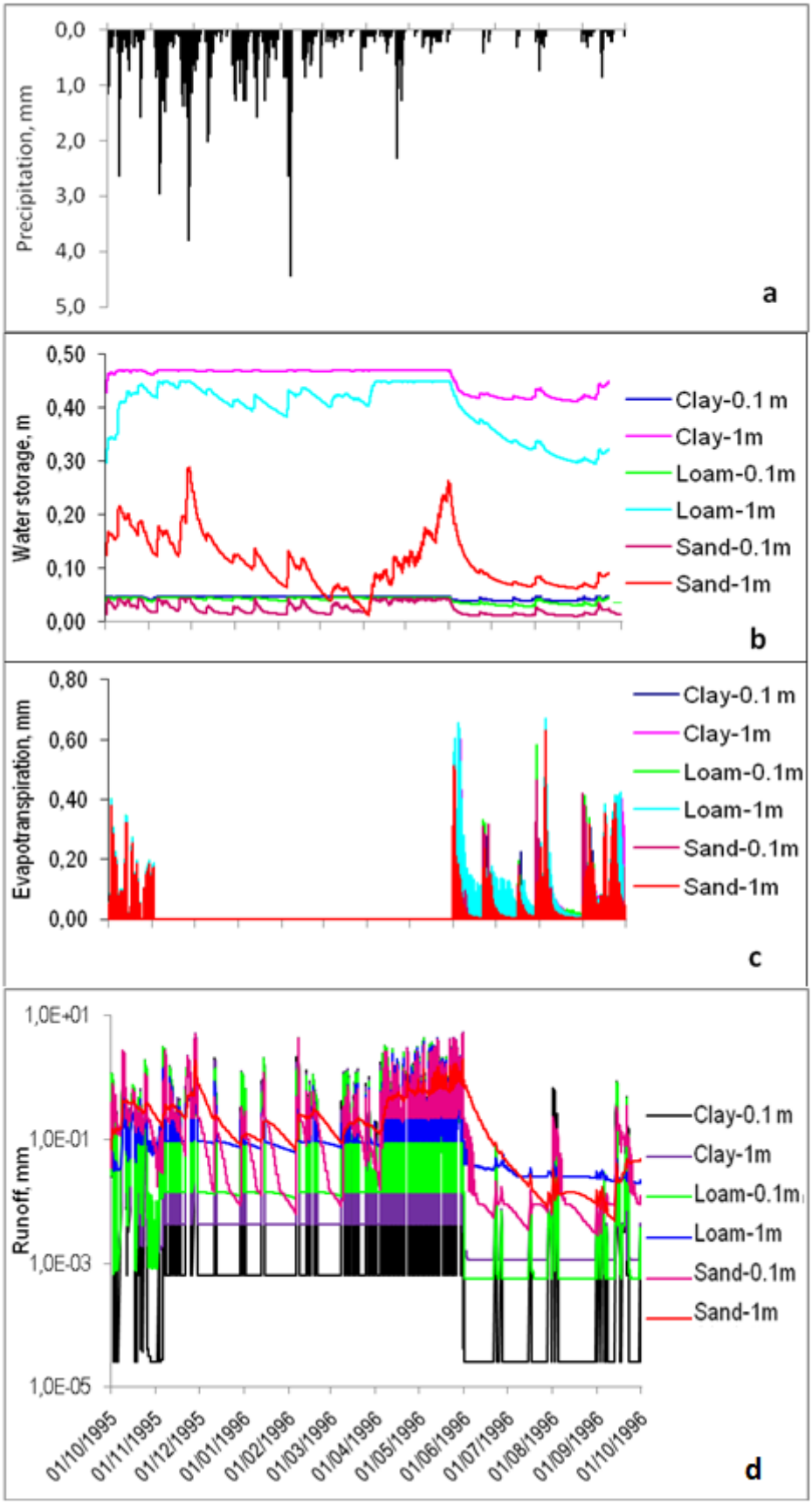

Figure 4-3 Sensitivity of DHSVM mass balance outputs to soil depth (a) precipitation (b) soil moisture (c) evapotranspiration (d) runoff

4.3.2.2 Effect on evaporation

Because soil depth was made to vary only on bare soil surfaces, its effect on evaporation from soil was evaluated. The effect of soil depth on evaporation is presented in Figure 4-3c. In the model evaporation is allowed to remove water from the upper bare soil layer. It could be noted that soil depth exhibited similar effects on all soil types. During the cold period evaporation is climate controlled and remained very low in both shallow and deep soils. During the dry period evaporation generally increased with depth as deeper soils have more water to sustain the process. An exception to this is, during the intermittent rain events, evaporation was higher in shallower soils due to availability of more moisture in the upper layer. The simulation results are in agreement to the explanations given by Meerveld and McDonnel (2006).

4.3.2.3 Effect on runoff

The sensitivity of runoff to soil depth is presented in Figure 4-3d using log-scale for better visualization. During low flow periods, runoff from deeper soils was greater as their higher moisture storage allowed them to sustain the supply. During high flow periods the effect of soil depth was insignificant in clay soil as the rapidly responding overland flow is the dominant process. In medium and coarse textured soils a slight increase in runoff could be noted on thinner soils and this could be due to the contribution of saturation excess overland flow. As thinner soils have low soil moisture deficit, they can get saturated rapidly and favor generation of saturation excess overland flow (Beven, 2001).

4.3.3 Sensitivity to soil parameters

DHSVM uses soil parameters to model various processes that include evaporation from soil, transpiration, soil moisture balance, unsaturated flow and saturated subsurface flow. Soil parameters affect these processes through their influence on water holding capacity and movement. Whipkey and Kirkby (1978) considered physical properties of soils as major controlling factors of subsurface flow.

4.3.3.1 Effect on soil moisture

The effects of soil parameters on soil moisture are indicated in Figure 4-4a. In the model the soil moisture balance of each soil layer is computed by considering different fluxes that include infiltrated precipitation, downward water discharged in each soil layer, evaporation from soil, evapotranspiration, water supplied by a rising water table and a return flow. Porosity appeared to have a significant effect in all soil types which could be due its use in the computation of the various fluxes mentioned. The apparent effects of field capacity and wilting point could also be partly attributed to that of porosity as in some cases conjoint variation of these parameters was made to ensure that wilting point < field capacity < porosity. Soil moisture in coarse-grained soils was also sensitive to other parameters including lateral and vertical saturated hydraulic conductivities, maximum infiltration capacity, and pore size distribution. This could be explained by the relatively better infiltration and drainage capacity of coarse textured soils.

4.3.3.2 Effect on evapotranspiration

The effect of soil parameters on evapotranspiration is presented in Figure 4-4b. The significance of soil properties in controlling evapotranspiration becomes apparent during the dry period when soil moisture deficit is large (Brutsaert, 2005). Porosity affected evapotranspiration noticeably in all soil types. The influence was more pronounced on vegetation-covered surfaces which could be due to its involvement in the computation of evapotranspiration from the different soil layers. Other parameters that had moderate effect on evapotranspiration included field capacity, wilting point, lateral and vertical saturated hydraulic conductivities, maximum infiltration capacity, pore size distribution and bubbling pressure. The relative effect of lateral saturated hydraulic conductivity was high on coarse grained soil due to its good drainage. In general, a larger number of soil parameters had moderate influence on evapotranspiration in all soil types. This moderate effect on fine textured soil was not, however, reflected on soil moisture balance as seen in Figure 4-4a. This could be due to the comparatively lower contribution of evapotranspiration to soil moisture balance variability.

4.3.3.3 Effect on runoff

The effect of soil parameters on runoff was noticeable mainly on deep coarse textured soil with steeper slope as shown in Figure 4-4c. In deep and well-drained soils subsurface flow is the dominant streamflow generating process (Dunne, 1978). The parameters with noticeable effect included porosity, field capacity, lateral saturated hydraulic conductivity, vertical saturated hydraulic conductivity, maximum infiltration capacity, and pore size distribution. These parameters influence runoff volume through their effect on soil moisture movement. In fine and medium textured soils the relative contribution of overland flow to runoff volume could be dominant. Consequently, the influence of subsurface flow and hence soil parameters on long-term runoff volume is insignificant.

4.3.3.4 Effect on streamflow hydrograph

Low flow

The sensitivity of low flow to soil parameters is presented in Figure 4-4d. Subsurface flow is the dominant source of low flow (Jones, 1997). The influence of few soil parameters was relatively higher in deeper and steeper coarse textured soils which could be due to their better drainage characteristic. Parameters with noticeable effect included lateral saturated hydraulic conductivity and its rate of exponential decrease, porosity, field capacity, and pore-size distribution. In the model these parameters are involved in the computation of saturated subsurface flow. The effect of vertical saturated hydraulic conductivity is low as percolation from the lower zone is negligible during the dry period. Most of the soil parameters did have no or insignificant effect on low flow in fine and medium textured soils and this could be related to their low lateral and vertical saturated hydraulic conductivities.

Medium flow

Medium flow became more sensitive to various coarse grained soil parameters that affected low flows as shown in Figure 4-4e. The increase in the level of sensitivity could be associated to availability of more soil moisture. In shallow and flat bare coarse soils the effect of these sensitive parameters was negligible which could be due to enhancement of saturation excess overland flow. The influences of pore size distribution and vertical hydraulic conductivity were negligible on flat slopes which could be due to the relatively lower variability of soil moisture. Parameters of fine grained soils that are bare or covered by understory vegetation

did not have any effect on medium flows and this could be due to the dominance of overland flow contribution. In forest-covered clay soil the contribution of subsurface flow could have become noticeable due to canopy interception so that porosity, field capacity and infiltration showed influence on medium flow.

High flow

Most soil parameters that were responsible for variation of medium flows also affected high flows generated in coarse grained soils as shown in Figure 4-4f. The effects of porosity, field capacity and pore size distribution became insignificant on deep bare soil with flat slope. This could be due to the enhancement of saturation excess overland flow on flatter slopes. The effect of saturated vertical hydraulic conductivity became pronounced which could be due to the greater availability of soil moisture for percolation. As overland flow is the dominant pathway in fine and medium textured soils during high flow period, most of the soil parameters had no or negligible effect on high flow. The considerable effect of porosity on high flows coming from forest-covered fine and medium soils could be related to the enhancement of subsurface flow by forest that has the potential to reduce rainfall intensity through interception storage.

Overall hydrograph

The influence of the soil parameters on the overall hydrograph showed similar pattern as that of low flows (Figure 4-4g). This could be due to the dominance of low flows in the whole simulation period. This concealed the significance of some parameters in medium and high flow regimes. It is therefore important to make sensitivity analysis for different flow regimes.

4.3.4 Sensitivity to vegetation parameters

Vegetation cover plays a significant role in the hydrological cycle through its effect on interception storage, evapotranspiration and infiltration (Brooks *et al.,* 2003). For instance, the proportion of precipitation that will be yielded as streamflow will be greatest for bare soil and least for forested area. Evapotranspiration is potentially higher in forested lands than areas with bare soil or shrublands. In the model vegetation parameters are used to compute interception storage and evapotranspiration.

4.3.4.1 Effect on soil moisture

Soil moisture of coarse textured soils on steep slope was sensitive to most of the vegetation parameters as presented in Figure 4-5a. This could be related to the variability of soil moisture in these soils due to their higher permeability. For other land surface types, vegetation parameters with moderate effect on soil moisture included fractional coverage, minimum stomatal resistance, vapor pressure deficit, rooting depth and fraction, and leaf area index. Soil moisture dynamics is controlled by evapotranspiration and subsurface water movement. The influence of vegetation parameters on soil moisture is realized through transpiration process.

4.3.4.2 Effect on evapotranspiration

The effects of the various vegetation parameters on evapotranspiration are presented in Figure 4-5b. Generally, fractional coverage, height of vegetation, stomatal resistance, understory moisture threshold, vapor pressure deficit, rooting depth, root fraction, and leaf area index appeared to have moderate effect on evapotranspiration. The model uses the Penman-Monteith approach to estimate evapotranspiration. The various vegetation parameters influence the process by controlling the radiation budget and/or rate of moisture transfer to the atmosphere. Fractional coverage and leaf area index could also influence evapotranspiration by limiting moisture availability through interception storage. In the model water that is intercepted by the understory and overstory vegetation is assumed to evaporate at potential rate. It could be observed that the effects of vegetation parameters of the overstory overshadowed that of understory when two canopy layers existed. Rooting depth appeared to have influence on bare soil and this is due to the use of this parameter in the calculation of soil moisture balance.

4.3.4.3 Effect on runoff

The variation of vegetation parameters did not have noticeable effect on the long-term runoff as indicated in Figure 4-5c. This could be due to the relatively smaller amount of water loss by evapotranspiration. During the longer winter period evapotranspiration was negligible as observed for the reference parameter values (Figure 4-2c).

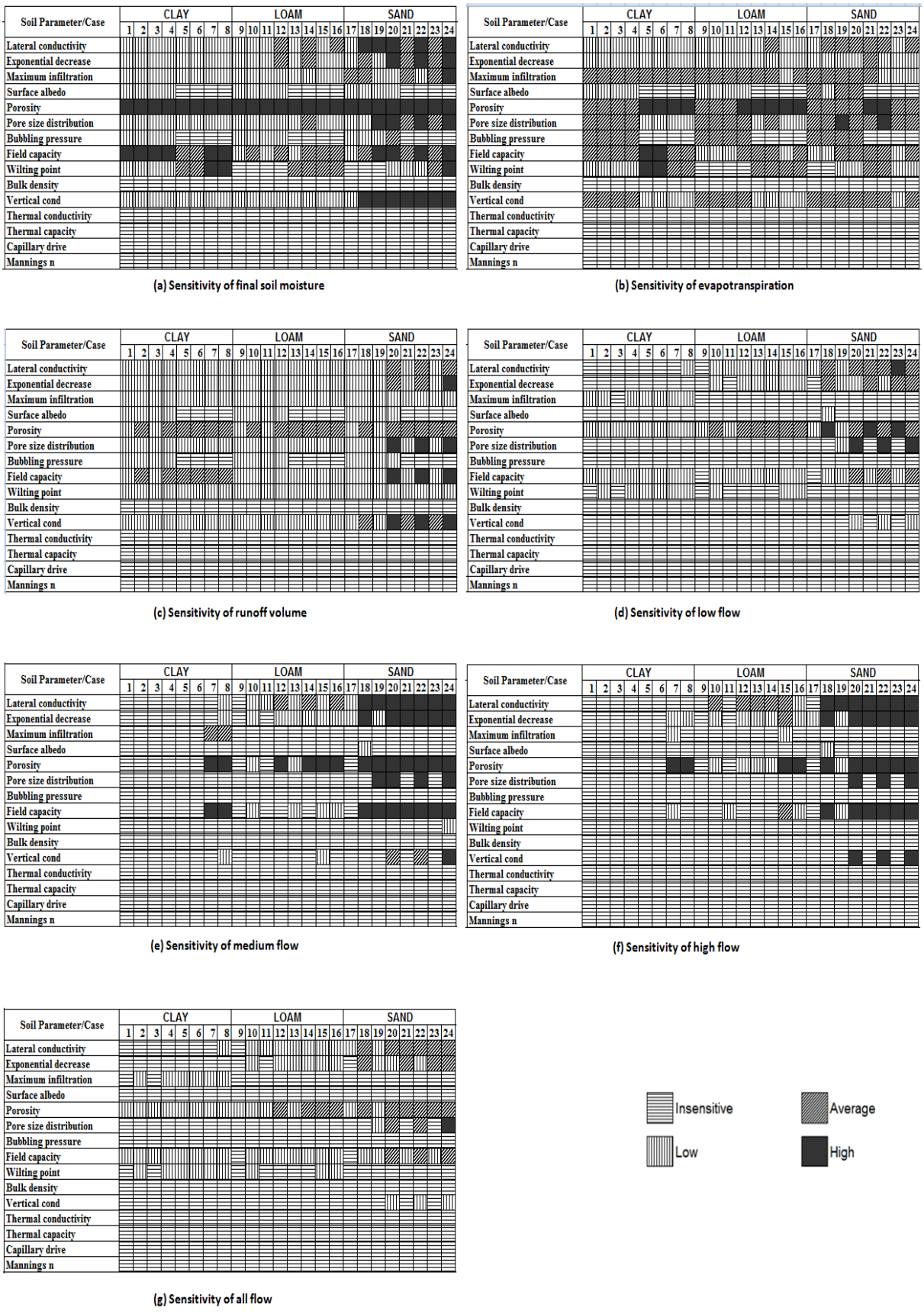

Figure 4-4 Sensitivity of DHSVM outputs to soil parameters

4.3.4.4 Streamflow hydrograph

Low flow

Most parameters did have no or little effect on low flow as indicated in Figure 4-6a. Low flows occur during winter months when most of the water is retained in snowpack or dry periods when moisture deficit is large. Due to the weak radiation energy in winter and large moisture deficit in summer, evapotranspiration and its effect on low flow are negligible. The observed moderate influences of fractional coverage, radiation attenuation and overstory leaf area index could be related to evapotranspiration that occurred during the intermittent rain showers in summer. Reference to the model equations indicated that these three parameters are involved in the computation of radiation budget which is the driver of evapotranspiration.

Medium flow

The three parameters that had moderate influence on low flows also showed significant effects on medium flows in all soil types (Figure 4-6b). The relative increase in their influence could be related to availability of greater soil moisture during medium flow period. For coarse textured soil additional vegetation parameters with considerable effect included maximum snow interception capacity, aerodynamic attenuation, overstory height, minimum stomatal resistance, and rooting depth. The sensitivity of medium flows to these additional parameters could be due to the relatively high variability of soil moisture in coarse textured soils caused by quicker soil water movement. In the fine and medium textured soils, soil moisture variability is low and hence lesser influence on medium flows.

High flow

High flows were found to be sensitive to fractional coverage, and maximum snow interception capacity in all soil types as indicated Figure 4-6c. As overland flow is the dominant pathway in fine and medium textured soils, the effect of these parameters on high flows could be related to interception storage. The influence of other vegetation parameters was apparent only on coarse textured soil with relatively higher moisture variability. These parameters included trunk space, radiation attenuation, aerodynamic attenuation, height and LAI of overstory, minimum stomatal resistance, and rooting depths.

Overall hydrograph

The sensitivity of the overall storm hydrograph was similar to that of low flow (Figure 4-6d) since the streamflow period is dominated by low flows. The influential parameters that were

observed in medium and high flows could not be detected when the overall streamflow hydrograph is analyzed.

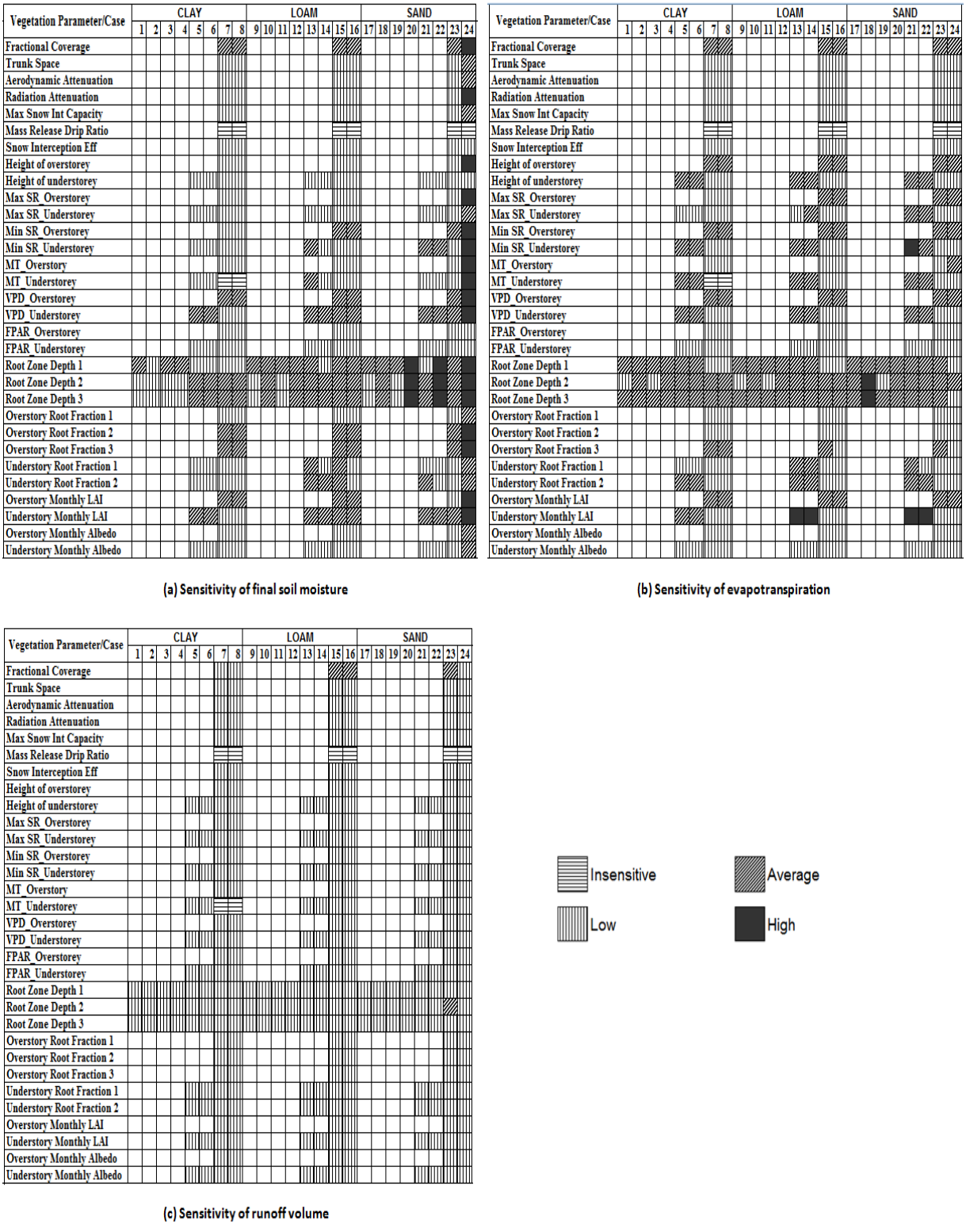

(a) Sensitivity of final soil moisture

(b) Sensitivity of evapotranspiration

(c) Sensitivity of runoff volume

Figure 4-5 Sensitivity of DHSVM mass balance outputs to vegetation parameters

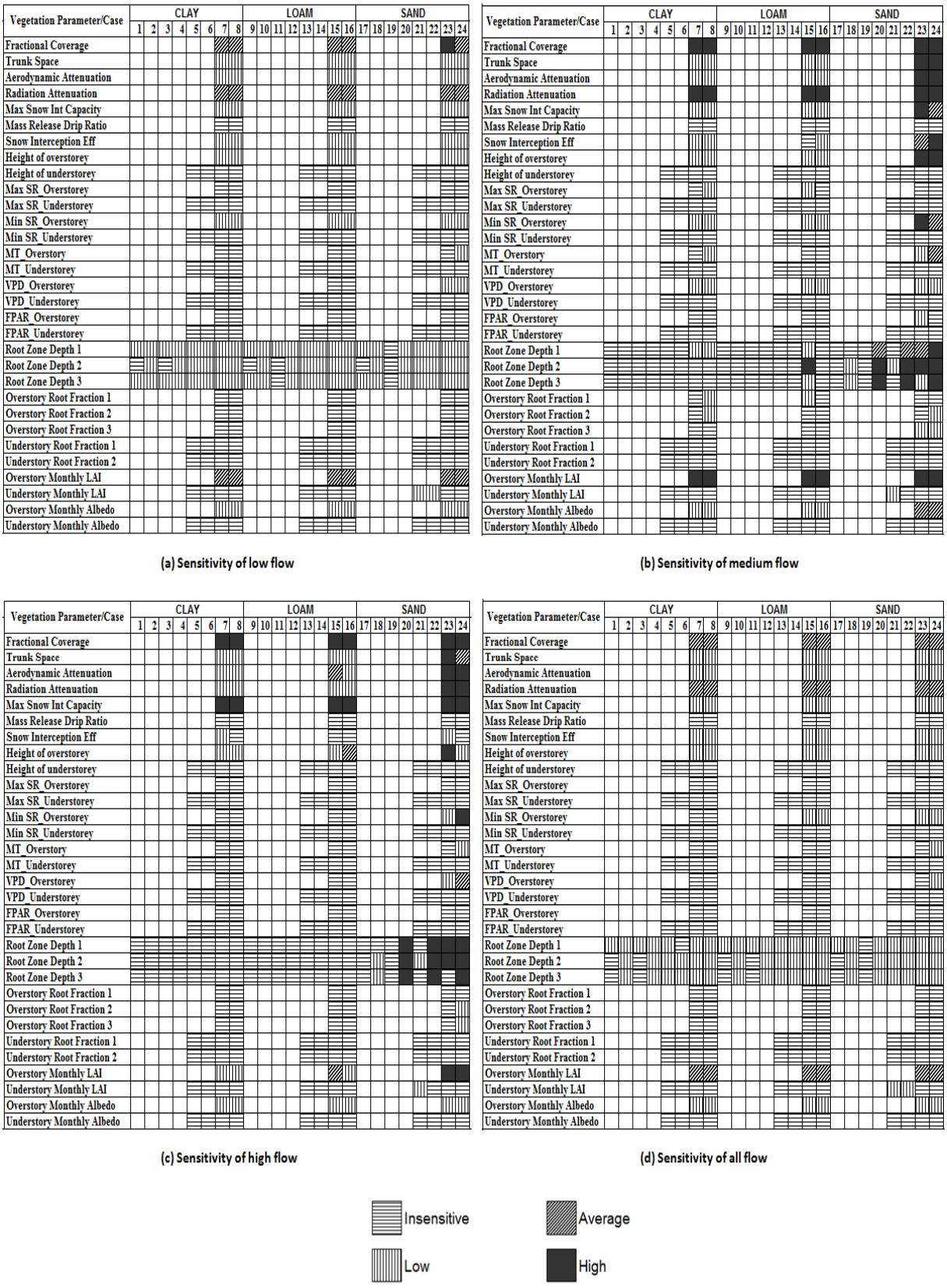

Figure 4-6 Sensitivity of DHSVM hydrograph simulations to vegetation parameters

4.4 Conclusions

The main objective of this study was to assess the sensitivity of different outputs of DHSVM to soil and vegetation parameters. The OFAT sensitivity analysis method was used for this purpose by considering virtual catchments representing twenty four different land surface characteristics. The effects of slope and soil depth on the outputs of the model were also assessed.

Outputs of the simulation are in general agreement with results reported in literatures for hillslope scale studies. The study enabled to identify the relative influence of parameters of the model on different outputs. Use of the identified parameters in the calibration of the model for real catchments could be noted.

The fact that actual catchments are large and complex may result in some variations to the outcomes of the assessment when applied to real world problems. Nonetheless, the results can be used as a guide to calibrate parameters of the model. They could also be taken as screening level results for making further analysis using global sensitivity method.

The findings of the study can be particularly useful in making better runoff simulations by adjusting few influential parameters. Soil depth can be considered as an important calibration parameter for adjusting low flows in different soil types. Porosity and saturated lateral hydraulic conductivity can be used as calibration parameters in coarse, medium and forest-covered fine textured soils. Vegetation parameters are influential in forest-covered surfaces with fractional coverage, radiation attenuation and leaf area index showing greater effect in all soil types. Adjustment of additional soil and vegetation parameters may be required in coarse textured soils.

Chapter 5

5 DHSVM Input Data Creation for Lake Tana Basin

5.1 Introduction

Hydrological modeling using DHSVM was done at temporal and spatial resolutions of 1 hour and 90 m, respectively. The available and derived hydro-meteorological and spatial datasets were processed using different techniques and tools to create the input files at the required resolutions and formats (Figure 5-1). This chapter presents the methodologies employed in the creation of these input datasets and parameterization of the distributed hydrological model. Meteorological forcings at a temporal resolution of one hour were created by disaggregating the daily data series. The specific disaggregation techniques used for the various meteorological elements is discussed in relevant sections. Spatial datasets and initial model state files were created in the required format using relevant GIS tools and executable programs supplied with the DHSVM source code. The methods used in assigning *a priori* values for soil and vegetation parameters are also presented.

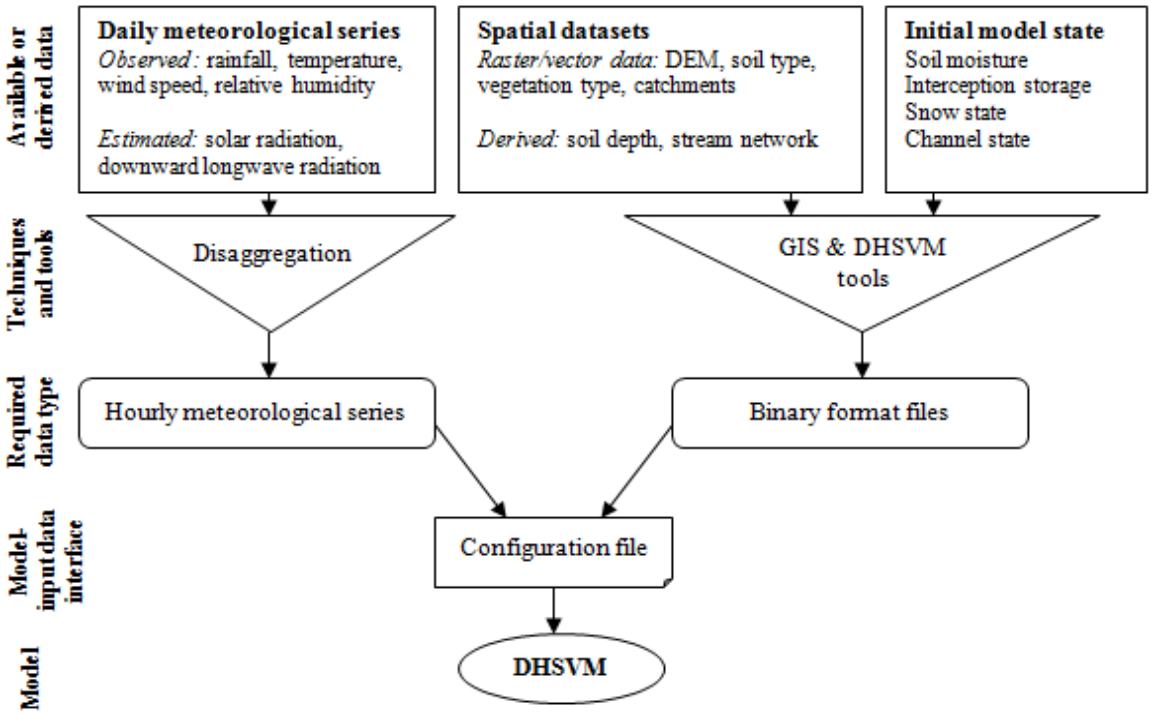

Figure 5-1 Required input files for DHSVM

5.2 Weather data disaggregation

The weather data required by the model include rainfall, temperature, wind speed, relative humidity, shortwave radiation, and downward longwave radiation. Observed daily time series for the first four meteorological elements are available. Daily solar radiation and downward longwave radiation were estimated by empirical equations that relate these variables to temperature, which has a relatively better coverage in the study area. The observed and estimated daily meteorological time series were then disaggregated into hourly time scale using appropriate techniques that are presented in the following sections. The use of weather data disaggregation techniques to generate meteorological forcings at finer temporal resolution for simulating hydrological processes is common (Bormann *et al.,* 1997; Waichler and Wigmosta, 2002; Debele *et al.,* 2007).

5.2.1 Rainfall

This section represents part of a paper submitted to Journal of Hydrology for publication (Engida and Esteves, 2010). The revised manuscript is presented in Annex A.

Rainfall disaggregation models are used to obtain rainfall time series at subdaily scale from daily values. The different approaches of rainfall disaggregation can be classified into four groups (Onof *et al.,* 2000): complex process-based meteorological models, multi-scale stochastic models such as multi-fractal cascades, statistical models developed on the bases of observed statistics and point-process stochastic models. The commonly used point process stochastic models are the Bartlett-Lewis and Neyman-Scott cluster models. The point-process models have practical advantage of summarizing the many rainfall characteristics by few parameters and representing the hierarchical nature of rainfall structure conveniently (Onof *et al.,* 2000).

In this study, the Modified Bartlett-Lewis Rectangular Pulse Model (MBLRPM) was used to generate hourly rainfall series from daily data. The MBLRPM has got relatively wider applications in different climates with reported good performance levels (Glasbey *et al.,* 1995; Khaliq and Cunnane, 1996; Smithers *et al.,* 2002; Campo *et al.,* 2008). Figure 5-2 illustrates how rainfall processes are represented in the model (Rodriguez-Iturbe *et al.*, 1988; Koutsoyiannis and Onof, 2001). Storms are assumed to originate at times $\mathbf{t_i}$ following a Poisson process at a rate λ; each storm is then assumed to generate rain cells at times $\mathbf{t_{ij}}$ according to a Poisson process at a rate β; Generation of cells corresponding to a storm

terminates after a time $\mathbf{x_i}$ that is exponentially distributed with parameter γ. Rain depth of each cell $\mathbf{y_{ij}}$ is a random constant exponentially distributed with mean μ_x. Each cell has a random duration $\mathbf{x_{ij}}$ that is exponentially distributed with parameter η which is assumed to vary from storm to storm with a gamma distribution having a scale and shape parameters of α and ν, respectively. The parameters β and γ are also made to vary with storms so that $\kappa = \beta/\eta$ and $\phi = \gamma/\eta$ remain constant. The rainfall amount in any time interval T is then represented by the sum of all active cells in that period. The model equations are indicated in Annex A.

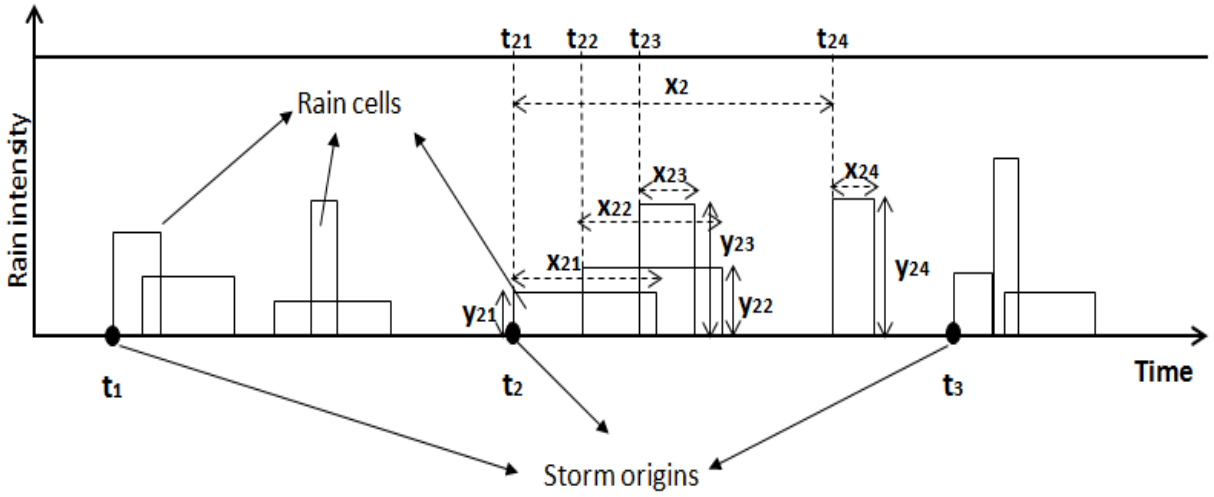

Figure 5-2 Rainfall process as assumed in the MBLRPM

5.2.1.1 Evaluating the performance of MBLRPM

The applicability of the MBLRPM to the rainfall pattern of the study area was first evaluated based on the available limited hourly data of Bahir Dar and Gonder meteorological stations. The six parameters of the MBLRPM were estimated using the method of moments where non-linear equations that relate observed and analytical moments are solved simultaneously. Inclusion of moments that describe depth processes and dry probabilities are deemed to be necessary in order to arrive at reasonable parameter values (Onof and Wheater, 1993). Based on the recommendation of Khaliq and Cunnane (1996), the model parameters were determined from more moment equations than the number of unknowns. The moments included mean, variance, lag-1 autocovariance and dry probabilities for different levels of aggregation.

Many applications of the model recommend inclusion of subdaily rainfall statistics in the estimation of the model parameters (Khaliq and Cunnane, 1996). In this study the estimation was done based on two sets of rainfall statistics depending on the relative length of available hourly rainfall records. For the main wet months, i.e. June, July, August, and September, rainfall statistics calculated from 1-, 6-, 24- and 48-hours historical data were used to estimate the model parameters. For the other months the estimation was based on only 24- and 48-hours rainfall statistics as the length of the hourly data is very short. There are studies which estimate parameters of the model from 24- and 48-hours rainfall statistics and yet conclude good performance of the model. Bo and Islam (1994) are able to infer satisfactorily subdaily rainfall statistics from 24 hours and 48 hours data. Similarly, Campo *et al.* (2008) reasonably infer 10 min, 30 min, 1 hours, 2 hours, 6 hours and 12 hours rainfall statistics using parameters estimated from accumulated 24- and 48-hours rainfalls. Successful parameter estimation is also reported by Smithers *et al.* (2002) who make the determination with and without subdaily rainfall statistics. The optimum parameter values of the MBLRPM for each station are presented in Annex A.

Disaggregation of the observed daily rainfall into hourly series was then done using the computed optimum parameter values. A repetition technique with proportional adjustment was followed during the disaggregation to ensure that daily rainfall equals the sum total of disaggregated hourly rainfalls. This method is recommended by Koutsoyiannis and Onof (2001) and is incorporated in a disaggregation model developed by Gyasi-Agyei (2005). The approach enables to obtain consistent finer time scale rainfalls by distributing the error proportionally to each of the disaggregated results. A computer program called Hyetos[6] in which the Bartlett-Lewis model and the adjusting procedures are implemented (Koutsoyiannis and Onof, 2000) was employed in the disaggregation. Debele *et al.* (2007) reported very good performance of the model in disaggregating daily rainfall data into hourly data.

The direct outputs of the MBLRPM did not match well the average diurnal rainfall pattern of the study area during the main wet season (See Figure 5-3 for Bahir Dar). The performances of the model as measured by the mean square error (MSE) varied from 15% to 25%. Similarly, poor performance was noted for Gonder meteorological station. The MBLRPM stochastically generated rainfalls at any hour of the day following the Poisson process. This resulted in a mismatch between the observed and disaggregated rainfalls during the morning day hours which hardly receive rainfall. Rainfall in the study region is convective and most of

[6] http://www.itia.ntua.gr/en/softinfo/3/

it occurs in the afternoon and night hours (Nyssen *et al.* 2005; Haile *et al.*, 2009). Outputs of the MBLRPM were, therefore, stochastically redistributed to mimic the diurnal rainfall pattern of the study area.

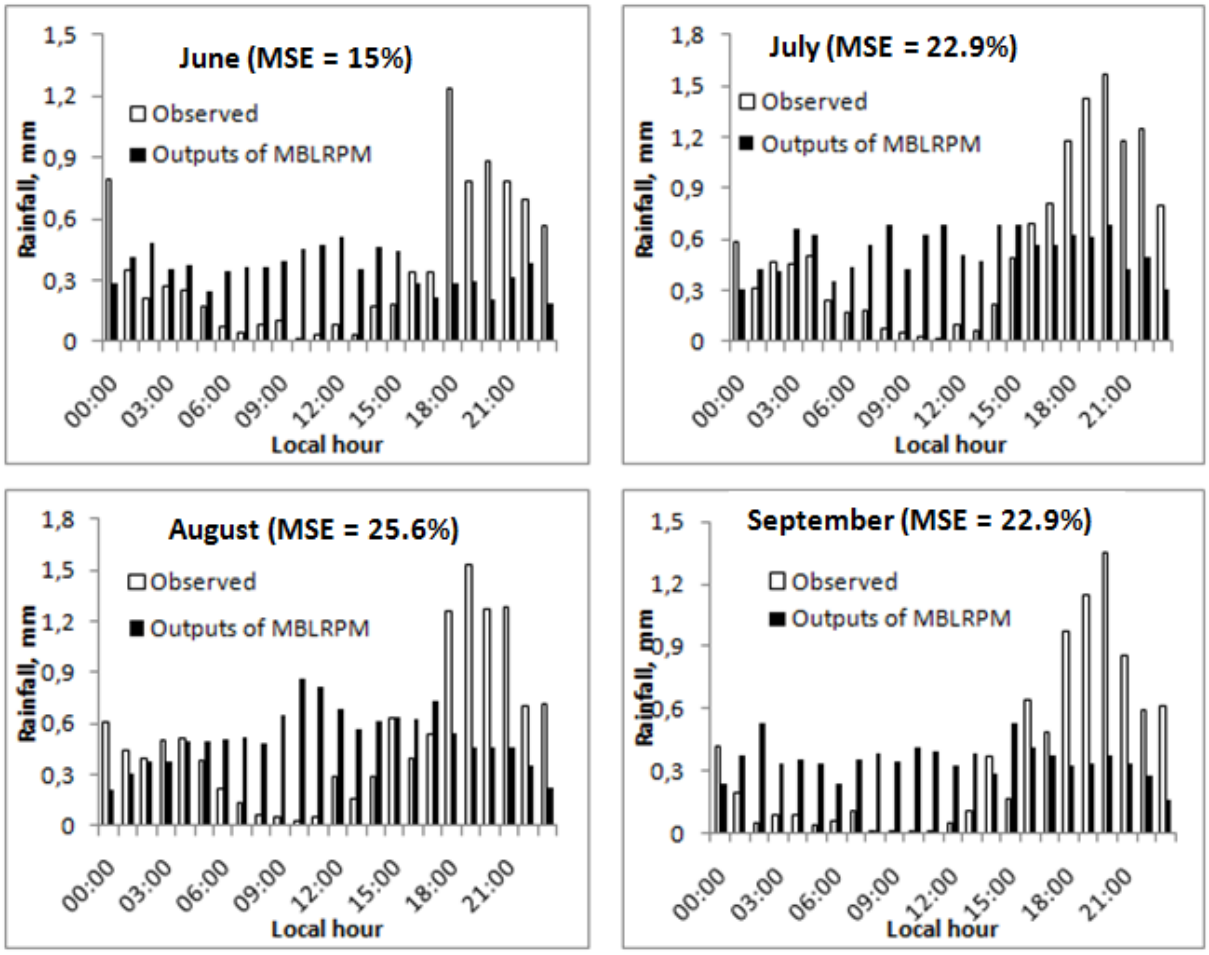

Figure 5-3 Comparison between observed and disaggregated mean hourly rainfall of Bahir Dar station for the wet months. The mean square errors (MSE) are also indicated.

5.2.1.2 Adjustment of the MBLRPM outputs

Stochastic redistribution of the direct outputs of MBLRPM was done using Beta distribution function (Equation 5-1) which was found to better describe the diurnal rainfall patterns of Bahir Dar and Gonder meteorological stations. During the main rainfall season, the daily rainfall pattern at Bahir Dar and Gonder meteorological stations showed a Beta distribution starting from 11:00-13:00 hour local time (See Figure 5-4 for Bahir Dar). Use of Beta probability distribution function to simulate rainfall occurrence time in a day could be found in the literature (Hershenhorn and Woolhiser, 1987; Connolly *et al.,* 1998).

$$f(t;a,b)=\frac{\Gamma(a+b)}{\Gamma(a)\Gamma(b)}t^{a-1}(1-t)^{b-1} \quad \text{for } 0<t<1, a>0, b>0$$
$$=0 \quad \text{otherwise}$$

Equation 5-1

Where t is scaled hour of the day between 0 and 1; a = scale parameter; b = shape parameter.

The optimum parameters of the Beta probability distribution function could be estimated from the mean and variance of the observed hourly rainfall occurrence hours using Equation 5-2. The estimated average Beta distribution parameters for Bahir Dar were a = 2.8 and b = 3.8 and that for Gonder were a = 2.0 and b =3.7.

$$E(t)=\frac{a}{a+b}$$

Equation 5-2

$$Var(t)=\frac{ab}{(a+b+1)(a+b)^2}$$

Where E(t) is the mean rainfall occurrence hour; Var(t) is the variance of the rainfall occurrence hour, i.e., $E(t^2)$-$[E(t)]^2$.

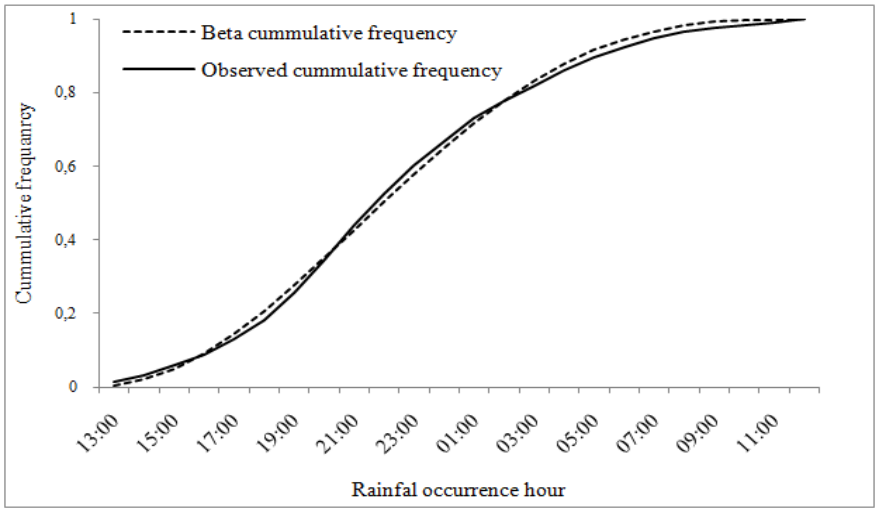

Figure 5-4 Typical distribution of rain start hour for Bahir Dar station

The redistribution was done by generating a scaled random rainfall occurrence hour from the Beta distribution. The redistributed hourly rainfall showed a better fit to the observed data as indicated by the relatively smaller MSE values and the graphical similarity (See Figure 5-5 for Bahir Dar station). Similar improvements could be obtained for Gonder meteorological

station. See Annex A for more results and discussions on the performance of the MBLRPM and its subsequent adjustments using the Beta distribution.

For the other stations the rainfall disaggregation was done following the same procedure. The Beta distribution parameters of either Bahir Dar or Gonder were used for the redistribution depending on which station is close to the station concerned.

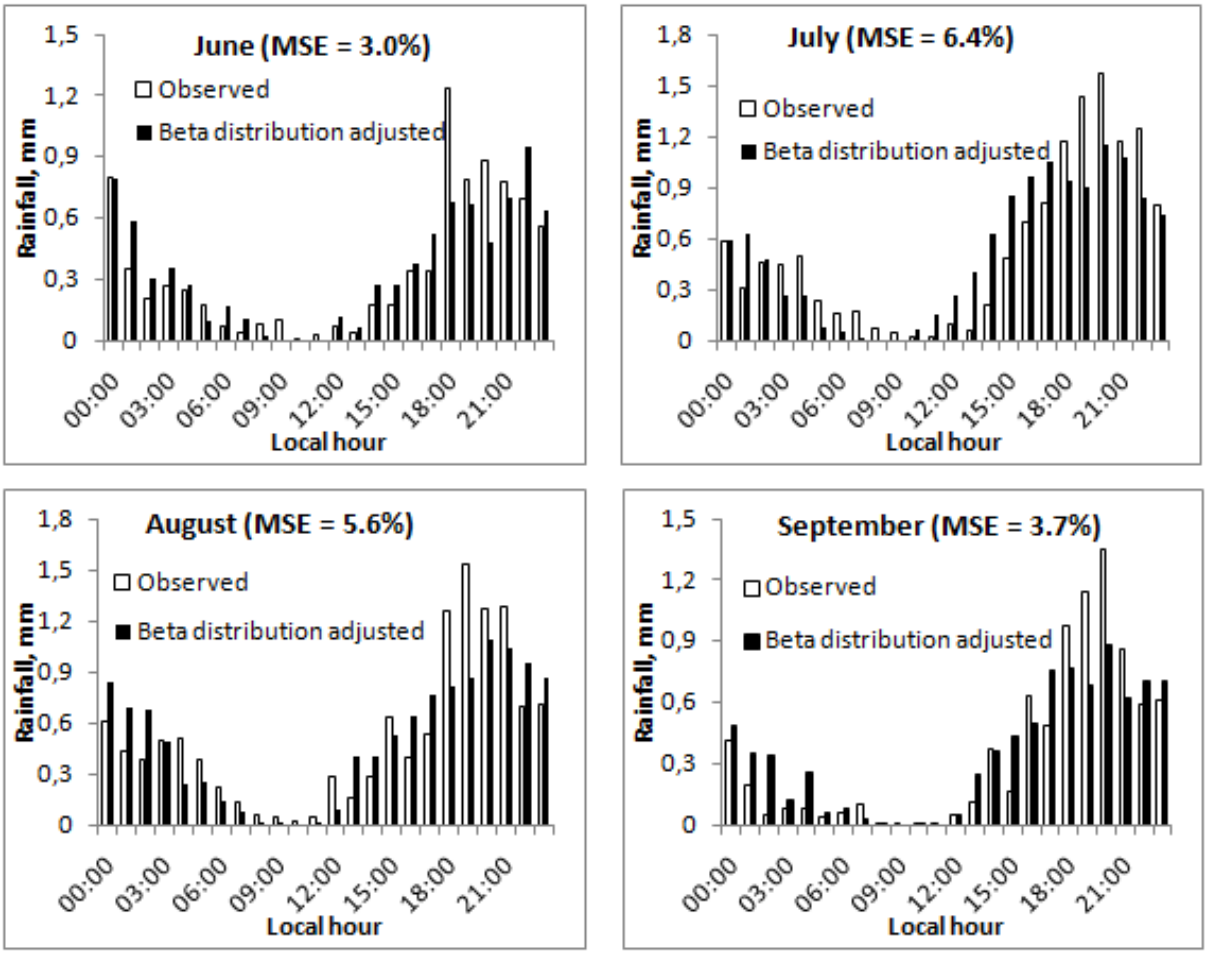

Figure 5-5 Comparison between observed and disaggregated hourly rainfall after adjustment. Bahir Dar, for the main rainy season.

5.2.2 Temperature

Observed temperature data at most meteorological stations is often limited to daily minimum and maximum records. Simple to complex disaggregation models are, therefore, usually used to determine the diurnal temperature pattern. The methods that are in use include simpler models based on sinusoidal curves or Fourier analysis and complex energy balance relations (Reicosky *et al.,* 1989; Sadler and Schroll, 1997). The simpler methods have a practical advantage of using commonly available daily minimum and maximum temperature observations (Sadler and Schroll, 1997). In this study the daily air temperature was

disaggregated using a sinusoidal model originally proposed by De Wit (1978). This model has got different applications with reported good performance levels (Baker, 1988; Bilbao *et al.*, 2002; Debele *et al.*, 2007). The model uses three sinusoidal segments to connect the times of minimum and maximum daily air temperatures. The temperature at any hour t is then calculated using the following equations.

$$T(t) = \frac{T_{min} + T_{max}}{2} - \frac{T_{max} - T_{min}}{2} \times \cos\left(\pi \frac{t - t_{max} + 24}{t_{min} - t_{max} + 24}\right) \quad 1 \le t \le t_{min} \qquad \textbf{Equation 5-3}$$

$$T(t) = \frac{T_{min} + T_{max}}{2} - \frac{T_{max} - T_{min}}{2} \times \cos\left(\pi \frac{t - t_{min}}{t_{max} - t_{min}}\right) \quad t_{min} \le t \le t_{max} \qquad \textbf{Equation 5-4}$$

$$T(t) = \frac{T_{min} + T_{max}}{2} - \frac{T_{max} - T_{min}}{2} \times \cos\left(\pi \frac{t - t_{max}}{t_{min} - t_{max} + 24}\right) \quad t_{max} \le t \le 24 \qquad \textbf{Equation 5-5}$$

Where, T(t) is temperature at any hour t in °C; T_{min} is minimum daily temperature in °C; T_{max} is maximum daily temperature in °C; t_{min} and t_{max} are hours at which minimum and maximum daily temperatures occur, respectively.

Minimum and maximum temperatures of a day are assumed to occur at 06:00 and 15:00 hours, respectively. These hours correspond to the minimum and maximum temperature observation hours of the Ethiopian National Meteorological Agency. The average diurnal temperature patterns for Class 1 stations that are located within the basin are indicated in Figure 5-6. Due to lack of observed hourly temperature data, it was not possible to check the performance of the disaggregation model.

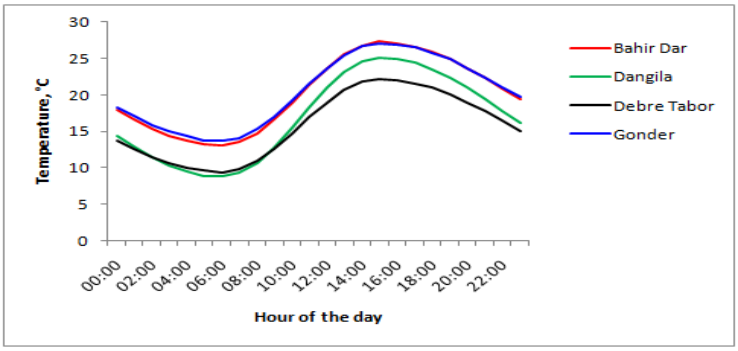

Figure 5-6 Average diurnal temperature pattern of four Class 1 stations in the Lake Tana basin (Based on disaggregated daily data).

5.2.3 Wind speed

Wind speed disaggregation models include direct use of the average daily wind speed (Waicheler and Wigmosta, 2002), curve-fitting like cosine function (Debele *et al.,* 2007) or simple random distribution-based model (Neitsch *et al.,* 2001). In this study disaggregation of daily wind speed was done using a simple random distribution-based model given in Equation 5-6. A similar method is incorporated in the Soil and Water Assessment Tool (SWAT) model for calculating daily wind speed from monthly values (Neitsch *et al.,* 2001). Debele *et al.* (2007) used this model to disaggregate daily wind speed into hourly data and obtained reasonable results.

$$w_h = w_d\left[-\ln\left(rnd[0,1]\right)\right]^{0.3} \qquad \textbf{Equation 5-6}$$

Where, w_h is estimated hourly wind speed, m/s; w_d is mean daily wind speed, m/s and *rnd*[0,1] represents a random number between 0 and 1.

The disaggregation resulted in a longterm average diurnal pattern that closely matched the longterm mean daily wind speed. However, a notable variation in hourly wind speed could be seen in any single day. For instance, the average range of wind speed in a day was 1.7 m/s for Gonder and 0.7 m/s for Bahir Dar. The diurnal wind speed pattern for a typical day at Gonder meteorological station is shown in Figure 5-7. Lack of observed hourly wind speed data could not allow assessment of the performance of the disaggregation.

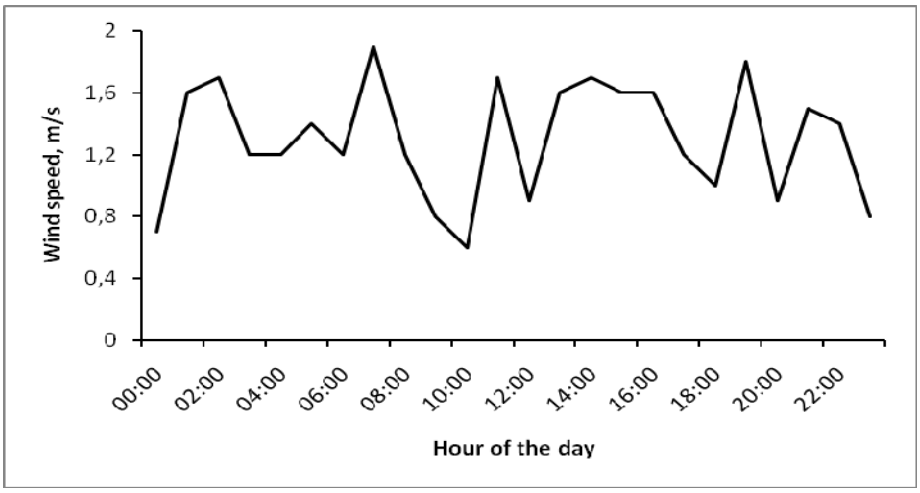

Figure 5-7 Diurnal wind speed pattern on a typical day at Gonder (Based on disaggregated daily data)

5.2.4 Relative humidity

Disaggregation of relative humidity was done using Equation 5-7. The method requires data on dew point temperature and hourly ambient air temperature. The daily minimum temperature is usually taken as a surrogate of dew point temperature or it is estimated from regression equations developed from observed minimum and maximum daily temperatures (Hubbard *et al.*, 2003; Andersson-Sköld *et al.*, 2008). In this study, use of daily minimum temperature as dew point temperature was first tested. The disaggregated hourly temperature series obtained from Section 5.2.2 were taken as the ambient air temperature.

$$RH(t) = \frac{e_d}{e_a} \times 100\% \qquad \textbf{Equation 5-7}$$

Where e_d and e_a are vapor pressures at dew point and ambient air temperatures, respectively. They can be computed from known temperature values using Equation 5-8.

$$e = 0.611 \exp\left(\frac{17.27T}{237.3 + T}\right) \qquad \textbf{Equation 5-8}$$

Where, T in °C is dew point temperature for e_d and ambient air temperature for e_a.

The disaggregated relative humidity at 12:00 and 18:00 hours were compared against five year observations (1999-2003) made at Bahir Dar, Dangila, Debre Tabor and Gonder stations. The performance of the disaggregation as measured by the Nash-Sutcliffe efficiency was found to vary from 0.22 for Dangila to 0.31 for Bahir Dar. This poor performance may be related to the use of minimum temperature as dew point temperature. Although this assumption is often used, its unsuitability in sites with arid and semi-arid climate characteristics is also reported (Kimball *et al*., 1997). Regression based desegregation models were also tried but they did not show better performance. The diurnal pattern of relative humidity is illustrated in Figure 5-8.

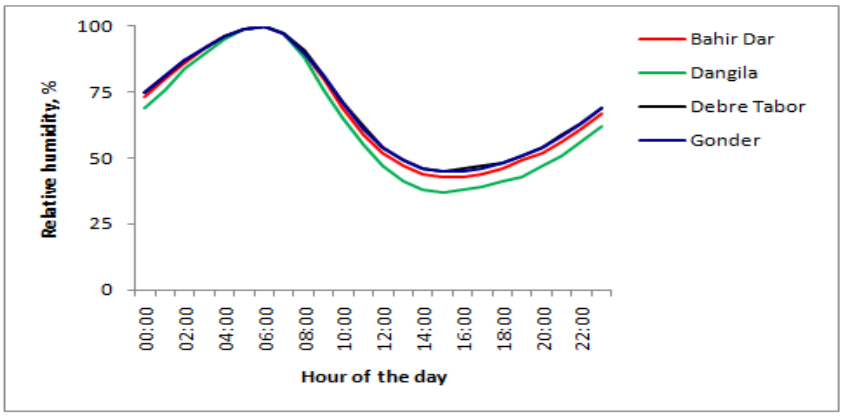

Figure 5-8 Mean diurnal pattern of relative humidity in the Lake Tana basin (Based on disaggregation of daily average values)

5.2.5 Solar radiation

In DHSVM solar radiation data is involved in the simulation of snow melt and evapotranspiration processes. Hourly solar radiation data was determined by disaggregating estimated daily solar radiation. As direct observation of daily solar radiation is limited, it is often estimated from sunshine hour or temperature measurements (Podesà *et al.*, 2004). One commonly used simpler method is the Angström–Prescott (A-P) equation which requires data on daily sunshine hour (Liu *et al.,* 2009). As discussed in Chapter 3 the spatial coverage of sunshine hour data in the study area is highly inadequate. An alternative method that makes use of temperature data, which has a relatively better spatial and temporal coverage, was therefore employed. The Hargreaves equation (Equation 5-9) is one such method that enables estimation of global solar radiation from observed minimum and maximum daily temperatures. The method has got applications in data sparse regions with reported good performance levels (Chineke, 2008). The daily solar radiation obtained from the Angström–Prescott and the Hargreaves equations were compared for Bahir Dar station and the results are indicated in Figure 5-9. The coefficients of the Angström–Prescott equation used were a = 0.385 and b = 0.348 as reported in Mulugeta and Drake (1996). It appeared that the two methods give comparable estimates of daily solar radiation.

$$R_{sd} = 0.16 R_e \left(T_{\max} - T_{\min}\right)^{0.5} \qquad \textbf{Equation 5-9}$$

Where, R_{sd} is daily solar radiation in MJ/m^2; R_e is extraterrestrial solar radiation in MJ/m^2 and T_{min} and T_{max} are minimum and maximum temperatures, respectively, in °C.

The extraterrestrial solar radiation is a function of latitude, day of the year, solar declination, and solar constant (Alam *et al.*, 2005).

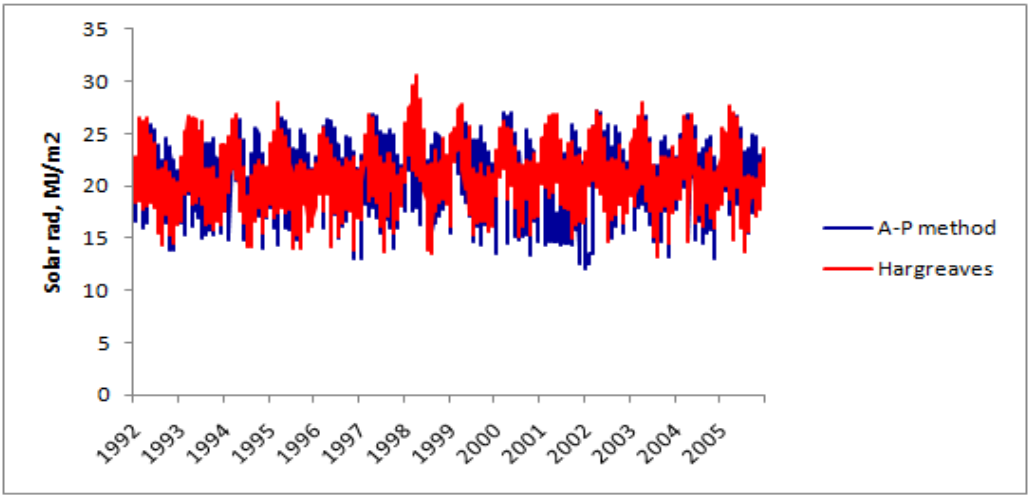

Figure 5-9 Comparison of daily solar radiation values computed by the A-P and Hargreaves equations at Bahir Dar meteorological station for the period 1992-2005.

The estimated daily solar radiation was then disaggregated into hourly data using Equation 5-10. This method is proposed by Kaplanis (2006) and is considered to be good in generating hourly solar radiation values that can closely match the observed data.

$$R_s(t) = a_i + b_i \cos\left(\frac{2\pi t}{24}\right) \qquad \textbf{Equation 5-10}$$

Where, $R_s(t)$ is the hourly solar radiation in W/m^2; t is the hour at which solar radiation is computed which varies from 00:00 to 23:00; a_i and b_i are constants to be determined for each day.

The two constants, a_i and b_i, were calculated for each day from two boundary conditions given by Equations 5-11 and 5-12.

$$R_{sd} = a_i\left(t_{ss} - t_{sr}\right) + b_i \times \frac{24}{\pi}\sin\left(\frac{\pi t_{ss}}{12}\right) \qquad \textbf{Equation 5-11}$$

$$0 = a_i + b_i \cos\left(\frac{\pi t_{ss}}{12}\right) \qquad \textbf{Equation 5-12}$$

The parameters t_{sr} and t_{ss} represent, respectively, sunrise and sunset hours of a particular day. They can be computed as a function of latitude and solar deflection angle. Equation 5-5b ensures equality of the sum total of hourly solar radiation to the daily global solar radiation. The second boundary condition ensures that the solar radiation at sunrise and sunset equals zero. The two equations were solved simultaneously on each day to determine the constants. The average diurnal solar radiation pattern for Class 1 stations is indicated in Figure 5-10. No solar radiation data could be obtained to evaluate the performance of the disaggregation.

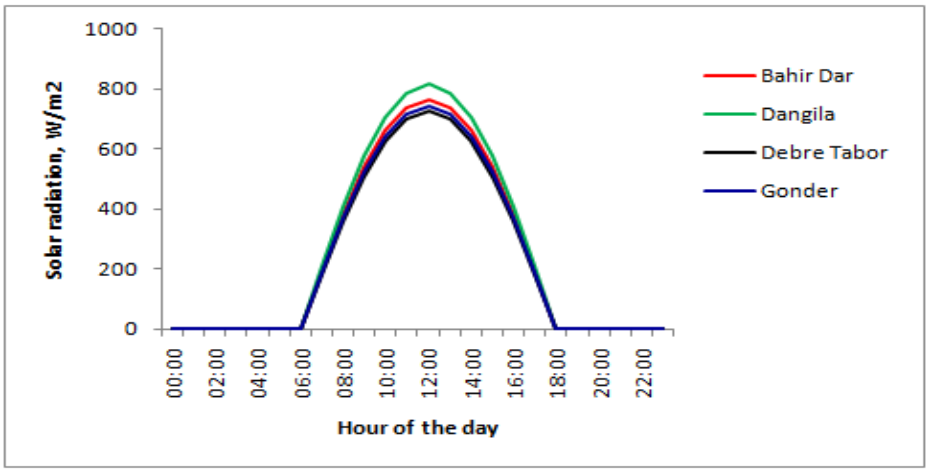

Figure 5-10 Average diurnal pattern of solar radiation in the Lake Tana basin (Based on disaggregation)

5.2.6 Downward longwave radiation

The distributed hydrological model requires data on downward longwave radiation to compute the energy balance. Because, direct measurement of downward longwave radiation is difficult and expensive, it is often estimated with radiation models that use readily available air temperature and/or humidity data (Duarte *et al.*, 2006). Clear sky downward longwave radiation is usually computed by a relation given in Equation 5-13.

$$R_{lc}\downarrow = \varepsilon_{ac}\sigma T^4 \qquad \textbf{Equation 5-13}$$

Where, R_{lc} is clear sky downward longwave radiation, in W/m^2; ε_{ac} is effective clear-sky atmospheric emissivity; σ represents the Stefan–Boltzmann's constant (5.67×10^{-8} $Wm^{-2}K^{-4}$); T is air temperature near the ground surface in Kelvin.

Different methods are available for estimating the atmospheric emissivity as a function of temperature and/or humidity. Considering the availability of data in the study area, the simpler Idso and Jackson (1969) method was selected (Equation 5-14). The method uses only air temperature as input and it has got applications associated with evapotranspiration and soil moisture dynamics studies (Brandes and Wilcox, 2000; Ward and Trimble, 2004). Moreover, after having compared the performance of five simpler models under clear and cloudy sky conditions, Finch and Best (2004) considered this method as the best choice.

$$\varepsilon_{ac} = 1 - 0.261 \exp\left[-7.77 \times 10^{-4} (273 - T)^2\right] \qquad \textbf{Equation 5-14}$$

Where, T is temperature in °K.

In reality the sky is covered by cloud and this increases the amount of longwave radiation reaching the ground surface. Therefore, the clear sky downward longwave radiation should be adjusted for cloud cover. A method proposed by Sugita and Brutsaert (1993) was used in this study. Accordingly, the actual downward longwave radiation in the presence of cloud cover (R_{la}) was estimated by Equation 5-15.

$$R_{la} \downarrow = R_{lc} \downarrow \left(1 + 0.0496 C^{2.45}\right) \qquad \textbf{Equation 5-15}$$

Where, C is fractional cloud cover. As this data is not available, a method suggested by Crawford and Duchon (1999) was used to estimate it from global and extraterrestrial solar radiation (Equation 5-16). Use of this method in estimating cloud fraction where observed data is lacking could be found in the literature (Duarte *et al.*, 2006; Kruk *et al.* 2010).

$$C = 1 - \frac{R_s}{R_e} \qquad \textbf{Equation 5-16}$$

Where, R_s and R_e are global and extraterrestrial solar radiations, respectively, in MJm^{-2}.

The hourly downward longwave radiation was directly computed using the disaggregated hourly temperature. The average diurnal downward longwave radiation pattern is presented in Figure 5-11.

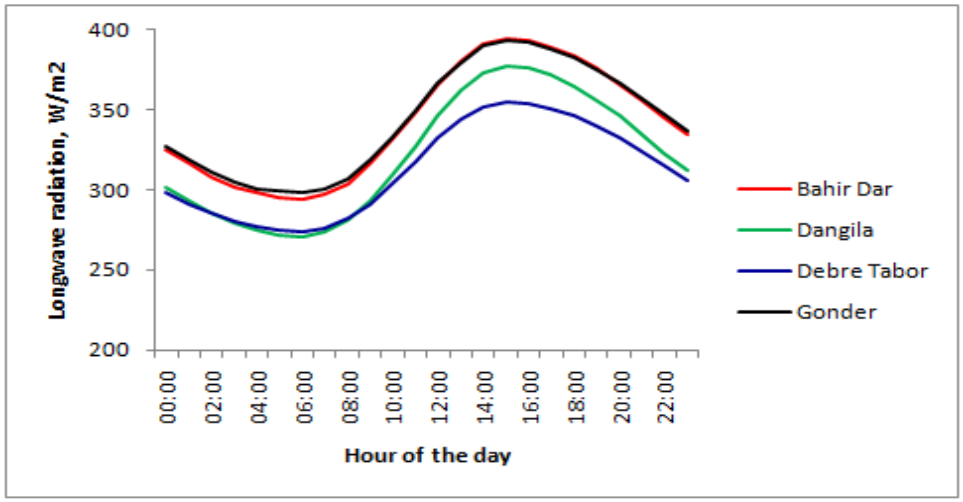

Figure 5-11 Mean diurnal pattern of downward longwave radiation in the Lake Tana basin (based on disaggregation)

5.3 Spatialization of meteorological data

DHSVM solves water and energy balance equations at grid scale, which in this study was 90 m by 90 m. As the meteorological forcings were not available at this fine grid scale, they had to be spatialized by interpolation from the observed values. The model has built-in alternative interpolation methods that include nearest neighbor, inverse distance and Cressman techniques. In this study the nearest neighbor method was selected and all rainfall stations that had influence on any single pixel of a simulation catchment were involved. In case the rainfall station lacks data on other meteorological elements, time series obtained by interpolation from neighboring stations was used. Accordingly, the meteorological stations involved in the interpolation per catchment were determined as shown in Table 5-1.

Table 5-1 Meteorological stations used for simulation catchments in the Lake Tana basin

Gauged catchment	Meteorological stations used
Megech	Amba-Giorgis, Gonder, Maksegnit, Shebekit
Rib	Adis Zemen, Debre Tabor, Enfraz, Wereta, Yifag
Gumara	Debre Tabor, Wanzaye, Wereta
Gilgel Abay	Adet, Dangila, Engibara, Meshenti, Sekela

5.4 Creation of spatial datasets

DHSVM requires certain spatial datasets in binary format. These datasets include DEM, maps of soil and vegetation types, catchment-specific mask file, and soil depth map. In addition to these maps, stream network files are required. A brief presentation of the procedures followed in creating these files is presented below.

5.4.1 Soil and land cover maps

The soil and land cover maps obtained from the MoWR have coarse resolutions. This is evident from the representation of the basin by few soil and land cover types. The great majority of the basin is designated as cropland with four soil types and this appeared to be against the natural heterogeneity of the land surface. Soil types were differentiated based on the FAO-UNESCO classification system as obtained from the MoWR. A suitable classification system, however, was followed for land cover types. The original classification gives very general classes like 'dominantly cultivated', 'moderately cultivated', etc. which were found to be inconvenient for the parameterization of vegetation properties. Consequently, a better classification system based on the IGBP-DISCover land cover legend was adopted. The IGBP-DISCover legend comprises 17 classes and has been used in global-scale modeling of climate, biogeochemistry and other Earth system processes (FAO, 2000; ISLSCP, 2009). Data on the percentage distribution of specific land cover types was used in the classification and the final outcome was a basin-wide land cover map with eleven classes.

5.4.2 Soil depth

As data on soil depth in the study area is highly limited, a method that relates soil depth to basic topographic attributes was used. Because information on soil depth is usually lacking, its derivation from digital elevation data is common (Boer *et al.*, 1996; Ziadat, 2010). In this study soil depth at grid scale was estimated using a regression equation provided with the DHSVM source code (Westrick, 1999). The formula (Equation 5-17) relates soil depth to slope, upslope contributing area, and elevation. All these basic topographic attributes could be derived from the digital elevation data. Maximum values of these topographic attributes at which they cease to have effect on soil depth are also required. Values of the parameters used

for the soil depth calculation are presented in Annex C-2. The computed soil depth map is indicated in Figure 5-12.

Soil depth map at grid scale was created in a GIS environment by writing an appropriate batch file. A binary map of soil depth was created following the procedure discussed in the next section.

$$Sd_{ij} = Sd_{\min} + (Sd_{\max} - Sd_{\min}) \times \left[a\left(1 - \frac{S_{ij}}{S_{\max}}\right)^{A} + b\left(1 - \frac{A_{ij}}{A_{\max}}\right)^{B} + c\left(1 - \frac{Z_{ij}}{Z_{\max}}\right)^{C} \right] \quad \textbf{Equation 5-17}$$

Where Sd_{ij} is soil depth at any point; Sd_{min} and Sd_{max} are minimum and maximum soil depth limits, respectively; S_{ij} and S_{max} are local and maximum slopes, respectively; A_{ij} and A_{max} represent local and maximum upslope areas, respectively; Z_{ij} and Z_{max} indicate local and maximum elevations, respectively; a, b and c are weights; A, B and C are exponents. Optimum weights and exponents could be determined from field data, if available.

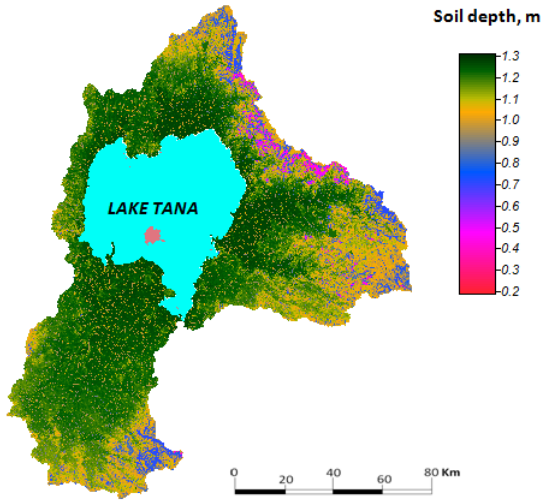

Figure 5-12 Soil depth map of Lake Tana basin derived from topographic attributes

5.4.3 Binary maps

All maps that were in shapefile format (soil and vegetation types and individual catchment boundaries) were first converted to raster data format in SAGA[7] GIS environment. These raster grids, the soil depth map and the 90-m digital elevation model were then converted to ascii data format in the GIS environment. Finally, the required files in binary format were

[7] SAGA (**S**ystem for **A**utomated **G**eoscientific **A**nalyses) is a free open source GIS software and can be downloaded from http://www.saga-gis.org/en/index.html

created from the ascii files using the relevant executable program provided at the DHSVM official web site[8].

5.4.4 Stream files

The stream network files required by the model are three- stream class, stream network map and stream network. These files are required for routing channel flows to the basin outlet. The files were created from DEM using MS-DOS executable program developed by Hydrowide, a company associated with Laboratoire d'Etude des Transferts en Hydrologie et Environnement (LTHE) and that has been active in developing modeling tools for DHSVM. The D8 algorithm was used to generate the stream networks and it was assumed that they have five orders with manning roughness coefficient of 0.035-0.060. This value for manning roughness is in the range recommended for natural streams. Streams were assumed to be created when the upslope contributing area exceeds 0.25 km^2. Typical vegetation and stream class inputs used for creating the stream files are given in Annex C-3.

5.5 Creation of initial model state files

Noto *et al.* (2008) stated the importance of defining initial models states carefully to better simulate watershed responses. The initial state files required by DHSVM include soil moisture, canopy interception, snow state and channel state. These files were created by the relevant executable programs downloaded from the official DHSVM web site. No snow fall is expected in the study area throughout the year. As the model start time was January, which is a dry month, initial soil moisture close to the field capacity was used. The decrease in soil moisture occurs very slowly once it reaches its field capacity (Dingman, 1994). The average catchment temperature at the model starting day was made to represent the soil surface temperature. As data on soil temperature of the root zone could not be found, it was calculated by adding 1°C to the ambient air temperature. Use of this assumption could be found in the Abay Master Plan study report (BCEOM, 1999c). Initial water depth of 0.1 m was assumed in the creation of the channel state file. To improve the initial state files, the model was run for a year using the state files created by the above procedures. The model state files obtained at the end of the one-year model run were used as initial state files for the calibration and validation

[8] ftp://ftp.hydro.washington.edu/pub/HYDRO/tools/dhsvm/DHSVMPC/executables/

of the model. Use of a similar approach in creating improved model initial states could be found in the literature (Refsgaard, 1997). The text file used for creating the initial model state files is presented in Annex C-4.

5.6 Parameterization of soil and vegetation properties

This section discusses the methods employed in assigning *a priori* parameter values for the fifteen soil and thirty-one vegetation properties. Measured parameter values for some soil hydraulic properties could be obtained from the Abay Master Plan study and other project-specific studies. These measured values were used directly or with some modifications as *a priori* parameter estimates. Moreover, for soil parameters without measured data relevant literatures and pedotransfer functions were used to estimate parameter values based on information on soil texture.

A priori saturated lateral hydraulic conductivity values were set by increasing the measured values to account for the difference between the scale of measurement and the larger scales at which hydrological processes take place. Saturated lateral hydraulic conductivities found in soil survey reports represent point scale measurements which usually underestimate the actual hillslope/watershed-scale values (Brooks *et al.*, 2004). This is related to difficulties in measurement setups and preferential flows that may become important at larger scales. Therefore, hillslope-scale saturated hydraulic conductivities could be one to two orders of magnitude greater than those obtained from point scale measurements (Brooks *et al.,* 2004). In assigning *a priori* saturated hydraulic conductivity, first average values of the reported point measurements were calculated for each soil type. The computed average values were then increased by one order of magnitude to obtain the *a priori* saturated hydraulic conductivities. The exponential rate of decrease of hydraulic conductivity was estimated from measured values at 60 cm and 100 cm depth.

As field data on vertical hydraulic conductivity of the soils could not be found, it was assumed to be one order of magnitude less than the saturated hydraulic conductivity. Brooks *et al.* (2004) found the vertical saturated conductivity as having this kind of relation with lateral conductivity.

Measured values of infiltration capacity and bulk density were directly taken as *a priori* estimates. The observed soil bulk densities were further used to estimate porosities of the various soil types. *A priori* values of field capacity and permanent wilting point were determined with the help of pedotransfer functions developed from available measurements

and the percentage of clay, silt and sand (Annex B-7). The regression coefficients of the pedotransfer functions were determined from the observed field capacity, permanent wilting point and soil texture values.

Parameter values of the remaining soil hydraulic properties were fixed from relevant literatures based on information on soil texture type (Rawls *et al.,* 1982; Sumner, 2000; Bonan, 2002; Kozak *et al.*, 2005). The sensitivity analysis results presented in the previous chapter indicated these parameters as having negligible or no influence on the various outputs of the model. Accordingly, the use of appropriate literature values could be reasonable.

As there are no measured data on the required properties of the different vegetation types of the study area, the values of the parameters were assigned by referring to relevant literatures (Vörösmarty *et al.,* 1989; Asner *et al.,* 2003; Xavier and Vettorazzi, 2003; Chen *et al.,* 2005; Cuo *et al.*, 2006; Thanapakpawin, 2006). For leaf area index and photosynthetically active radiation parameters, reference to MODIS satellite products was also made. For cropland/natural vegetation mosaics the average properties of the two land cover types were used.

The *a priori* parameter values for the various soils and land covers of the study area are given in the typical configuration file presented in Annex C-5. The values of the critical soil and vegetation parameters were further adjusted during the model calibration.

5.7 Creation of configuration file

The configuration file could be considered as an interface between the input datasets and the model. It is a text file which comprises different sections that describe the methods to be used by the model, the spatial and temporal extent and resolution for the modeling, locations of the input meteorological, spatial and initial state files, values of constants and parameters, and the types and locations of the output files. A typical configuration file for the Rib catchment is presented in Annex C-5.

5.8 Concluding remarks

The chapter presented various techniques employed in creating the various hydro-meteorological and spatial input files. Creation of good quality input datasets is a crucial step in hydrological modeling for reliable and useful outputs. Otherwise, the old adage, Garbage

in-Garbage out, would be the result. In this study effort has been exerted to create the input meteorological datasets from the quality-controlled observed time series using commonly used disaggregation techniques. The use of weather data disaggregation techniques can be considered as an important strategy to get fine resolution datasets. This is particularly true in developing countries where most of the existing data are found at coarse resolution and the potential for making observations at finer scales is low due to resource constraints. It is often difficult to get some spatial datasets like soil types and properties at the resolution of distributed hydrological model grids. Data from different sources including field measurements, use of remotely sensed data and pedotransfer functions could serve as good strategies in bridging the gap. In this study effort has been exerted to create the required spatial inputs from datasets obtained from limited observations and relevant literatures. In view of the highly heterogeneous nature of soil hydraulic properties, the coverage of the observed data could be considered as inadequate. The few influential soil and vegetation parameters identified through the sensitivity analysis could be used as calibration parameters to improve model simulation.

Chapter 6

6 Application of DHSVM to Selected Catchments in the Lake Tana Basin

6.1 Introduction

There has been a surge in the development and use of physically-based distributed hydrological models despite difficulties in their parameterization and calibration (Beven, 2001). Some of the scientific and practical reasons behind this include the need to better predict erosion and sediment transport in a catchment, and assessment of the hydrological impacts of changes in land use and catchment characteristics.

This chapter evaluates the performance of the distributed hydrology-soil-vegetation model in predicting streamflows on selected catchments in the study area. The application of the model to predict sediment yield was abandoned as it gave results that were unrealistically low when applied to catchments in the study basin and others. The team that is working actively on DHSVM at LTHE is trying to sort out and solve the problem. A brief literature review on calibration and validation of distributed hydrological models is made at the outset. This is followed by a detailed presentation on the calibration and validation of the model on Megech and Rib catchments. A modeling period of 14 years at a temporal resolution of 1 hour for Megech and 3 hours for Rib catchment was used. Reference to the results of the sensitivity analysis study presented in Chapter 4 was made in the calibration of the model parameters. The model inputs created using the different methods discussed in Chapter 5 were utilized.

6.2 Calibration and validation of models: Literature review

6.2.1 Calibration

Model calibration is done in order to arrive at parameter values that result in outputs which are in close agreement with observed quantities. In principle, a fully physically-based distributed hydrological model would not require calibration as it contains parameters which can be obtained from measurements (Refsgaard and Storm, 1996; Beven, 2001). The natural heterogeneity and complexity of catchment characteristics, however, make impractical and

impossible to take measurements at the scale required by a distributed model (Madsen, 2003; Ajami *et al*., 2004). For this reason model calibration is still a requirement for physically based distributed hydrological models for better simulation results. Unlike empirical and lumped conceptual models, however, the variation in parameter values is restricted to a relatively narrow interval during the calibration.

Two broad classes of model calibration can be identified- manual and automatic methods. Automatic calibration involves use of optimization algorithms that can identify optimum parameter sets that minimize an objective function. Several applications of this method in calibrating conceptual and distributed hydrological models could be found in the literature (Eckhardt and Arnold, 2001; Madsen, 2003; Ajami *et al*., 2004; Francés *et al*., 2007). In manual calibration adjustment to selected parameter values is done systematically until the difference between the model outputs and observed quantities is within acceptable range. The manual methods are time consuming and demand a skilled modeler (Francés *et al*., 2007). This weakness of manual calibration methods can, however, be overcome by following systematic approaches like the one proposed by Vieux and Moreda (2003).

6.2.2 Validation

Model validation is the process of demonstrating that a given site-specific model is capable of making accurate predictions for periods outside the calibration period (Refsgaard, 1997). A model is said to be validated if its accuracy and predictive capability in the validation period is proved to be within acceptable limits or errors. Klemeš (1986) recommends four hierarchical validation schemes for hydrological models.

- Split-sample test: this is the classical method in which the available time series is split into two parts each of which should be used in turn for calibration and validation and the results from both arrangements compared. The model is considered acceptable only if the model validation results are satisfactory in both cases.
- Differential split-sample test: this is similar to the previous but the data is split based on a criterion that is consistent with the change in the catchment condition. This is done to ascertain the validity of the model in environmental conditions that are different from those used during the calibration. For instance, if simulation of the effects of climate change is the objective, the historical record could be divided into two- one with a higher average precipitation, and the other with a lower average precipitation. If the model is

intended to simulate streamflow for a wet climate scenario, then it should be calibrated on a dry segment of the historical record and validated on a wet segment.

- Proxy-basin test: this should be applied to test the geographic transferability of the model in a region that is assumed to be hydrologically and climatologically homogeneous. If, for example, streamflow has to be predicted in ungauged catchment Z, two gauged catchments X and Y within the region should be selected. The model should be calibrated on catchment X and validated on catchment Y and vice versa. Only if the two validation results are acceptable, should one consider the model as having a basic level of credibility with regard to its ability to simulate the streamflow in catchment Z adequately.
- Proxy-basin differential split-sample test: this is the most involved model validation test which combines features of the second and third methods. The test requires splitting of the observed data of each catchment into two sets based on a certain environmental criteria. Then, one of the datasets of the first catchment is used to calibrate the model and the contrasting dataset from the second catchment is used to validate the model. This can help, for instance, to assess whether a rainfall-runoff model calibrated with a dry climate on basin X can simulate streamflow of basin Y under wet condition, and *vice versa*.

Refsgaard and Storm (1996) recommend multi-criteria and multi-site calibration/validation for distributed hydrological models to be consistent with their level of complexity. But this requires availability of observed data on different variables such as streamflow, groundwater table, soil moisture, etc.

6.2.3 Model performance measures

For a model to be considered acceptable it is required that model outputs during the calibration and validation periods are sufficiently close to the observed data. The goodness-of-fit of model predictions to observations can be measured by methods that range from subjective graphical techniques to objective statistical criteria (Moriasi *et al*., 2007). The graphical method is usually the first step in model evaluation and relies on visual assessment of the fit between the simulated and observed quantities. Hydrographs and percent exceedance plots are widely used graphical techniques. The final decision on the performance of a model is often made based on methods that rely on objective criteria. A range of methods that could be grouped into three broad classes could be identified: error index, dimensionless and regression-based methods. Commonly used techniques in the error index category include

mean absolute error (MAE), mean square error (MSE), root mean square error (RMSE), ratio of mean square error to standard deviation (RSR) and percent bias (PBIAS). The most widely used dimensionless model performance measure is the Nash-Sutcliffe efficiency (NSE). Regression-based techniques in common use include the coefficient of determination (R^2), Pearson's correlation coefficient (r), and slope and y-intercept. A detailed presentation is made on three of the statistical techniques, i.e., RSR, PBIAS and NSE, which were used in this study.

6.2.3.1 Ratio of root mean square error to standard deviation (RSR)

The RSR is calculated as the ratio of the root mean square error to the standard deviation of the observed quantity (Equation 6-1). The RSR assumes values that are greater than or equal to zero, with 0 indicating a perfect fit. RSR value less than or equal to 0.7 is considered as appropriate threshold to judge the model performance as satisfactory (Moriasi *et al*., 2007).

$$RSR = \frac{RMSE}{Stdev_{obs}} = \frac{\sqrt{\sum_{i=1}^{n}\left(Q_{i-obs} - Q_{i-sim}\right)^2}}{\sqrt{\sum_{i=1}^{n}\left(Q_{i-obs} - \overline{Q}_{obs}\right)^2}} \qquad \textbf{Equation 6-1}$$

Where $Q_{i\text{-}obs}$ is observed quantity; $Q_{i\text{-}sim}$ is simulated quantity, $\overline{Q}_{obs}$ mean of the observed quantity.

6.2.3.2 Percent bias (PBIAS)

The PBIAS measures the average tendency of the simulated data to be larger or smaller than their observed counterparts (Gupta *et al*., 1999) and is computed using Equation 6-2. The optimal value of PBIAS is 0.0 with positive values indicating underestimation by the model and negative values signifying model overestimation bias. Generally, the performance rating of hydrological models has been reported as very good if the absolute value of PBIAS is less than 10% and satisfactory if it is in the range of 10% to 25 % (Moriasi *et al*., 2007).

$$PBIAS = \frac{\sum_{i=1}^{n}\left(Q_{i-obs} - Q_{i-sim}\right)}{\sum_{i=1}^{n}\left(Q_{i-obs}\right)} \times 100\% \qquad \textbf{Equation 6-2}$$

6.2.3.3 Nash-Sutcliffe efficiency (NSE)

The NSE is a normalized measure that compares the mean square error generated by a particular model simulation to the variance of the observed data (Nash and Sutcliffe, 1970). It is computed by Equation 6-3 and assumes values in the range –inf to 1.0. NSE value of 1.0 indicates perfect match of the model and NSE value of 0.0 shows that the model performs only as good as the mean of the observed data, and NSE less than 0.0 indicates the unsuitability of the model. NSE values between 0.0 and 1.0 are, therefore, considered as acceptable levels of model performance. Moriasi *et al*. (2007) sets a minimum threshold of 0.5 to judge the model performance as satisfactory. They also give references that have rated hydrological model performances as satisfactory with NSE values > 0.36.

$$NSE = 1 - \frac{\sum_{i=1}^{n}\left(Q_{i-obs} - Q_{i-sim}\right)^2}{\sum_{i=1}^{n}\left(Q_{i-obs} - \overline{Q}_{obs}\right)^2} \qquad \textbf{Equation 6-3}$$

6.3 Selected catchments

The selection of catchments for the model evaluation purpose was based on the following criteria:

- Availability of at least three meteorological stations within and adjacent to the catchment, with at least one of them being Class 1 station.
- Availability of observed daily runoff data for the period 1992-2005 with less than 10% missing data.
- Spatial representativeness of the catchment in terms of geographic location and soil and vegetation types.

Four catchments were selected based on the above criteria. The location of the catchments and their description with respect to the criteria are presented in Figure 6-1 and Table 6-1. The distribution of the soil types for Megech and Rib catchments is also given in Figure 6-2. Land cover is mainly cropland.

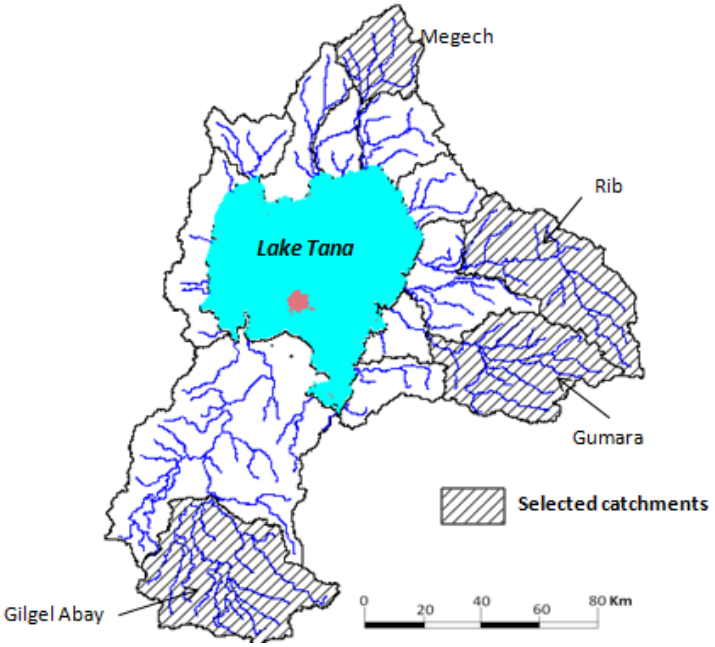

Figure 6-1 Catchments on which DHSVM was evaluated

Table 6-1 Characteristics of the simulation catchments

Catchment	Area km^2	No. of nearby meteorological stations	% of missing daily runoff data	Major soil type(s)†	Major vegetation type(s) ††
Megech	514	4	0.3	LPe, NTh	LC1
Rib	1448	5	0.9	LPe,LVc,FLe	LC1, LC7
Gumara	1279	3	3.6	LVh	LC1, LC2
Gilgel Abay	1641	5	0.4	LVh, ALh	LC1

†LPe- Eutric Leptosols; NTh- Haplic Nitosols; LVc-Chromic Luvisols; LVh-Haplic Luvisols; FLe- Eutric Fluvisols; ALh- Haplic Alisols
††LC1- cropland; LC2- cropland/grassland mosaic; LC7- shrubland

The model was run for the period 1992-2005 at a temporal resolution of 1 hour for the smaller catchments and 3 hours for the larger catchments. The period was divided into three sub-periods as "warming-up period", calibration period and validation period. This kind of simulation periods classification is common in hydrological model applications (Ahl *et al.*, 2008). The first two years period was used as "warming-up period" and is meant for minimizing the effects of incorrect initial states. The period 1994-2000 was used for calibrating the model parameters and the remaining years were used for validation.

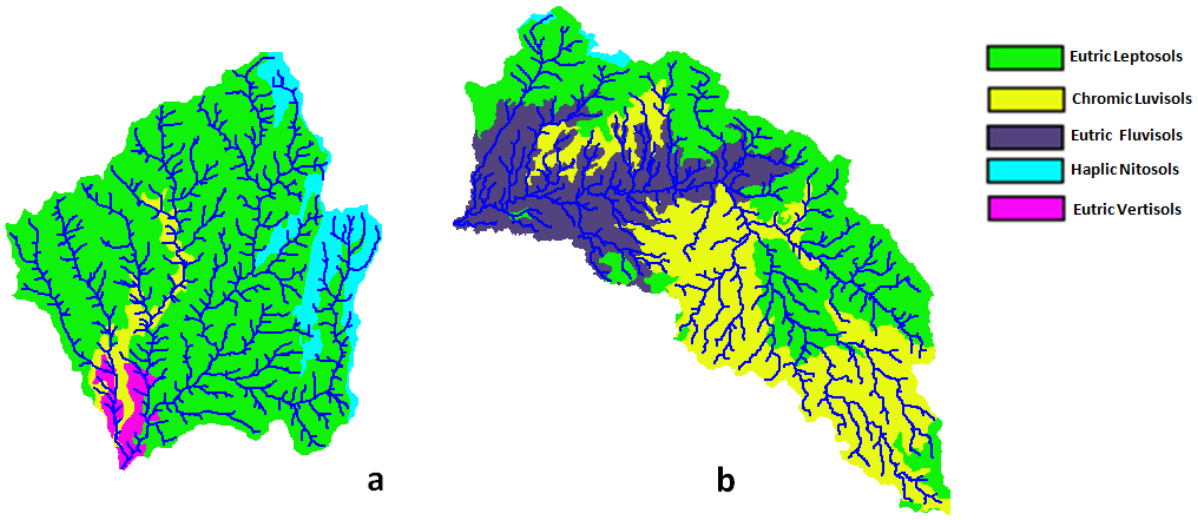

Figure 6-2 Distribution of soil types in (a) Megech and (b) Rib catchments

6.4 Calibration and validation of the model

The model was calibrated against observed daily streamflow records and monthly runoff volumes. The simulated hourly discharges were used to calculate the daily average simulated streamflow. Lack of observed data on other state variables like watertable, soil moisture, etc. did not allow multi-objective calibration. Calibration of DHSVM was limited to sensitive parameters of the dominant soil and vegetation types of the selected catchments.

A systematic manual calibration procedure similar to that recommended by Vieux and Moreda (2003) was followed:

- Assign *a priori* parameter values based on field data and relevant literatures
- Make sensitivity study of the streamflow hydrograph to the different parameters and identify key calibration parameters based on the results
- Run the model using *a priori* parameter values
- Evaluate of the level of agreement between the model outputs and observed discharge
- In case of poor model performance, change the values of the calibration parameters and run the model repeatedly until better agreements between simulated and observed discharges and runoff volumes are obtained.

The model was assigned with *a priori* soil and vegetation parameter values obtained from field measurements and relevant literatures as discussed in Chapter 5. Sensitivity of streamflow hydrograph to soil and vegetation parameters of the model was studied using a

small virtual catchment in Chapter 4. In light of the dominant soil and vegetation types of the selected catchments and the sensitivity analysis results, five key calibration parameters were identified: porosity, lateral hydraulic conductivity and its rate of exponential decrease, rooting depth and soil depth. The model was run repeatedly by changing the values of these calibration parameters until a relatively good agreement between simulated and observed hydrographs was obtained.

The performance of the calibrated model was then validated using the standard split-sample technique. Some adjustments to the manning roughness coefficients of streams were made in case of clear timing mismatch between the simulated and observed hydrographs.

6.5 Results and discussion

The performance of DHSVM during the calibration and validation periods is presented for only Megech and Rib catchments. The model goodness-of-fit was very poor for Gumara and Gilgel Abay catchments with consistent underestimation of streamflows. These two catchments are relatively larger and wetter with higher baseflow contributions. The dominant soil and land cover types are similar to that of Megech and Rib catchments. Different values of the calibration parameters that favor high flows were tried, but the simulated hydrograph remained low in each case. Further investigation is required to better explain the issue. For Megech and Rib catchments, the performance of the model was evaluated at daily and monthly time scales. Three statistical performance measures were used to evaluate the level of agreement between the model outputs and observed discharges. Moreover, graphical plots were used to visualize the agreement between the simulated and observed hydrographs.

6.5.1 Performance of the model at daily time step

The model was calibrated manually by changing porosity (θ), lateral saturated hydraulic conductivity (K_s) and its rate of exponential decrease (λ), and soil and rooting depths. For Megech catchment, a relatively better performance was obtained when the upper and lower rooting depths of the dominant land cover type, i.e., cropland were 0.2 m each with a total depth of 1.2 m. The *a priori* upper and lower rooting depths and total soil depth were, respectively, 0.105 m, 0.28 m and 0.70 m. The following calibrated parameter values were used for the dominant soil types with the *a priori* values indicated in brackets, if different: Eutric Leptosols- θ = 0.59 (0.53), K_s = 2.0 x 10^{-4} m/s (8.4 x 10^{-5} m/s), λ = 0.6 (1.1); Haplic

Nitosols- $\theta = 0.53$, $K_s = 1.7 \times 10^{-4}$ m/s (7.7×10^{-5} m/s), and $\lambda = 1.10$. For Rib catchment a relatively better result was obtained when the upper and lower rooting depths of cropland were 0.06 m and 0.160 m, respectively with a total depth of 0.40 m. The *a priori* depths were the same as those used for Megech catchment. The parameter values used for the three dominant soil types were: Eutric Leptosols- same values used for Megech; Chromic Luvisols- $\theta = 0.53$, $K_s = 1.0 \times 10^{-6}$ m/s (6.38×10^{-5} m/s), $\lambda = 0.3(1.1)$; Eutric Fluvisols- $\theta = 0.5$, $K_s = 2.0 \times 10^{-6}$ m/s (4.55×10^{-5} m/s), $\lambda = 0.2$ (1.1).

The performance of the model at daily time step in each year is indicated in Table 6-2 and Figure 6-3 for Megech and Table 6-3 and Figure 6-4 for Rib catchment. The level of agreement between the observed and simulated discharges should be evaluated in light of the meteorological and spatial input datasets, the streamflow data used for calibration/validation purposes, and the size of the catchments. The meteorological forcings were created by disaggregating observed/estimated daily average values and parts of the catchments are not adequately covered by the existing observation stations. The soil and vegetation maps have coarse resolution with one or two soil and vegetation types covering most of the catchments. For instance, Megech was represented mainly by Leptosols (81%) and cropland (97%). The observed streamflow data could not truly represent the daily average value as stage measurements are taken once or twice a day. The simulated daily average discharge was calculated, however, from the hourly simulation results. The catchments are large in size making spatial variations of rainfall and soil characteristics greater.

Table 6-2 DHSVM performance at daily time step on Megech catchment

Calibration				Validation			
Year	NSE	RSR	PBIAS	Year	NSE	RSR	PBIAS
1994	0.59	0.64	-18.90	2001	0.47	0.73	17.65
1995	0.55	0.67	-0.46	2002	0.30	0.83	-17.80
1996	0.43	0.76	-10.30	2003	0.38	0.79	25.84
1997	0.54	0.68	-18.60	2004	0.27	0.86	21.66
1998	0.44	0.75	-5.13	2005	0.21	0.89	45.24
1999	0.32	0.82	25.83				
2000	0.39	0.78	30.40				
Overall	**0.46**	**0.73**	**2.80**	**Overall**	**0.35**	**0.81**	**22.26**
Overall	**0.25**	**0.87**	**10.11**				

In light of these facts and model performance ratings discussed in Section 6.2.3, the goodness-of-fit for Megech catchment could be considered as satisfactory during the calibration period and poor in the validation period. In some years the three model performance measures were

all within the recommended acceptable limits. There was a general underestimation of streamflow during both calibration and validation periods. In the period 1994-1998 an overestimation of the model could be observed and this is mainly related to dry period flows. In the validation period, however, the model resulted in lower dry period flows. The model could not capture the peak discharges during the wet season. The observed peaks may be instantaneous and could not therefore be representative of daily average values.

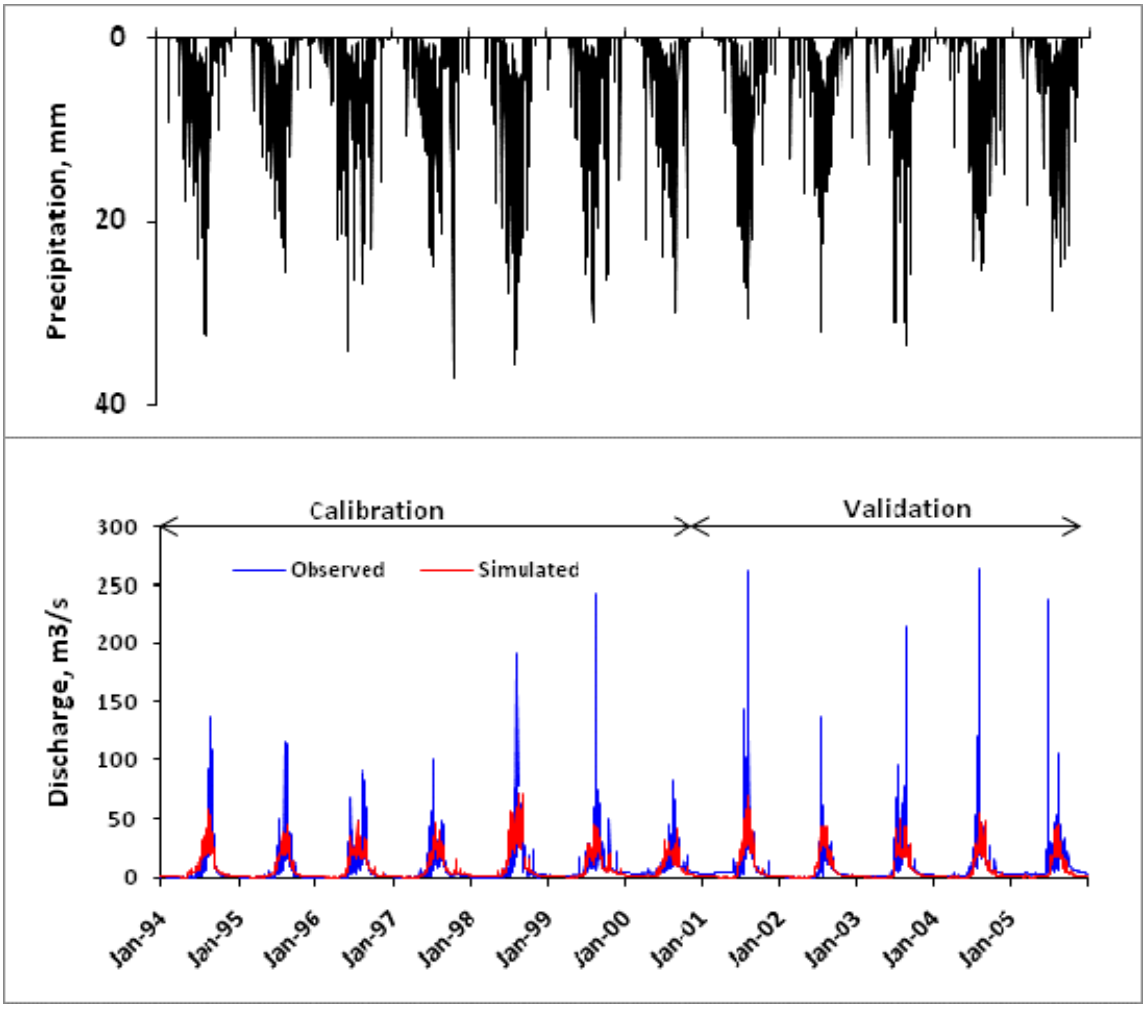

Figure 6-3 Measured and simulated hydrographs for Megech catchment

The overall performance of the model in Rib catchment appeared to be satisfactory during both the calibration and validation periods with NSE value greater than 0.6 in some years. A significant underestimation could, however, be seen in most of the years. This could be associated to sedimentation and overbank flow upstream of the gauging station which is reported to be a common problem (SMEC, 2008a). This can result in unrealistically high observed streamflows, particularly in the days following flooding. As evidence to this, the

streamflow data analysis in Chapter 3 indicated constant and high flows for successive days. The considerable underestimation by the model may not therefore be a real one. But if the observed flow is accepted as real one, then the underestimation may be caused by poor representation of the areal rainfall pattern. In Chapter 3 it was indicated that notable area in the middle part of Rib did not fulfill the recommended minimum network density of WMO. To get an insight into the effect of rainfall pattern, the model was run by taking the meteorological forcings of Class 1 station (Debre Tabor) alone. An improvement in the overall goodness-of-fit was noted in both the calibration and validation periods (Table 6-4 and Figure 6-4c). This suggests the importance of having good quality rainfall data with adequate spatial coverage for better model predictions.

Table 6-3 DHSVM performance at daily time step on Rib catchment when all nearby meteorological stations were used

Calibration				Validation			
Year	NSE	RSR	PBIAS	Year	NSE	RSR	PBIAS
1994	0.57	0.66	41.01	2001	0.16	0.91	70.23
1995	0.46	0.74	48.68	2002	0.48	0.72	-24.9
1996	0.24	0.87	43.54	2003	0.69	0.56	30.71
1997	0.14	0.93	60.89	2004	0.71	0.54	15.23
1998	0.33	0.82	64.61	2005	0.63	0.61	24.91
1999	0.61	0.63	46.93				
2000	0.67	0.57	2.26				
Overall	**0.47**	**0.73**	**42.58**	**Overall**	**0.52**	**0.69**	**28.30**

Table 6-4 DHSVM performance at daily time step on Rib catchment when Debre Tabor meteorological station was used

Calibration				Validation			
Year	NSE	RSR	PBIAS	Year	NSE	RSR	PBIAS
1994	0.75	0.50	9.53	2001	0.77	0.48	13.91
1995	0.75	0.50	16.55	2002	0.62	0.62	7.76
1996	0.51	0.70	33.75	2003	0.64	0.60	29.20
1997	-0.23	1.11	-53.24	2004	0.62	0.62	18.5
1998	0.64	0.60	6.64	2005	0.69	0.56	7.93
1999	0.62	0.62	24.35				
2000	0.67	0.58	4.03				
Overall	**0.59**	**0.64**	**8.18**	**Overall**	**0.69**	**0.56**	**15.89**
Overall ***(a priori)***	**0.25**	**0.86**	**56.39**				

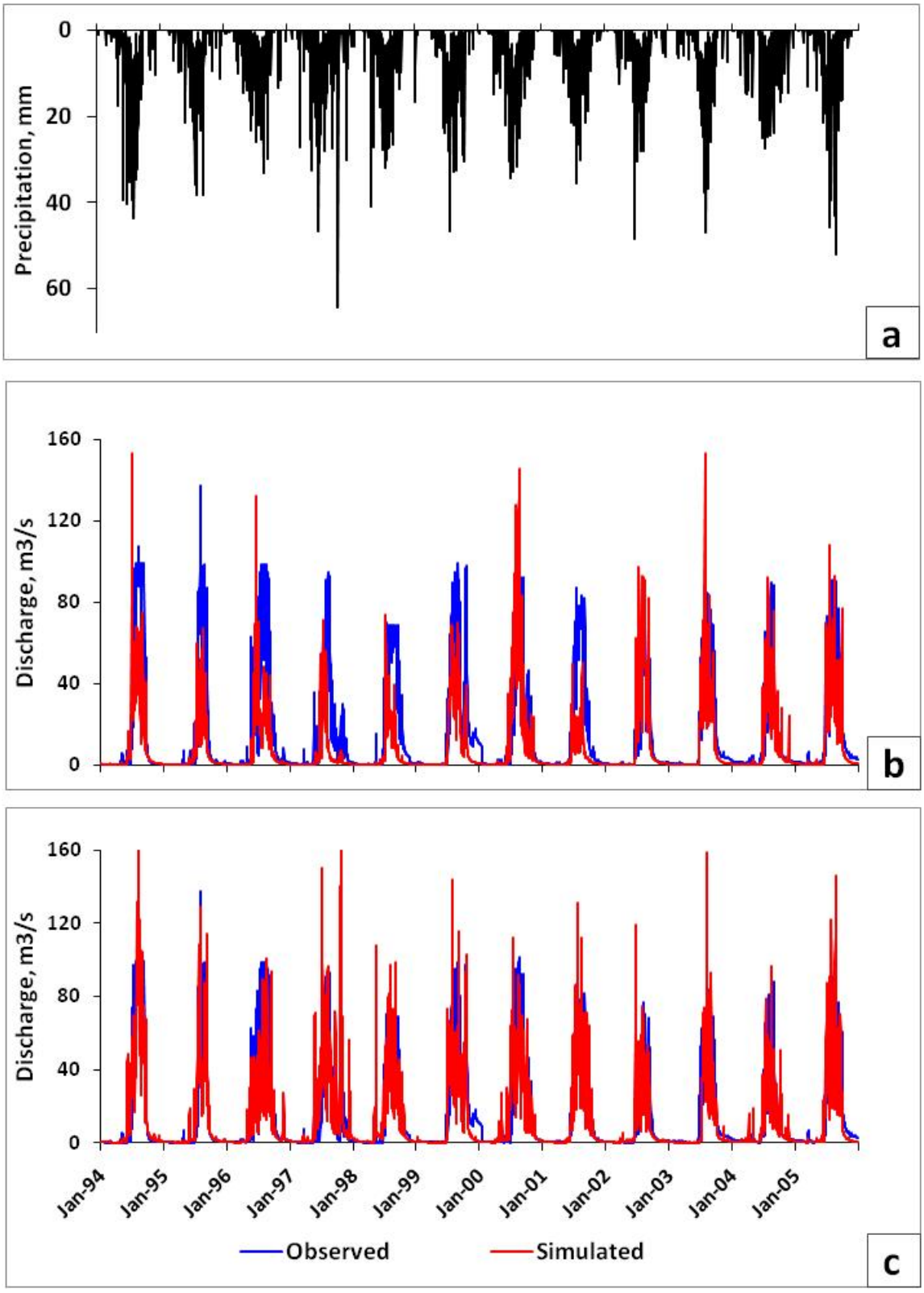

Figure 6-4 Measured and simulated hydrographs for Rib catchment (a) precipitation (b) when all nearby meteorological stations were used (c) when only Debre Tabor meteorological station was used

6.5.2 Performance of the model at monthly time step

This evaluation was done to see how well the model could reproduce the runoff volume at a monthly time scale. The results are shown in Table 6-5 and Figure 6-5. The overall goodness-of-fit appeared to be relatively good, particularly for Megech catchment with all performance measures being well within the recommended limits. The goodness-of-it in the dry period, however, was weak, especially during the validation period where the model predicted consistently lower flows. For Rib catchment, a considerable difference between the observed and simulated runoff volumes could be seen in the wet and subsequent dry months when all nearby meteorological stations were used. A better match could, however, be obtained when the model prediction was based on meteorological datasets of Debre Tabor station.

Table 6-5 DHSVM performance at monthly time step on Megech and Rib catchments

	Calibration			Validation		
	NSE	RSR	PBIAS	NSE	RSR	PBIAS
Megech						
Overall	0.85	0.39	1.75	0.81	0.43	24.71
Wet	0.73	0.52	0.63	0.67	0.57	14.01
Dry	0.51	0.7	7.22	-0.49	1.22	62.43
Rib (using all surrounding meteo stations)						
Overall	0.67	0.57	38.56	0.66	0.58	28.32
Wet	0.27	0.86	34.03	0.11	0.94	25.72
Dry	0.45	0.74	64.71	0.41	0.77	52.32
Rib (using only Debre Tabor meteo station)						
Overall	0.85	0.39	-0.55	0.89	0.33	15.92
Wet	0.73	0.52	4.10	0.73	0.52	14.89
Dry	0.23	0.88	-27.40	0.41	0.77	25.40

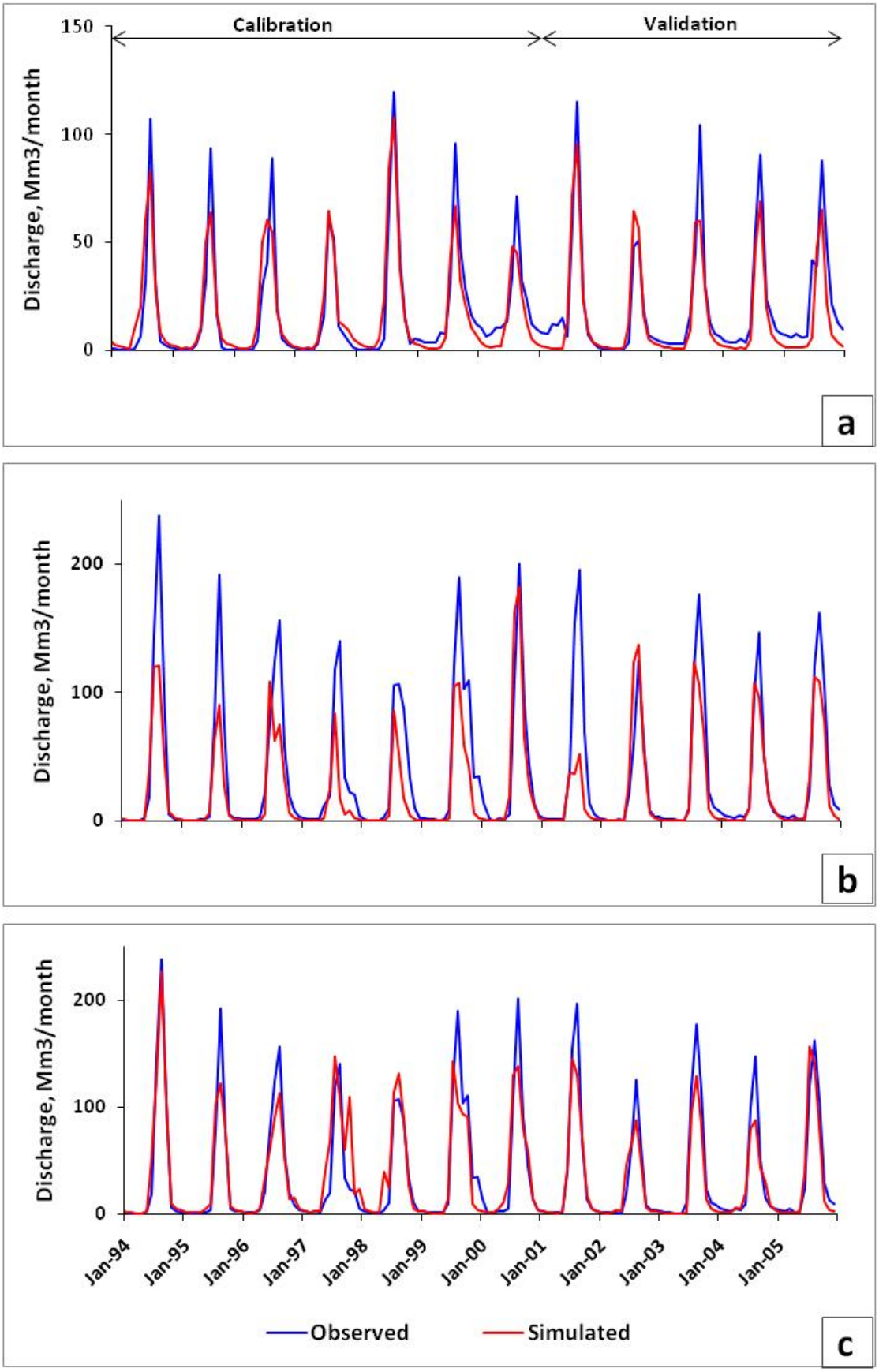

Figure 6-5 Measured and simulated monthly discharges (a) Megch (b) Rib using all nearby meteorological stations (c) Rib using only Debre Tabor meteorological station

6.6 Conclusion

The aim of this chapter was to assess the applicability of the distributed hydrological model, DHSVM, on selected catchments in the study area. The assessment indicated a relatively better goodness-of-fit on Megech and Rib catchments and it was very poor in Gilgel Abay and Gumara catchments. In view of the coarse temporal and spatial resolutions of the observed datasets used to calibrate and validate the model, the performance of the model can be judged satisfactory. Testing the model on other catchments that have hydro-meteorological and spatial datasets with better quality and spatial coverage would be important. It would also be useful to test the model's capability in predicting other state variables like groundwater table, soil moisture content, etc if data is available. DHSVM is a physically-based model that simulates various hydrological processes, soil erosion and sediment transport with reported good performances on experimental and mesoscale catchments. It would therefore be helpful to consider this model as an important tool in future water, and soil erosion and sediment transport related researches.

Chapter 7

7 Water and Suspended Sediment Balances of Lake Tana

7.1 Introduction

Worldwide, lakes represent the major reserves of readily available freshwater resources (WWAP, 2009). They provide human beings with multitude of goods and services. Unsustainable land development activities and water uses, however, have endangered the quality and quantity of lake water resources. For instance, the area of Lake Chad has shrunk by 95% from a surface area of 22902 km^2 in 1963 to 304 km^2 in 2001 due to both climatic and human factors (UNEP, 2006). In Ethiopia, the storage capacity of Lake Alemaya is reported to have shown a rapid decrease due to erosion and sedimentation (Muleta *et al.*, 2006). Major rift valley lakes of Ethiopia are also threatened by unsustainable land and water resources management (Legesse and Tenalem, 2006). The management of lakes and reservoirs is difficult due to their unique features that include their role as integrating sink of pollutants, longer water residence times and complex response dynamics (Jorgensen and Rast, 2007).

Water and sediment balance of lakes provide basic information that contribute to sustainable management of these important resources. Previous studies on water balance of Lake Tana indicate different results which could be due to the difference in the data period and methods used to estimate the various components. Summary of the major water balance components obtained in previous studies is presented in Table 7-1. It could be seen that the difference in some of the water balance components (e.g. inflow from rivers) is large. Meaningful studies on suspended sediment balance of the lake could not be found.

The purposes of this study are twofold (i) to make an update to the water balance of Lake Tana based on representative hydro-meteorological datasets and (ii) to provide an estimate of its suspended sediment balance which could be useful for planning level applications. The lake water balance modeling comprised estimation of the various components of the water balance based on quality controlled hydro-meteorological datasets and relevant computational methods. The specific methods used for each of the water balance components are presented in the respective sections. The estimate for longterm suspended sediment balance of the lake involved use of rating curves and a regional suspended sediment yield model.

Table 7-1 Reported magnitudes of major Lake Tana water balance components

Water balance component†	Kebede *et al.*,2006	SMEC, 2008a	Wale *et al.*, 2009
Rainfall, mm	1451	1264	1220
River inflow, mm	1162	1650	2160
River outflow, mm	1113	1240	1520
Evaporation, mm	1478	1675	1690

†Some of the values were directly reported in unit of mm. For those reported in volumetric unit a conversion to unit of mm was made by dividing it by the lake area.

7.2 Lake water balance model

A lake water balance model comprises three major components- inflow, outflow and storage. Mathematically, it is defined by a continuity equation that establishes mass balance among the various components for any temporal resolution (See Figure 7-1 and Equation 7-1). Inflow may comprise on-lake precipitation, surface inflow from contributing catchments and influx from aquifer systems. Outflow may consist of river discharge, water withdrawal for various purposes, evaporation and leakage through the bottom of the lake. The storage component at any time can be positive or negative depending on the relative magnitudes of inflows and outflows.

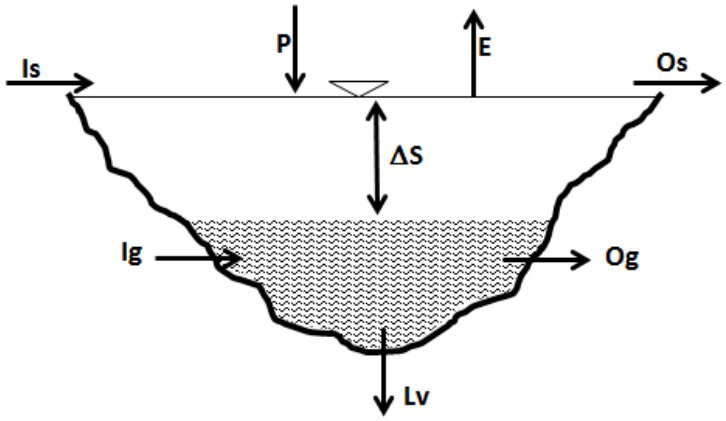

Figure 7-1 Components of Lake water balance

$$I_s + I_g + P - E - O_s - O_g - L_v - \Delta S = 0 \qquad \textbf{Equation 7-1}$$

Where, I_s is surface inflow; I_g is lateral groundwater inflow; P represents on-lake precipitation; E is evaporation from the lake surface; O_s is surface outflow; O_g is lateral groundwater outflow; L_v indicates vertical leakage through the bottom of the lake; ΔS is change in water storage.

The relative magnitudes of the water balance components vary from season to season and in most cases the groundwater component is small compared to the other inflow and outflow components (Ferguson and Znamensky, 1981). In reality, the water balance equation defined by Equation 7-1 is not satisfied due to uncertainties associated with measurements and estimates of the different components. The equation is, therefore, usually modified by including a closure term (Equation 7-2).

$$I_s + I_g + P - E - O_s - O_g - L_v - \Delta S \pm \delta = 0 \qquad \textbf{Equation 7-2}$$

Where, δ is the error of closure. It can be positive or negative depending on the relative magnitudes of total inflow, outflow and storage. The relative discrepancy can be calculated by dividing the absolute value of the closure error by the maximum of the total inflow or outflow.

7.3 Computation of the water balance components of Lake Tana

Lake Tana is an open lake with several feeder rivers and a single natural outflow to the Abay River. The major water balance components of the lake and their relative magnitudes are presented in this section. They include on-lake precipitation, river inflow from gauged and ungauged catchments, evaporation, river outflow and interaction with the groundwater system.

7.3.1 Rainfall

On-lake precipitation represents a major water balance component as the lake has a large surface area and is located in a region where the annual rainfall exceeds 1000 mm. Accurate estimation of areal precipitation on the lake is, therefore, important. Previous water balance studies applied different methods that include use of a nearby point rainfall data (Kebede *et al.,* 2006), Thiessen polygon and inverse distance weighing (SMEC, 2008a; Wale *et al*., 2009). The estimated on-lake precipitation varied from 1220 mm to 1450 mm.

In this study three spatial rainfall interpolation methods were compared: Thiessen, inverse distance square, and multiquadric methods. A brief presentation on different spatial interpolation methods was made in Chapter 3. More information on the methods could be found in Dingman (1994). Quality-controlled rainfall data of stations that have relatively low data gaps and are within a buffer distance of 0.5° from shoreline were included in the

calculation (Figure 7-2). The mean annual areal rainfall on Lake Tana as estimated by the different methods is presented in Table 7-2.

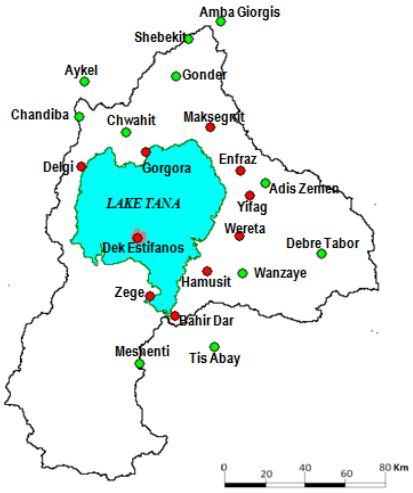

Figure 7-2 Stations used for spatial rainfall interpolation. Stations in red were used for the Thiessen method. Both stations in red and green were used for the other methods.

Table 7-2 Estimated mean annual on-lake precipitation for Lake Tana (1992-2005)

Method	Mean annual rainfall, mm
Thiessen	1250
Inverse distance square	1222
Multiquadric	1225

The multiquadric and inverse distance square interpolation methods gave comparable annual areal rainfall estimates. The mean annual areal rainfall on Lake Tana was taken to be 1225 mm, considering the positive comments on the superiority of kriging or multiquadric interpolation methods (Tabios and Salas, 1985). The corresponding mean monthly areal rainfall pattern is also indicated in Table 7-3. The estimated mean annual rainfall is in close agreement to two of the previous studies despite the difference in the periods and stations used in the estimation. The difference is, however, notable with that reported by Kebede *et al. (*2006) who used the rainfall records of Bahir Dar station alone and this appeared to be an overestimation. Observed mean annual rainfalls at stations close to the lake indicated low values (<1000 mm) in the western part and high values (>1400 mm) in the southern part of the lake.

Table 7-3 Mean monthly on-lake precipitation on Lake Tana (1992-2005)

Month	Annual	Jan	Feb	Mar	Apr	May	Jun	Jul	Aug	Sep	Oct	Nov	Dec
Rainfall, mm	1225	0.8	0.7	11.5	19.2	65.1	193.4	344.0	337.9	150.7	90.8	10.0	1.3

7.3.2 Inflow from contributing catchments

Lake Tana is surrounded by different contributing catchments that have a total surface area of 12108 km^2, some of them being gauged in their upstream parts. Two methods were used to estimate the contributions of these catchments depending on streamflow data availability. Direct utilization of historical streamflow data was made to those catchments for which data could be obtained. For some of the gauged catchments data could not be obtained and a large part of the basin is ungauged. The contribution of these catchments was estimated by using a conceptual hydrologic model. The model was also used to fill data gaps in the gauged catchments. Figure 7-3 shows areas to which these methods were applied.

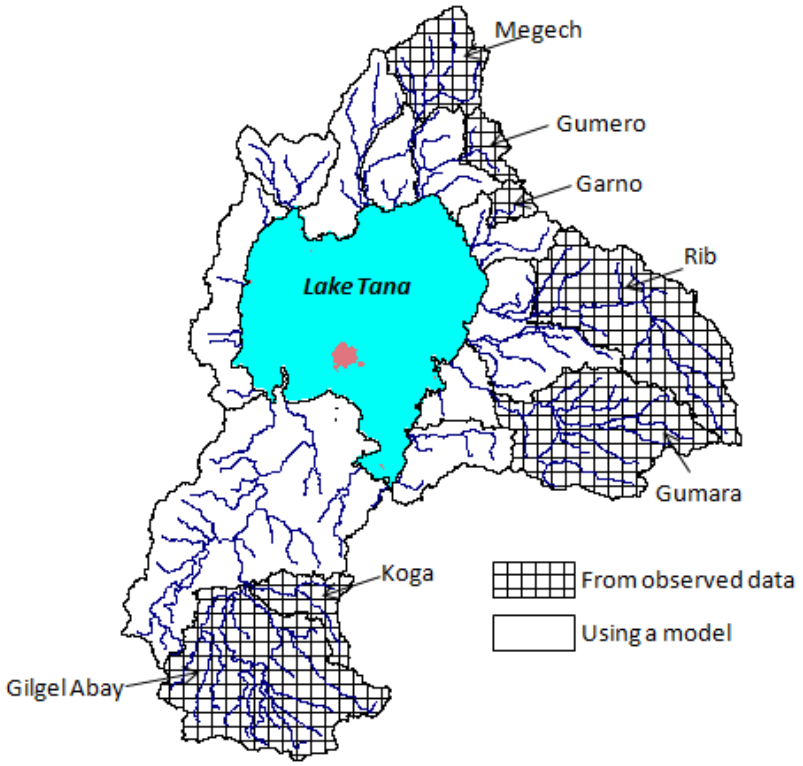

Figure 7-3 Methods used to estimate inflow contributions

7.3.2.1 Inflow from the major gauged catchments

The monthly runoff time series of each gauged station was created from the observed daily data for the period 1992-2005. The mean monthly and annual contributions of the major gauged catchments are presented in Table 7-4.

Table 7-4 Contributions of major gauged catchments to surface inflow into Lake Tana (1992-2005)

Catchment	Annual ($x 10^6 m^3$)	Mean monthly contribution ($x 10^6 m^3$)											
		J	F	M	A	M	J	J	A	S	O	N	D
Garno	30	0.8	1.0	0.8	0.8	1.3	5.2	11.2	4.0	1.6	1.3	1.0	1.1
Gilgel Abay	1700	9.6	5.6	5.4	5.7	20.6	136.9	403.9	496.3	350.4	179.7	57.8	28.1
Gumara	1126	12.1	6.3	6.2	5.2	7.5	46.1	244.3	410.9	232.2	95.9	37.3	21.7
Gumero	47	0.5	0.5	0.5	0.5	0.8	3.9	10.7	19.8	5.7	1.9	1.0	0.8
Koga	167	4.3	2.9	2.7	2.6	3.5	9.6	31.9	43.7	27.2	22.5	9.8	6.2
Megech	212	2.9	2.4	2.9	3.1	4.3	12.7	42.1	88.7	30.3	12.1	6.2	4.6
Rib	473	2.9	1.2	1.3	2.1	4.6	18.7	119.7	189.4	86.3	27.3	13.5	5.9
Total, Mm^3	**3755**	**33.1**	**19.9**	**19.8**	**20**	**42.6**	**233.1**	**863.8**	**1253**	**733.7**	**340.7**	**126.6**	**68.4**
Total, mm†	**1247**	**11**	**6.6**	**6.6**	**6.6**	**14.1**	**77.4**	**286.8**	**416**	**243.6**	**113.1**	**42**	**22.7**

†The total in mm was obtained by dividing the total in Mm^3 by the lake's average surface area, i.e., 3012 km^2.

7.3.2.2 Inflow from other catchments

Notable area in the Lake Tana basin is ungauged and data from few gauged catchments could not be obtained. Hydrological models are often used to estimate streamflows that are unavailable. Physically-based distributed hydrological models are considered to be useful for predicting runoff in ungauged catchments. However, as the performance of DHSVM was found to be unsatisfactory in some of the major gauged catchments, its use for estimating runoff from ungauged catchments was not considered.

Consequently, a lumped conceptual water balance model was used to estimate the contributions of catchments that are lacking streamflow data. The model was first calibrated and validated against runoff data obtained from gauged catchments. Then, a regionalization technique was used to establish values of the model parameters to each catchment with unavailable data.

7.3.2.2.1 The model

A parsimonious and dynamic water balance model developed based on Budyko framework was used. The original Budyko method takes into account only the dominant factors that control the longterm water balance, i.e., precipitation and evapotranspiration (Budyko, 1958). Zhang *et al.* (2008) have extended the original version of the model by including more features that simulate soil moisture dynamics and baseflow. These additional features of the model enable simulation at shorter time scales (e.g. daily and monthly time steps). Three key strengths of the model are noted by the developers- consistency in predictions across different time scales, parsimoniousness and robustness. Based on promising simulation results obtained in a number of catchments, the model is considered to be a good candidate for predicting streamflow in ungauged catchments (Zhang *et al.,* 2008). The various model equations and the calculation steps are indicated in Figure 7-4.

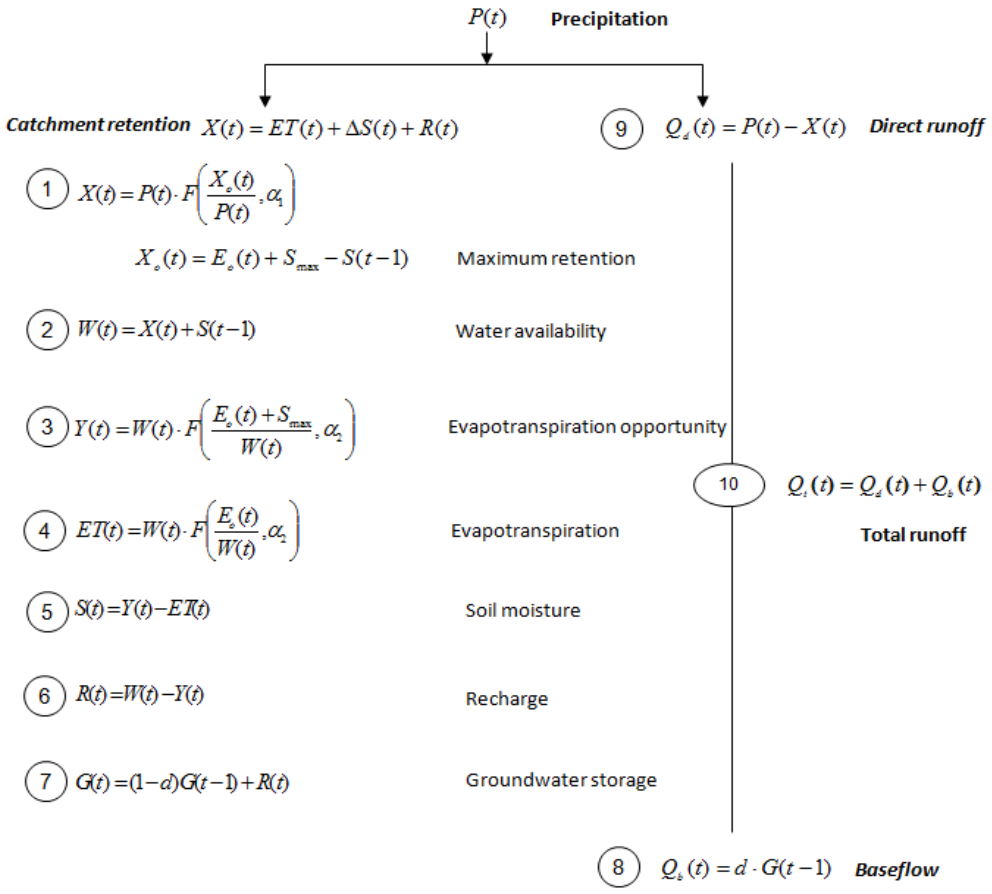

- The index t represents the current time step and t-1 the previous time step
- Inputs: rainfall P(t), potential evapotranspiration, Eo(t)
- Model parameters: α_1, α_2, d and maximum soil storage capacity (S_{max})
- Initial conditions: Soil moisture, S(t=0) and groundwater storage G(t=0)
- $\Delta S(t)$ is change in soil moisture: S(t)-S(t-1)

- X(t), Y(t), and ET(t) are calculated using Fu's function F(u, α) defined as:

$$F(u,\alpha) = 1 + u - \left[1 + u^{\frac{1}{1-\alpha}}\right]^{1-\alpha}$$

Where u is a variable and α is model parameter. For instance, for X(t), $u = \frac{X_o(t)}{P(t)}$ and $\alpha = \alpha 1$

Figure 7-4 The model Equations (Developed based on the model description given in Zhang *et al.,*2008)

7.3.2.2.2 Creation of inputs for the model

The water balance model was run at a monthly time step using rainfall and potential evapotranspiration as meteorological forcings. For each catchment, first the daily average rainfall and potential evapotranspiration series were computed using the Thiessen polygon and then aggregated to a monthly time step. The daily potential evapotranspiration was computed by the Penman method.

7.3.2.2.3 Calibration and validation of the model

The model was first calibrated and validated against observed monthly streamflow series of seven gauged catchments. The data for the period 1993-1997 and 1998-2002 were used, respectively, for calibration and validation purposes. Three measures were used to evaluate the performance of the model- NSE, RSR and PBIAS (refer to Chapter 6 for their definition). The quantitative thresholds indicated in Table 7-5 were used to decide the performance rating of the model.

Table 7-5 Recommended model performance ratings for monthly streamflow (Moriasi *et al.*, 2007)

Performance rating	NSE	RSR	PBIAS (%)†
Very good	0.75 – 1.00	0.00 – 0.50	< 10
Good	0.65 – 0.75	0.50 – 0.60	15 – 30
Satisfactory	0.50 – 0.65	0.60 – 0.70	30 – 55
Unsatisfactory	< 0.50	> 0.70	> 55

†PBIAS can assume negative and positive values; the thresholds indicated are absolute values.

For each gauged catchment, the optimum values of the four parameters of the model (α_1, α_2, d and S_{max}) were determined by the Microsoft Office Excel Solver tool which uses the generalized reduced gradient nonlinear optimization code. The optimum values of the model parameters are presented in Table 7-6. The calibrated model was then tested in the validation period. The results of calibration and validation are indicated in Figure 7-5 and Table 7-7. With reference to the recommended model performance ratings (Table 7-5), the level of performance in five of the catchments could be considered as good or very good. The performance of the model was poor in Garno and Gumero catchments.

Table 7-6 Optimum model parameter values for the gauged catchments

Catchment	α_1	α_2	d	S_{max}
Gilgel Abay	0.69	0.51	0.90	185.56
Gumara	0.61	0.40	0.90	251.55
Megech	0.47	0.80	0.50	406.80
Rib	0.53	0.89	0.50	600.00
Koga	0.51	0.59	0.61	596.49
Gumero	0.43	0.66	0.90	600.00
Garno	0.43	0.90	0.50	600.00

Table 7-7 Goodness-of-fit of the conceptual model during the calibration and validation periods

Catchment	Calibration (1993-1997)			Validation (1998-2002)		
	NSE	RSR	PBIAS	NSE	RSR	PBIAS
Gilgel Abay	0.91	0.3	2.76	0.91	0.29	-16.3
Gumara	0.88	0.35	0.44	0.71	0.53	-32.31
Megech	0.71	0.53	-3.19	0.85	0.38	21.98
Rib	0.8	0.44	-0.61	0.84	0.4	3.86
Koga	0.73	0.52	3.27	0.82	0.42	0.35
Gumero	0.5	0.7	11.16	0.7	0.55	12.32
Garno	0.39	0.77	13.35	0.3	0.83	26.28

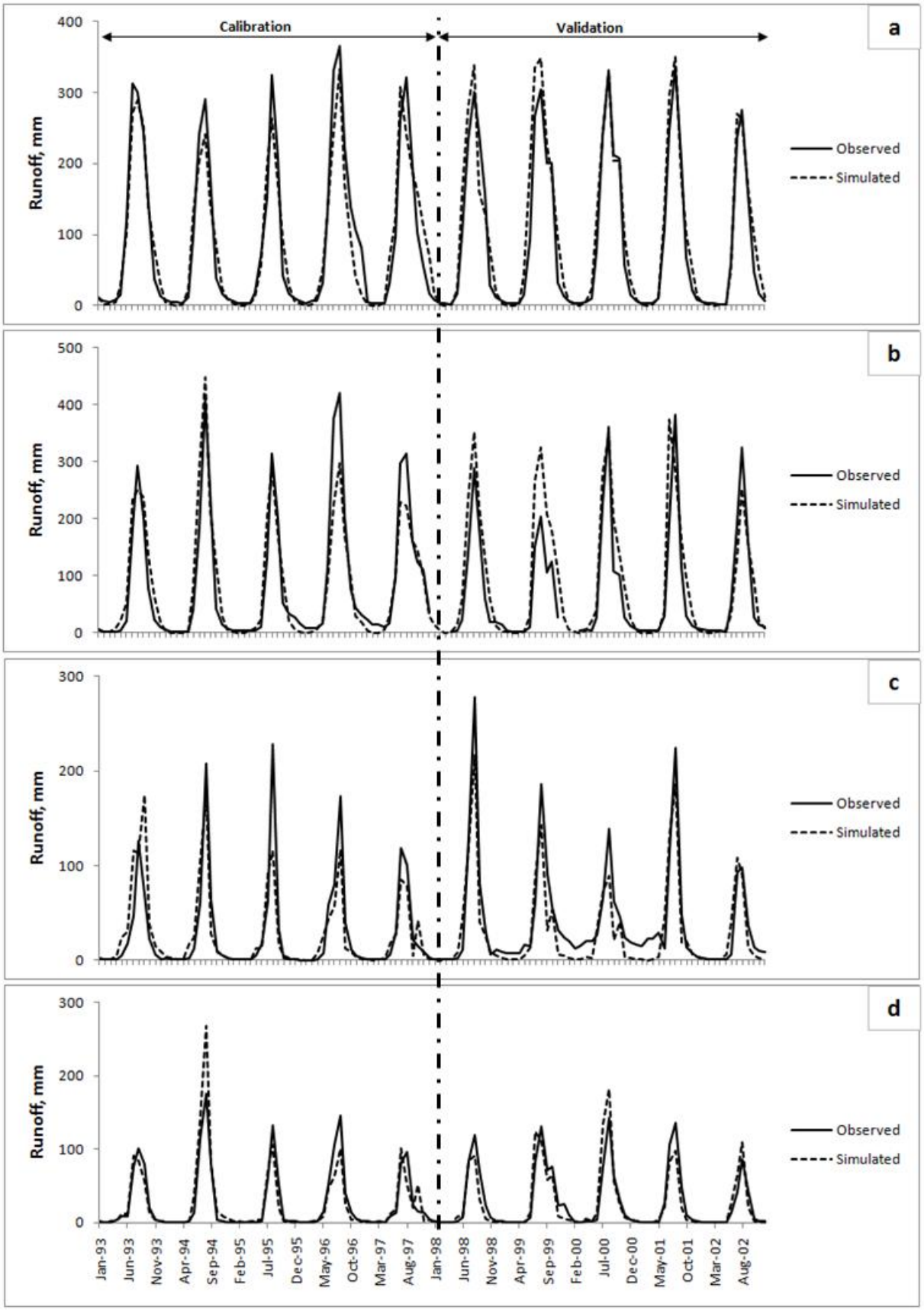

Figure 7-5 Calibration and validation results of the conceptual rainfall-runoff model (a) Gilgel Abay (b) Gumara (c) Megech (d) Rib. Period of calibration is 1993-1997 and that of validation is 1998-2002

7.3.2.2.4 Parameter regionalization

In order to apply the model in the ungauged parts of the basin, appropriate parameter values should first be established. Model parameters for ungauged catchments are often extrapolated from those obtained at gauged catchments using regionalization techniques. Parameter regionalization is commonly accomplished by using regression equations that relate model parameters to physiographic attributes of a catchment (Parajka *et al.*, 2005). Direct transfer of calibrated parameters from nearby gauged catchments is also possible. Kim and Kaluarachchi (2008) listed specific parameter regionalization techniques used in different studies. In this study a regression equation that relates the model parameters to area, slope and mean annual rainfall of a catchment was used for the regionalization (Equation 7-3). Slope was calculated as the mean of slopes of all grid cells found in a particular catchment. The calibrated model parameters of the five catchments that showed good performance were used in the regionalization.

$$Y^k = \beta^k X^k \qquad \textbf{Equation 7-3}$$

Where Y^k is matrix of the k^{th} parameter, and β^k is the corresponding matrix of the regression coefficients; X^k is matrix of the catchment characteristics.

The analysis resulted in regression coefficients shown in Table 7-8. These coefficients, together with the three watershed characteristics, have been used to estimate the model parameters of each catchment without streamflow data.

Table 7-8 Regression coefficients used to estimate the regional model parameters

Model parameter, p †		Regression coefficients				
		β_0	β_1	β_2	β_3	R^2
$p = \beta_0 + \beta_1 \times Area + \beta_2 \times Slope + \beta_3 \times ARF$	α_1	0.8505	0.0002	-	-	0.79
	α_2	-3.2451	-	0.1089	0.0022	0.66
	S_{max}	-822.15	-	31.734	0.8692	0.53
	d	3.567	0.0007	-	-	0.65

†Catchment area is in km^2; mean watershed slope is in %; ARF is mean annual catchment rainfall in mm
†p stands for any of the model parameters (α_1, α_2, S_{max}, d)

As the number of the gauged catchments was limited, they were all used in the parameter regionalization and thus it was not possible to use a proxy basin test for validating the regional model. Instead, the validity of the regression equations was tested by comparing

runoff computed using parameters obtained from the regional equation against observed streamflows for the period 2003-2005 in each of the gauged catchments. Wale *et al.*(2009) used the same approach in validating the regional equation for the HBV model parameters. The validation result is shown in Table 7-9. By and large, the performance of the regional model parameter equations appeared to be good. The poor performance in the Rib catchment could be related to the unique feature of this catchment as mentioned in Chapter 3 where the observed runoff appeared to be low in comparison to its large area and rainfall.

Table 7-9 Validation results of the regional model parameters equations (2003-2005)

Catchment	Performance measures		
	NSE	RSR	PBIAS
Gilgel Abay	0.96	0.2	-1.67
Gumara	0.91	0.3	6.72
Megech	0.72	0.52	42.46
Rib	0.25	0.85	-71.08
Koga	0.77	0.47	-14.71

After having established values of the model parameters using the regional equation, runoff contribution of each ungauged catchment and gauged area for which data could not be accessed were estimated. Summary of the simulation results is presented in Table 7-10.

Table 7-10 Runoff contribution of catchments without streamflow data (1992-2005)

Catchment	**Annual ($x 10^6 m^3$)**	**Mean monthly contribution ($x 10^6 m^3$)**											
		J	F	M	A	M	J	J	A	S	O	N	D
Dirma	149.5	0.5	0.2	0.3	1	4	21.5	44.7	46.6	15.6	11.2	2.6	1.3
Gabi Kura	107.4	0.8	0.5	0.3	1	3.2	15	26.2	28.7	17.1	9.6	3.4	1.6
Garno†	81.4	0.3	0	0.3	0.5	1.3	8.6	27.3	32.1	6.7	3.2	0.8	0.3
Gelda	243.7	3.5	1.2	0.5	0.3	1.6	11.9	52.8	68.8	45.1	31.1	18.1	8.8
Gilgel Abay†	2309	1.1	0	0.3	1	29.2	238.5	747.3	738.2	344.5	157	44.6	7
Gumara†	176.6	2.4	1	0.5	0.3	1.1	8.6	39.1	51.4	30.8	22	13	6.4
Gumero†	89.4	0	0	0.3	0.8	2.4	9.8	31.1	35.6	6.2	2.4	0.5	0.3
Megech†	78	0.3	0	0.3	0.5	2.1	11.4	24.1	24.6	7.3	5.6	1.3	0.5
Rib†	202.4	0.5	0.2	0.3	0.5	1.6	13.2	65.9	85.7	23.3	8.8	1.6	0.8
West Tana	148.1	0.3	0.2	0.3	1.3	4.3	18.1	45	47.7	18.9	10.2	1.3	0.5
Total, Mm^3	**3585**	**9.7**	**3.3**	**3.4**	**7.2**	**50.8**	**356.6**	**1103.5**	**1159.4**	**515.5**	**261.1**	**87.2**	**27.5**
Total, mm	**1191**	**3.3**	**1**	**1**	**2.3**	**16.9**	**118.5**	**366.5**	**384.8**	**171.3**	**86.7**	**28.9**	**9.3**

†Represent areas other than the gauged parts indicated in Figure 7-3

7.3.3 Evaporation

Tropical regions are characterized by high energy fluxes, making evaporation to be a dominant process. Open water evaporation should, therefore, be considered as an important water balance component in the planning and management of surface water resources. As supply of water is not a limiting factor, evaporation from lakes is controlled by climatic factors and occurs at potential rate (Dingman, 1994; Ward and Trimble, 2004). Evaporation from lakes is often estimated using indirect methods due to the difficulties involved in making direct observations (WMO, 1994). Different approaches are available to estimate evaporation indirectly which include water budget, energy balance, mass transfer and combined approaches. The combined approach considers both energy balance and mass transfer processes. The Penman approach is the most widely used combined method and it is considered to be theoretically sound (Dingman, 1994).

In this study the Penman approach (Equation 7-4), was used to estimate evaporation from Lake Tana. Use of this method in estimating evaporation from lakes that are located in Ethiopia and the wider East African region could be found in the literature (Yin and Nicholson, 1998; Vallet-Coulomb *et al.*, 2001; Kebede *et al.*, 2006).

$$E = \frac{\Delta}{\Delta + \gamma} \cdot \frac{R_n}{\lambda} + \frac{\Delta}{\Delta + \gamma} \cdot \frac{6.43(f_u)(e_s - e_a)}{\lambda} \qquad \textbf{Equation 7-4}$$

Where E is open water (potential) evaporation in mm/d; Δ is the slope of saturation vapour pressure curve (kPa/°C); γ is psychrometric coefficient (kPa/°C); R_n is the net radiation at the surface (MJ/m^2/d); λ is latent heat of vaporization (MJ/kg); f_u is wind function; e_s and e_a are saturation and actual vapour pressures, respectively in kPa.

This equation does not include other energy balance terms such as heat exchange with the ground, water advected energy or change in heat storage. But, its application for monthly or daily evaporation estimations is considered to be acceptable (Shuttleworth, 1993; Allen *et al.,*1998). The different methods used to compute the various terms of the Penman equation are presented in Annex D. Brief notes on the methods used to determine the wind function, temperature and albedo, however, are presented below.

Wind function

The wind function, f_u, is calculated by the empirical relation given in Equation 7-5.

$$f_u = a_u + b_u u \qquad \textbf{Equation 7-5}$$

Where u is wind speed at 2 m height in m/s; a_u and b_u are wind function coefficients.

In the original Penman formulation a_u is taken as 1.0 and b_u as 0.536. The use of 1.0 for a_u, however, makes evaporation from open water bodies unrealistically high and a lower value of 0.5 is suggested (Cohen *et al.*, 2002). Making the value of a_u 0.0 is considered to be more appropriate for estimating evaporation from large lakes (Valiantzas, 2006). In this study the a_u value was made to be zero and the wind function was calculated as $f_u = 0.536u$.

Temperature

Minimum, maximum and average daily temperatures were used to calculate the various terms of the Penman equation. The areal temperature of Lake Tana was computed from point observations using the nearest neighbor method adjusted for elevation. Temperature observations of six stations (Bahir Dar, Enfranz, Gorgora, Maksegnit, Wereta and Zege) were used.

Albedo

Albedo is a measure of the light reflectance properties of surfaces and therefore controls the amount of shortwave radiation received by a surface. It assumes values between 0 and 1 depending on the whiteness of the surface. A constant albedo value between 0.05 and 0.10 is often taken for a water surface (Dingman, 1994). In this study monthly albedo values were derived from the MODIS white and black sky albedos with a temporal resolution of 16 days and spatial resolution of a quarter degree. The complete data for year 2002 could be obtained from the ISLSCP initiative website[9]. The actual or blue sky albedo was computed by linearly combing the white and black sky albedos using Equation (7-6).

$$\alpha_{actual} = \alpha_{white-sky} \times skyl - \alpha_{black-sky}(1 - skyl) \qquad \textbf{Equation 7-6}$$

Where, skyl is diffusivity which is a function of solar zenith angle, optical depth and solar band.

[9] http://daac.ornl.gov/ISLSCP_II/islscpii.shtml

Evaporation was first calculated at daily time step and then aggregated to monthly and annual periods. The mean monthly inputs and the estimated evaporation are given in Table 7-11. The estimated annual evaporation was 1687mm based on data of 1992-2005. This value is close to two of the previous estimates but Kebede *et al.* (2006) who used meteorological datasets of Bahir Dar and Addis Ababa stations for the period 1961-1992.

Table 7-11 Mean monthly and annual evaporation from Lake Tana using the Penman method (1992-2005)

Input/output	Annual mm	Mean monthly magnitude											
		J	F	M	A	M	J	J	A	S	O	N	D
Temperature, °C	20.4	19.3	20.8	21.9	22.7	22.4	20.7	19.3	19.2	19.7	20	19.8	19.3
Wind speed, m/s	1.1	1	1.1	1.2	1.2	1.2	1.2	1	1	1	0.9	0.9	0.9
Relative hum, %	61.5	50.1	44.6	44.6	46.7	55.3	72	81.3	82.1	76.3	69	61	54.8
Incoming SR†	22	20.8	22.7	24	24.2	23.5	21.8	19.9	19.8	20.9	20.5	20.1	20
Net LR†	-5.6	-5.8	-5.6	-5.4	-5.3	-5.3	-5.6	-5.7	-5.7	-5.7	-5.7	-5.7	-5.8
Evap., mm/d	1687	134.3	144.1	173.3	177.5	173.2	141.4	115.2	118.4	125.6	131.9	124.3	127.9

†The unit for incoming solar radiation (SR) and net longwave radiation (LR) is $MJm^{-2}d^{-1}$. Net longwave radiation is calculated as the difference between the incoming downward and outgoing longwave radiation.

7.3.4 Interaction with groundwater

Depending on the relative positions of the lake water and groundwater levels and the surrounding geologic conditions, there could be inflow to or outflow from the lake. Based on isotope studies, Kebede (2004) concludes that it is unlikely to have outflow from the lake to the surrounding groundwater aquifer system. They attribute this conclusion to the graben structure of the basin that dips towards Lake Tana from all directions. Moreover, considering the thick and compacted sediment deposits beneath the bottom of the lake (Lamb et al 2007), the vertical leakage could be assumed negligible. Kebede *et al.* (2006) considered the groundwater component of the water balance term to be generally low with an estimated contribution of less than 7% of the total inflow. There was no need for estimating groundwater separately in this study as this was already considered in the conceptual model that has a recharge and baseflow component.

7.3.5 River outflow

With its long years of streamflow data, the Abay River represents the only river outflow from the lake. The daily streamflow data for the period 1992-2005 was used to create the monthly

river outflow series. The mean annual and monthly outflows from the lake are shown in Table 7-12.

Table 7-12 Mean monthly and annual outflow from Lake Tana (calculated based on daily data of 1992-2005)

Unit	Annual	J	F	M	A	M	J	J	A	S	O	N	D
$x10^6$ m^3	**4228**	247.9	181	179.2	174.5	140.4	135.4	226.2	415.3	825	790.1	549.8	362.7
mm	**1404**	82.3	60.1	59.5	57.9	46.6	45	75.1	137.9	273.9	262.3	182.5	120.4

7.3.6 Floodplain evaporation

Lake Tana is surrounded by extensive floodplains and wetlands where considerable amount of water could be lost via evaporation and percolation into the aquifer system. Based on five years of satellite images (1998-2003), Daniel (2007) has been able to estimate the average extent of flooded areas during seven months (June-December). The mean annual basin-wide rainfall in this five years period was close to that calculated from the longer 1992-2005 period. The estimated average flooded areas could, therefore, be taken as representative of the water balance study period. These areas, together with the mean monthly evaporation rates estimated in Section 7.3.3, were used to estimate the loss of water from floodplains via evaporation. The results are shown in Table 7-13.

Table 7-13 Estimated evaporation from the floodplains that surround Lake Tana (1992-2005)

Month	Flooded area km^2	Monthly evaporation mm	Floodplain evaporation $x10^6$ m^3	Equivalent floodplain evaporation with respect to Lake Tana's area mm
June	112	141.4	15.8	5.2
July	349	115.2	40.2	13.3
August	563	118.4	66.7	22.1
September	432	125.6	54.3	18
October	411	131.9	54.2	18
November	209	124.3	26	8.6
December	193	127.9	24.7	8.2
Total			**282**	**94**

7.3.7 Change in lake water storage

The lake storage could be positive or negative depending on the relative magnitudes of the total inflow and outflow. During the dry months the storage becomes negative as there is no

significant inflow. The mean monthly and annual storage volume was estimated from the observed daily lake level records at Bahir Dar for the period 1992-2005. The results are shown in Table 7-14.

Table 7-14 Mean changes in Lake Tana water storage (from daily lake level at Bahir Dar, 1992-2005)

Unit	Annual	J	F	M	A	M	J	J	A	S	O	N	D
$x10^6$ m^3	29	-623.8	-559.3	-690.7	-598.2	-533.4	96.7	1803	2390.3	602.4	-395.8	-744.3	-658.4
mm	88	-207.1	-185.7	-229.3	-198.6	-177.1	32.1	598.6	793.6	200	-131.4	-247.1	-218.6

7.3.8 Summary of the major water balance components of Lake Tana

Summary of the water balance of the lake is shown in Table 7-15. The relative discrepancy varied from a minimum of 1.7% in December to 43.1% in June. A criterion recommended by Ferguson and Znamensky (1981) was used to decide whether the computed discrepancy is acceptable or not. The criterion is that the discrepancy should not exceed the square root of the sum of the squares of the error limits of the water balance components (Equation 7-7).

$$\delta \le \sqrt{\delta_1^2 + \delta_2^2 + ...+\delta_m^2} \qquad \textbf{Equation 7-7}$$

Where δ is the maximum acceptable discrepancy; δ_1, $\delta_{2, ...,}$ δ_m are error limits of the different water balance components.

For catchments with good network density, the long-term mean monthly, seasonal or annual error limits may be set as ±10-20% for precipitation and evaporation, ±5% for runoff and ±1 cm for lake level measurements (Ferguson and Znamensky, 1981).

In this study the allowable discrepancy was calculated by using error limits of ±20% for precipitation and evaporation, ±5% for inflow from gauged catchments, and ±20% for catchment inflow estimated by the conceptual model. The model catchment inflow was estimated based on precipitation and potential evaporation data. This resulted in the maximum acceptable relative discrepancies indicated in the last row of Table 7-15. The relative discrepancies for the average year and nine of the months were found to be less than the acceptable limit. For the months of May, June and July, however, the relative discrepancies were greater than the allowable limit. The major source of this discrepancy could be the runoff estimated by the model. These months, particularly from late May to end of June, represent rainfall onset period in the study area where the major runoff mechanism could be

subsurface flow. Analysis of the rainfall-runoff data in Chapter 3 hinted this could be the case until the antecedent rainfall reaches a certain threshold after which saturated excess overall flow would occur. Most of the rainfall in these months may, therefore, recharge the groundwater aquifer instead of directly contributing to the lake. The model result, however, indicated direct runoff to be the dominant pathway. It could be reasonable to consider only the subsurface flow part of the model as the contribution to the lake in May, June, and the beginning of July. With this adjustment the mean annual total inflow to the lake was found to be 3350 mm with respect to the lake's average surface area and the relative discrepancy reduced to 6.9%. It is also important to note that the model indicated a total annual baseflow contribution of 250 mm which equaled 7.5% of the total inflow. This appeared to be a further confirmation to the estimate of Kebede *et al. (*2006), who assumed it to be about 7% of the total inflow.

Table 7-15 Mean monthly and annual water balance of Lake Tana (1992-2005)

Water balance component†	Annual	J	F	M	A	M	J	J	A	S	O	N	D
Inflow													
On-lake rainfall, mm	1225(34%)	0.8	0.7	11.5	19.2	65.1	193.4	344	337.9	150.7	90.8	10	1.3
††Catchment inflow, mm	2344(66%)	14.3	7.6	7.6	8.9	31	190.7	640	778.6	396.9	181.8	62.3	23.8
Total, mm	3569	15.1	8.3	19.1	28.1	96.1	384.1	984	1116.5	547.6	272.6	72.3	25.1
Outflow													
Lake evaporation, mm	1687(47%)	134.3	144.1	173.3	177.5	173.2	141.4	115.2	118.4	125.6	131.9	124.3	127.9
River outflow, mm	1403(39%)	82.3	60.1	59.5	57.9	46.6	45	75.1	137.9	273.9	262.3	182.5	120.4
Total , mm	3090	216.3	204.1	232.3	235.5	220.2	186.4	190.2	256.4	399.6	393.9	307.3	247.9
Change in storage, mm	30 (1%)	-207	-186	-229	-199	-177	32	599	794	200	-131	-247	-219
Actual discrepancy, %	12.6	2.7	4.9	6.9	3.7	24.1	43.1	19.8	6	9.5	2.6	3.9	1.7
Allowed discrepancy, %	13.4	12.6	14.2	15	15.2	16.9	13.8	10.4	9.4	9.8	9.5	8.6	10.3

†The water balance components in volumetric units could be obtained by multiplying the values in mm by the average lake surface area, i.e., 3012 km^2

††Catchment inflow was calculated as: observed surface inflow + simulated catchment inflow – floodplain evaporation

Catchment inflow represented about 66% of the total mean annual water influx. A breakdown of the total catchment inflow indicated that 85% of the contribution came from four watersheds (54% Gilgel Abay, 18% Gumara, 9% Rib and 4% Megech). The contribution of direct precipitation was limited to 34%. Loss of water by evaporation from the lake exceeded on-lake precipitation by 38%. These percentages of inflow and evaporation are different from that reported by Kebede *et al.* (2006) who used rainfall data of a single station, meteorological

data of Addis Ababa to estimate evaporation and assumed negligible contributions from the ungauged parts. The results are, however, in close agreement to Wale *et al.* (2009) who estimated average areal rainfall and evaporation from more point measurements and found the contribution of the ungauged part to be notable. A difference in the observed outflow quantity was also noted among the various studies due to the data period used. For instance, Wale *et al.* (2009) took data of a short period (1995-2001), where the recorded outflow appeared to be relatively high in most of the years.

7.3.9 Simulation of lake level fluctuation

To further verify the degree of accuracy of the estimated water balance components of Lake Tana, the observed mean monthly water level time series of the lake was compared against that simulated using the model rewritten in the form of Equation 7-8 without the closure term.

$$H(t) = H(t-1) + P(t) - E(t) + \frac{I_s(t) - O_s(t)}{A(h)} \qquad \textbf{Equation 7-8}$$

Where, H(t) and H(t-1) in meters represent lake levels at the current and previous months respectively; P(t) is on-lake precipitation in meters; E(t) evaporation in meters; $I_s(t)$ and $O_s(t)$ are river inflow and outflow, respectively in m^3/month; A(h) is lake surface area in m^2 corresponding to the lake level at the current time step.

A relationship between the lake level and the corresponding water surface area was established based on the bathymetric data obtained for year 2006. A polynomial function of third degree fitted well the observed data.

Equation 7-20 is a nonlinear function of the unknown lake level. The following procedure was followed to determine lake level that satisfies the equation at each time step.

1. Take the lake level of the previous time step H(t-1) as the initial state. For instance, if a monthly water balance model starts in January 1992, then lake level recorded in December 1991 represents the initial state
2. Assume lake level at the current time step and compute A(h)
3. Compute H(t) using Equation 7-8
4. Compare the calculated and assumed lake levels of the current time step
5. Repeat steps 2-4 until the difference between the calculated and assumed lake levels is within a tolerable limit
6. Repeat 2-5 for the next time step using the lake level just computed as the initial state

These steps were automatically executed in a Matlab environment. A constrained nonlinear optimization algorithm was employed to obtain optimum values that could minimize the difference between the assumed and calculated lake levels at each time step.

Simulation result of the lake level fluctuation is shown in Figure 7-5. Closer investigation of Figure 7-6a generally indicated that the rising limb of the simulated lake level lagged behind that of the observed. This systematic phase difference between the simulated and observed lake levels could be attributed to the effect of routing in the lake. This was also evident from the computed stronger lag-1 autocorrelation coefficient between the observed and simulated levels. The performance of the water balance model was, therefore, reevaluated by comparing the simulated lake levels against the observed by considering a phase shift of one month. A better performance could be noted as indicated in Figure 7-6b. In light of the good reproducibility of the amplitude and timing of the monthly water level fluctuations, the water balance model appeared to have captured the dominant processes that control the lake level.

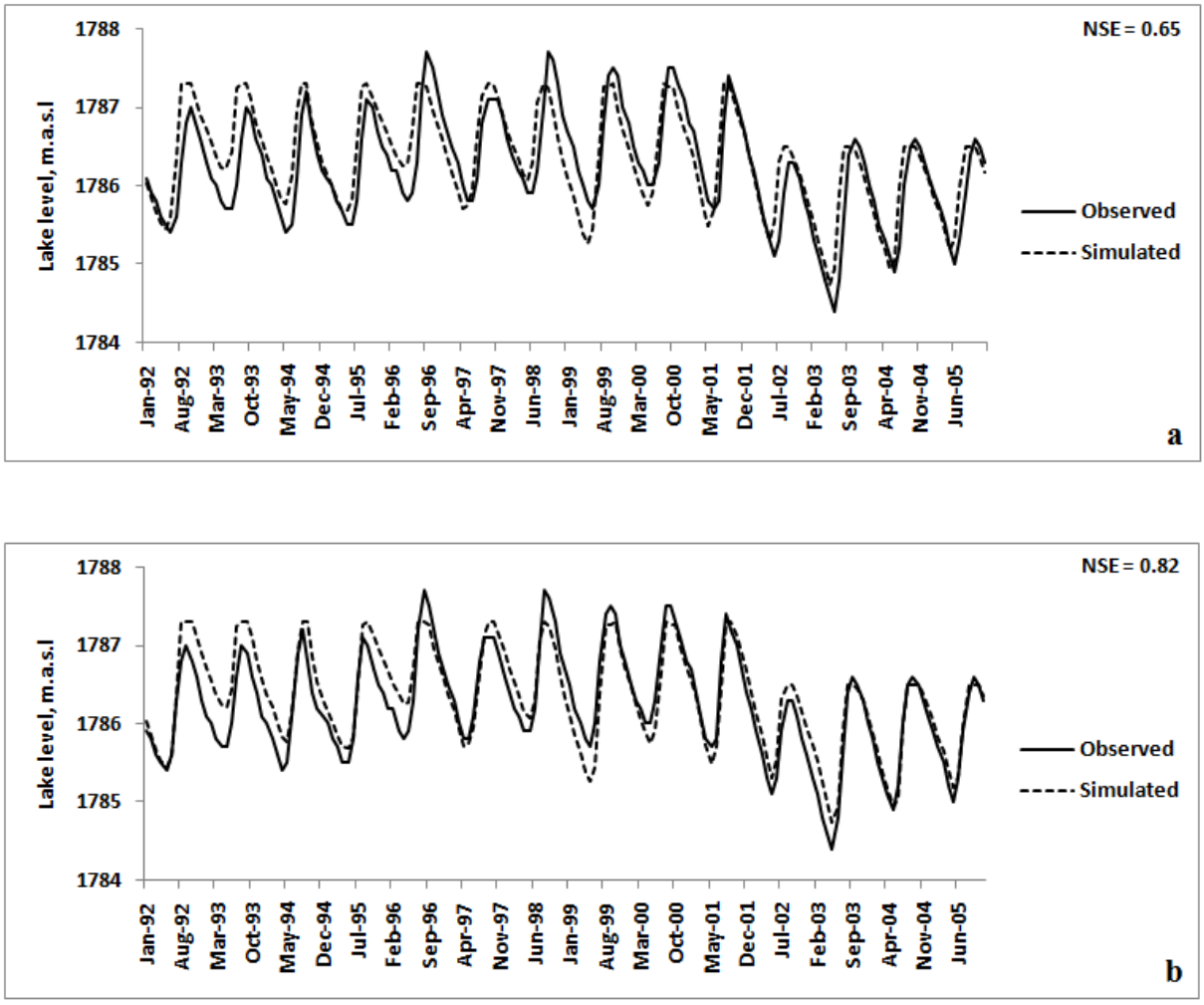

Figure 7-6 Comparison of observed and simulated levels of Lake Tana (a) without the lake's routing effect (b) considering the routing effect of the lake

7.4 Suspended sediment balance of Lake Tana

The suspended sediment balance modeling involved different parts that aimed at estimating the various components of the mass balance. It was not possible to exploit the erosion and sediment transport capability of DHSVM as it gave sediment yields that were too low. First, the suspended sediment rating curves developed in Chapter 3 were used to estimate the mean annual sediment load contributed by the gauged catchments. Then, a regional model that relates specific suspended sediment yield to catchment area was used to estimate suspended sediment discharge from watersheds without rating curves. Figure 7-7 illustrates parts of the basin for which each of these methods were applied. The suspended sediment outflow was estimated by using a rating curve obtained in the Abay Master Plan study report (BCEOM, 1999b). Finally, the calculated mean annual suspended sediment influx and outflow were used to estimate the sediment trap efficiency of the lake and the mean deposition rate.

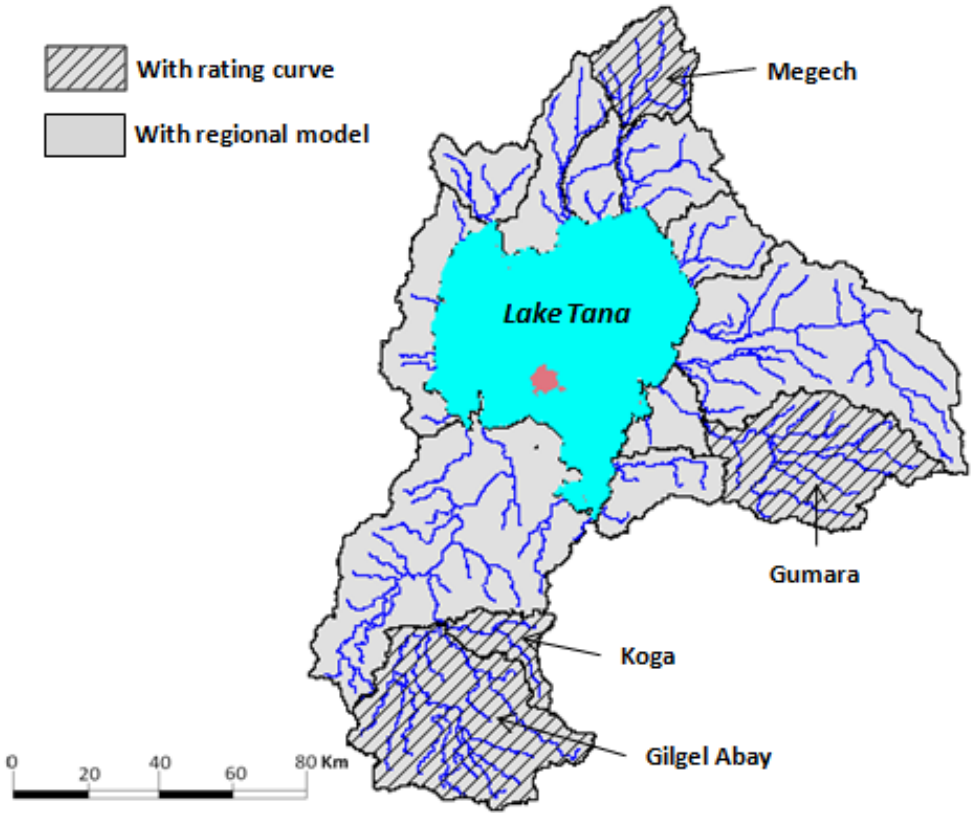

Figure 7-7 Catchments to which rating curves or regional models were applied to estimate suspended sediment discharges

7.4.1 Suspended sediment discharge from gauged catchments

The contributions of gauged catchments for which suspended sediment data could be obtained were estimated by using rating curves. Suspended sediment rating curves, with and without correction for bias, were established for the gauged parts of Gilgel Abay, Gumara, Koga and Megech catchments in Chapter 3. The rating curve equations together with the corresponding Nash-Sutcliffe efficiencies are presented in Table 7-16. Rating curve equations with better performance were used to estimate the mean annual sediment load.

Table 7-16 Suspended sediment rating curve equations of four gauged catchments in the Lake Tana basin

Catchment	Rating curve equation† $SS = aQ^b$ x CF			NSE	
	a	b	CF	Without correction	With correction
Gilgel Abay	4.155	1.698	1.11	0.68	0.70
Gumara	23.087	1.428	2.42	0.56	0.41
Koga	7.686	1.825	1.35	0.45	0.46
Megech	20.969	1.194	2.08	0.35	0.67

†SS is suspended sediment load in t/d; Q in m^3/s; a and b are rating curve parameters; CF is correction for bias

The mean annual suspended sediment discharge was first estimated based on the monthly streamflow series for the period 1992-2005. It represents suspended sediment load at the gauging stations which are located upstream of floodplains and wetlands that surround Lake Tana. Overbank deposition on floodplains during flood events usually represents a major sink to suspended sediment and may account for as much as 40-50% of the load delivered to the main channel system (Walling, 2005). A sediment budget study in Zambia by Walling (2001) indicated a 30% suspended sediment loss in a floodplain. Nyssen *et al.* (2004) indicates absence of any study related to sediment deposition rates in floodplains in Ethiopia. It could be assumed that a considerable amount of the suspended sediment load obtained at the gauging stations would be deposited in the low-lying areas. In fact, sedimentation in the lower reaches of the main rivers in the Lake Tana basin was already reported to be the major cause of overbank flow and flooding (SMEC, 2008a). The suspended sediment load contribution of the gauged catchments to the lake was, therefore, estimated by considering floodplain deposition. It is assumed that 30% of the suspended sediment load obtained at the gauging stations during the main rain season would be stored in the downstream floodplains. The estimated suspended sediment loads are presented in Table 7-17.

The specific suspended sediment loads at the gauging stations for Gumara and Gilgel Abay appeared to be high. Previous modeling studies in the Lake Tana basin also indicated high soil erosion potential and sediment yield in these catchments (Awulachew and Tenaw, 2009; Setegn *et al.,*2009).

Table 7-17 Suspended sediment discharges from four gauged catchments in the Lake Tana basin

Catchment	Area km^2	Annual SS load at the gauging station $x10^3$ tons	Specific SS load at the gauging station t $km^{-2}year^{-1}$	Estimated annual SS load reaching Lake Tana $x10^3$ tons
Gilgel Abay	1641	2720	1658	1983
Gumara	1280	2109	1648	1535
Megech	514	204	396	137
Koga	297	199	670	107
Total		5232		3762

7.4.2 Suspended sediment discharge from streams with no data

A large part of the basin with notable flat areas does not have observed suspended sediment data. Estimation of mean annual suspended sediment yields from these catchments without rating curves could be done by using empirical models that relate specific suspended sediment yields to catchment area and/or discharge. Akrasi (2005), for instance used this approach to estimate suspended sediment inputs to Lake Volta from the ungauged catchments. The limited number of catchments with observed/estimated suspended sediment loads, however, became a constraint to developing similar relationship in the study area. Moreover, relations developed based on data from the gauged catchments that are found in the upstream parts of the basin may not adequately represent the flatter downstream areas. It was therefore decided to use a regional suspended sediment-catchment area relationship developed for the wider central and Northern Ethiopian highlands. The model was developed by Nyssen *et al. (*2004) based on existing suspended sediment yield data (Equation 7-9).

$$SSy = 2595A^{-0.29} \quad (n = 20;\ r^2 = 0.59) \qquad \textbf{Equation 7-9}$$

Where *SSy* is specific suspended sediment yield in t km^{-2} $year^{-1}$; A is area in km^2

The model indicates an inverse relationship between suspended sediment yield and catchment size. The explanation to this inverse relationship is often associated to the increased

opportunity for sediment deposition as it moves through the channel system and into flatter areas and well-developed floodplains (Walling and Webb, 1996). On the contrary there are cases that show increase in suspended sediment yield with increase in catchment area and Dedkov (2004) related this to the increase in discharge with area which leads to higher rate of channel erosion. Considering the existence of a sizeable floodplain area all around the lake, the opportunity for sediment deposition could be high in the study area. The use of the regional area-specific suspended sediment yield equation could, therefore, be considered as acceptable. The mean annual suspended sediment contributions of catchments without rating curves are presented in Table 7-18.

Table 7-18 Estimated mean annual suspended sediment discharges from catchments without rating curves

Catchment	Area km^2	Mean annual suspended sediment load x 10^3 tons
Dirma	568	234
Gabikura	377	175
Garno	402	183
Gelda	411	186
Gilgel Abay†	2657	701
Gumara†	300	149
Gumero	548	228
Megech†	299	149
Rib	2193	611
West Tana	621	250
Total		2866

†Represent parts of the catchment excluding the gauged areas shown in Figure 7-7

7.4.3 Total suspended sediment inflow

The total suspended sediment discharge was finally calculated as the sum total of those estimates obtained for catchments with and without rating curves. The estimated mean annual suspended influx was found to be 6.6 x 10^6 tons. Dividing this total suspended sediment load by the basin's area (excluding the water surface) resulted in a specific suspended sediment yield of 545 t km^{-2} $year^{-1}$. The calculated specific suspended sediment yield is within the range indicated for Ethiopian highlands by Walling and Webb (1983). A recent study on sediment export from medium-sized catchments in the northern highlands of Ethiopia has also shown suspended sediment yields that vary from 497 to 6543 t km^{-2} $year^{-1}$ (Vanmaereke *et al.,*2010).

7.4.4 Suspended sediment outflow

The measured suspended sediment concentration at the Abay River gauging station which is located close to the lake's outfall could not be obtained. But, the suspended sediment rating curve equation developed based on data collected during 1961-1995 could be found in the Abay Master Plan study report (BCEOM, 1999b). The rating curve has a power function form and is given in Equation 7-10. It could be seen that the rating curve exponent is relatively low (b = 1.163) in comparison to that of the contributing rivers. This could be related mainly to the effect of the high sediment trap efficiency of the lake.

$$SSy = 10.86Q^{1.163} \qquad \textbf{Equation 7-10}$$

Application of the rating curve equation to monthly outflow series for the period 1992-2005 resulted in a mean annual suspended sediment outflow of 1.3 x 10^6 tons.

7.4.5 Suspended sediment deposition

A net annual suspended sediment deposition of 5.3 x 10^6 tons could be calculated from the estimated influxes and outflows. Dividing this mass by the bulk density of sediment particles could give the equivalent volumetric deposition rate. Use of reported bulk density of 1250 kg/m^3 resulted in a volumetric suspended sediment deposition rate of 4.2 x 10^6 m^3 per year. Dividing this volume by the mean lake surface area gave a uniform suspended sediment deposition rate of 1.4 mm/year. Uniform sediment accumulation pattern is, however, unusual. The suspended sediment trap efficiency of Lake Tana was also calculated from the estimated fluxes using Equation 7-11. The result indicated a trap efficiency value of 80%. This is different from the 50% trap efficiency used in the Abay Master Plan study (BCEOM, 1999a). Corresponding to the lake's average volume and mean annual catchment inflow, the commonly used Brune's curve (Morris, 1998), however, indicated trap efficiency greater than 90%.

$$TE = \left[1 - \frac{SS_{out}}{SS_{in}}\right] \times 100\% \qquad \textbf{Equation 7-11}$$

Where TE is suspended sediment trap efficiency in %; SS_{in} and SS_{out} are suspended sediment inflow and outflow, respectively, in tons per year.

The floodplain and wetland systems that are found all around the lake play an important role in preventing a large amount of sediment from reaching the lake. With the estimated suspended sediment deposition rate, it requires 65 years for the lake to lose 1% of its volume corresponding to the average water surface level. The situation would be different for reservoirs located in the upstream parts of the basin because of a higher suspended sediment yield and lower storage capacity of reservoirs. The problem of suspended sediment deposition in the lake should also be assessed in terms of its impact on water quality. Fine sediments and associated nutrients and contaminants are major sources of water pollution with adverse effects on the ecology of lakes (Donohue and Molinos, 2009). Adverse effects associated with fine sediments in the Lake Tana ecosystem has already been noted by Dejene *et al. (*2004). Management efforts to reducing suspended sediment discharge to the lake should, therefore, be driven by issues related to its effects on both storage capacity and water quality.

7.5 Concluding remark

The study on water and suspended sediment balance of Lake Tana provided useful outputs that could contribute to its sustainable management. It indicated the relative contributions of the different water balance components. The contribution from ungauged parts is not negligible as assumed in some of the previous studies. It is important to ensure minimal disruptions to the hydrologic regimes of the few catchments that contribute most of the surface inflow. In recent years Lake Tana basin has seen major water resource development projects, some completed and some ongoing. The projects have the effect of modifying inflows coming from the major catchments and bringing in a new outflow component via the direct transfer of water from the lake to a downstream basin. It would, therefore, be important to update the water balance of the lake by considering these major developments.

The mean annual suspended sediment load was estimated based on rating curves developed from limited data, a regional area-specific sediment yield model and an assumption on sediment loss in the floodplains. Considering these facts, the result could only be taken as a firsthand estimate useful for planning level applications. It would be important to make a concerted sediment measuring campaign at representative locations both in the upstream and downstream reaches. This would contribute to better understand sediment export processes and the role of floodplains and wetlands in the study area.

General conclusion and perspectives

Summary and conclusion

This study had three major components that include evaluation and analysis of the existing meteorological and spatial datasets in the Lake Tana basin, assessment of the applicability of a physically-based distributed hydrological model, and modeling the water and suspended sediment balance of the lake. Overall, the daily hydro-meteorological dataset could be considered as having good quality. A notable part of the basin, however, failed to meet the minimum rainfall network density of the WMO. The hourly rainfall data of Bahir Dar and Gonder meteorological stations were found to be by far inadequate and unreliable. In view of the spatially heterogeneous nature of soil properties, the available data could be considered as inadequate for carrying out studies that require higher resolution. The existing data on suspended sediment solids is limited to very few days in a year and is highly fragmented. The sensitivity analyses of soil and vegetation parameters of DHSVM enabled identification of few influential parameters and this has greatly simplified calibration of the model in the selected catchments. In light of the coarse spatial and/or temporal resolutions of the hydro-meteorological and spatial datasets used, the distributed hydrological model showed a promising performance in Megech and Rib catchments. The magnitudes of the estimated water balance components of Lake Tana could be considered acceptable, as the relative discrepancy was in general found to be within recommended limits. This was further supported by the ability of the water balance model to closely simulate the lake level fluctuation. Runoff from the contributing catchments of the lake was found to be a major component of the annual water balance of Lake Tana. Considering the limit in the spatial and temporal representativeness of the existing suspended sediment data, the results of the lake's sediment balance analysis should be considered relevant for planning level applications. The lake was found to be an important sink to the incoming suspended sediment.

Watersheds in Ethiopia in general, and Lake Tana basin in particular, are faced by a number of critical issues that include erosion and sedimentation, water availability, flooding, and nonpoint source pollution. The search for sustainable management options that effectively and efficiently address these issues requires a hydro-meteorological and spatial database with adequate quality, quantity and resolution as well as sound analysis tools. For Lake Tana basin it is important to strengthen the network density of rainfall gauging stations in different parts of the basin. A major improvement in the acquisition and quality control of data from the

recording rain gauges is required. Availability of adequate and reliable rainfall data at finer time scales is important to make scientific studies on some of the key issues of the basin that include soil erosion, water quality and flooding. The use of relevant disaggregation techniques should also be considered as an alternative strategy to generate meteorological data at the required temporal resolution.

In light of the seriousness of soil erosion and sedimentation problems and the ongoing major water resources development endeavors in the study region, a concerted effort should be exerted to acquiring, analyzing and archiving suspended sediment data. Physically-based distributed hydrological models are considered to be good for making predictions in ungauged catchments. They also have strengths that enable to carry out scientific researches on soil erosion and hydrological impacts of land use and climate changes. It, therefore, of great value to further test and apply the distributed hydrological model used in this study and other similar models in different catchments in the country.

This study has shown how demanding and challenging is making hydrological studies under poor data conditions. The various methods and results of the study could be considered as useful for managing water resources in the region and making relevant scientific researches. The key contributions of this dissertation could be summarized as follows:

- Systematic approach for building a reliable hydro-meteorological database which can be used to carry out similar studies.
- Quality controlled continuous daily hydro-meteorological database for Lake Tana basin for the period 1992-2005.
- Methodological contribution on daily rainfall disaggregation where convective rain producing mechanisms are dominant. Stochastic redistribution of the outputs of the MBLRPM by Beta probability function could reproduce the diurnal rainfall pattern.
- The sensitivity analysis of soil and vegetation parameters of DHSVM helped to identify few influential parameters and this could serve as a guide in calibrating the model.
- Useful body of knowledge on the spatial and temporal characteristics of hydrological and meteorological elements such as the variation of rainfall and temperature with altitude/latitude, baseflow indices, and insight on rainfall-runoff relationships.
- Updated water balance of Lake Tana based on quality controlled and representative datasets
- Longterm suspended sediment balance of Lake Tana based on comprehensive analysis

Perspectives

The study has enabled to explore and identify key areas for further research that would enhance its scientific and practical values. Four lines of research have been identified.

Uncertainty and sensitivity analysis

Uncertainty in outputs of the model is a major issue in hydrological and environmental modeling. The sources of uncertainty may include data uncertainty and model uncertainty. Data uncertainty is related to the quality, and spatial and temporal representativeness of observed quantities like precipitation, streamflow, soil hydraulic properties, etc. Model uncertainty is associated to the representations of the real world system and physical processes and parameter values.

This study involved use of simpler models associated with water and suspended sediment balance of Lake Tana and a complex physically-based model associated with the evaluation of the applicability of DHSVM. The quality and areal coverage of the daily rainfall data could be a major source of uncertainty in the lake water balance model. As discharges are estimated by rating curves, the quality of the observed streamflows could also be a major source of uncertainty. Moreover, the estimated discharges from the ungauged catchments could be affected by uncertainties due to the use of the conceptual model and the corresponding driving meteorological inputs. The distributed hydrological model used meteorological forcings derived from few stations that may not fully represent the catchment. This could be a major source of uncertainty in the outputs of the model. Conducting further studies on uncertainty analysis of the lake water balance and predictions of the distributed hydrological model would therefore be useful in refining the modeling results and defining the level of efforts that must be invested in acquiring the required inputs. Moreover, it would be relevant to assess the sensitivity of the water balance of Lake Tana to the different water resource developments as well as land use and climate changes.

Meteorological data disaggregation

In this study various disaggregation techniques were used to generate meteorological time series at hourly temporal resolution. But due to lack of observed hourly data for most of the meteorological elements in the study area, it was not possible to evaluate the level of performance of the disaggregation techniques. Lack of meteorological data at shorter time

scales is a general problem in the country and may continue so due to resource constraints. The use of weather data disaggregation techniques should, therefore, be considered as an important strategy. Evaluation of the performances of the disaggregation models based on data that could be obtained from synoptic meteorological stations of the country like Addis Ababa should, therefore, be regarded as an important line of research.

Testing DHSVM on other catchments

Evaluation of the performances of DHSVM in the study area gave mixed results- satisfactory in some and poor in others. Good performance of the model from field to watershed scale is reported in the literature. Further evaluation of the model would be required to reach a better judgment on its performance. It is, therefore, important to test the applicability of the model on other catchments with better hydro-meteorological and spatial data coverage and resolution. Moreover, it would be good to evaluate the capability of the model in predicting other state variables like groundwater level and soil moisture content if data is available.

Further study on suspended sediment

The study on suspended sediment yield provided the order of magnitude of the problem. In light of the seriousness of soil erosion and sedimentation problems in the study area as well as the ongoing and planned major water resource developments in the study region, more research is required on the issue. Further studies using representative and good quality data on sources and yield of suspended sediment would strengthen the scientific bases of watershed management alternatives that aim at reducing the onsite and offsite impacts of soil erosion. Research on suspended sediment yields is also important to make related studies such as estimation of nonpoint source pollution loads. In this regard, it is of great value to further exploit the erosion and sediment transport capabilities of DHSVM.

References

Abbott, M., Bathurst, J., Cunge, J., O'Connell, P., and Rasmussen, J. (1986). An introduction to the European Hydroloigcal system – Système Hydrologique Européen, SHE, 2: Structure of a physically based distributed modelling system. *Journal of Hydrology* **87**: 61-77.

Abdo,K.S., Fiseha, B.M., Rientjes, H.M., Gieske, A.S.M., Haile, A.T. (2009). Assessment of climate change impacts on the hydrology of Gilgel Abay catchment in Lake Tana basin, Ethiopia. *Hydrological Processes* **23**: 3661-3669.

Achamyeleh, K. (2003). Ethiopia: Integrated flood management . WMO/GWP Associated Program on Flood Management.

Acres International and Shawel Consult (1995). *Feasibility Study of Birr and Koga Irrigation Project*. Koga catchment and irrigation studies, Annex L, Soil conservation. Addis Ababa: Ministry of Water Resources.

Ahl, R.S., S.W. Woods, H.R. Zuuring (2008). Hydrologic calibration of SWAT in a snow-dominated rocky mountain watershed, Montana, USA. *Journal of the American Water Resources Association* **44(6)**: 1411-1430.

Ahrens, C.D. (1991) *Meteorology today: An Introduction to Weather, Climate, and the Environment,* 4th ed. West Publishing Company, USA.

Ajami, N.K., H. Gupta, T. Wagener, S. Sorooshian (2004). Calibration of a semi-distributed hydrologic model for streamflow estimation along a river system. *Journal of Hydrology* **298**: 112-135.

Akrasi, S.A. (2005). The assessment of suspended sediment inputs to Volta Lake. *Lakes & Reservoirs: Research and Management* **10**: 179-186.

Aksoy, H., N. E. Unal, A. O. Pektas (2008). Smoothed minima baseflow separation tool for perennial and intermittent streams. *Hydrological Processes* **22**, 4467-4476.

Alam, M.S., S.K. Saha, M.A.K. Chowdhury, Md. Saifuzzaman and M. Rahman (2005). Simulation of solar radiation. *American Journal of Applied Sciences* **2(4)**: 751-758.

Alemayehu, T., McCartney, M., Kebede, S. (2009). Simulation of water resources development and environmental flows in the Lake Tana subbasin. In: Awulachew, S. B.; Erkossa, T.; Smakhtin, V.; Fernando, A. (Comp.). *Improved water and land management in the Ethiopian highlands: Its impact on downstream stakeholders dependent on the Blue Nile*. *Intermediate Results Dissemination Workshop held at the International Livestock Research Institute (ILRI), Addis Ababa, Ethiopia.* Colombo, Sri Lanka: International Water Management Institute. doi:10.3910/2009.201

Allen, R.G., Pereira, L.S., Raes, D., Smith, M., 1998. *Crop Evapotranspiration: Guidelines for Computing Crop Water Requirements.* FAO Irrigation and Drainage Paper, 56, Rome, 300 pp.

Ananda, J. and Herath, G. (2003). Soil erosion in developing countries: a socio-economic appraisal. *Journal of Environmental Management* **68**: 343-353.

Andersson-Sköld, Y., D. Simpson and V. Odedaard (2008). Humidity parameters from temperature: test of a simple methodology for European conditions. *International Journal of Climatology* **28**: 961-972.

Anderton, S., Latron, J. and Gallart, F. (2002). Sensitivity analysis and multi-response, multi-criteria evaluation of a physically based distributed model. *Hydrological Processes* **16**: 333-353.

ASCE (1996). *Hydrology Handbook*, 2nd ed. American Society of Civil Engineering.

Asner, G.P., J.M.O. Scurlock and J.A. Hicke (2003). Global synthesis of leaf area index observations: implications for ecological and remote sensing studies. *Global Ecology & Biogeography* **12**: 191-205.

Asselman, N.E.M. (2000). Fitting and interpretation of sediment rating curves. *Journal of Hydrology* **234**: 228-248.

Awulachew, S. B. and Mequanint Tenaw (2009). Micro-watershed to basin scale impacts of widespread adoption of watershed management interventions in the Blue Nile Basin. In: Humphreys, E. and Bayot, R.S. (eds.), *Increasing the productivity and sustainability of rainfed cropping systems of poor smallholder farmers.* Proceedings of the CGIAR Challenge Program on Water and Food International Workshop on Rainfed Cropping Systems, Tamale, Ghana, 22-25 September 2008, pp. 223-231, The CGIAR Challenge Program on Water and Food, Colombo, Sri Lanka.

Awulachew, S. B., McCartney, M. Steenhuis, T. S. Ahmed, A. A. (2008). *A Review of Hydrology, Sediment and Water Resource Use in the Blue Nile Basin*. Colombo, Sri Lanka: International Water Management Institute. 87p. (IWMI Working Paper 131)

Awulachew, S. B.; Yilma, A. D.; Loulseged, M.; Loiskandl, W., Ayana, M.; Alamirew, T. (2007). *Water Resources and Irrigation Development in Ethiopia*. Colombo, Sri Lanka: International Water Management Institute. 78p. (Working Paper 123).

Ayana, Essayas K. (2007). Validation of radar altimetri lake level data and its application in water resources management. M.Sc thesis, ITC, Enschede, The Netherlands.

Ayenew, Tenalem (2007). Water management problems in the Ethiopian rift: challenges for development. *Journal of African Earth Sciences* **48**: 222-236.

Ayenew, Tenalem., Demile, M., Wohnlich, S. (2008). Hydrological framework and occurrence of groundwater in the Ethiopian aquifers. *Journal of African Earth Sciences* **52**: 97-113.

Ayenew, Tenalem (2009). *Natural Lakes of Ethiopia.* Addis Ababa: Addis Ababa University Press.

Bahremand, A. and De Smedt, F. (2008). Distributed hydrological modeling and sensitivity analysis in Torysa watershed, Slovakia. *Water Resources Management* **22**: 393-408.

Baker, J.M., Reicosky, D.C. and baker, D.G. (1988). Estimating the time dependence of air temperature using daily maxima and minima: a comparison of three methods. *Journal of Atmospheric and Oceanic Technology* **5**: 736-742.

Banadda, E.N., Kansiime, F.,.Kigobe, M., ; Kizza, M., Nhapi, I. (2009). Landuse-based nonpoint source pollution: a threat to water quality in Murchison Bay, Uganda. *Water Policy* **11**: Supplement 1, 94-105.

BCEOM (1999a). *Abay River Integrated Development Master Plan Project*. Phase 3, Vol I: Main Report, Addis Ababa: Ministry of Water resources.

BCEOM (1999b). *Abay River Integrated Development Master Plan Project.* Phase 2, Section II, Volume III: Hydrology. Addis Ababa: Ministry of Water Resources.

BCEOM (1999c). *Abay River Integrated Development Master Plan Project*. Phase 2, Section II, Volume IX: Semi-detailed soils survey. Addis Ababa: Ministry of Water Resources.

Becker, A. and Serban, P. (1990). Hydrological models for water resources system design and operation. In: *Operational Hydrology*, WMO Report No. 34, 80pp.

Bekele, Getachew and B. Palm (2009). Wind energy potential assessment at four typical locations in Ethiopia. *Applied Energy* **86**: 388-396.

Bergström, S. (1976). *Development and application of a conceptual runoff model for Scandinavian catchments.* SMHI Report RHO, No. 7.

Beven, Keith J. (2001). *Rainfall-Runoff Modeling.* Chichester: Johns Wiley & Sons Ltd.

Bewket, W., Conway, D. (2007). A note on the temporal and spatial variability of rainfall in the drought-prone Amhara region of Ethiopia. *International Journal of Climatology* **27**: 1467-1477.

Bewket, Woldeamlak, and Geert Sterk (2003). Assessment of soil erosion in cultivated fields using a survey methodology for rills in the Chemoga watershed, Ethiopia. *Agriculture, Ecosystems and Environment* **97**: 81-93.

Bilbao, J., A.H., de Miguel and H.D. Kambezidis (2002). Air temperature model evaluation in the North Mediterranean Belt area. *Journal of Applied Meteorology* **41**: 872-884.

Blanco, Humberto, and Rattal Lal (2008). *Principles of Soil Conservation and Management.* Springer.

Bo, Z. and Islam, S. (1994). Aggregation-disaggregation properties of a stochastic model. *Water Resources Research* **30 (12)**: 3423-3435.

Boer, M. G. D. Barrio and J. Puigdefàbregas (1996). Mapping soil depth classes in dry Mediterranean areas using terrain attributes derived from a digital elevation model. *Geoderma* **72**: 99-118.

Bonan, G.B. (2002). *Ecological Climatology: Concepts and Applications*. Cambridge University Press.

Bormann, H., B., Diekkrüger and O. Richter (1997). Effects of data availability on estimation of evapotranspiration. *Phys. Chem. Earth.* **21(3)**: 171-175.

Brandes, D. and Wilcox, B.P. (2000). Evapotranspiration and soil moisture dynamics on a semiarid ponderosa pine hillslope. *Journal of the American Water Resources Association* **36(5)**: 965-974.

Brooks, E.S., J. Boll and P.A. McDaniel (2004). A hillslope-scale experiment to measure lateral saturated hydraulic conductivity. *Water Resources Research* **40**: W04208, doi:10.1029/2003WR002858.

Brooks, Kenneth N., Peter F. Ffolliott, Hans M. Greresen, and Leonard F. Debango (2003). *Hydrology and the Management of Watersheds.* 3rd ed. Iowa: Iowa State Press.

Brustaert, W. (2005). *Hydrology- An Introduction.* Cambridge University Press: Cambridge.

Budyko, M.I. (1958). *The Heat Balance of the Earth's Surface*. US Department of Commerce, Washington, DC.

Burt, T.P. (1992). The hydrology of headwater catchments. In: Calow, P. and Petts, G.E. (eds), *The Rivers Handbook: Hydrological and Ecological Principles*. Oxford: Blackwell, 3-28.

Campo, M.A., Cirauqui, J.C., Lopez, J.J. (2008). Application of a stochastic rainfall model for disaggregation. *Geophysical Research abstracts* **10**: EGU2008-A-11799.

Campologo, F., Cariboni, J., Saltelli, A. (2007). An effective screening design for sensitivity analysis of large models. *Environmental Modeling & Software* **22**: 1509-1518.

Cariboni, J., Gatelli, D., Liska, R., Saltelli, A. (2007). The role of sensitivity analysis in ecological modeling. *Ecological Modeling* **203**: 167-182.

Carta, J.A., P.Ramirez and S. Velàzquez (2009). A review of wind speed probability distributions used in wind energy analysis: case studies in the Canary Islands. *Renewable and Sustainable Energy Reviews* **13**: 933-955.

Chapman, T. (1999). A comparison of algorithms for streamflow recession and baseflow separation. *Hydrological Processes* **13**: 701-714.

Chen, J.M., X. Chen, W. Ju and X. Geng (2005). Distributed hydrological model for mapping evapotranspiration using remote sensing inputs. *Journal of Hydrology* **305**: 15-39.

Cheung, W.H., Senay, G.B., Singh, A. (2008). Trends and spatial distribution of annual and seasonal rainfall in Ethiopia. *International Journal of Climatology, DOI: 10.1002/joc.1623*.

Chineke, T.C. (2008). Equations for estimating global solar radiation in data sparse regions. *Renewable Energy* **33**: 827-831.

Chorowicz, J., Collet, B., Bonavia, F.F., Mohr, P., Parrot, J.F. and Korme, T. (1998). The Tana basin, Ethiopia: intra-plateau uplift, rifting and subsidence. *Tectonophysics* **295**: 351-367.

Chow, V. T., Maidment, D.R., Mays, L.W. (1988). *Applied Hydrology*. McGraw-Hill, New York.

Christie, F., and J. Hanlon (2001). *Mozambique and the Great Flood of 2000*. International African Institute and James Currey, 176 pp.

Cloke, H.L., Pappenberge, F. and Renaud, J.P. (2008). Multi-method global sensitivity analysis for modeling floodplain *Hydrological Processes*. *Hydrological Processes* **22**: 1660-1674.

Cohen, S., Ianetz, A., Stanhill, G. (2002). Evaporative climate changes at Bet Dagan, Israel, 1964–1998. *Agricultural and Forest Meteorology* **111**: 83–91.

Connolly, R.D., Schirmer, J., Dunn, P.K. (1998). A daily rainfall disaggregation model. *Agricultural and Forest Meteorology* **92**: 105-117.

Conway, D. (2000). The climate and hydrology of the Upper Blue Nile River. *The Geographical Journal* **166(1)**: 49-62.

Crawford TM and Duchon CE (1999). An improved parameterization for estimating effective atmospheric emissivity for use in calculating daytime downwelling longwave radiation. *Journal of Applied Meteorology* **38 (4)**:474–480

CRED (2010). Centre for Research on the Epidemiology of Disasters. Database, http://www.emdat.be/database. Cited 12 May 2010

CSA (2008). *Summary and Statistical Report of the 2007 Population and Housing Census.* Central Statistical Agency of Ethiopia, Addis Ababa, Ethiopia.

Cugier, P., Billen, G., Guillaud, J.F., Garnier, J., Ménesguen, A. (2005). Modelling the eutrophication of the Seine Bight (France) under historical, present and future riverine nutrient loading. *Journal of Hydrology* **304**: 381-396.

Cuo L., Giambelluca T.W., Ziegler, A.D., Nullet, M.A. (2006). Use of the distributed hydrology soil vegetation model to study road effects on *Hydrological Processes* in Pang Khum Experimental Watershed, northern Thailand. *Forest Ecology and Management* **224**: 81–94

Cuo, L., Lettenmaier, D.P., Mattheussen, B.V., Storck, P., Wiley, M. (2008). Hydrologic prediction for urban watershed with the Distributed Hydrology-Soil-Vegetation Model. *Hydrological Processes* **22**: 4205-4213.

Cuo, L., Lettenmaier, D.P., Alberti, M. and Richey, E. (2009). Effects of a century of land cover and climate change on the hydrology of the Puget Sound basin. *Hydrological Processes* **23**: 907-933.

Daniel, Yohannes (2007). Remote sensing based assessment of water resource potential for Lake Tana basin. Master of Science Thesis, Civil Engineering Department: Addis Ababa University.

Davie, T. (2003). *Fundamentals of Hydrology*. Routledge Publishing

De Roo, A.P.J., Offermans, R.J.E., and Cremers, N.H.D.T. (1996). LISEM: A single-event, physically based hydrological and soil erosion model for drainage basins II: sensitivity analysis, validation and application, *Hydrological Processes* **10**: 1119-1126.

De Wit C.T. (1978). Simulation of assimilation, respiration and transpiration of crops, p.148.Wageningen: Pudoc.

Debele, B., Srinivasan, R., Parlange, J.Y. (2007). Accuracy evaluation of weather data generation and disaggregation methods at finer timescales. *Advances in water resources* **30(5)**: 1286-1300

Dedkov A. P. (2004). The relationship between sediment yield and drainage basin area. In*:* V. Golosov, V. Belyaev and D. E. Walling (eds.), *Sediment Transport Through the Fluvial System,* pp. 197–204. IAHS Press, Wallingford: United Kingdom.

Dejen, E., J. Vijverberg, L.A.J. Nagelkerke, and F. A., Sibbing (2004). Temporal and spatial distribution of microcrustacean zooplankton in relation to turbidity and other environmental factors in large tropical lake (L. Tana, Ethiopia). *Hydobiologia* **513**: 39-49.

Devi, Rani, Esubalew Tesfahune, Worku Legesse, Bishaw Deboch, and Abebe Beyene (2008). Assessment of siltation and nutrient enrichment of Gilgel Gibe Dam, Southwest Ethiopia. *Bioresource Technology* **99**: 975-979.

Dingman, S.L. (1994). *Physical Hydrology*. New Jersey: Prentice Hall.

Diplas, P. (2002). Integrated decision making for water resources management. *Journal of the American Water Resources Assosciation* 38(2): 37-340.

Diro, G.T., D.I.F. Grimes, E. Black, A. O'Neill and E. Pardo-Iguzqiza (2009). Evaluation of reanalysis rainfall estimates over Ethiopia. *International Journal of Climatology* **29**: 67-78.

Donohue, I. and Molinos, J.G. (2009). Impacts of increased sediment loads on the ecology of lakes. *Biological Reviews,* DOI:10.1111/j.1469-185X.2009.00081.x.

Doten, C.O. and D.P. Lettenmaier (2004). *Prediction of Sediment Erosion and Transport with the Distributed Hydrology-Soil-Vegetation Model*. Water Resources Series, Technical Report 178, University of Washington.

Doten, C.O., L.C. Bowling, E.P. Maurer, J.S. Lanini and D.P. Lettenmaier (2006). A spatially distributed model for dynamic prediction of sediment erosion and transport in mountainous forested watersheds. *Water Resources Research* **42(4)**: W0441710.1029/2004WR003829.

Driessen P, Deckers J, Spaargaren O, Nachtergaele F. (2001). *Lecture Notes on the Major Soils of the World*. World Soil Resources Reports, 94. Rome: Food and Agricultural Organization of the United Nations, 334 pp.

Duan, N. (1983). Smearing estimate: a nonparametric retransformation method. *Journal of the American Statistical* Association **78 (383)**: 605–610.

Duarte HF, Dias NL, Maggiotto SR (2006). Assessing daytime downward longwave radiation estimates for clear and cloudy skies in Southern Brazil. *Agricultural and Forest Meteorology* **139(3–4)**:171–181

Dubus, I.G., Brown, C.D. and Beulke, S. (2003). Sensitivity analysis for four pesticide leaching models. *Pest Manag. Sci.* **59**: 962-982.

Duda, A.M. (1996). Addressing nonpoint sources of pollution must become an international priority. *Water Science and Technology* **28(3-5)**: 1-12.

Dunne, T. (1978). Field studies of hillslope flow processes. In: M.J. Kirkby (ed), *Hillslope Hydrology*. Chichester: John Wiley & Sons, 227–293.

Eckhardt, K. (2008). A comparison of baseflow indices, which were calculated with seven different baseflow separation methods. *Journal of Hydrology* **352**: 168-173.

Eckhardt, K. and Arnold, J.G. (2001). Automatic calibration of a distributed catchment model. *Journal of Hydrology* 251: 103–109.

Edossa, Desalegn C., Mukand S. Babel (2010). Drought analysis in the Awash River Basin, Ethiopia. *Water Resources Management* **24**: 1441-1460.

Eischeid JK, Pasteris PA, Diaz HF, Plantico MS, Lott NJ. (2000). Creating a serially complete, national daily time series of temperature and precipitation for the Western United States. *Journal of Applied Meteorology* **39**: 1580–1591.

Elsheikh, S., A. Kaikai, and K. Andah (1991). Intensive sediment transport from the Upper Nile basin and water resources management in Sudan. In *Hydrology for the Water Management of Large River Basins.* Vienna: IAHS, 1991 291-300.

Engida, Agizew N. and Esteves, Michel (2010). Characterization and disaggregation of daily rainfall in the Upper Blue Nile Basin in Ethiopia. Submitted to Journal of Hydrology.

EWD (2007). *Regional Summary of Multi-agency Flood Impact Assessment of 2006*. Early Warning Department, Federal Disaster Prevention and Preparedness Agency, Addis Ababa, Ethiopia.

Ewen, J., Parkin, G. and O'Connell, P.E. (2000). SHETRAN: Distributed river basin flow and transport modeling system. *Journal of Hydrologic Engineering* **5**: 250-258.

Famiglietti,J.S., Rudnicki, J.W. and Rodell, M. (1998). Variability in surface moisture content along a hillslope transect: Rattlesnake Hill, Texas. *Journal of Hydrology* **210**: 259-281.

FAO (1988). *Soil Map of the World. Revised Legend.* Reprinted with corrections. World Soil Resources Report 60. FAO, Rome.

FAO (2000). Forest cover mapping and monitoring with NOAA-AVHRR and other coarse spatial resolution sensors. Forest Resources Assessment Program., Working Paper 29 Forestry Department

Federico, S., Avolio, E., Pasqualoni, L., Leo, L. D., Sempreviva, A. M., and Bellecci, C. (2009). Preliminary results of a 30-year daily rainfall database in southern Italy. *Atmospheric Research* **94**: 641-651.

Ferguson, H.L. and Znamensky, V.A. (1981). Methods of computation of the water balance of large lakes and reservoirs. A contribution to the International Hydrological Programme, Paris: UNESCO.

Ferguson, R.I. (1986). River loads underestimated by rating curves. *Water Resources Research* **22**: 74–76.

Finch, J.W. and M.J. Best (2004). The accuracy of downward short- and long-wave radiation at the earth's surface calculated using simple models. *Meteorol. Appl.* **11**: 33-39.

Fiorentino, M., s. Manfreda, and V. Iacobellis (2007). Peak runoff contributing area as hydrological signature of the probability distribution of floods. *Advances in Water Resources* **30**: 2123-2134.

Francés, F.,Vélez, J.I.,Vélez, J.J. (2007). Split-parameter structure for the automatic calibration of distributed hydrological models. *Journal of Hydrology* **332:** 226-240.

Franchini, M., J. Wendling, C. Obled, and E. Todini (1996). Physical interpretation and sensitivity analysis of the TOPMODEL. *Journal of Hydrology* **175**: 293-338.

Freehafer, P. (2008). Science and watershed management. *Journal of Contemporary Water Research & Education* **138**: 1-2.

Gautam, Madhur (2006). *Managing drought in sub-Saharan Africa: policy perspectives*. IAAE Conference on Drought: Economic consequences and policies for mitigation, Queensland, Australia.

Gebre, G. and Van Rooijen, D. (2009). Urban water pollution and irrigated vegetable farming in Addis Ababa. In Shaw, Rod (ed) *Proceedings of the 34th WEDC International Conference*, Addis Ababa, Ethiopia.

Giertz, S., B. Diekkrûger, and G. Steup (2006). Physically-based hydrological modelling in Benin. *Hydrol. Earth Syst. Sci.Discuss.* **3**: 595-651.

Glasbey, C.A., Cooper, G., McGechan, M.B. (1995). Disaggregation of daily rainfall by conditional simulation from a point-process model. *Journal of Hydrology* **165:** *1-9.*

Gonfa, Lemma (1996). *Climate Classifications of Ethiopia.* Meteorological Research Report Series, Addis Ababa: National Meteorolological Services Agency.

Gonzàlez-Rouco J, Jimenez J, Quesada V, Valero F. (2001). Quality control and homogeneity of precipitation data in the southwest of Europe. *Journal of Climate* **14**: 1345–1358.

Govindaraju, R.S. (2000). Artificial neural networks in hydrology I: preliminary concepts. *Journal of Hydrologic Engineering* **5 (2):** 115-123.

Grayson, R.B., I.D. Moore, and T.A. McMahon (1992). Physically based hydrologic modeling: a terrain-based model for investigative purposes. *Water Resources Research* **28(10)**: 2639-2658.

Gregersen, Hans M., Peter F.Ffolliott, and Kenneth N. Brooks (2007). *Integrated Watershed Management: Connecting People to their Land and Water.* Oxforshire: CAB International.

Griensven, A.V., Meixner, T., Grunwald, S., Bishop, T., Diluzio, M., Srinivasan, R. (2006). A global sensitivity analysis tool for parameters of multi-variable catchment models. *Journal of Hydrology* **324**: 10-23.

Grubbs, F.E. (1969). Procedures for detecting outlying observations in samples, *Technometrics* **11**: 1–21.

Guo, H., Q. Hu, and T. Jiang (2008). Annual and seasonal streamflow responses to climate and land-cover changes in the Poyang Lake basin, China. *Journal of Hydrology* **355**: 106-122.

Gupta, H. V., S. Sorooshian, and P. O. Yapo (1999). Status of automatic calibration for hydrologic models: Comparison with multilevel expert calibration. *Journal of Hydrologic Engineering* **4(2)**: 135-143.

Gyasi-Agyei, Y. (2005). Stochastic disaggregation of daily rainfall into one-hour time scale. *Journal of Hydrology* ***309***: *178–190*

Haile, A.T., Rientjes, T., Gieske, A. and Gebremichael, M. (2009). Rainfall variability over mountainous and adjacent lake areas: The case of Lake Tana Basin at the source of the Blue Nile River. *Journal of Applied Meteorology and Climatology* **48**: 1696-1717.

Hailemariam, Kinfe (1999). Impact of climate change on the water resources of Awash River Basin, Ethiopia. *Climate Research* **12**: 91-96.

Hamby, D.M. (1994). A review of techniques for parameter sensitivity analysis of environmental models. *Environmental Monitoring and Assessment* **32**: 135-154.

Hamouda, M.A., Nour El-Din, M.M. and Moursy, F.I. (2009). Vulnerability assessment of water resources systems in the Eastern Nile Basin. *Water Resources Management* **23**: 2697-2725.

Hassan, R. (2006). Assessing the impact of climate change on the water resources of the Lake Tana subbasin using Watbal model. Climate change and African Agriculture Policy Note No. 30, CEEPA, University of Pretoria.

Hautot, S., Whaler, K., Gebru, W., Desissa, M. (2006). The structure of a Mesozoic basin beneath the Lake Tana area, Ethiopia, revealed by magnetotelluric imaging. *Journal of African Earth Sciences* **44**: 331-338.

Helsel, D.R. and R.M. Hirsch (2002). *Statistical Methods in Water Resources.* U.S. Geological Survey.

Hengsdij, H., G.W. Meijerinkb, and M.E. Mosugu (2005). Modeling the effect of three soil and water conservation practices in Tigray, Ethiopia. *Agriculture, Ecosystems and Environment* **105**: 29-40.

Hershenhorn, J., Woolhiser, D.A. (1987). Disaggregation of daily rainfall. *Journal of Hydrology* **95***: 229-322.*

Hessel, R., R.van den Bosch, and O.Vigiak (2006). Evaluation of the LISEM soil erosion model in two catchments in the East African Highlands. *Earth Surface Processes and Landforms* **31**: 469-486.

Holvoet, K., Griensven, A., Seuntjens, P., Vanrolleghem, A.A. (2005). Sensitivity analysis for hydrology and pesticide supply towards the river in SWAT. *Phys. Chem. Earth.* **30**: 518-526.

Horowitz, A.J (2003). An evaluation of sediment rating curves for estimating suspended sediment concentrations for subsequent flux calculations. *Hydrological Processes* **17**: 3387-3409.

Hubbard, K.J., R. Mahmood and C. Carlson (2003). Estimating daily dew point temperature for the Northern Great plains using maximum and minimum temperature. *Agronomy Journal* **95**: 323-328.

Hulme, M. (1996). Climate change within the period of meteorological records. In W.M. Adams, A.S. Goudie and A.R. Orme (eds.), *The Physical Geography of Africa*, pp. 88-102. Oxford: Oxford University Press.

Hurni, H. (1990). Degradation and conservation of soil resources in the Ethiopian highlands. *Mountain Research and Development* **8(2-3)**: 123– 130.

Hurni, H. (1993). Land degradation, famine, and land resource scenarios in Ethiopia. In D. Pimentel (ed), *World Soil Erosion and Conservation*, pp. 27-61. Cambridge: Cambridge University Press.

Idso SB and Jackson RD (1969) Thermal radiation from the atmosphere. *J Geophys Res* **74(23)**:5397–5403

ISLSCP (2009). The International Satellite Land-Surface Climatology Project, Initiative II. http://islscp2.sesda.com/ISLSCP2_1/html_pages/groups/veg/edc_landcover_xdeg.html. Accessed in May 2009

Jansson, M.B. (1995). Estimating a sediment rating curve of the Reventazon River at the Palomo using logged mean loads within discharge classes. *Journal of Hydrology* **183**; 227-241.

Jones, J.A.A. (1997). *Global Hydrology: processes, resources and environmental management.* London: Longman.

Jorgensen, S.E. and Rast, W. (2007). The use of models for synthesizing knowledge for integrated lake basin management, and facilitating implementation of the World Lake Vision. *Lakes & Reservoirs: Research and Management* **12**:3-13.

Kannan, N., White, S.M., Worrall, F. and Whelan, M.J. (2007). Sensitivity analysis and identification of best evapotranspiration and runoff options for hydrological modeling in SWAT-2000. *Journal of Hydrology* **336**: 456-466.

Kaplanis, S.N. (2006). New methodologies to estimate the hourly global solar radiation: comparisons with existing models. *Renewable Energy* **31**: 781-790.

Kassahun B. (1999). Ye'ayer mezabat'na tinbi'ya k'Itiopia antsar [Climate change and forecast in Ethiopia]. Paper presented at *Ye'ayer Mezabat, Dirk'na ye'adega mekalakel 'Itiopia*, August 1999, DPPC, Addis Ababa.

Kaur, R., O. Singh, R. Srinivasan, S.N. Das, and K. Mishra (2004). Comparison of a subjective and a physical approach for identification of priority areas for soil and water management in a watershed –A case study of Nagwan watershed in Hazaribagh District of Jharkhand, India. *Environmental Modelling and Assessment* **9**: 115-127.

Kebede, S. (2004). Environmental isotopes and geochemistry in investigating groundwater and lake hydrology: cases from the Blue Nile basin and the Ethiopian Rift (Ethiopia). PhD dissertation, Université d'Avignon et des Pays de Vaucluse, France.

Kebede, S., Y. Travi, T. Alemayehu and T. Ayenew (2005). Groundwater recharge, circulation and geochemical evolution in the source region of the Blue Nile River, Ethiopia. *Applied Geochemistry* **20**: 1658-1676

Kebede, S. Travi Y, Alemayehu T, Marc V. (2006). Water balance of Lake Tana and its sensitivity to fluctuations in rainfall, Blue Nile basin, Ethiopia. *Journal of Hydrology* **316(1–4):** 233–247.

Khaliq, M.N., Cunnane, C. (1996). Modeling point rainfall occurrences with the modified Bartlett-Lewis Rectangular Pulse Model. *Journal of Hydrology* **180***: 109-138.*

Kim, U. and Kaluarachchi, J.J. (2008). Application of parameter estimation and regionalization methodologies to ungauged basins of the Upper Blue Nile River Basin, Ethiopia. *Journal of Hydrology* **362**: 39-56.

Kimball, J.S., S.W. Running, R.Nemani (1997). An improved method for estimating surface humidity from daily minimum temperature. *Agricultural and Forest Meteorology* **85:** 87-98.

Kindie, Abye (2001). Wetlands distribution in Amhara Region, their importance and current threats. In Dixon, A.B., A. Hailu and A.P. Wood (eds.), *Proceedings of the Wetland awareness creation and activity identification workshop in Amhara National Regional State*, Ethiopia.

Kinghton, D. (1998). *Fluvial Forms and Processes: a new perspective*. New York: Oxford University Press Inc.

Kirkby, M.J. (1978). *Hillslope Hydrology*. Chichester: John Wiley & Sons

Klemes V. (1986). Operational testing of hydrological simulation models. *Hydrological Sciences Journal* **31**: 13–24.

Korecha, D., and A.G. Barnston (2006). Predictability of June-September rainfall in Ethiopia. *Monthly Weather Review* **135**: 628-650.

Koutsoyiannis, D. and Onof, C. (2000). A computer program for temporal rainfall disaggregation using adjusting procedures. XXV General Assembly of European Geophysical Society, Nice, *Geophysical Research Abstracts*.

Koutsoyiannis, D. and Onof, C. (2001). Rainfall disaggregation using adjusting procedures on poisson cluster model. *Journal of Hydrology* **246***: 109-122.*

Kozak, J.A., L.R. Ahuja, L. Ma and T.R. Green (2005). Scaling and estimation of evaporation and transpiration of water across soil textures. *Vadoze Zone Journal* **4**: 418-427.

Krause, P., Boyle, D.P., and Bäse, F. (2005). Comparison of different efficiency criteria for hydrological model assessment. *Advances in Geosciences* **5**: 89-97.

Kruk, N.S., I. F. Venrrame, H. R. da Rocha, S. C. Chou and O. Cabral (2010). Downward longwave radiation estimates for clear and all-sky conditions in the Sertaozinho region of Sao Paulo, Brazil. *Theor Appl Climatol* **99:** 115-123.

Kulshreshtha, S. (1998). A global outlook for water resources to the year 2025. *Water Resources Management* **12**: 167-184.

Kundzewicz, Z.W., and Z. Kaczmarek (2000). Copying with hydrological extremes. *Water International* **25 (1)**: 66-75.

Kundzewicz, Z.W., S. Budhakooncharoen, A. Bronstert, H. Hoff, D. Lettenmaier, L. Menzel, R. Schulze (2002). Coping with variability and change: floods and droughts. *Natural Resources Forum* **26**: 263-274.

Lal, R. (2001). Soil degradation by erosion. *Land Degradation and Development* **12**: 519–539.

Lamb, H.F., Bates, C.R., Coombes, P.V., Marshall, M.H., Umer, M., Davies, S.J., Dejene, E. (2007). Late Pleistocene desiccation of Lake Tana, source of the Blue Nile. *Quaternary Science Reviews* **26**: 287-299.

Legesse, D., C. Vallet-Coulomb, and F. Gasse (2003). Hydrological response of a catchment to climate and land use changes in Tropical Africa: case study South Central Ethiopia. *Journal of Hydrology* **275**: 67-85.

Legesse, Dagnachew and Ayenew Tenalem (2006). Effect of improper water and land resource utilization on the central Main land Ethiopian lakes. *Quaternary International* **148**: 8-18.

Lenhart, T., Eckhardt, K., Fohrer, N. and Frede, H.G. (2002). Comparison of two different approaches of sensitivity analysis. *Phys. Chem. Earth.* **27**: 645-654.

Leung, C. K., M. A. F. Mateo and A. J. Nadler (2007). An effective multi-layer model for controlling the quality of data. 11th International Database Engineering and Applications Symposium, IEEE.

Leung, L.R., and M.S. Wigmosta (1999). Potential climate change impacts on mountain watersheds in the Pacific Northwest. *Journal of American Water Resources. Association* **35**: 1463-1471.

Liebscher, Hans-Jürgen, Robin Clarke, John Rodda, Gert Schultz, Andreas Schumann, Lucio Ubertini and Gordon Young (eds.) (2009). The Role of Hydrology in Water Resources Management. *Proceedings of the symbosium held on the island of Capri, Italy, 2008.* IAHS Publ. 327.

Liu, X., X. Mei, Y. Li, Y. Zhang, Q. Wang, J.R. Jensen, J.R. Porter (2009). Calibration of the Angström-Prescott coefficients (a,b) under different time scales and their impacts in estimating global solar radiation in the Yellow River basin. *Agricultural and Forest Meteorology* **149**: 697-710.

Liu, Z., and E. Todini (2002). Towards a comprehensive physically-based rainfall-runoff model. *Hydrol. Earth Syst. Sci* **6**: 859-881.

Ludwig, R. and Philipp Schneider (2006). Validation of digital elevation models from SRTM X-SAR for applications in hydrological modeling. *Journal of Photogrammetry & Remote Sensing* **60**: 339-358.

Madsen, H. (2003). Parameter estimation in distributed hydrological catchment modelling using automatic calibration with multiple objectives. *Advances in Water Resources* **26**: 205-216.

McCartney, M.P., A. Shiferaw, and Y. Seleshi (2009). Estimating environmental flow requirements downstream of the Chara Chara weir on the Blue Nile River. *Hydrological Processes*, DOI: 10.1002/hyp.7254.

McGregor, G.R., Nieuwolt, S. (1998). *Tropical Climatology: an Introduction to the Climates of the Low Latitudes*, 2nd ed. Chichester: John Willey and Sons Ltd.

Meerveld , H.J.T., McDonnell, J.J. (2006). On the interrelations between topography, soil depth, soil moisture, transpiration rates and species distribution at the hillslope scale. *Advances in Water Resources* **29**: 293-310.

Mishra, A., S. Kar, and V.P. Singh (2007). Prioritizing structural management by quantifying the effect of land use and land cover on watershed runoff and sediment yield. *Water Resources Management* **21**: 1899-1913.

MoFED (2006). *Ethiopia: Building on Progress, A plan for accelerated and sustained development to end poverty (PASDEP).* Addis Ababa, Ethiopia: Ministry of Finance and Economic Development.

Mohamed, Y.A., and M. Loulseged (2008). *The Nile Basin Water Resources: Overview of key research questions pertinent to the Nile Basin Initiative.* Sri Lanka: International Water Management Institute.

Mohammed, H., F. Yohannes, and G. Zeleke (2004). Validation of agricultral nonpoint source (AGNPS) pollution model in Kori watershed, South Wollo, Ethiopia. *International Journal of Applied Earth Observation and Geoinformation* **6:** 97-109.

Mohr, P. A. (1962). *The Geology of Ethiopia*. Addis Ababa University-College Press, pp. 268, Addis Ababa.

Moore, I.D., Grayson, R.B. and Ladson, A.R. (1993). Digital Terrain Modeling: A review of hydrological, geomorphological and biological applications: In Beven, K.J. and Moore, I.D. (eds), *Terrain Analysis and Distributed Modeling in Hydrology*. Chichester: John Wiley & Sons pp. 7-34

Moreda, F., V. Koren, Z. Zhang, S. Reed, and M. Smith (2006). Parametrization of distributed hydrological models: learning from the experiences of lumped modeling. *Journal of Hydrology* **320**: 218-237.

Moriasi, D.N., Arnold J.G., Van Liew, M.W., Binger, R.L., Harmel, R.D., Veith, T. (2007). Model evaluation guidelines for systematic quantification of accuracy in watershed simulations. *Transactions of the ASABE* **50(3)**: 885–900.

Morita, M. (2008). Flood risk analysis for determining optimal flood protection levels in urban river management. *J. Flood Risk Management* **1**: 142-149.

Morris, Gregory L. and Fan, Jiahua (1998). *Reservoir Sedimentation Handbook.* New York: McGraw-Hill Book Co.

MoWR (2002). *Water Sector Development Program: Main Report*, Volume 2. Addis Ababa, Ethiopia: Ministry of Water Resources.

MoWR, UNESCO and GIRDC (2004). *National Water Development Report for Ethiopia.* Addis Ababa: Ministry of Water Resources.

Muleta, M.K., Nicklow, J.W. (2005). Sensitivity and uncertainty coupled with automatic calibration for a distributed watershed model. *Journal of Hydrology* **306**: 127-145.

Muleta, S., F. Yohannes, and S.M. Rashid (2006). Soil erosion assessment of Lake Alemaya Catchment, Ethiopia. *Land Degradation and Development* **17**: 333-341.

Mulugeta, Yacob and F. Drake (1996). Assessment of solar and wind energy resources in Ethiopia II: wind energy. *Solar Energy* **57(4)**: 323-334.

Nagle, G.N., T.J. Fahey, and J.P. Lassoie (1999). Management of sedimentation in tropical watersheds. *Environmental Management* **23**: 441-452.

Nash JE, Sutcliffe JV (1970). River flow forecasting through conceptual models. Part I: a discussion of principles. *Journal of Hydrology* **10**: 282–290.

Neitsch, S.L., Arnold, J.G., Kiniry, J.R. and Williams, J.R. (2001). Soil and water assessment tool theoretical documentation. Blackland Research Center, Texas Agricultural Experiment Station, Temple, Texas.

Nigussie, Agizew (1999). Evaluation of water quality and suggested improvement measures: the case of the Little Akaki River, Addis Ababa, Ethiopia. Master of Science Degree Thesis No. 406, Stockhom: Division Of Hydraulic Engineering, The Royal Institute of Technology.

Nishat, S., Guo, Y. and Baetz, B.W. (2007). Development of a simplified continuous simulation model for investigating long-term soil moisture fluctuation. *Agricultural Water Management* **92**: 53-63.

NMA (2009) National Meteorological Agency of Ethiopia: Access to data/information, http://www.ethiomet.gov.et/ Accessed in June 2009.

NMSA (1996). Climatic and Agroclimatic Resources of Ethiopia. *Meteorological Research Report Series, vol. 1, No. 1*, Addis Ababa.

Noto, L.V., V.Y. Ivanov, R.L. Bras, E.R. Vivoni (2008). Effects of initialization on response of a fully-distributed hydrologic model. *Journal of Hydrology* **352**: 107-125.

Novotony, V., and H. Olem (1994). *Water Quality: Prevention, Identification, and Management of Diffuse Pollution* . New York: Van Nostrand Reinhold.

Novotony, V. (1995). *Nonpoint Pollution and Urban Stormwater Management.* PA: Technomic Publishing Company.

Ntiba, M.J., W.M. Kudoja, and C.T. Mukasa (2001). Management issues in the Lake Victoria watershed. *Lakes & Reservoirs: Research and Management* **6**: 211-216.

Nyssen, J., J. Poesen, J. Moeyersons, J. Deckers, Mitiku Haile, and A. Lang (2004). Human impact on the environment in the Ethiopia and Eritrean highlands- a state of the art. *Earth-Science Reviews* **64**: 273-320.

Nyssen, J., Vandenreyken, H., Poesen, J., Moeyersons, J., Deckers, J., Mitiku Haile, Salles, C., Govers, G. (2005). Rainfall erosivity and variability in the Northern Ethiopian Highlands. *Journal of Hydrology* **311**: 172-187.

Nyssen, J., J. Poesen, M. Veyret-Picot, J. Moeyersons, Mitiku Haile, J. Deckers, J. Dewit, J. Naudts, Kassa Teka and G. Govers (2006). Assessment of gully erosion rates through interviews and measurements: a case study from the northern Ethiopian highlands. *Earth Surf. Process. Landforms* **27**: 1267-1283.

Oki, T., C. Valeo, and K. Heal (2006). *Hydrology 2020: An integrating science to meet world water challenges*. IAHS Press.

Oldeman, L., R. Hakkeling, and W. Sombroek (1991). *World map of the status of human-induced soil degradation: an explanatory note.* Nairobi: UNEP.

Oliver JE. (1980). Monthly precipitation distribution: a comparative index. *Professional Geographer* **32**: 300–309.

Onof, C., Wheater, H.S. (1993). Modeling of British rainfall using a random parameter Bartlett-Lewis rectangular pulse model. *Journal of Hydrology* **149**: 67-95.

Onof, C., Chandler, R.E., Kakou, A., Northrop, P., Wheater, H.S., Isham, V. (2000). Rainfall modeling using Poisson-cluster processes: a review of developments. *Stochastic Environmental Research and Risk Assessment* **14**: 384-411.

Ouyang, Wei, Fang-Hua Hao, and Xue-lei Wang (2008). Regional nonpoint source organic pollution modeling and critical area identification for watershed best environmental management. *Water Air Soil Pollut* **187**: 251-261.

Owens, P. N. (2005). Conceptual models and budgets for sediment management at the river basin scale. *Journal of Soils and Sediments* **5**: 201–212.

Owens, P.N. and A.J. Collins (2006). *Soil Erosion and Sediment Redistribution in River Catchments: Measurement, Modelling and Management in the 21st century.* Oxfordshire: CAB International.

Pandey, A., V.M Chowdary, B.C. Mal, and M. Billib (2008). Runoff and sediment yield modeling from a small agricultural watershed in India using the WEPP model. *Journal of Hydrology* **348**: 305-319.

Parajka, J., Merz, R. and Blöschl, G. (2005). A comparison of regionalisation methods for catchment model parameters. *Hydrology and Earth Sciences* **9**: 157-171.

Peterson, TC, DR Easterling, TR Karl, P. Groisman, N. Nicholls, N. Plummer, S. Torok, I. Auer, R. Boehm, D. Gullett, L. Vincent, R. Heino, H. Tuomenvirta, O. Mestre, T. Szentimrey, J. Salinger, EJ Førland, I. Hanssen-Bauerj, H. Alexandersson, P. Jones and D. Parker (1998). Homogenity adjustments of in situ atmospheric climate data: a review. *International Journal of Climatology* **18**: 1493-1517.

Piggott, A.R., S. Moin, C. Southam (2005). A revised approach to the UKIH method for the calculation of baseflow. *Hydrological Sciences Journal* **50(5)**: 911-920.

Pik, R., Deniel, A., Coulon, C., Yirgu, G., Hofmann, C., Ayalew, D. (1998). The northwestern Ethiopian Plateau flood basalts: classification and distribution of magma types. *Journal of Volcanology and Geothermal Research* **81**: 91-111.

Plate, Erich J. (2002). Flood risk and flood management. *Journal of Hydrology* **267**: 2-11.

Podestà, G.P., L. Nùñez, C.A. Villanueva and M.A. Skansi (2004). Estimating daily solar radiation in the Argentine Pampas. *Agricultural and Forest Meteorology* **123**: 41-53.

Prochnow, S.J., J.D. White, T. Scott, and C.D. Filstrup (2008). Multi-scenario simulation analysis in prioritizing management options for an impacted watershed system. *Ecohydrology & Hydrobiology* **8 (1)**: 3-15.

Ramos-Calzado, P., J. Gomez-Camacho, F. Perez-Bernal and M.F. Pita-Lopez (2008). A novel approach to precipitation series completion in climatological datasets: application to Andalusia. *International Journal of Climatology* **28**: 1525-1534.

Rawls, W.J., D.L. Brakensiek, and K.E. Saxton (1982). Estimation of soil water properties. *Trans. ASAE* **25**:1316–1320.

REDECO and HSD (2002). Assessment and monitoring of erosion and sedimentation problems in Ethiopia: *Volume III- Geomorphological investigation of erosion processes in eight selected watersheds.*, REDECO Consulting and Hydrology Studies Department, Addis Ababa, Ethiopia: Ministry of Water Resources.

Refsgaard, J.C. (1997). Parameterization, calibration and validation of distributed hydrologic models. *Journal of Hydrology* **198**: 69–97.

Refsgaard, J.C. and B. Storm (1996). Construction, calibration and validation of hydrological models. In A.B. Abbott and J.C. Refsgaard (eds), *Distributed Hydrological Modelling*. The Netherlands: Kluwer Academic Publishers.

Refsgaard, J.C., H.J. Henriksen, W.G. Harrar, H. Scholten, and Ayalew Kassahun (2005). Quality assurance in model based water management- review of existing practice and outline of new approaches. *Environmental Modelling & Software* **20**: 1201-1215.

Refsgaard., J.C., and H.J. Henriksen (2004). Modelling guidelines- terminology and guiding principles. *Advances in Water Resources* **27**: 71-82.

Reicosky, D.C., L.J. Winkelman, J.M. Baker and D.G. Baker (1989). Accuracy of hourly air temperatures calculated from daily minima and maxima. *Agricultural and Forest Meteorology* **46**: 193-209.

Ridolfi, L., D'Odoricoc, P., Porporato, A. and Rodriguez-Iturbe, I. (2003). Stochastic soil moisture dynamics along a hillslope. *Journal of Hydrology* **272**: 264-275.

Rijsberman, F.R. (2006). Water scarcity: fact or fiction. *Agricultural Water Management* **80**: 5-22.

Riverside, Tropics Consulting Engineers and Shebele Consults (2009). Flood risk mapping consultancy for pilot areas in Ethiopia, Interim report. Addis Ababa: ENTRO.

Rodriguez-Iturbe, I., Cox, D.R. Isham, V. (1988). A point process model for rainfall: further developments. *Proc. R.Soc.London, A,* **417**: 283-298.

Romero, R., Guijarro, J., C.Ramis and S.Alonso (1998). A 30-year (1964-1993) daily rainfall database for the Spanish Mediterranean regions: first exploratory study. *International Journal of Climatology* **18**: 541-560.

Rovira, A. and Batalla, R. (2006). Temporal distribution of suspended sediment transport in a Mediterranean basin: The Lower Tordera (NE Spain). *Geomorphology* **79**: 58-71.

Sadler, E.J and R.E. Schroll (1997). An empirical model of diurnal temperature patterns. Agronomy Journal 89(4), 542-548.

Saltelli, A., Ratto, M., Tarantola, S., Campolongo, F. (2006). Sensitivity analysis practices: Strategies for model-based inference. *Reliability Engineering and System Safety* **91**: 1109-1125.

Saltelli, A., Torantola, S., Chan, K.P.S. (1999). A quantitative model-independent method for global sensitivity analysis of model output. *Technometrics* **41 (1)**: 39–56.

Schaefli, B. and Gupta, H.V. (2007). Do Nash values have value? *Hydrological Processes* **21(15)**: 2075-2080

Segele, Zewdu.T. and Lamb, P.J. (2005). Charcaterization and variability of Kiremt rainy season over Ethiopia. *Meteorol Atmos Phys* **89**: 153-180.

Seleshi, Y., Zanke, U. (2004). Recent trends in rainfall and rainy days in Ethiopia. *International Journal of Climatology* **24**: 973-983.

Setegn, Shimelis G., Ragahavan Srinivasan, Bijan dargahi, and Asefa M.Melesse (2009). Spatial delineation of soil erosion vulnerability in the Lake Tana Basin, Ethiopia. *Hydrolojical Processes*, DOI:10.1002/hyp.

Shahin, M. (2003). *Hydrology and Water Resources of Africa*. New York: Kluwer Academic Publishers

Shibru, D., W. Rieger, and P. Strauss (2003). Assessment of gully erosion using photogrammetric techniques in eastern Ethiopia. Catena. *Catena* **50**: 273– 291.

Shuttleworth, W.J. (1993). Evaporation. In Maidment, D.R. (ed.), *Handbook of Hydrology*. McGraw-Hill, New York, pp. 4.1–4.53 (Chapter 4)

Singh, Vijay, and Donald Frevert (2006). *Watershed Models.* Boca Raton: CRC Press.

Sivapalan, M. (2003). Predictions in ungauged basins : a grand challenge for theoretical hyrology. *Hydrol. Process*. **17**: 3163-3170.

Sivapalan, M., K. Takeuchi, S.W. Franks, V.K. Gupta, H. Karambiri, V. Lakshmi, X. Liang, J.J. McDonnell, E.M. Mendiondo, P.E. O'Connell, T. Oki, J.W. Pomeroy, D. Schertzer, S. Uhlenbrook and E. Zehe (2003). IAHS Decade on Predictions in Ungauged Basins (PUB), 2003-2012: Shaping an exciting future for the hydrological sciences. *Hydrological Sciences Journal* **48(6)**: 857-880

Sivapalan, M., T. Wagener, S. Uhlenbrook, E. Zehe, V. Lakshmi, X. Liang, Y. Tachikawa, P. Kumar (eds.) (2006). *Predictions in Ungauged Basins: Promise and Progress*. IAHS Publication 303, Wallingford: IAHS Press

Smakhtin, V.U. (2001). Low flow hydrology: a review. *Journal of Hydrology* **240**: 147-186.

SMEC (2008c). *Hydrological study of the Tana-Beles Sub-basins: Main Report*. Addis Ababa, Ethiopia: Ministry of Water Resources.

SMEC (2008b). *Hydrological study of the Tana-Beles Sub-basins: Groundwater investigation*. Ministry of Water Resources, Addis Ababa, Ethiopia.

SMEC (2008a). *Hydrological study of the Tana-Beles Sub-basins: Surface water investigation*. Addis Ababa, Ethiopia: Ministry of Water Resources.

Smithers, J.C., Pegram, G.G.S., Schulze, R.E. (2002). Design rainfall estimation in South Africa using Bartlett-Lewis rectangular pulse rainfall models. *Journal of Hydrology* **258**: 83-99.

Snell, S.E., Gopal, S., Kaufmann, R.K. (2000). Spatial interpolation of surface air temperature using artificial neural networks: evaluating their use for downscaling GCMs. *Journal of Climate* **13**: 886-895.

Stahl, K., Moore, R.D., Floyer, J.A., Asplin, M.G., McKendry, I.G. (2006). Comparison of approaches for spatial interpolation of daily air temperature in a large region with complex topography and highly variable station density. *Agricultural and Forest Meteorology* **139**: 224-236.

Sugita M. and Brutsaert WH (1993). Cloud effect in the estimation of instantaneous downward longwave radiation. *Water Resources Research* **29(3)**: 599–605

Sumner, M.E. (2000). *Handbook of Soil Science*. Florida: CRC Press.

Sutcliffe, J. V., Parks, Y. P. (1999). *The Hydrology of the Nile*. IAHS Special Publication no. 5, Institute of Hydrology, Wallingford, Oxfordshire OX10 8BB, UK.

Tabios, G.Q. and J.D. Salas (1985). A comparative analysis of techniques for spatial interpolation of precipitation . *Water Resources Bulletin* **21**: 365-380.

Tadesse, Girma, Fentaw Abegaz, and Taye Gidelew (2007). The water quality of the Middle Awash Valley, Ethiopia. *Middle-East Journal of Scientific Research* 2, no. 2.

Tamene, L., S.J. Park, and P.L.G. Vlek (2006). Reservoir siltation in the semi-arid highlands of northern Ethiopia: sediment yield-catchment area relationship and a semi-quantitative approach for predicting sediment yield. *Earth Surf. Process. Landforms* **31**: 1364-1383.

Tamene, L. and Paul L.G. Vlek (2008). Soil erosion studies in Northern Ethiopia. In Ademola K. Braimoh and Paul L.G. Vlek (eds.), *Land Use and Soil Resources,* 73-100. Springer Netherlands.

Tang, W.Y., Kassim, A.H.M., Abubakar, S.H. (1996). Comparative studies of various missing data treatment methods- Malaysian experience. *Atmospheric Research* **42**: 247-262.

Tang, Y., Reed, P., Wagener, T., Werkhoven, K. (2007). Comparing sensitivity analysis methods to advance lumped watershed model identification and evaluation. *Hydrol. Earth Syst. Sci*. **11**: 793-817.

Tebebu, Tigist Y., Abiy, Anteneh Z., Adzo, Assefa, Dahlke, Helen E., White, Erick D., Collick, Amy S., Kidanu, Selamyihun, Dadgari, F. Steenhuis, Tammo S. (2009). Assessment of hydrological controls on gully erosion and upland erosion near Lake Tana, northern highlands of Ethiopia. In: Awulachew, S. B.; Erkossa, T.; Smakhtin, V.; Fernando, A. (Comp.). *Improved water and land management in the Ethiopian highlands: Its impact on downstream stakeholders dependent on the Blue Nile. Intermediate Results Dissemination Workshop held at the International Livestock Research Institute (ILRI), Addis Ababa, Ethiopia*. Colombo,Sri Lanka: International Water Management Institute. doi:10.3910/2009.201

Teegavarapu, R.S.V. and Chandramouli, V. (2005). Improved weighting methods, deterministic and stochastic data-driven models for estimation of missing precipitation records. *Journal of Hydrology* **312**: 191-206.

Teklemariam, A. and Wenclawiak, B. (2005). Water quality monitoring within the Abaya-Chamo drainage basin. In Förch, G. and Thiemann, S. (eds), *Lake Abaya Research Symposium 2004 Proceedings,* Vol 4, University of Siegen, Germany.

Teshale, Berhanu, Lee, Ralp, Zawdie, Girma (2001). Development initiatives and challenges for sustainable resource and livelihood in the Lake Tana region of northern Ethiopia. In ANRS and EWNRA (eds.), *Proceedings of the Wetland Awareness Creation and Activity Identification Workshop in Amhara National Regional State*, *Bahir Dar*.

Thanapakpawin, P., J. Richey, D. Thomas, S. Rodda, B. Campbell, and M. Logsdon (2006). Effects of landuse change on the hydrologic regime of the Mae Chaem river basin, NW Thailand. *Journal of Hydrology* **334**: 215– 230.

Todini, E. (2007). Hydrological catchment modelling: past, present and future. *Hydrol. Earth Syst. Sci.* **11(1)**: 468-482.

Tripathi, M.P., Panda, R.K. and Rghuwanshi (2003). Identification and prioritisation of critical sub-watershed for soil conservation management using the SWAT model. *Biosystems Engineering* **85(3)**: 365-379.

Ulke, A., G. Tayfur and S. Ozkul (2009). Predicting suspended sediment loads and missing data for Gediz River, Turkey. *Journal of Hydrologic Engineering* **14(9)**: 954-965.

UNEP (2006). *Africa's Lakes: Atlas of our changing environment*. United Nations Environment Programme, Nairobi, Kenya.

USBR (1964). *Land and Water Resources of the Blue Nile Basin-Ethiopia*. Addis Ababa: Ministry of Water Resources.

USDA-NRCS (1986). *Urban Hydrology for Small Watersheds: Technical Release No. 55.* Washington DC: United States Department of Agriculture, Natural Resources Conservation Service.

Valiantzas, J.D. (2006). Simplified versions for the Penman evaporation equation using routine weather data. *Journal of Hydrology* **331**: 690-702.

Vallet-Coulomb, C., Dagnachew Legesse, F. Gasse, Y. Travi, Tesfaye Chernet. (2001). Lake evaporation estimates in tropical Africa (Lake Ziway, Ethiopia). *Journal of Hydrology* **245**:1-18.

Vanmaercke, M., Amanuel Zenebe, J. Poesen, J. Nyssen, G. Verstraeten, J. Deckers (2010). Sediment dynamics and the role of flash floods in sediment export from medium-sized catchments: a case study from the semi-arid tropical highlands in northern Ethiopia. *J Soils Sediments* **10**: 611-627.

Vieux, and B.E., Moreda, F.G. (2003). Ordered physics-based parameter adjustment of a distributed model. In: Duan, Q., Sorooshian, S., Gupta, H.V., Rousseau, A.N., Turcotte, R. (eds.), Chapter 20, *Advances in Calibration of Watershed Models*, Monograph Series on Water Resources. American Geophysical Union, ISBN 0-87590-355-X, pp. 267–281.

Vörösmarty, C.J., A.L. Grace, m.P. Gildea, J.M. Melillo, B.J. Peterson, E.B. Rastetter and P.A. Steudler (1989). Continental scale models of water balance and fluvial transport: an application to South America. *Global Biogeochemical Cycles* **3(3)**: 241-265.

Waichler, S.R. and M. Wigmosta (2003). Development of hourly meteorological values from daily data and significance to hydrological modeling at H.J. Andrews experimental forest. *Journal of Hydrometeorology* **4**: 251- 263.

Wainwright, J. and Mulligan, M. (2004). Modeling and Model Building. In: Wainwright, J. and Mulligan, M. (eds), *Environmental Modeling: finding simplicity in complexity*, pp. 7-73. Chichester:John Wiley & Sons.

Wale, A., T.H.M. Rientjes, A.S.M. Gieske and H.A. Getachew (2009). Ungauged catchment contributions to Lake Tana's water balance. *Hydrological Processes* **23**: 3682-3693.

Walling, D. E. and Webb, B. W. (1983). Patterns of sediment yield. In: K. J. Gregory (ed.), *Background to Palaeohydrology*, 69-100. Chichester:John Wiley & Sons

Walling, D. E. and Webb, B. W. (1996). Erosion and sediment yield: Global overviews. In Walling, D.E. and Webb, B.W. (eds.), *Erosion and Sediment Yield:Global and Regional Perspectives* pp. 3–19. IAHS Press, Wallingford, United Kingdom.

Walling, D.E. and Horowitz, A.J. (2005). Sediment Budgets: Proccedings of symposium held during the seventh IAHS Scientific Assembly at Foz do Ignaçu, Brazil. IAHS Publ. 291.

Walling, D.E., Collins, A.L., Sichingabula, H.M. and Leeks, G.J.L. (2001). Integrated assessment of catchment sediment budgets: a Zambian example. *Land Degradation and Development* **12**: 387–415.

Wang, L. and H. Liu (2006). An efficient method for identifying and filling surface depressions in digital elevation models for hydrologic analysis and modelling. International *Journal of Geographical Information Science* **20(2)**: 193-213.

Wanger, S., H. Kunstmann, A. Bárdossy, C. Conrad, and R.R. Colditz (2009). Water balance estimation of a poorly gauged catchment in West Africa using dynamically downscaled meteorological fields and remote sensing information. *Phys. Chem. Earth.* **34**: 225-235.

Ward, A., and Trimble, S. (2004). *Environmental Hydrology*. London: CRC Press.

Werkhoven, K., Wagener, T., Reed, P. and Tang, Y. (2008). Characterization of watershed model across a hydroclimatic gradient. *Water Resources Research* **44**: W01429.

Westrick, K. (1999). Soil depth calculation "aml" script downloaded from the internet at: http://www.hydro.washington.edu/Lettenmaier/Models/DHSVM/index.shtml accessed February, 2009.

Westrick, K.J., Storck, P., and Mass, C.F. (2002). Description and evaluation of a hydrometeorological forecast system for mountainous watersheds. *Weather and Forecasting* **17(2)**: 250-262.

Whipkey, R.Z. and Kirkby, M.J. (1978). Flow within the soil. In: Kirkby, M.J (ed.), *Hillslope Hydrology*, pp. 121-144. Chichester: John Wiley & Sons.

Wigmosta, M.S., Vail, L.W. and Lettenmaier, D.P. (1994). A distributed hydrology-vegetation model for complex terrain. *Water Resources Research* **30(6)**: 1665-1679.

Wigmosta, M.S, B. Nijssen, and P. Storck. (2002). The Distributed Hydrology Soil Vegetation Model. In: Singh, V.P. and Frevert, D.K. (eds.), *Mathematical Models of Small Watershed Hydrology and Applications*, pp. 7-42. Water Resources Publications, Highlands Ranch, CO.

Wiley, M.W. and Palmer, R.N. (2008). Estimating the impacts and uncertainty of climate change on a municipal water supply system. *Journal of Water Resources Planning and Management* **134 (3)**: 239-246.

WMO (1994). *Guide to Hydrological Practices*, WMO No. 168. World Meteorological Organization, Geneva.

Wondie, Tenagne A. (2009). The impact of urban storm water runoff and domestic waste effluent on water quality of Lake Tana and local groundwater near the city of Bahir Dar, Ethiopia. M.Sc Thesis: Faculty of Graduate School, Cornell University.

World Bank (2006). *Ethiopia: Managing Water Resources to Maximize Sustainable Growth.* Washington: The World Bank Agriculture and Rural Development Department.

Wösten, J.H.M., Pachepsky, Ya.A. and Rawls, W.J. (2001). Pedotransfer functions: bridging the gap between available basic soil data and missing soil hydraulic characteristics. *Journal of Hydrology* **251**: 123-150.

Woube, Mengistu (1999). Flooding and sustainable land-water management in the lower Baro-Akobo river basin, Ethiopia. *Applied Geography* **19**: 235-251.

Wudneh, Tesfaye (1998). Biology and management of fish stocks in Bahir Dar Gulf, Lake Tana, Ethiopia. PhD thesis, Fish Culture and Fisheries Group, Wageningen Institute of Animal Science, Wagnen Agricultural University, The Netherlands.

WWAP (World Water Assessment Programme) (2009). *The United Nations World Water Development Report 3: Water in a Changing World.* Paris: UNESCO, Earthscan.

WWDSE and TAHAL (2007a). *Megech dam design: Final feasibility report, Vol. 2, Geological and geotechnical investigations*. Addis Ababa, Ethiopia: Ministry of Water Resources.

WWDSE and TAHAL (2007b). *Rib dam design: Final feasibility report, Vol. 2, Geological and geotechnical investigations*. Addis Ababa, Ethiopia: Ministry of Water Resources.

WWDSE and TAHAL (2008). *Jemma dam design: Final feasibility report, Vol. 2, Geological and geotechnical investigations*. Addis Ababa, Ethiopia: Ministry of Water Resources.

Xavier, A.C. and Vettorazzi, C.A. (2003). Leaf area index of ground covers in a subtropical watershed. *Scientia Agricola* **60(3)**: 425-431.

Xevi, E., Christiaens, K., Espino, A., Sewnandan, W., Mallants, D., Sorensen, H., and Feyen, J. (1997). Calibration, validation and sensitivity analysis of MIKE-SHE model using the Neuenkirchen Catchment as case study. *Water Resources Management* **11**: 219-242.

Xia, Y., P. Fabian, A. Stohl and M. Winterhalter (1999). Forest climatology: estimation of missing values for Bavaria, Germany. *Agricultural and Forest Meteorology* **96**: 131-144.

Yin, X. and S.E. Nicholson (1998). The water balance of Lake Victoria. *Hydrological Sciences Journal* **43(5)**: 789-811.

Yoganath, A. and Junichi, Y. (2009). *Global trends in water-related disasters: an insight for policy makers.* World Water Assessment Programme side publications series: insights*;* Paris: UNESCO.

Yoshimura C, Maichun Z, Kiem AS, Fukami K, Prasantha HHA, Ishidaira H, Takeuchi K (2009). 2020s scenario analysis of nutrient load in the Mekong River Basin using a distributed hydrological model. *Science of the Total Environment* **407**: 5356-5366.

Zhang, J. and Jørgensen, S.E. (2005). Modelling of point and non-point nutrient loadings from a watershed. *Environmental Modelling & Software* **20**: 561-574.

Zhang, Lu, N.Potter, K. Hickel, Y. Zhang, Q. Shao (2008). Water balance modeling over variable time scales based on the Budyko framework- Model development and testing. *Journal of Hydrology* **360**: 117-131.

Ziadat, F.M. (2010). Prediction of soil depth from digital terrain data by integrating statistical and visual approaches. *Pedosphere* **20(3)**: 361-367.

Zinabu, G.M., Elizabete Kebede and Zerihun Desta (2002). Longrem changes in the chemical feature of water of seven Ethiopian rift-valley lakes. *Hydrobiologia* **477**: 81-91.

Zinabu, G.M., J. Nicolas and G. Pierce (2003). Concentrations of heavy metals and related trace elements in some Ethiopian rift valley lakes and their inflows. *Hydrobiologia* **429**: 171-3178.

Zoras, S., Triantafyllou, A.G., and Hurley, P.J. (2007). Grid sensitivity analysis for the calibration of a prognostic meteorological model in complex terrain by a screening experiment. *Environmental Modeling & Software* **22**: 33-39.

Annexes

Annex A: Paper submitted for journal publication

Characterization and Disaggregation of Daily Rainfall in the Upper Blue Nile Basin in Ethiopia

Agizew N. Engida, Michel Esteves

LTHE- Laboratoire d'Etude des Transferts en Hydrologie et Environnement, BP 53, 38 041 Grenoble cedex 9, France

Abstract

In Ethiopia, available rainfall records are mainly limited to daily time steps. Though rainfall data at shorter time steps are important for various purposes like modeling of erosion processes and flood hydrographs, they are hardly available in Ethiopia. The objectives of this study were i) to study the temporal characteristics of daily rains at two stations in the region of the Upper Blue Nile Basin (UBNB) and ii) to calibrate and evaluate a daily rainfall disaggregation model. The analysis was based on rainfall data of Bahir Dar and Gonder Meteorological Stations. The disaggregation model used was the Modified Bartlett-Lewis Rectangular Pulse Model (MBLRPM). The mean daily rainfall intensity varied from about 5 mm in the dry season to 17 mm in the wet season with corresponding variation in raindays of 0.4-26 days per month. The observed maximum daily rainfall varied from 13 mm in the dry month to 200 mm in the wet month. The average wet/dry spell length varied from 1/21 days in the dry season to 6/1 days in the rainy season. Most of the rainfall occurs in the afternoon and evening periods of the day. Daily rainfall disaggregation using the MBLRPM alone resulted in poor match between the disaggregated and observed hourly rainfalls. Stochastic redistribution of the outputs of the model using Beta probability distribution function improved the agreement between observed and calculated hourly rain intensities. In areas where convective rainfall is dominant, the outputs of MBLRPM should be redistributed using relevant probability distributions to simulate the diurnal rainfall pattern.

Key words: Ethiopia, Rainfall, Disaggregation, Bartlett-Lewis model

1. Introduction

Rainfall is the main driving force for runoff generation and soil erosion by water. Availability of rainfall data at relevant time scales is therefore important for water resources management. In Ethiopia, rainfall data are usually available at time scales of daily and above. Automatic gauges that record instantaneous rainfall rates are found only in limited meteorological stations. Investigation of the hourly rainfall records of Bahir Dar and Gonder meteorological stations indicated a significant mismatch between the daily rainfall calculated from the hourly chart data and that measured by the non-recording gauges in many cases. Moreover, the data from the automatic gauges is characterized by a long series of missing data with notes indicating the malfunctioning of the recorder.

Previous studies on rainfall of Ethiopia focused mainly on variability and trend analyses of annual and seasonal rainfall (Seleshi and Zanke, 2004; Cheung *et al.*, 2008; Bewket and Conway, 2007; Conway *et al.*, 2004). There are also few studies on daily/subdaily rainfall variability at local scale (Nyssen *et al.*, 2005; Bitew *et al.*, 2009). Studies on disaggregation of daily rainfall records to subdaily scales could not be found. But certain hydrologic applications require rainfall data at subdaily time scales (Khaliq and Cunnane, 1996; Connolly *et al.,* 1998; Smithers *et al.*, 2002; Onof *et al.*, 2000). Such applications include modeling of erosion and sediment transport, flood analysis, water quality modeling, design of hydraulic structures, etc. It is therefore of practical and academic importance to have hourly rainfall series for hydrological and soil erosion related studies.

Rainfall disaggregation models are used to obtain rainfall time series at subdaily scale from daily values. Onof *et al.* (2000) have classified the different approaches of rainfall disaggregation into four groups: complex process-based meteorological models, multi-scale stochastic models such as multi-fractal cascades, statistical models developed on the bases of observed statistics and point-process stochastic models. The point process stochastic models commonly used are the Bartlett-Lewis and Neyman-Scott cluster models. The point-process models have practical advantage of summarizing the many rainfall characteristics by a few parameters and representing the hierarchical nature of rainfall structure conveniently (Onof *et al.*, 2000).

In this study the application of the Modified Bartlett-Lewis Rectangular Pulse Model (MBLRPM) in disaggregating daily rainfall data into hourly time series was evaluated. Rainfall data of Bahir Dar and Gonder Meteorological Stations, which are located in the

Upper Blue Nile Basin (UBNB), were used for the purpose. The outputs of the model were compared against average diurnal rainfall patterns of the stations. Observed diurnal pattern close to the study area indicates the dominance of convective rains where most of the rainfall occurs in the afternoon and evening hours (Nyssen *et al.*, 2005). Similar diurnal rainfall pattern is noted for the wider Sub-Saharan Africa region (Mohr, 2004). The MBLRPM was selected because of its relatively wider application under different climates (Campo *et al.*, 2008; Khaliq and Cunnane, 1996; Glasbey *et al.*, 1995; Smithers *et al.*, 2002).

The objectives of this study were twofold. First the daily and hourly rainfall characteristics of the stations were summarized using relevant descriptors. The descriptors used included daily rainfall intensity and its variation, number of raindays, dry/wet spell lengths, maximum daily rainfall intensity and diurnal rainfall pattern. Second, the performance of the MBLRPM in disaggregating daily rainfall into hourly data was evaluated using optimum parameter values derived from 24-, 48-hours and subdaily rainfall statistics.

2. Data and methods

2.1. The study area

The study area is located in the UBNB in Ethiopia (Abay Basin) where the regional climatic feature is relatively low rainfall with complicated distribution pattern showing a general increase from north to south (McGregor and Nieuwolt, 1998). Ethiopia has a total area of 1.13 x 10^6 km^2 with complex topography that varies in altitude from 120 m below sea level in the northeast to over 4000 m above sea level in the northern highlands. The UBNB comprises 17.7 percent of the total area and is dominated by highland topography (Figure 1). It is the largest tributary of the main Nile River with more than 50 % contribution to annual runoff (Conway, 2000; Sutcliffe and Parks, 1999).

The rainfall climate of the study area is influenced by various regional and global weather systems that include the seasonal northward movement of the inter-tropical convergence zone (ITCZ) that drives the summer monsoon, the positions and strengths of the nearby subtropical high-pressure systems, upper-level jet streams and tropical cyclones (NMSA, 1996). Orographic and convective factors also shape the spatial and temporal patterns of rainfall in Ethiopian highlands (Korecha and Barnston, 2006). Analysis of the rainfall data of Bahir Dar

and Gonder stations indicated a monomodal pattern with more than 75% of the annual rainfall volume occurring between June and September.

The UBNB is relatively wet with mean annual rainfall varying from 1000 mm in the northeast to 2000 mm in the southwest (Conway, 2000). The rainfall climate is highly seasonal with more than 70% of the rainfall occurring in the wet season called *Kiremt* (June to September) (Korecha and Barnston, 2006). The remaining rainfall occurs in the light wet season called Belg (February to May) and dry season called Bega (October to January).

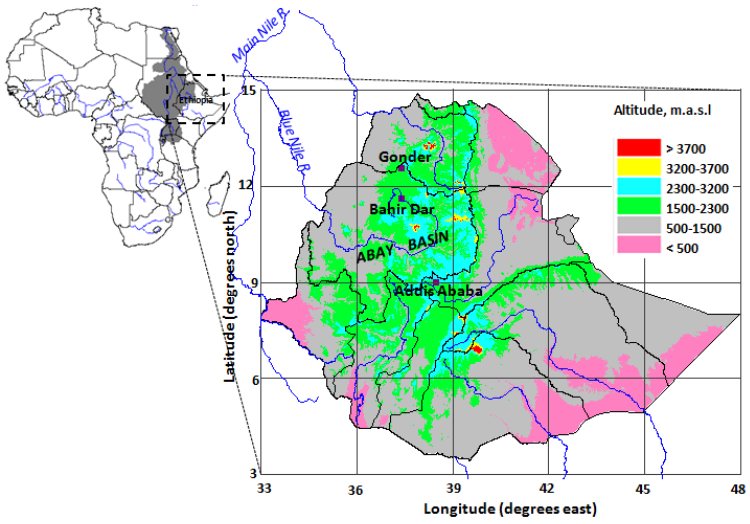

Figure 1 The stations in the Upper Blue Nile Basin (Abay)

2.2. The rainfall data

In this study we used observed daily and hourly rainfall data of two meteorological stations that have long periods of historical records- Bahir Dar station (11.60N, 37.42E, 1824 m.a.s.l) and Gonder station (12.55N, 37.42E, 2094 m.a.s.l). Bahir Dar and Gonder stations are classified as Class I meteorological stations where observations of essential climatological elements are made at daily and subdaily scales. The data were obtained from the National and /or Regional Meteorological offices which make observations using non-recording standard rain gauges for daily rainfall and float-type recording gauges for hourly rainfalls. Daily rainfall records starting from 1961 for Bahir Dar and 1953 for Gonder are available. We used

daily rainfall data for the period 1965-2006. The percentage of missing daily data for Bahir Dar in the analysis period is 0.97% and that for Gonder is 3.56%.

There are also limited reliable hourly rainfall data for the stations. Hourly rainfall records starting from year 1964 for Bahir Dar and 1976 for Gonder meteorological stations are available. The records are, however, characterized by long periods of missing data with notes indicating the malfunctioning of the recording gauges as observed in the data record sheets.

2.3. Daily and hourly rainfall data analyses

Daily rainfall data analysis included temporal characterization of rainfall and computation of statistical variables that are relevant for the disaggregation task. The observed records were checked for outliers and obvious errors prior to the analyses using Grubbs test. Grubbs test is used for normally or log-normally distributed data and has some examples of applications in hydro-meteorological areas (Chow *et al.*, 1988; Tang *et al.*, 1996). The daily rainfall data of both stations was found to be log-normally distributed.

The pluviometric regime of the stations was described by variables that included average daily rainfall intensity and its variability, mean number of raindays, mean wet/dry spell lengths and maximum daily rainfall. These variables were computed for each month of the year. As the magnitude of average statistical variables would not be noticeably affected by some missing daily rainfall data, no effort was made to replace the data gaps by interpolation (Lana *et al.*, 2004). The calculation was based on daily rainfall amounts that exceeded 1 mm which was set to be the minimum threshold for defining a rainday following Seleshi and Zanke (2004). In the literature the use of different thresholds like 0.1 mm, 0.25 mm, 1 or 5 mm to define a rainday could be found (Bewket and Conway, 2007; Lana *et al.*, 2004; McGregor and Nieuwolt, 1998). The use of a higher threshold is, however, recommended in warmer climates for reasons related to practical usages like agriculture and water supply (McGregor and Nieuwolt, 1998).

The statistical parameters relevant to the rainfall disaggregation task included mean, variance, lag-1 autocovariance and dry probability of rainfall time series at different levels of aggregation. In the computation of these variables both dry (rainfall < 1mm) and rainy days data were considered. The probability of dry day for each month was computed as the ratio of number of raindays to total number of days in a month.

As the hourly rainfall data record is fragmented with notes stating the malfunctioning of the equipment, a check on the validity of the records preceded the analysis. The validity of the hourly records was checked by comparing the hourly totals of a day against daily observations obtained from the non-recording standard gauges. We considered data obtained from the standard non-recording rain gauges to be more reliable than the hourly totals (Srivastava, 2008). Hourly records were rejected when the absolute difference between the sum of the hourly rainfalls and the daily record exceeded 25% of the daily observation. The diurnal pattern of the rainfall was described in terms of the relative proportion of rainfall amounts at different hours of a day.

2.4. Temporal characteristics of rainfall

2.4.1. Daily rainfall frequency and intensity

The mean daily rainfall intensity, the number of raindays, mean dry/wet spell days and the mean monthly rainfall of each month are presented in Table 1 and Table 2. The average number of raindays could vary from 0.4 days in the dry month to 26 days in the wet period. Comparison of raindays of the two stations indicated a slightly higher number wet days at Bahir Dar station during the *Kiremt* season. The greater difference in the number of raindays during the late wet months could be related to the retreat of the ITCZ southwards. The mean wet/dry spell length varied from 1/21 days in the dry season to 6/1 days in the rainy season. This indicated the occurrence of wet and dry spell days in groups which is caused by the persistence of synoptic scale weather systems. The results obtained corresponded to the general characteristics of tropical rainfall climatology (McGregor and Nieuwolt, 1998).

The variability of the daily rainfall intensity was high in all months as depicted by larger coefficients of variation. The mean daily rainfall intensity varied from about 4 mm in the dry season to 17 mm in the wet season. Overall, the daily rainfall intensity at Bahir Dar was greater than at Gonder station. This may be due to the location of Bahir Dar at a lower latitude and elevation that favor development of intense rain producing convective systems. The observed maximum daily rainfall varied from 13 mm in the dry month to 200 mm in the wet month.

Table 1 Daily rainfall characteristics of Bahir Dar Meteorological Station

Month	Mean rainfall intensity (mm/d)	CV	Mean raindays	No. of wet/dry spell days	Max. intensity (mm/d)	Monthly rainfall (mm)
Jan	4.8	0.81	0.6	1/21	16	2.8
Feb	6.5	0.86	0.4	1/21	19.6	2.5
Mar	5.2	1.54	1.6	1/14	57.2	9
Apr	8.9	1.12	2.3	1/11	52.8	21.3
May	11.3	1.35	7	2/5	116.3	81.4
Jun	12.7	1.09	15	3/2	94.8	192.3
Jul	16.7	0.98	26	6/1	133.2	437.1
Aug	15.2	1.05	25.1	5/1	200.3	384
Sep	11.1	1.08	17.9	3/2	80.6	201.1
Oct	11.2	0.98	8.4	2/5	88.5	95.4
Nov	7.3	1.1	2.3	1/12	38.8	16.7
Dec	5.3	0.74	0.5	1/22	14.8	3

Table 2 Daily rainfall characteristics of Gonder Meteorological Station

Month	Mean rainfall intensity (mm/d)	CV	Mean raindays	No. of wet/dry spell days	Max intensity (mm/d)	Monthly rainfall (mm)
Jan	5.3	0.8	0.6	1/21	17	3.8
Feb	3.9	1	0.7	1/18	13.4	3.4
Mar	5.8	1.3	2.7	1/10	47.8	18.1
Apr	6.6	1.2	4.4	2/7	65.4	34.2
May	8	1.1	9.6	2/4	56.7	86.6
Jun	10	1.1	15.7	2/2	82	161.2
Jul	12	1	24.8	5/1	161.1	309.7
Aug	11.1	0.9	23.4	5/1	70.5	278.9
Sep	8.3	1.1	12.4	2/3	69.5	114.8
Oct	9.3	1.1	7.1	2/5	72.3	70.8
Nov	6.2	1.2	3.2	1/8	40.3	22.4
Dec	6	1	1.3	1/17	25.1	8.1

2.4.2. Temporal variation of hourly rainfall

Overall, the hourly rainfall totals in a day did not match daily observations obtained from the standard rain gauges. For instance, investigation of wet season hourly rainfall data of Bahir Dar Meteorological Station showed more than 25% difference between hourly totals and daily observed values for 60% of the records. For Gonder similar difference was obtained in 40% of the records. Most of the hours in the data sheets are blank with notes indicating the malfunctioning of the recorder.

The percentage of rainfall amounts during different periods of a day in the *kiremt* season is presented in Figure 2. It could be seen that most of the rainfall occurred in the afternoon and evening hours. This could be explained by the dominance of convective rains caused by the heating of the land surface during the morning day hours. A similar diurnal rainfall pattern was observed in the Northern Ethiopian highlands where eighty four percent of the rain volume occurs between afternoon and midnight (Nyssen *et al.*, 2005).

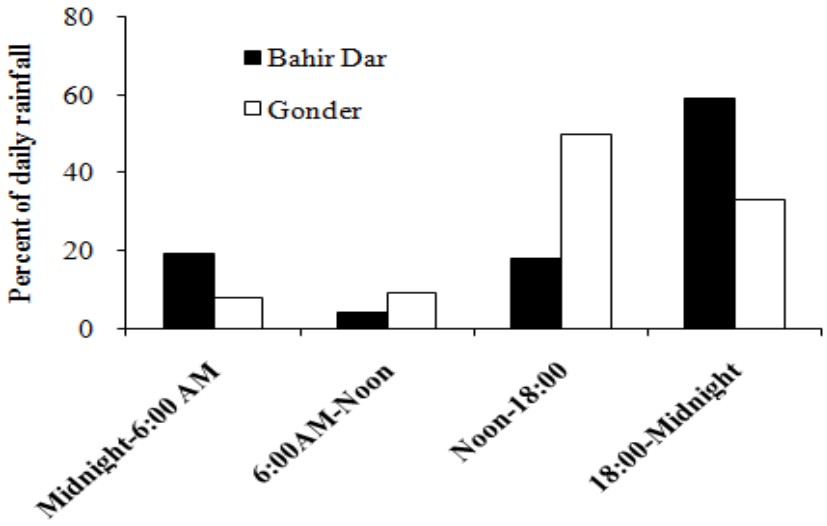

Figure 2 Percentage of rainfall volume during different periods of the day in wet season

2.5. Description of the MBLRPM

The MBRRPM is a stochastic point process rainfall model and is illustrated in Figure 3 (Rodriguez-Iturbe *et al.*, 1988; Koutsoyiannis and Onof, 2001). Storms are assumed to originate at times $\mathbf{t_i}$ following a Poisson process at a rate λ; each storm is then assumed to generate rain cells at times $\mathbf{t_{ij}}$ according to a Poisson process at a rate β; Generation of cells corresponding to a storm terminates after a time $\mathbf{x_i}$ that is exponentially distributed with parameter γ. Rain depth of each cell $\mathbf{y_{ij}}$ is a random constant exponentially distributed with mean μ_x. Each cell has a random duration $\mathbf{x_{ij}}$ that is exponentially distributed with parameter η which is assumed to vary from storm to storm with a gamma distribution having a scale and shape parameters of α and ν, respectively. The parameters β and γ are also made to vary with storms so that $\kappa = \beta/\eta$ and $\phi = \gamma/\eta$ remain constant. The rainfall amount in any time interval T is then represented by the sum of all active cells in that period.

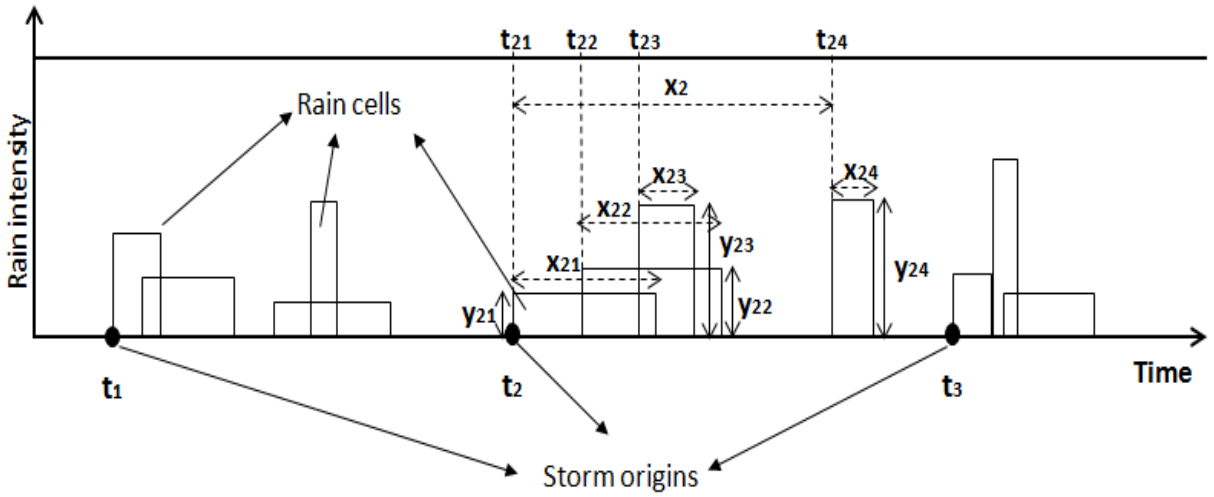

Figure 3 Representation of rainfall process in the MBLRPM model

The different parameters of the model were computed by equating simulated second-order statistics to observed statistics. The second-order statistics of the accumulated process over time interval T are computed by the following equations.

- Mean storm depth ($\overline{X}_T$)

$$\overline{X}_T = \lambda \mu_x \left(1+\frac{\kappa}{\phi}\right)\left(\frac{\nu}{\alpha-1}\right) T \quad (1)$$

- Variance (Var_T) and Lag-1 Autocovariance ($ACov1_T$)

$$Var_T = \frac{2\nu^{2-\alpha}}{\alpha-2}\left(k_1-\frac{k_2}{\phi}\right)-\frac{2\nu^{2-\alpha}}{(\alpha-2)(\alpha-3)}\left(k_1-\frac{k_2}{\phi^2}\right)+\frac{2}{(\alpha-2)(\alpha-3)}\left(k_1(T+\nu)^{3-\alpha}-\frac{k_2}{\phi}(\phi T+\nu)^{3-\alpha}\right) \quad (2)$$

$$ACov1_T = \frac{k_1}{(\alpha-2)(\alpha-3)}\left\{\nu^{3-\alpha}+(2T+\nu)^{3-\alpha}-2(T+\nu)^{3-\alpha}\right\}+\frac{k_2}{\phi^2(\alpha-2)(\alpha-3)}\left\{2(\phi T+\nu)^{3-\alpha}-\nu^{3-\alpha}-(2\phi T+\nu)^{3-\alpha}\right\} \quad (3)$$

Where,

$$k_1 = 2\lambda\left(1+\frac{\kappa}{\phi}\right)\mu_x^2+\left(\frac{\lambda\left(1+\frac{\kappa}{\phi}\right)\mu_x^2\phi}{\phi^2-1}\right)\left(\frac{\nu^\alpha}{\alpha-1}\right) \quad (4)$$

$$k_2 = \left(\frac{\lambda\left(1+\frac{\kappa}{\phi}\right)\kappa}{\phi^2-1}\right)\left(\frac{\nu^\alpha}{\alpha-1}\right) \quad (5)$$

- Dry probability (PD_T)

$$PD_T = e^{(-\lambda T-f_1+f_2+f_3)} \quad (6)$$

Where,

$$f_1 = \frac{\lambda\nu}{\phi(\alpha-1)}\left\{1+\phi\left(\kappa+\frac{\phi}{2}\right)-\frac{1}{4}\phi(\kappa+\phi)(\kappa+2\phi)+\frac{\phi(\kappa+\phi)(4\kappa^2+27\kappa\phi+36\phi^2)}{72}\right\} \quad (7)$$

$$f_2 = \frac{\lambda\nu}{(\kappa+\phi)(\alpha-1)}\left(1-\kappa-\phi+\frac{3}{2}\phi\kappa+\phi^2+\frac{\kappa^2}{2}\right) \quad (8)$$

$$f_3 = \frac{\lambda \nu}{(\kappa+\phi)(\alpha-1)}\left(\frac{\nu}{\nu+T(\kappa+\phi)}\right)^{\alpha-1}\left(1-\kappa-\phi+\frac{3}{2}\phi\kappa+\phi^2+\frac{\kappa^2}{2}\right) \quad (9)$$

2.6. Estimation of the MBLRPM parameters

The six parameters of the MBLRPM were estimated using the method of moments where non-linear equations that relate observed and analytical moments are solved simultaneously. Inclusion of moments that describe depth processes and dry probabilities are deemed to be necessary in order to arrive at reasonable parameter values (Onof and Wheater, 1993). Based on the recommendation of Khaliq and Cunnane (1996), the model parameters were determined from more moment equations than the number of unknowns. The moments included mean, variance, lag-1 autocovariance and dry probabilities for different levels of aggregation.

Many applications of the model recommend inclusion of subdaily rainfall statistics in the estimation of the model parameters (Khaliq and Cunnane, 1996). In this study the estimation was done based on two sets of rainfall statistics depending on the relative length of available hourly rainfall records. For the main wet months, i.e. June, July, August, and September, rainfall statistics calculated from 1-, 6-, 24- and 48-hours historical data were used to estimate the model parameters. For the other months the estimation was based on only 24- and 48-hours statistics as the length of the hourly data is very short. There are studies which estimate parameters of the model from 24- and 48-hours rainfall statistics and yet conclude good performance of the model. Bo and Islam (1994) are able to infer satisfactorily subdaily rainfall statistics from 24 hours and 48 hours data. Similarly, Campo *et al.* (2008) reasonably infer 10 min, 30 min, 1 hours, 2 hours, 6 hours and 12 hours rainfall statistics using parameters estimated from accumulated 24- and 48-hours rainfalls. Successful parameter estimation is also reported by Smithers *et al.* (2002) who make the determination with and without subdaily rainfall statistics.

Analytical moments defined by the various equations given in Section 2.5 were equated to the corresponding observed statistics. The resulting systems of nonlinear equations were solved simultaneously to determine the optimum parameter sets for each month. This was achieved by minimizing the objective function given in Equation 10 using the Excel Solver tool. Use of

similar objective function is found in the literature (Smithers *et al.*, 2002; Velghe *et al.*, 1994). Parameter estimates on monthly basis was done to account for seasonal effects (Onof and Wheater, 1993; Debele *et al.*, 2007)

$$Z = \min \sum_{i=1}^{n} \left(1 - \frac{\text{Simulated statistics}_i}{\text{Observed statistics}_i} \right)^2 \quad (10)$$

Where n is the number of statistics (moments) used

The goodness-of-fit of the rainfall statistics calculated using the calibrated parameters to those obtained from the historical records was evaluated based on the absolute deviate statistics (Equation 11). This statistics is used by Velghe *et al.* (1994) to measure the overall performance of the model in reproducing the historical rainfall statistics.

$$F = \frac{1}{n} \left[\sum_{i=1}^{n} \left| 1 - \frac{S_{i-sim}}{S_{i-obs}} \right| \right] \times 100\% \quad (11)$$

Where, $S_{i\text{-}m}$ is the computed statistic; $S_{i\text{-}obs}$ is the corresponding observed statistic; n is the number of statistics evaluated.

2.7. Disaggregation of daily rainfall

Disaggregation of observed daily rainfall into hourly series was done using the computed optimum parameter values. A repetition technique with proportional adjustment was followed during the disaggregation to ensure that daily rainfall equals the sum total of disaggregated hourly rainfalls. This method is recommended by Koutsoyiannis and Onof (2001) and is incorporated in a disaggregation model developed by Gyasi-Agyei (2005). The approach enables to obtain consistent finer-time scale rainfalls by distributing the error proportionally to each of the disaggregated results.

Daily rainfalls for which corresponding hourly observations exist were first disaggregated using a computer program called Hyetos in which the Bartlett-Lewis model and the adjusting

procedures are implemented (Koutsoyiannis and Onof, 2000). Debele *et al.* (2007) reported very good performance of the model in disaggregating daily rainfall data into hourly data.

2.8. Adjusting time of rainfall occurrence

Adjustments to the outputs of the MBLRPM model were made to mimic the observed diurnal rainfall pattern by stochastically redistributing the outputs using Beta probability distribution. Beta distribution to simulate rainfall occurrence time in a day is used by different researchers (Hershenhorn and Woolhiser, 1987; Connolly *et al.*, 1998). The Beta distribution function is defined by two parameters as shown in Equation 11.

$$f(t;a,b) = \frac{\Gamma(a+b)}{\Gamma(a)\Gamma(b)} t^{a-1}(1-t)^{b-1} \quad \text{for } 0 < t < 1, a > 0, b > 0$$
$$= 0 \quad \text{otherwise} \tag{11}$$

Where t is scaled hour of the day between 0 and 1; a = scale parameter; b = shape parameter.

The scale and shape parameters can be determined from the mean and variance of the observed hourly rainfall.

$$E(t) = \frac{a}{a+b} \tag{12}$$

$$Var(t) = \frac{ab}{(a+b+1)(a+b)^2} \tag{13}$$

Where E(t) is the mean rainfall occurrence hour; Var(t) is the variance of the rainfall occurrence hour, i.e., $E(t^2)$-$[E(t)]^2$.

A small computer program was written in a Matlab environment with required inputs including the outputs of the MBLRPM, the two parameters of the Beta function and the

average hour starting from which the diurnal rainfall pattern could be defined by the Beta probability distribution. First, scaled random rainfall occurrence hours that correspond to each of the disaggregated hourly rain events were generated from a Beta distribution. The scaled hour could be converted to equivalent actual hour of the day by multiplying it by 24. The outputs of the MBLRMP were then redistributed such that they would correspond to the random hours generated from the Beta distribution.

3. Disaggregation results and discussion

3.1. Calibration of the MBLRPM parameters

Optimum parameters for the MBLRPM were derived from 24-, 48-hours and sub-daily rainfall statistics. A typical observed daily rainfall statistics is shown in Table 3. Subdaily rainfall statistics of 1- and 6-hours rainfalls were considered only for the main wet months, i.e., June, July, August and September. The lag-1 autocovariances of both stations were found to be positive indicating persistence, which is a clear characteristic of tropical rainfall (McGregor and Nieuwolt, 1998). The magnitudes of dry probabilities indicated the seasonality of rainfall with most of the wet season days getting rainfall. The optimum magnitudes of the model parameters for each month are presented in Table 4 and Table 5. The computed values were generally within ranges reported in literatures (Segond *et al.*, 2006; Schnorbus and Alila, 2004). Higher values of Poisson arrival rates and mean cell rain depths corresponded to the wettest months of July and August that have negligible dry probabilities. The daily rainfall data analysis indicated these months as having mean dry spell length of 1 day.

Table 3 Observed daily rainfall statistics for Bahir Dar and Gonder Meteorological Stations

Month	Daily rainfall variance (mm^2)		Daily rainfall covariance (mm^2)		Daily dry probability	
	Bahir Dar	Gonder	Bahir Dar	Gonder	Bahir Dar	Gonder
Jan	0.62	1.01	0.03	0.09	0.97	0.97
Feb	0.83	0.8	0.03	0.16	0.96	0.95
Mar	4.34	6.45	0.10	0.62	0.91	0.87
Apr	18.00	17.72	4.69	2.62	0.87	0.79
May	73.59	40.22	12.68	3.89	0.67	0.54
Jun	132.47	113.67	17.87	9.27	0.37	0.31
Jul	263.10	108.22	27.40	4.01	0.07	0.08

Aug	237.79	94.64	11.56	1.4	0.09	0.1
Sep	115.12	51.3	6.14	5.22	0.28	0.43
Oct	57.46	36.84	7.54	4.18	0.67	0.66
Nov	8.36	10.82	1.67	0.57	0.89	0.85
Dec	0.81	2.69	0.13	0.32	0.97	0.94

Table 4 Optimum MBLRPM model parameter values for Bahir Dar Meteorological Station

Month	$\lambda(h^{-1})$	$\kappa = \beta/\eta$	$\phi = \gamma/\eta$	α	ν (h)	μ_x (mmh^{-1})
Jan	0.001	0.399	0.222	10.534	6.759	1.340
Feb	0.001	1.372	1.552	7.423	8.386	1.195
Mar	0.002	2.722	1.356	6.848	3.949	2.628
Apr	0.006	2.499	0.588	2.503	0.547	2.727
May	0.008	0.048	0.018	3.384	1.933	4.597
Jun	0.028	0.053	0.022	2.968	0.514	8.556
Jul	0.101	0.270	0.099	2.978	0.24	11.206
Aug	0.088	0.124	0.082	4.855	0.722	11.281
Sep	0.031	0.010	0.010	13.278	5.769	8.164
Oct	0.013	0.467	0.061	21.952	7.803	3.124
Nov	0.003	0.171	0.047	7.524	4.289	2.522
Dec	0.006	0.113	1.096	4.263	1.275	1.739

Table 5 Optimum MBLRPM model parameters for Gonder Meteorological Station

Month	$\lambda(h^{-1})$	$\kappa = \beta/\eta$	$\phi = \gamma/\eta$	α	ν (h)	μ_x (mmh^{-1})
Jan	0.001	0.762	0.172	15.925	10.980	1.011
Feb	0.001	0.523	0.112	11.644	4.984	1.493
Mar	0.005	0.209	0.496	6.565	8.599	1.630
Apr	0.004	0.029	0.010	4.799	3.363	3.337
May	0.025	0.199	0.065	3.282	0.553	4.558
Jun	0.027	0.024	0.010	2.668	0.597	4.859
Jul	0.089	0.055	0.045	22.125	4.329	9.158
Aug	0.086	0.417	0.106	8.914	0.675	9.999
Sep	0.021	0.037	0.021	19.224	9.093	4.704
Oct	0.010	0.020	0.010	4.505	2.981	3.754

Nov	0.006	0.612	0.240	9.621	5.316	2.547
Dec	0.002	0.578	0.111	10.109	5.936	1.112

The various rainfall statistics computed from the optimum parameters sets were compared against the observed ones. The overall performance of the model in reproducing the observed statistics appeared to be good for all months as shown in Table 6. A general improvement in goodness-of-fit could be seen in the main wet months which could be due to the inclusion of subdaily rainfall statistics.

Table 6 Absolute deviate of the overall rainfall statistics computed by using the optimum parameter values of the MBLRPM (in percent)

Station	Jan	Feb	Mar	Apr	May	Jun	Jul	Aug	Sep	Oct	Nov	Dec
Bahir Dar	8.61	3.03	10.44	4.70	1.57	2.30	2.65	1.52	1.72	8.73	4.39	10.46
Gonder	9.48	2.65	2.51	2.70	7.97	6.37	1.68	1.08	2.73	2.34	9.15	4.44

3.2. Disaggregation of daily rainfall into hourly data

The performance of the model was further evaluated by comparing the disaggregated hourly rainfalls with the reliable observed hourly data. Graphical comparisons of these data for the wet months at Bahir Dar station are presented in Figure 4. A poor match between observed and disaggregated rainfalls in the morning hours of a day could be seen. This poor performance of the MBLRPM was also supported by the larger mean square errors (MSE) (See Table 7). Similar results were obtained for Gonder station.

The MBLRPM model generated rainfall cells stochastically at any moment along the day hours that could not be consistent with the diurnal rainfall pattern of the study area. The differences are particularly clear in the morning hours of the day that hardly see rainfall. The diurnal rainfall pattern of the study region is mainly influenced by convective rain producing mechanisms where most of the rainfall occurs in the afternoon and evening hours. A research done in the Northern Ethiopian highlands close to the study area indicated that only 4 % of the daily rainfall occurs in the morning hours (Nyssen *et al.*, 2005). A recent study on the spatio-temporal rainfall variability in the Lake Tana basin further revealed the dominance of convection in the late afternoon and evening hours (Haile *et al.*, 2009).

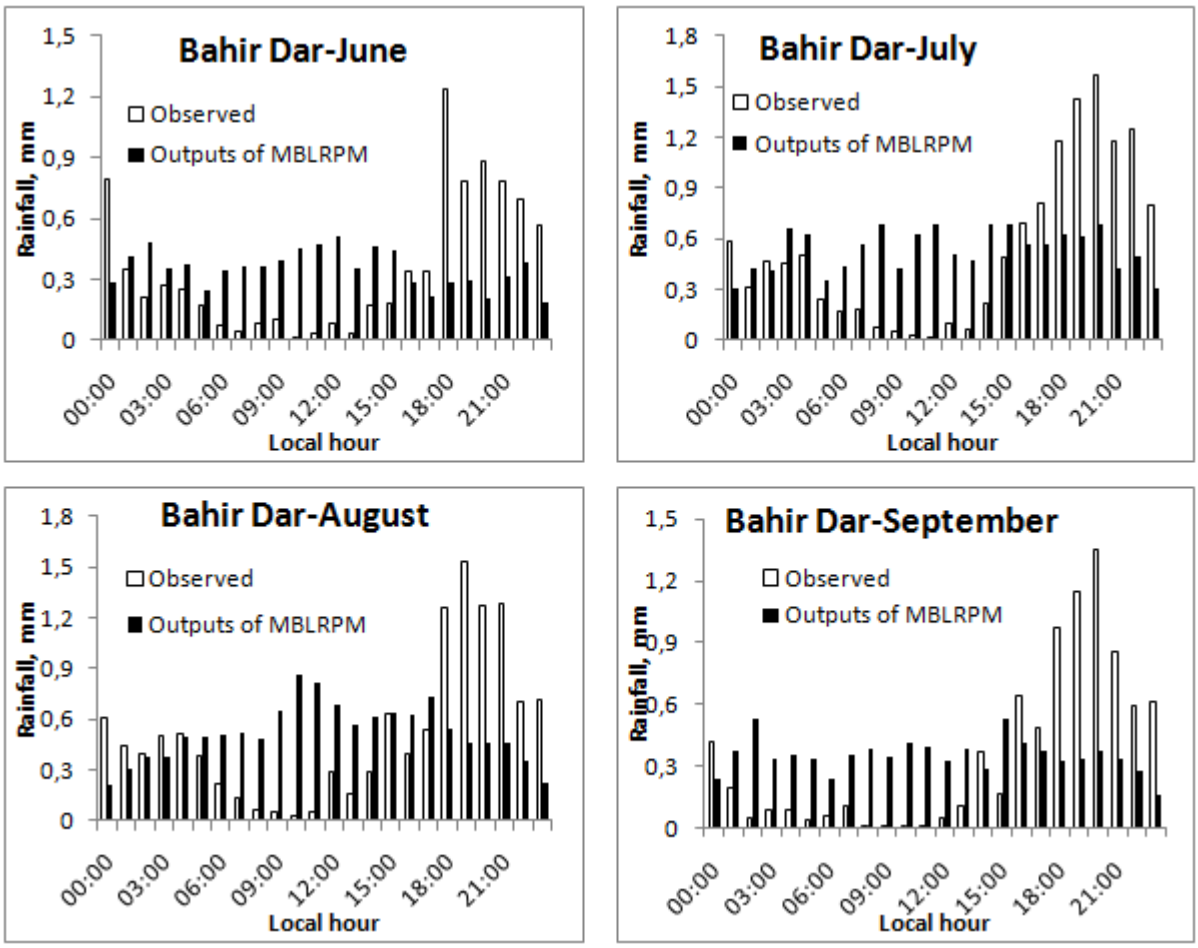

Figure 4 Comparison between observed and disaggregated mean hourly rainfall of Bahir Dar Station for the wet months

3.3. Adjustment of outputs of MBLRPM

In order to mimic the diurnal rainfall pattern of the stations, adjustments to the direct outputs of the MBLRPM were made through stochastic redistribution using Beta probability distribution. The use of Beta probability distribution function was justified after having analyzed the available hourly data at the two stations. During the dominant rainfall months, the daily rainfall pattern at Bahir Dar and Gonder Stations showed a Beta distribution starting from 11:00-13:00 hour local time (See Figure 5 for Bahir Dar). The estimated average Beta distribution parameters for Bahir Dar were a = 2.8 and b = 3.8 and that for Gonder were a = 2.0 and b =3.7.

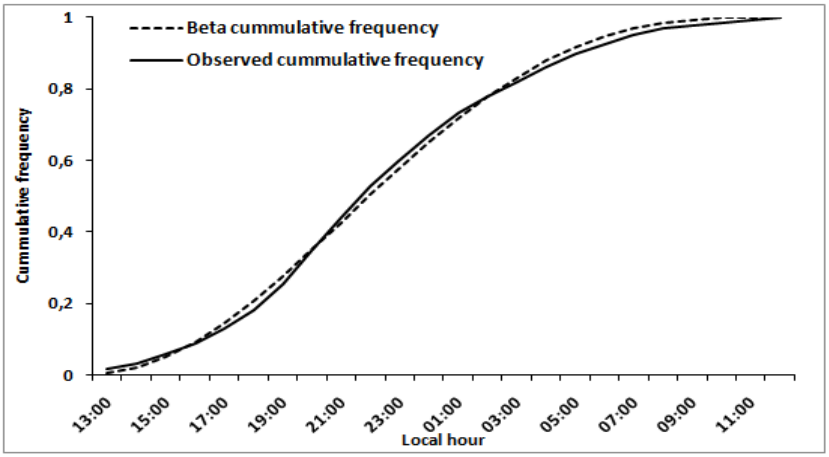

Figure 5 Typical distribution of rain start hour for Bahir Dar station

Rainfall occurrence hours of the MBLRPM outputs were adjusted following the method discussed in Section 2.8. The redistributed hourly rainfall showed a better fit to the observed data as indicated by the smaller MSE (Table 7) and the graphical similarity (Figure 6 and Figure 7) for both Bahir Dar and Gonder stations. The morning hours appeared to have insignificant rainfall which is consistent with the average diurnal pattern of the study region.

Table 1 Performance of the MBLRPM

Month	MSE. %			
	MBLRPM alone		With adjustment using Beta	
	Bahir Dar	Gonder	Bahir Dar	Gonder
June	15.0	9.0	3.0	6.0
July	22.9	10.1	6.4	4.2
August	25.6	9.6	5.6	5.2
September	17.2	3.3	3.7	1.5

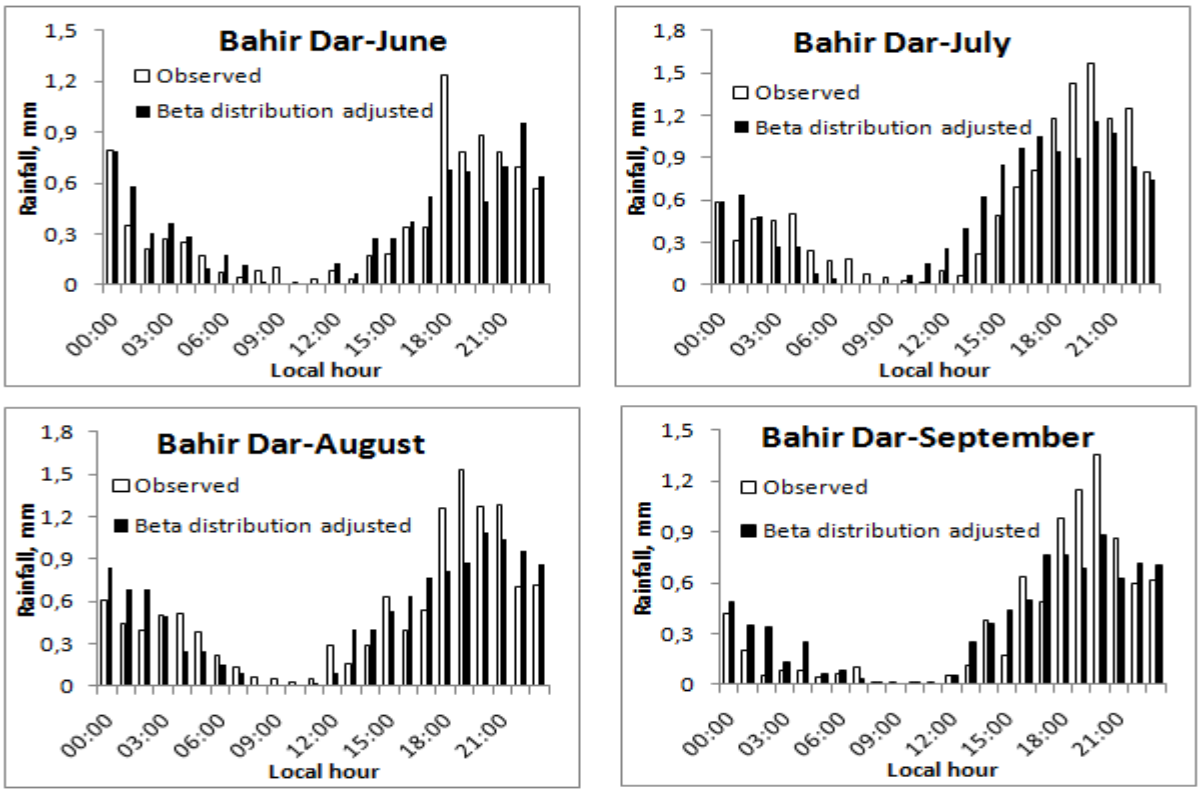

Figure 6 Comparison between observed and disaggregated mean hourly rainfall after adjustment for the wet months - Bahir Dar

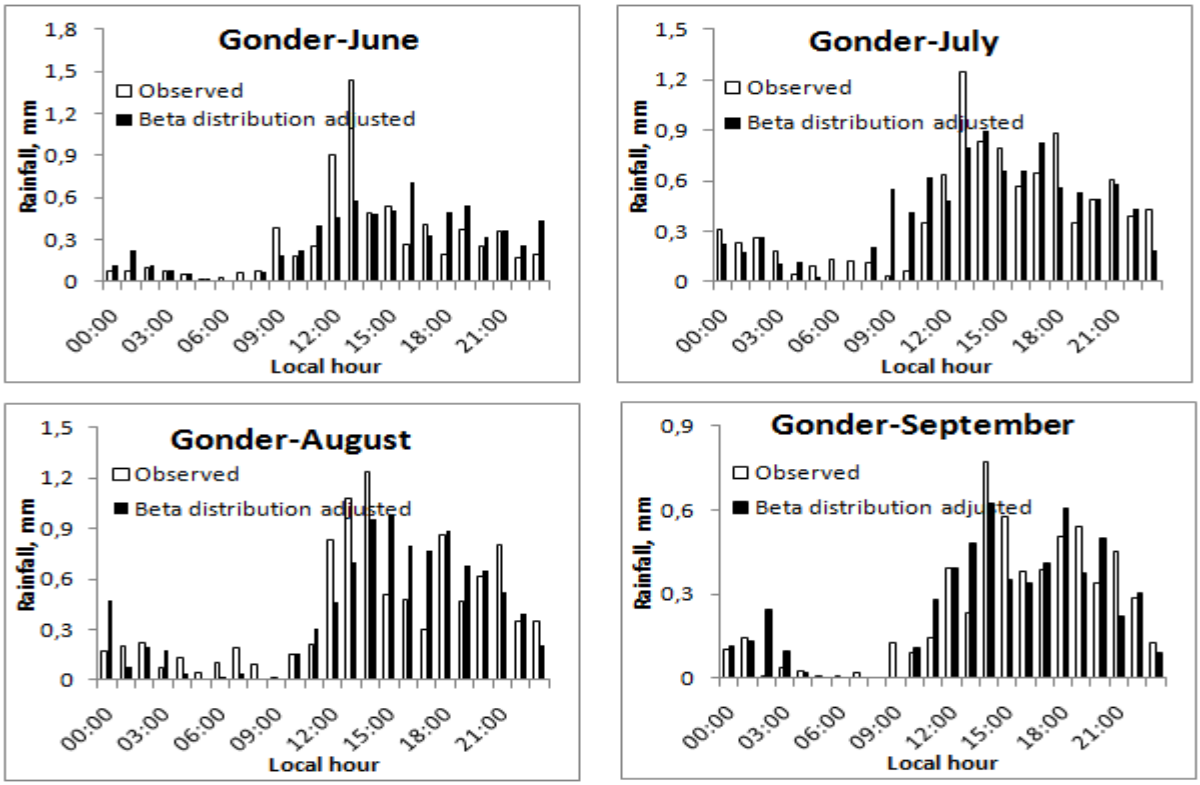

Figure 7 Comparison between observed and disaggregated mean hourly rainfall after adjustment- Gonder for the wet months

4. Conclusions

The objectives of this study were to investigate the temporal characteristics of rainfall data of two meteorological stations located in the Upper Blue Nile Basin in Ethiopia and to calibrate and evaluate the performance of a daily rainfall disaggregation model. The rainfall is highly seasonal with more than 75% of the rainfall occurring in the wet season from June to September. The daily rainfall showed characteristics similar to tropical climates. Most of the rainfall occurred in the afternoon and evening hours which could be explained by the dominance of convective rain producing mechanisms.

The disaggregation task was done in two major steps- determination of optimum parameter values and disaggregation of observed daily rainfall data. Several studies on the subject accomplish the first step and reach conclusion on the performance of the model by comparing the observed and simulated statistics of the rainfall. If the objective of the modeling exercise is to generate rainfalls at finer scales from coarse measurements, its performance should further be evaluated by comparing the observed and disaggregated rainfalls. We compared observed and disaggregated mean hourly rainfalls at both Bahir Dar and Gonder meteorological stations.

The MBLRPM stochastically generated rainfalls at any hour of the day following the Poisson process. This resulted in a mismatch between the observed and disaggregated rainfalls during the morning day hours which hardly receive rainfall. To improve the fit, stochastic adjustment to the disaggregated hourly rainfall pattern was made by using Beta probability distribution function. Redistribution of outputs of MBLRPM using Beta probability distribution improved the fit between the observed and disaggregated rainfalls. In areas where convective rainfalls are dominant, the outputs of MBLRPM should be redistributed using relevant probability distributions to simulate the diurnal rainfall pattern.

Acknowledgements

We would like to express our gratitude to the French Ministry of Foreign Affairs for providing Agizew N. Engida with a financial assistance. We are grateful to the Ethiopian National Meteorological Agency for the meteorological data.

References

Bewket, W., Conway, D., 2007. A note on the temporal and spatial variability of rainfall in the drought-prone Amhara region of Ethiopia. *Int. J. Climatol.* **27***: 1467-1477*.

Bitew, M.M., Gebremichael, M., Hirpa, F.A., Gebrewubet, Y.M., Seleshi, Y., Girma, Y., 2009. On the local-scale spatial variability of daily summer rainfall in the humid and complex terrain of the Blue Nile: observational evidence. *Hydrol. Process*. **23**, 3670-3674.

Bo, Z., Islam, S.,1994. Aggregation-disaggregation properties of a stochastic model. *Water Resources Research* **30** (12), 3423-3435.

Campo, M.A., Cirauqui, J.C., Lopez, J.J., 2008. Application of a stochastic rainfall model for disaggregation. *Geophysical Research abstracts* **10,** *EGU2008-A-11799*.

Cheung, W.H., Senay, G.B., Singh, A., 2008. Trends and spatial distribution of annual and seasonal rainfall in Ethiopia. *Int. J. Climatol., DOI: 10.1002/joc.1623*.

Chow, V. T., Maidment, D.R., Mays, L.W., 1988. *Applied Hydrology*. McGraw-Hill, New York.

Connolly, R.D., Schirmer, J., Dunn, P.K., 1998. A daily rainfall disaggregation model. *Agricultural and Forest Meteorology* **92***, 105-117.*

Conway, D. (2000). The climate and hydrology of the Upper Blue Nile River. *The Geographical Journal,* **166**(1):49-62.

Conway, D., Mould, C., Bewket, W., 2004. Over one century of rainfall and temperature observations in Addis Ababa, Ethiopia. *Int. J. Climatol.* **24**: 77-91.

Debele, B., Srinivasan, R., Parlange, J.Y., 2007. Accuracy evaluation of weather data generation and disaggregation methods at finer timescales. *Advances in Water Resources* **30**(5), 1286-1300

Glasbey, C.A., Cooper, G., McGechan, M.B., 1995. Disaggregation of daily rainfall by conditional simulation from a point-process model. *Journal of Hydrology* **165**: 1-9.

Gyasi-Agyei, Y., 2005. Stochastic disaggregation of daily rainfall into one-hour time scale. *Journal of Hydrology* **309**: 178–190

Haile, A.T., Rientjes, T., Gieske, A. and Gebremichael, M., 2009. Rainfall variability over mountainous and adjacent lake areas: The case of Lake Tana Basin at the source of the Blue Nile River. *Journal of Applied Meteorology and Climatology* **48**: 1696-1717.

Hershenhorn, J., Woolhiser, D.A., 1987. Disaggregation of daily rainfall. *Journal of Hydrology* **95:** 229-322.

Khaliq, M.N., Cunnane, C., 1996. Modeling point rainfall occurrences with the modified Bartlett-Lewis Rectangular Pulse Model. *Journal of Hydrology* **180:** 109-138.

Korecha, D., Barnston, A.G., 2006. Predictability of June-September rainfall in Ethiopia. *Mon. Wea. Rev.,* **135**: 628-650.

Koutsoyiannis, D., Onof, C., 2000. A computer program for temporal rainfall disaggregation using adjusting procedures. XXV General Assembly of European Geophysical Society, Nice, Geophysical Research Abstracts.

Koutsoyiannis, D., Onof, C., 2001. Rainfall disaggregation using adjusting procedures on poisson cluster model. *Journal of Hydrology* **246**: 109-122.

Lana, X., Martinez; M.D., Serra, C., Burgueno, A., 2004. Spatial and temporal variability of the daily rainfall regime in Catalonia (Northeastern Spain), 1950-2000. *Int. J. Climatol.* **24**, 613-641.

McGregor, G.R., Nieuwolt, S., 1998. Tropical Climatology: an introduction to the climates of the low latitudes, 2nd ed. John Willey and Sons ltd., England.

Mohr, K., 2004. Interannual, monthly, and regional variability in the wet season diurnal cycle of precipitation in Sub-Saharan Africa. *J. Climate* **17**, 2441-2453.

NMSA, 1996. Climatic and Agroclimatic Resources of Ethiopia. *Meteorological Research Report Series, vol. 1, No. 1*, Addis Ababa.

Nyssen, J., Vandenreyken, H., Poesen, J., Moeyersons, J., Deckers, J., Mitiku Haile, Salles, C., Govers, G., 2005. Rainfall erosivity and variability in the Northern Ethiopian Highlands. *Journal of Hydrology* **311**: 172-187.

Onof, C., Wheater, H.S., 1993. Modeling of British rainfall using a random parameter Bartlett-Lewis rectangular pulse model. *Journal of Hydrology* **149**: 67-95.

Onof, C., Chandler, R.E., Kakou, A., Northrop, P., Wheater, H.S., Isham, V., 2000. Rainfall modeling using Poisson-cluster processes: a review of developments. *Stochastic Environmental Research and Risk Assessment* **14**, 384-411.

Rodriguez-Iturbe, I., Cox, D.R. Isham, V., 1988. A point process model for rainfall: further developments. *Proc. R. Soc. London,* A, **417**: 283-298.

Schnorbus, M., AlilaY., 2004. Generation of an hourly meteorological time series for an Alpine Basin in British Columbia for use in numerical hydrologic modelling. *Journal of Hydrometeorology,* **5**, 862-882.

Segond, M.L., Onof, C., Wheater, H.S., 2006. Spatial–temporal disaggregation of daily rainfall from a generalized linear model. *Journal of Hydrology* **331**: 674-689.

Seleshi, Y., Zanke, U., 2004. Recent trends in rainfall and rainy days in Ethiopia. *Int. J. Climatol.* **24**: 973-983.

Smithers, J.C., Pegram, G.G.S., Schulze, R.E., 2002. Design rainfall estimation in South Africa using Bartlett-Lewis rectangular pulse rainfall models. *Journal of Hydrology* **258**: 83-99.

Srivastava, G.P., 2008. *Surface Meteorological Instruments and Measurement Practices*. Atlantic Publishers: New Delhi.

Sutcliffe, J. V., Parks, Y. P., 1999. *The Hydrology of the Nile*. IAHS Special Publication no. 5, Institute of Hydrology, Wallingford, Oxfordshire OX10 8BB, UK.

Tang, W.Y., Kassim, A.H.M., Abubakar, S.H., 1996. Comparative studies of various missing data treatment methods- Malaysian experience. *Atmospheric Research* **42**, 247-262.

Velghe, T., Troch, P.A., De troch, F.P., Van de Velde, J., 1994. Evaluation of cluster-based rectangular pulses point process models for rainfall. *Water Resources Research* **30**(10), 284-2857.

Annex B: Information on hydro-meteorological and spatial characteristics of Lake Tana basin

B-1 Meteorological stations within and near Lake Tana basin

Station	Class	Geodetic coordinates		UTM coordinates		Altitude, m.a.s.l
		Latitude degree	Longitude degree	East m	North m	
Adis Zemen	3	12.13	37.78	367246.68	1341225.90	1970
Adet	1	11.26	37.47	332986.66	1245163.53	2195
AmbaGiorgis	4	12.77	37.60	348029.77	1412111.60	2900
Arb Gebeya	4	11.63	37.74	362643.09	1285944.83	2305
Aykel	1	12.53	37.05	288111.20	1385943.64	2172
Bahir Dar	1	11.60	37.42	327733.01	1282800.77	1824
Chandiba	3	12.39	37.03	285822.25	1370469.98	2071
Chwahit	4	12.33	37.22	306441.23	1363687.05	1890
Dangila	1	11.25	36.83	263090.20	1244497.86	2127
Debre Tabor	1	11.85	38.01	392165.34	1310158.37	2700
Dek Estifanos	4	11.91	37.27	311585.17	1317188.85	1808
Delgi	4	12.19	37.04	286748.65	1348334.05	1814
Enfranz	3	12.18	37.68	356390.40	1346806.91	1882
Enjibara	4	10.98	36.92	272710.90	1214554.10	2574
Gassay	3	11.79	38.14	406306.09	1303476.13	2850
Gonder	1	12.55	37.42	328339.37	1387887.20	2094
Gorgora	3	12.25	37.30	315086.98	1354780.61	1786
Hamusit	4	11.78	37.55	342011.91	1302634.88	1939
Korata	3	11.83	37.63	350757.13	1308121.36	1797
Kunzila	4	11.87	37.03	285406.42	1312937.65	1808
Maksegnit	3	12.35	37.56	343432.98	1365677.35	1897
Mekane Yesus	3	11.60	38.06	397519.81	1282492.12	2373
Merawi	3	11.25	37.15	298038.47	1244258.57	2020
Meshenti	4	11.41	37.28	312338.89	1261871.33	2056
Sekela	4	11.00	37.22	305516.76	1216556.03	2626
Shebekit	4	12.70	37.47	333869.74	1404448.00	2471
Tis Abay	4	11.48	37.58	345115.44	1269436.19	1648
Wanzaye	3	11.77	37.69	357263.36	1301453.82	1934
Wereta	3	11.92	37.68	356252.06	1318049.50	1801
Wetet Abay	3	11.37	37.05	287206.46	1257605.12	1922
Yifag	4	12.08	37.72	360690.95	1335725.63	1849
Zege	3	11.68	37.32	316879.60	1291712.71	1786

B-2 Double mass curve of annual rainfall (black line): X-axis and Y-axis represent cumulative mean annual rainfall for the base and target stations, respectively. Red line is linear trendline.

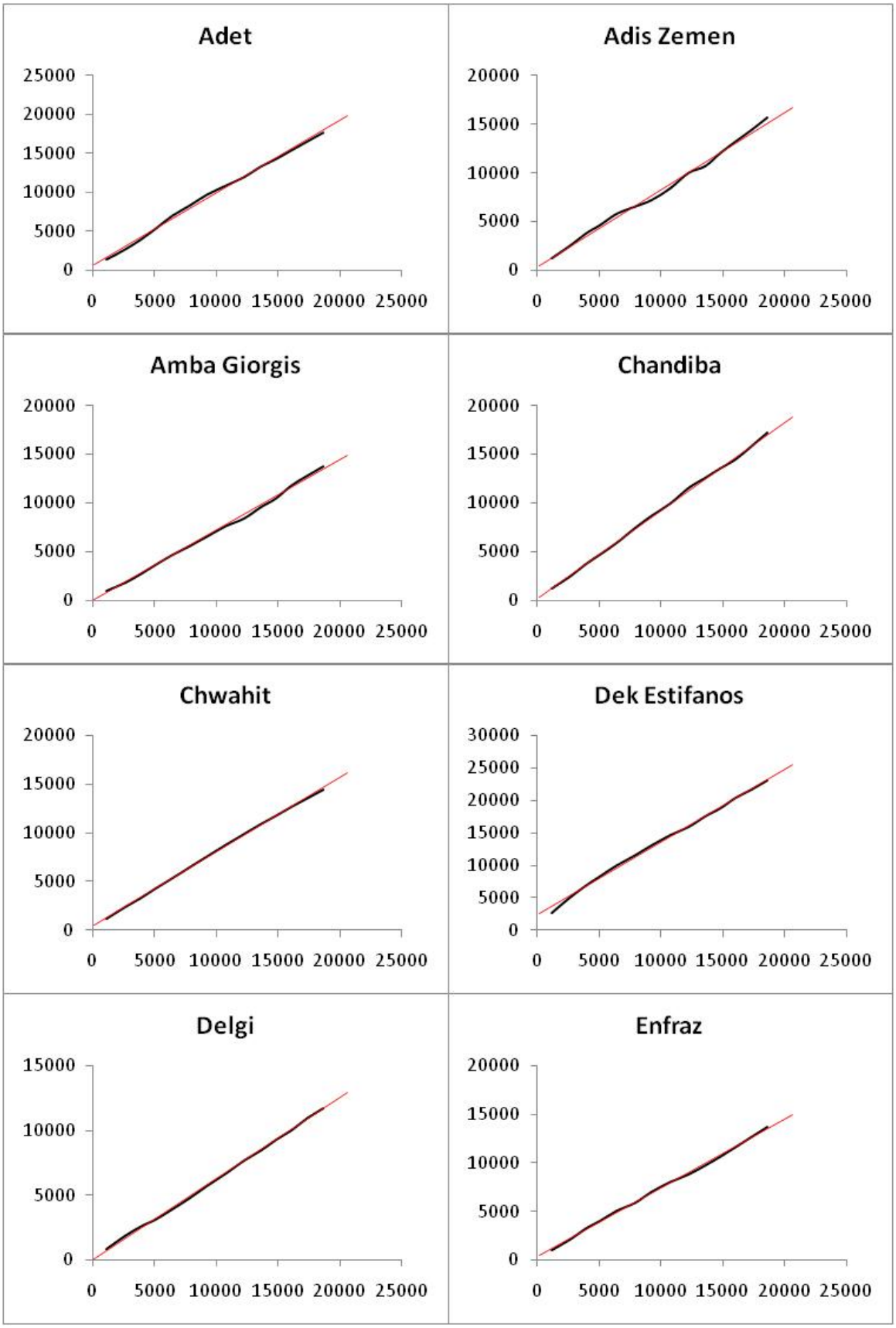

B-2 Double mass curve of annual rainfall- continued…

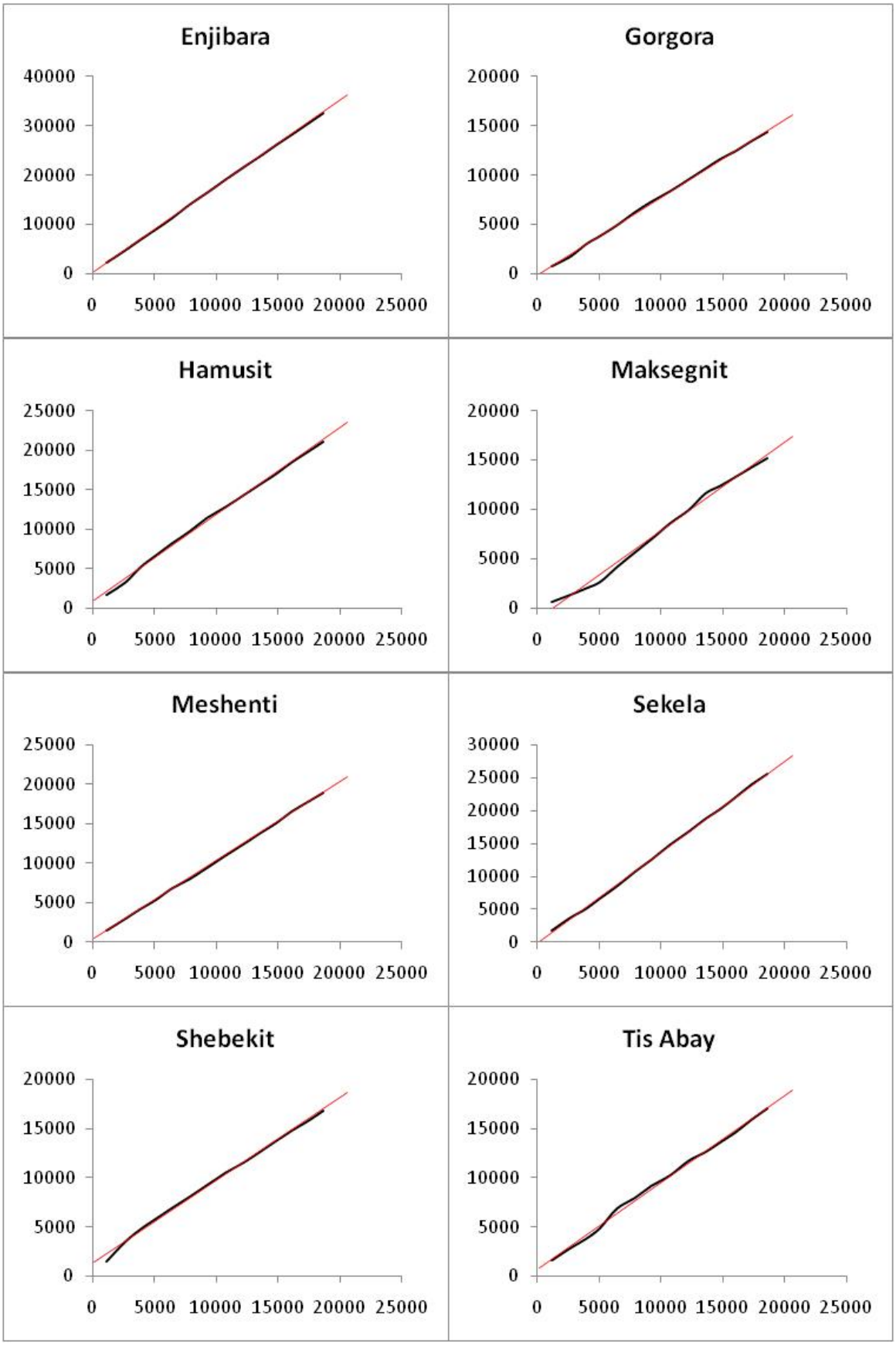

B-2 Double mass curve of annual rainfall- continued…

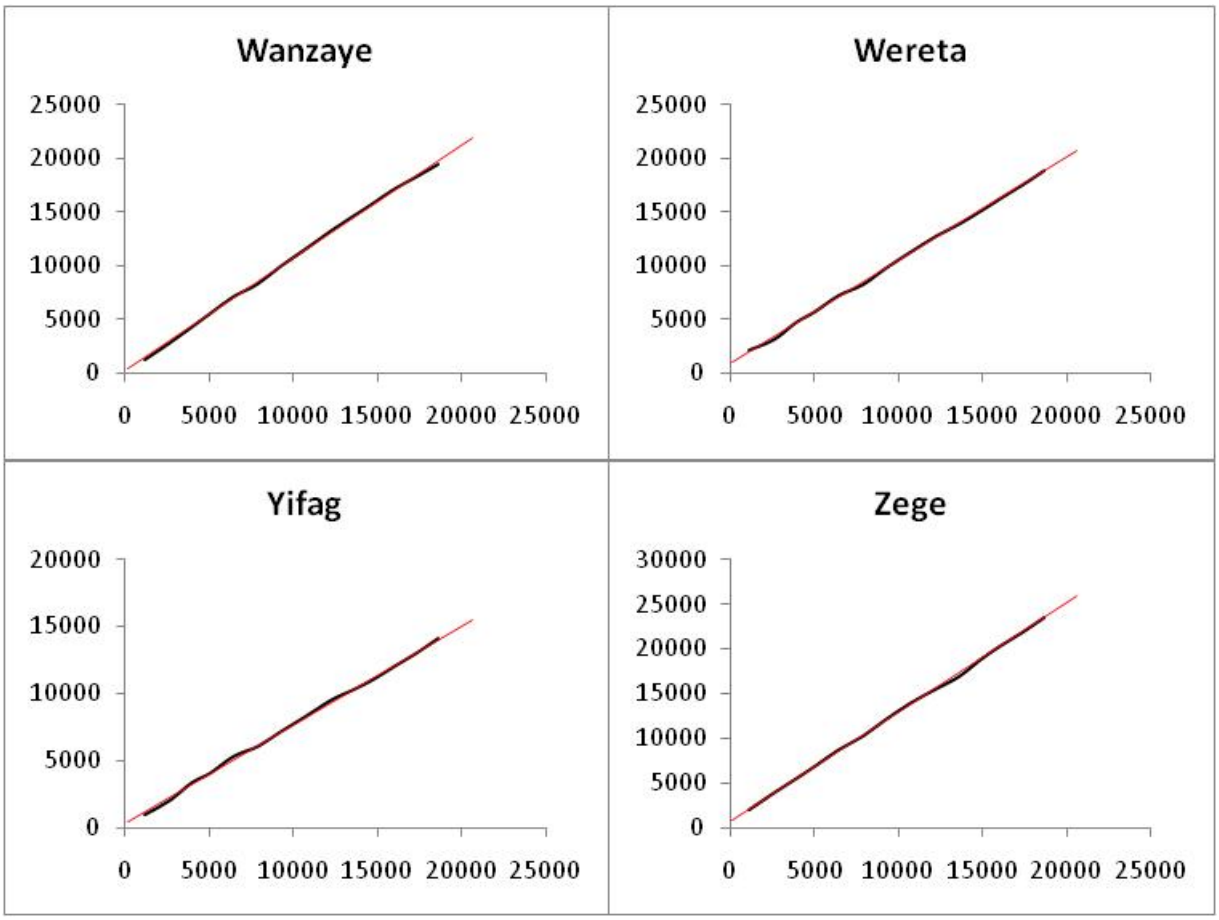

B-3 Double mass curve for mean annual minimum temperature (black line). X- & Y-axis represent cumulative temperature for base and target stations, respectively. Red line is linear trendline

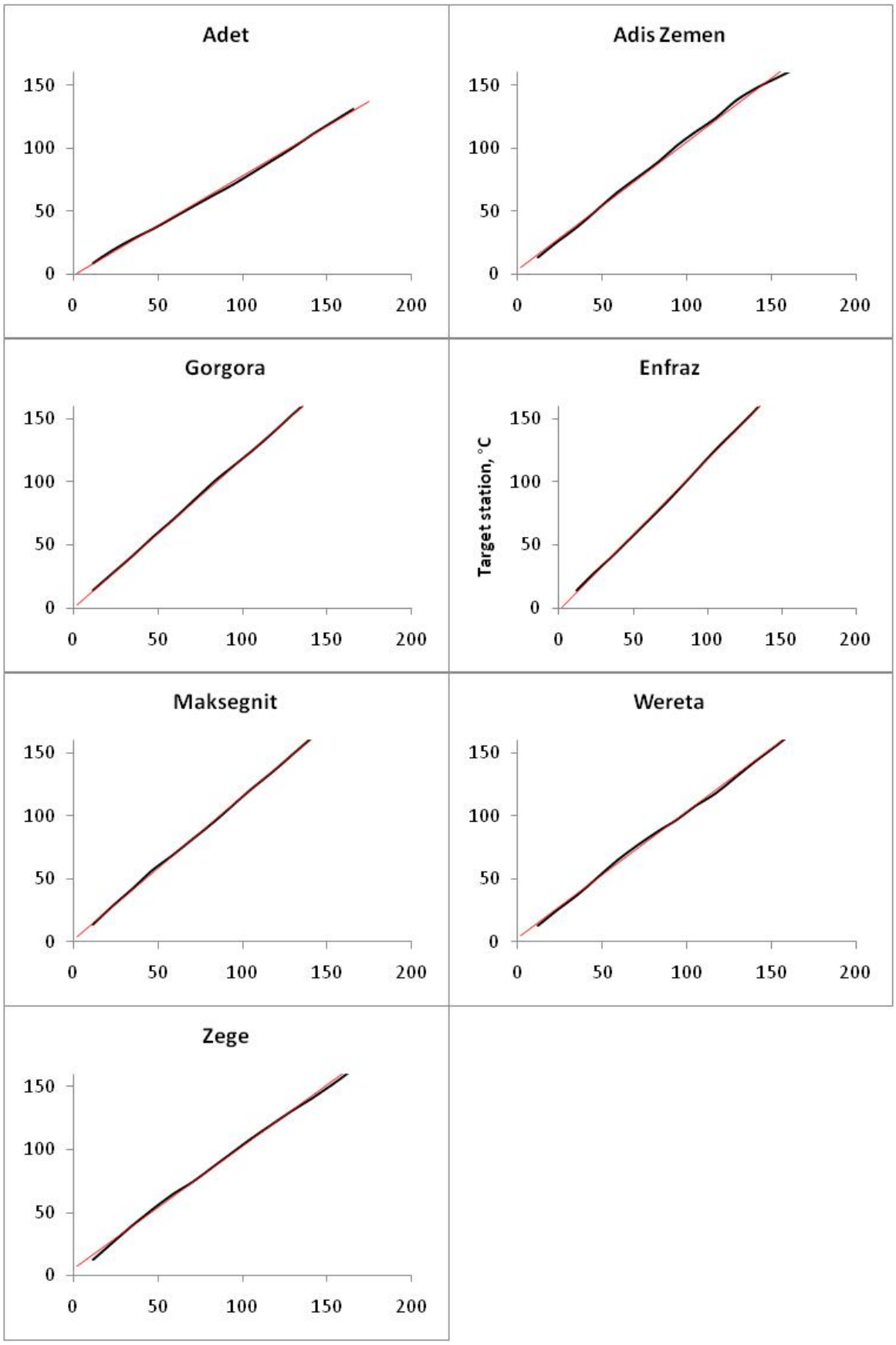

B-4 Double mass curve for mean annual maximum temperature (black line). X- & Y-axis represent cumulative temperature for base and target stations, respectively. Red line is linear trendline

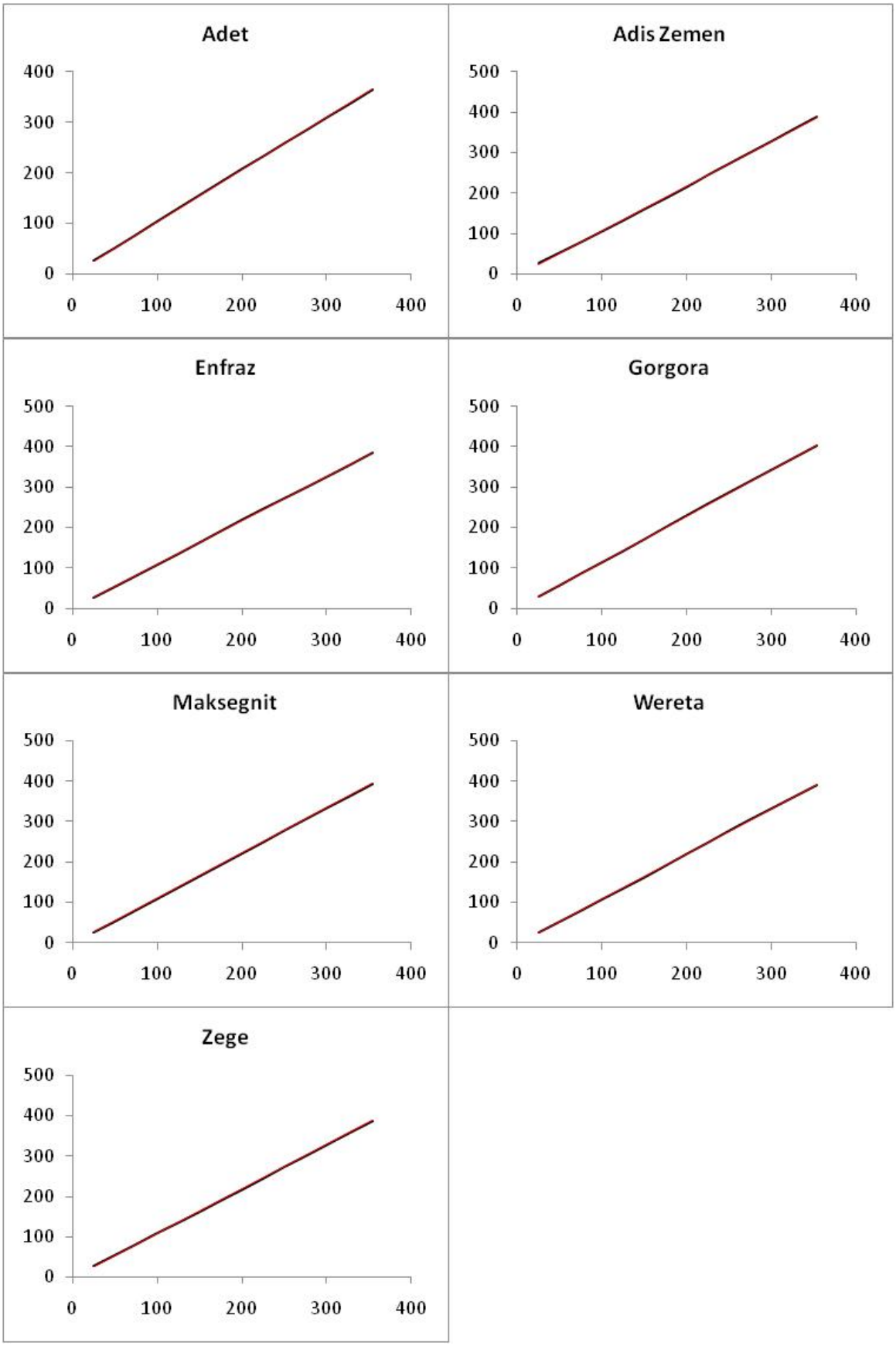

B-5 Physical characteristics of catchments in the Lake Tana basin

Catchment	Total area, km^2	Altitude, m.a.s.l	Slope %	Mean annual rainfall, mm	Median annual rainfall, mm
Dirma	568	1959	6.7	1063	1071
Gabi-Kura	377	1894	4.5	1089	1101
Garno	402	2136	17.8	979	1030
Gelda	411	1954	6.3	1407	1402
Gilgel Abay	4595	2080	6.5	1635	1592
Gumara	1579	2188	20.3	1439	1389
Gumero	548	2048	12	913	950
Megech	813	2158	13.4	1044	1036
Rib	2194	2139	12.1	1346	1395
West of Tana	621	1911	7.5	944	883
Lake Tana	3012	1786	0	1225	1225
Whole basin	15120	2025	9.3	1345	1330

B-6 Distribution of soil types in the Lake Tana basin (in percent)

Catchment	LVh	LVc	LPe	VRe	FLe	ALh	LPl	NTh	RGe	CMe
Dirma	8.6	31	48.8	11.6				0		
Gabi-Kura		11.9	0.6	70.1	17.4			0		
Garno		2.5	56.1	25	8.6			1.4	6.4	
Gelda	46.3	50.1	0.7	2.9						
Gilgel Abay	42	16.2	0.5	8.7	3.2	16.2	10.2	2.1	0.9	
Gumara	52.3	28.9	7	8.1	3.7			0		
Gumero		13.6	43	39.5	0.8			1.1	2	
Megech		6.8	51.6	29.9	4.6			7.1		
Rib	4.2	27	30.7	6	31.6			0.5		
West of Tana	10.5	27.5		3	58.8					0.2
Whole Tana basin	26	20.9	16.3	13	11.6	6.2	3.9	1.5	0.6	

LVh-Haplic Luvisols; LVc-Chromic Luvisols; LPe- Eutric Leptosols; VRe-Eutric Vertisols; FLe- Eutric Fluvisols; ALh- Haplic Alisols; LPl- Lithic Leptosols; NTh- Haplic Nitosols; RGe- Eutric Regosols; CMe- Eutric Cambisols.

B-7 Average soil physical properties in the Lake Tana basin

(Based on data reported in the Abay Master Plan (BCEOM, 1999)

Soil	Clay %	Silt %	Sand %	FC %	PWP %	BD kg/m^3	Porosity	IC m/d	Ks_60 m/d	Ks_100 m/d
Haplic Luvisols	57.7	26.1	16.2	0.43	0.23	1250	0.53	-	-	-
Chromic Luvisols	61.7	25.5	12.8	0.44	0.24	1250	0.53	2.1	0.3	0.3
Eutric Leptosols	59	24.7	16.3	0.43	0.23	1250	0.53	2.8	-	-
Eutric Vertisols	76.3	18.5	5.6	0.47	0.27	1250	0.53	0.7	0.2	0.1
Eutric Fluvisols	51.6	41.2	7.2	0.45	0.24	1300	0.51	2.3	0.2	0.1
Haplic Alisols	54.2	30.4	15.1	0.44	0.23	1250	0.53	3.2	0.5	0.8
Haplic Nitisols	46.4	35.4	18.3	0.41	0.21	1250	0.53	2.6	0.3	0.3
Eutric Regosols	54	35	11	0.44	0.24	1250	0.53	-	-	-
Eutric Cambisols	46.6	34.6	18.5	0.42	0.21	1250	0.53	0.8	0.1	0.1

FC: field capacity; PWP: permanent wilting point; BD: bulk density; IC: infiltration capacity; Ks_60 and Ks_100: saturated hydraulic conductivity at 60 cm and 100 cm soil depth, respectively;

Field capacity and permanent wilting point were determined by the following pedotransfer functions developed from limited measurements.

Field capacity:

FC(%) = -1.245 x %Clay – 1.351 x %Silt – 1.623 x %Sand + 176.574 (n = 34, RMSE = 3.8%)

Permanent wilting point:

PWP(%) = 0.062 x %Clay – 0.066 x %Silt – 0.244 x %Sand + 25.274 (n= 34, RMSE = 1.8%)

Porosity was calculated from the bulk density by the following relation:

$$Porosity = 1 - \frac{\text{bulk density}}{\text{particle density}}$$

B-8 Distribution of land cover types in the Lake Tana basin (in percent)

Catchment	LC1	LC2	LC3	LC4	LC5	LC6	LC7	LC8	LC9	LC10
Dirma	92.0	1.2	6.6						0.2	
Gabi-Kura	98.8	1.1							0.1	
Garno	24.0		32.6				43.4			
Gelda	83.0	5.7	9.4	1.3						0.6
Gilgel Abay	79.4	7.2	3.3	0.4	1.1	0.1	8.4		0.1	
Gumara	71.8	23.3	1.3			0.4	3.1		0.1	
Gumero	63.7	0.5	35.7						0.1	
Megech	96.5	1.7	0.7			0.3			0.8	
Rib	78.6	8.4	0.7	1.0			10.8	0.4	0.1	
West of Tana	89.8	7.6	0.4		1.3	0.8			0.1	
Whole Tana basin	63.0	6.5	3.9	0.1	0.5	0.2	5.6	0.1	0.1	20.0

LC1: cropland; LC2: cropland/grassland mosaic; LC3: cropland/shrubland mosaic; LC4: cropland/woodland mosaic; LC5: cropland/woody savanna mosaic; LC6: grassland; LC7: open shrubland; LC8: plantation; LC9: urban area; LC10: water

Annex C: Main processes of DHSVM and typical input files

C-1 Main processes and equations of the DHSVM model

The major hydrological processes represented in the DHSVM model are shown in Figure C-1. Some of the mathematical equations used to model these processes are also given. The equations that represent snow accumulation and melt processes are not given. The model solves water and energy balance equations simultaneously at grid scale.

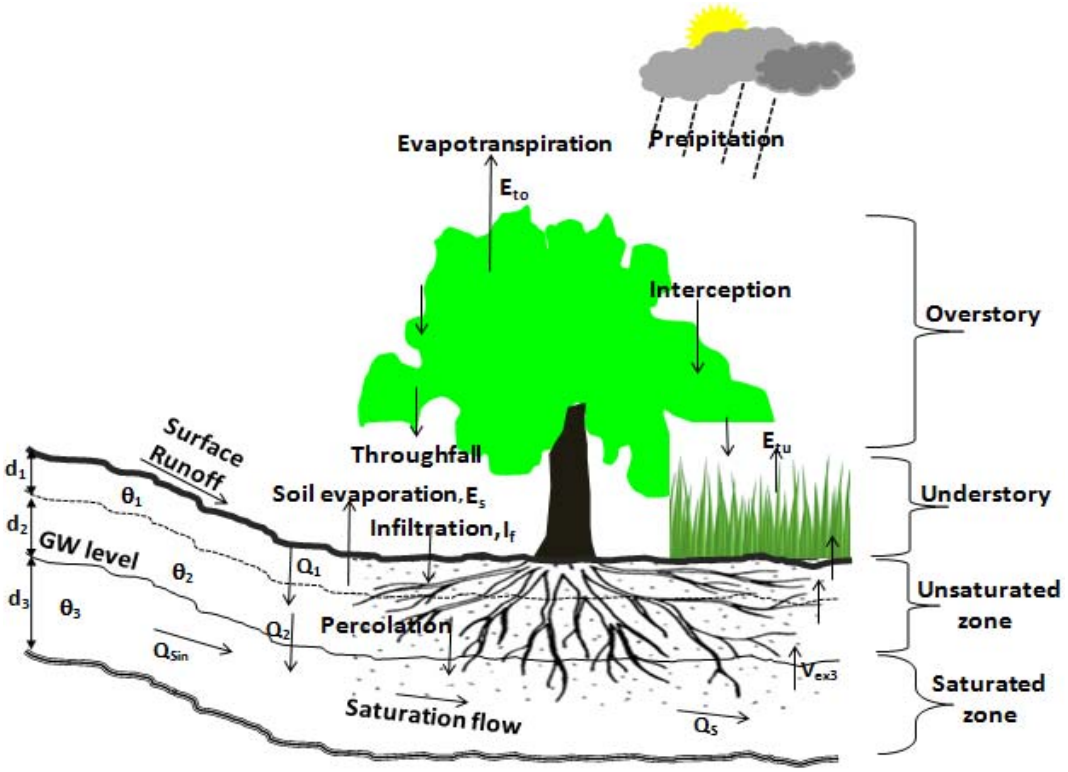

Figure C-1 major hydrological processes in DHSVM

Interception and throughfall

Precipitation is assumed to be stored on the surfaces of overstory and understory vegetation until maximum storage capacities defined by Equations C-1 and C-2 are reached.

$$I_{co} = 10^{-4} LAI_o F \qquad \text{Equation C-1}$$

$$I_{cu} = 10^{-4} LAI_u \qquad \text{Equation C-2}$$

Where, I_c represents maximum interception storage; LAI is leaf area index; F stands for the fraction of ground surface covered by overstory; the subscripts o and u indicate the overstory and understory, respectively.

Throughfall is generated when the canopy storage calculated by Equation C-3 exceeds the maximum interception storage.

$$S_{ij}^{t+\Delta t} = S_{ij}^{t} + P - E_{ij} \qquad \textbf{Equation C-3}$$

Where, the subscript j denotes separate values for the overstory (j = o) and the understory (j = u). S_{ij}^{t} and $S_{ij}^{t+\Delta t}$ represent the actual interception storage at time t and t + Δt, respectively. For $S_{ij}^{t+\Delta t} > I_{cj}$, throughfall is calculated as $S_{ij}^{t+\Delta t} - I_{cj}$ and $S_{ij}^{t+\Delta t}$ is set equal to I_{cj}. P is equal to the overstory throughfall when Equation C-3 is applied to the understory.

Evapotranspiration

Evaporation and transpiration are calculated independently for the overstory and understory in a stepwise fashion. Evaporation of intercepted water from wet vegetation surfaces is assumed to occur at the potential rate. Transpiration from dry vegetation surface over the time period Δt is calculated using the Penman-Monteith approach given by Equation C-4.

$$E_{ij} = \frac{\Delta R_{nj} + \rho c_p (e_s - e)/r_{aj}}{\lambda_v \left[\Delta + \gamma(1 + r_{cj}/r_{aj}\right]} \Delta t \qquad \textbf{Equation C-4}$$

Where, Δ is the slope of the saturated vapor pressure; R_{nj} is the net radiation flux density; ρ is the density of moist air; c_p is the specific heat of air at constant pressure; e_s and e are the saturation and actual vapor pressure, respectively; r_{aj} is the aerodynamic resistance to vapor transport; r_{cj} is the canopy resistance to vapor pressure; λ_v is the latent heat of vaporization of water; γ is the psychrometric constant. R_{nj}, r_{aj} and r_{cj} are calculated separately for the overstory and understory. Different equations for calculating aerodynamic resistance to vapor transfer depending on the vegetation covers are given Wigmosta et al (1994). Vegetation parameters like height, fractional coverage, and leaf area index are involved in the calculations. Canopy resistance is represented as a summation of the stomatal resistance of individual leaves, r_{sj}, which is dependent on vegetation type and environmental factors. The various vegetation parameters involved in the computation of stomatal resistance include minimum and maximum stomatal resistance, vapor pressure deficit, fraction of photosynthetically active radiation, and plant wilting point.

First, evaporation of intercepted water from the overstory (E_{ij}) is calculated as the minimum of the interception storage amount or the potential evaporation demand (E_{pj}) which is obtained by setting r_{cj} in Equation C-4 to zero. Then transpiration from the dry surface (E_{tj}) is computed by Equation C-5.

$$E_{tj} = (E_{pj} - E_{ij})\frac{\Delta + \gamma}{\Delta + \gamma(1 + r_{cj} / r_{aj})}$$ **Equation C-5**

Evaporation from soil is calculated as the minimum of potential evaporation demand (E_{ps}) or the soil desorption volume, F_e (Equation C-5) which refers to the rate at which soil delivers water to the surface.

$$F_e = S_e \Delta t^{1/2}$$ **Equation C-6**

$$S_e = \left[\frac{8\phi K(\theta_s)\psi_b}{3(1+3m)(1+4m)}\right]^{1/2}\left[\frac{\theta}{\phi}\right]^{(1/2m)+2}$$ **Equation C-7**

Where, ϕ is porosity; θ_s is saturation soil moisture which is taken to be ϕ; θ is actual soil moisture; $K(\theta_s)$ is saturated lateral hydraulic conductivity; ψ_b is the soil bubbling pressure; m is the pore size distribution index.

Unsaturated flow

Unsaturated moisture movement is simulated using a multi-soil layer representation. Each vegetation layer may remove water from one or more soil layers, and each soil layer may contain roots from one or more vegetation layers. Transpiration by a given canopy is first calculated for each soil layer using the approach discussed above, then multiplied by the root fraction in that soil layer. Soil evaporation is restricted to the upper zone. For three-soil layers (see Figure C-3), the mass balance equations are given by the following equations:

$$d_1(\theta_1^{t+\Delta t} - \theta_1^t) = I_f - Q_1(\theta_1) - E_{to1} - E_{tu1} - E_{s1} + V_{ex2} - V_{ex1}$$ **Equation C-8**

$$d_2(\theta_2^{t+\Delta t} - \theta_2^t) = Q_1(\theta_1) - Q_2(\theta_2) - E_{to2} - E_{tu2} + V_{ex3}$$ **Equation C-9**

$$d_3(\theta_3^{t+\Delta t} - \theta_3^t) = Q_2(\theta_2) + (Q_{Sin}^t - Q_S^t)\Delta t$$ **Equation C-10**

Where,

d_k (k= 1, 2, 3) is thickness of k^{th} soil layer; θ_k and Q_k are, respectively, average soil moisture and percolation in soil layer k; E_{tok} and E_{tuk} are evapotranspiration from overstory and understory respectively; E_{s1} evaporation from top soil layer; V_{exk} exfiltration from layer k; Q_{sin} and Q_s are the volumes of lateral subsurface inflow and outflow in the saturated zone at the start of the time step, respectively.

The percolation in each soil layer, Q_k, is computed as a function of the actual vertical hydraulic conductivity (Equation C-11)

$$Q_k = \left[\frac{K_v(\theta_k^t) + K_v(\theta_k^*)}{2} \right] \Delta t \qquad \textbf{Equation C-11}$$

Where, $K_v(t)$ is the soil vertical unsaturated hydraulic conductivity; $\theta_k^* = \theta_k^t + (Q_{k-1}/d_k)$. The Brooks-Corey equation is used to calculate the unsaturated hydraulic conductivity (Equation C-12).

$$K_v(\theta) = K_v(\theta_s) \left[\frac{\theta - \theta_r}{\phi - \theta_r} \right]^{2/m+3} \qquad \textbf{Equation C-12}$$

θ_r is the residual soil moisture content which is assumed to be equal to zero (i.e. $\phi = \theta_s$).

Saturated subsurface flow

The model employs a cell-by-cell approach to route subsurface flow. Model grid cells are centered on each DEM elevation point. Directions between a node and its neighbors are assigned the index k and numbered from 0 to 7 in a clockwise direction from north. The rate of saturated subsurface flow from cell i, j in the k direction is computed by Equation C-13.

$$q_{s\,i,j,k} = w_{i,j,k} \beta_{i,j,k} T_{i,j}(z, D) \qquad \textbf{Equation C-13}$$

Where $w_{i,j,k}$ is the grid cell flow width in the k-direction; $\beta_{i,j,k}$ is the water table slope in the k-direction; $T_{i,j}(z,D)$ is the grid cell transmissivity. Soil lateral saturated hydraulic conductivity is assumed to decrease exponentially with depth and soil transmissivity is calculated by Equation C-14.

$$T_{i,j}(z, D) = \frac{K_{i,j}}{f_{i,j}} (e^{-f_{i,j} \cdot z_{i,j}} - e^{-f_{i,j} \cdot D_{i,j}}) \qquad \textbf{Equation C-14}$$

Where $K_{i,j}$ is the grid cell lateral saturated hydraulic conductivity at the soil surface, $f_{i,j}$ is the rate of exponential decrease, and $D_{i,j}$ is the grid cell soil thickness. The total subsurface outflow from a grid cell, $Q_{Si,j}$, is equal to the sum of the component flows obtained from Equation C-13.

C-2 Parameter values used to estimate soil depth

Soil depth was estimated from topographic attributes using equation C-1.

$$Sd_{ij} = Sd_{\min} + \left(Sd_{\max} - Sd_{\min}\right) \times \left[a\left(1 - \frac{S_{ij}}{S_{\max}}\right)^{A} + b\left(1 - \frac{A_{ij}}{A_{\max}}\right)^{B} + c\left(1 - \frac{Z_{ij}}{Z_{\max}}\right)^{C} \right] \quad \text{Equation C-1}$$

Topographic attribute	Parameter	Value used
Soil depth limits	Sd_{min}, minimum soil depth (m)	0.1
	Sd_{max}, maximum soil depth, m	1.5
Slope	a, weight for slope	0.5
	A, exponent for slope	0.25
	S_{max}, maximum limiting slope(decimal)	0.35
Upslope area	b, weight for area	0.2
	B, exponent for upslope area	1.0
	A_{max}, maximum limiting area, m^2	1000000
Altitude	c, weight for altitude	0.3
	C, exponent for altitude	0.75
	Z_{max}, maximum limiting elevation (m)	2800

C-3 Typical vegetation and stream inputs used to create stream network files for Rib catchment

Vegetation class (Name)	Rooting depth, m
1 (Cropland)	0.7
2 (Cropland/grassland mosaic)	0.4
3 (Cropland/shrubland mosaic)	0.4
4 (Cropland/woodland mosaic)	1.0
5 (Cropland/woody savanna mosaic)	0.8
6 (Grassland)	0.2
7 (Open shrubland)	0.2
8 (Plantation)	1.2
9 (Urban area)	1.2
10 (Water)	0.1

Stream class	Width, m	Depth, m	Upslope area range, m^2	Manning n
1	2.0	0.25	0.25×10^6-1×10^7	0.03
2	6.0	0.4	1×10^7-5×10^7	0.03
3	10.0	0.8	5×10^7-5×10^8	0.06
4	25.0	1.5	5×10^8-1×10^9	0.06
5	50.0	2.5	1×10^9-2×10^9	0.06

C-4 Typical text file used to create initial model state file for Rib catchment

```
./Init_Model/          # Path for the output file
01/01/1992-00          # Date for the model state in mm/dd/yyyy-hh
642  631               # Number of rows (ny) and number columns (nx) of the catchment grid
2                      # Maximum number of vegetation layers
0.0   0.0              # Rain interception in m for each vegetation layer
0.0                    # Snow interception in m for top vegetation layer
0                      # Snow cover mask
365                    # Number of days since last snow fall
0.0                    # Snow water equivalent in m
0.0                    # Liquid water content in m of bottom layer of snowpack
20.0                   # Temperature in °C of bottom layer of snowpack
0.0                    # Liquid water content in m of top layer snowpack
20.0                   # Temperature in °C of top layer of snowpack
0.0                    # Cold content of snowpack
3                      # maximum number of root zone layers
0.4 0.4 0.4 0.4        # Volumetric soil moisture content of each layer (including the layer below the
                           lowest root zone layer)
20.0                   # Temperature in °C at soil surface
19.0 19.0 19.0         # Soil temperature in °C for each root zone layer
0.0                    # Ground heat exchange
0.0                    # Runoff
```

C-5 Typical configuration file used for Rib catchment

```
##############################################################################
# OPTIONS SECTION
##############################################################################
[OPTIONS]                    # Model Options
Format                = BIN            # BIN. BYTESWAP or NETCDF
Extent                = BASIN          # POINT or BASIN
Gradient                    = WATERTABLE       # TOPOGRAPHY or WATERTABLE
Flow Routing          = NETWORK        # UNIT_HYDROGRAPH or NETWORK
Sensible Heat Flux    = FALSE          # TRUE or FALSE
Sediment              = FALSE        # TRUE or FALSE
Sediment Input File   = ./TBsediment.MWM  # path for sediment c
Overland Routing      = CONVENTIONAL     # CONVENTIONAL or KINEMATIC
Interpolation         = NEAREST        # NEAREST or INVDIST or VARCRESS
MM5                   = FALSE          # TRUE or FALSE
QPF                   = FALSE          # TRUE or FALSE
PRISM                 = FALSE          # TRUE or FALSE
PRISM data path       = ./input/prism/PrismMap    # path for PRISM files
PRISM data extension       = bin            # file extension for PRISM files
Canopy radiation attenuation mode = FIXED # FIXED or VARIABLE
Shading                     = FALSE        # TRUE or FALSE
Shading data path     =              # path for shading files
Shading data extension     = bin           # file extension for shading files
Skyview data path     =                # path for skyview file
Snotel                = FALSE          # TRUE or FALSE
Outside               = TRUE         # TRUE or FALSE
Rhoverride                  = FALSE          # TRUE or FALSE
Precipitation Source = STATION         # STATION or RADAR
Wind Source           = STATION         # STATION or MODEL
Temperature lapse rate   = CONSTANT      # CONSTANT or VARIABLE
Precipitation lapse rate     = CONSTANT      # CONSTANT. MAP. or VARIABLE
Infiltration          = STATIC         # STATIC or DYNAMIC
Cressman radius       = 10             # in model pixels
Cressman stations     = 4              # number of stations

##############################################################################
# MODEL AREA SECTION
##############################################################################
[AREA]                       # Model area
Coordinate System          = UTM
Extreme North         = 1352173.0000
Extreme West          = 359927.0000
Center Latitude       = 11.97
Center Longitude      = 37.97
Time Zone Meridian         = 37
Number of Rows       = 642
Number of Columns          = 631
Grid spacing               = 90
Point North                =
Point East             =
```

```
################################## TIME SECTION#####################################
 [TIME]                          # Model period
Time Step                  = 3             # Model time step (hours)
Model Start                = 01/01/1992-00:00    # Model start time (MM/DD/YYYY-HH)
Model End             = 12/31/2005-21:00     # Model end time (MM/DD/YYYY-HH)
Number of Model State    = 0
Model State Date     = 0
################################## CONSTANTS SECTION ################################
 [CONSTANTS]                    # Model constants
Ground Roughness          = 0.02           # Roughness of soil surface (m)
Snow Roughness      = 0.02           # Roughness of snow surface (m)
Rain Threshold         = -1.0           # Minimum temperature at which rain occurs (°C)
Snow Threshold         = 0.5            # Maximum temperature at which snow occurs (°C)
Snow Water Capacity       = 0.03           # Snow liquid water holding capacity (fraction)
Reference Height      = 50.0           # Reference height (m)
Rain LAI Multiplier    = 0.0001          # LAI Multiplier for rain interception
Snow LAI Multiplier  = 0.0005          # LAI Mulitplier for snow interception
Min Intercepted Snow      = 0.005          # Intercepted snow that can only be melted (m)
Outside Basin Value         = 0              # Value in mask that indicates outside the basin
Temperature Lapse Rate   = -0.005      # Temperature lapse rate (C/m)
Precipitation Lapse Rate   = 0.0       # Precipitation lapse rate (m/m)

################################## TERRAIN INFORMATION SECTION ##################
 [TERRAIN]                      # Terrain information
DEM File                    =  ./Input_data/DEM/Rib_dem.bin     # path for DEM file
Basin Mask File         =  ./Input_data/Mask/Rib_mask.bin   # path for mask file

############################### ROUTING SECTION ################################
 [ROUTING] # Routing information. This section is only relevant if the Extent = BASIN
# The following three fields are only used if Flow Routing = NETWORK

Stream Map File       = ./Input_data/Stream/Rib_stream.map.dat      # path for stream map file
Stream Network File         = ./Input_data/Stream/Rib_stream.network.dat  # path for stream network file
Stream Class File      = ./Input_data/Stream/Rib_stream.class.dat    # path for stream class file

################################ METEOROLOGY SECTION ################################
 [METEOROLOGY]                  # Meteorological stations
Number of Stations  = 5               # Number of meteorological stations

Station Name     1     = Debre Tabor          # Name for station 1
North Coordinate 1  = 1310158.37         # North coordinate of station 1
East Coordinate  1    = 392165.34         # East coordinate of station 1
Elevation       1        = 2700           # Elevation of station 1 in m
Station File    1              = ./Input_data/Meteo/Debretabor.txt  # path for station 1 file

Station Name     2     = Addis Zemen          # Name for station 2
North Coordinate 2  = 1341225.90         # North coordinate of station 2
East Coordinate  2    = 367246.68         # East coordinate of station 2
Elevation       2        = 1970           # Elevation of station 2 in m
Station File    2              = ./Input_data/Meteo/Adiszemen.txt # path for station 2 file

Station Name     3     = Enfraz           # Name for station 3
North Coordinate 3  = 1346806.96         # North coordinate of station
East Coordinate  3    = 356390.40         # East coordinate of station 3
Elevation       3        = 1882           # Elevation of station 3 in m
Station File    3              = ./Input_data/Meteo/Enfraz.txt # path for station 3 file
```

```
Station Name    4    = Wereta         # Name for station 4
North Coordinate 4  = 1318049.50       # North coordinate of station 4
East Coordinate  4   = 356252.06       # East coordinate of station 4
Elevation       4    = 1801            # Elevation of station 4 in m
Station File    4            = ./Input_data/Meteo/Wereta.txt # path for station 4 file

Station Name    5    = Yifag           # Name for station 5
North Coordinate 5  = 1335725.63       # North coordinate of station 5
East Coordinate  5   = 360690.95       # East coordinate of station 5
Elevation       5    = 1849            # Elevation of station 5 in m
Station File    5            = ./Input_data/Meteo/Yifag.txt # path for station 5 file

################################### SOILS INFORMATION SECTION#############################
 [SOILS]                    # Soil information

Soil Map File           = ./Input_data/Soil/Rib_soil.bin
Soil Depth File         = ./Input_data/Soil/Rib_soildepth.bin
Number of Soil Types    = 10

Soil Description 1          =    Haplic Luvisols (C-C-C)
Lateral Conductivity 1      =    1.07E-06   # m/s
Exponential Decrease 1      =    1.10
Maximum Infiltration 1      =    2.95E-06   # m/s
Surface Albedo 1            =    0.17
Number of Soil Layers 1     =    3
Porosity 1        =    0.45 0.45 0.45
Pore Size Distribution 1    =    0.131      0.131      0.131
Bubbling Pressure 1 =    0.373      0.373      0.373      # m
Field Capacity 1        =    0.3   0.3   0.3
Wilting Point 1         =    0.15  0.15  0.15
Bulk Density 1          =    1250  1250  1250     # kg/m3
Vertical Conductivity 1     =    1.07E-06   4.44E-07   3.56E-07    # m/s
Thermal Conductivity 1      =    0.61 0.61 0.61
Thermal Capacity 1  =    2.25E+06  2.25E+06  2.25E+06
Capillary Drive 1           =    0.41
Mannings n 1            =    0.25

Soil Description 2          =    Chromic Luvisols (SiC-C-C)
Lateral Conductivity 2      =    1.0E-06
Exponential Decrease 2      =    0.3
Maximum Infiltration 2      =    3.0E-06
Surface Albedo 2            =    0.17
Number of Soil Layers 2     =    3
Porosity 2        =    0.53 0.53 0.53
Pore Size Distribution 2    =    0.127      0.131      0.131
Bubbling Pressure 2 =    0.342      0.373      0.373
Field Capacity 2        =    0.4   0.4   0.4
Wilting Point 2         =    0.25  0.25  0.25
Bulk Density 2          =    1250  1250  1250
Vertical Conductivity 2     =    1.07E-06   4.44E-07   3.56E-07
Thermal Conductivity 2      =    0.63 0.61 0.61
Thermal Capacity 2  =    2.25E+06  2.25E+06  2.25E+06
Capillary Drive 2           =    0.41
Mannings n 2            =    0.25
```

Soil Description 3 = Eutric Leptosols (CL - C - C)
Lateral Conductivity 3 = 2.0E-04
Exponential Decrease 3 = 0.3
Maximum Infiltration 3 = 2.0E-05
Surface Albedo 3 = 0.17
Number of Soil Layers 3 = 3
Porosity 3 = 0.59 0.59 0.59
Pore Size Distribution 3 = 0.194 0.131 0.131
Bubbling Pressure 3 = 0.256 0.373 0.373
Field Capacity 3 = 0.4 0.4 0.4
Wilting Point 3 = 0.19 0.25 0.25
Bulk Density 3 = 1250 1250 1250
Vertical Conductivity 3 = 6.79E-06 2.82E-06 2.26E-06
Thermal Conductivity 3 = 0.65 0.61 0.61
Thermal Capacity 3 = 2.28E+06 2.25E+06 2.25E+06
Capillary Drive 3 = 0.41
Mannings n 3 = 0.25

Soil Description 4 = Eutric Vertisols (C-C-C)
Lateral Conductivity 4 = 1.0E-07
Exponential Decrease 4 = 1.10
Maximum Infiltration 4 = 3.0E-06
Surface Albedo 4 = 0.17
Number of Soil Layers 4 = 3
Porosity 4 = 0.45 0.45 0.45
Pore Size Distribution 4 = 0.131 0.131 0.131
Bubbling Pressure 4 = 0.373 0.373 0.373
Field Capacity 4 = 0.3 0.3 0.3
Wilting Point 4 = 0.27 0.28 0.27
Bulk Density 4 = 1250 1250 1250
Vertical Conductivity 4 = 4.50E-06 1.85E-07 1.48E-07
Thermal Conductivity 4 = 0.61 0.61 0.61
Thermal Capacity 4 = 2.25E+06 2.25E+06 2.25E+06
Capillary Drive 4 = 0.41
Mannings n 4 = 0.25

Soil Description 5 = Eutric Fluvisols (SiC. SiC. C)
Lateral Conductivity 5 = 2.0E-06
Exponential Decrease 5 = 0.2
Maximum Infiltration 5 = 2.68E-06
Surface Albedo 5 = 0.17
Number of Soil Layers 5 = 3
Porosity 5 = 0.5 0.5 0.5
Pore Size Distribution 5 = 0.127 0.127 0.131
Bubbling Pressure 5 = 0.342 0.342 0.373
Field Capacity 5 = 0.35 0.35 0.35
Wilting Point 5 = 0.15 0.15 0.15
Bulk Density 5 = 1300 1300 1250
Vertical Conductivity 5 = 4.72E-06 1.93E-07 1.54E-07
Thermal Conductivity 5 = 0.63 0.63 0.61
Thermal Capacity 5 = 2.25E+06 2.25E+06 2.25E+06
Capillary Drive 5 = 0.41
Mannings n 5 = 0.25

Soil Description 6 = Haplic Alisols (C-CL-C)
Lateral Conductivity 6 = 1.69E-06
Exponential Decrease 6 = 1.10
Maximum Infiltration 6 = 3.74E-06
Surface Albedo 6 = 0.17
Number of Soil Layers 6 = 3
Porosity 6 = 0.45 0.45 0.45
Pore Size Distribution 6 = 0.131 0.194 0.131
Bubbling Pressure 6 = 0.373 0.256 0.373
Field Capacity 6 = 0.3 0.3 0.3
Wilting Point 6 = 0.15 0.15 0.15
Bulk Density 6 = 1250 1250 1250
Vertical Conductivity 6 = 1.69E-06 7.00E-07 5.62E-07
Thermal Conductivity 6 = 0.61 0.65 0.61
Thermal Capacity 6 = 2.25E+06 2.28E+06 2.25E+06
Capillary Drive 6 = 0.41
Mannings n 6 = 0.25

Soil Description 7 = Letic Leptosols (CL-CL-CL)
Lateral Conductivity 7 = 6.37E-06
Exponential Decrease 7 = 1.10
Maximum Infiltration 7 = 7.08E-06
Surface Albedo 7 = 0.17
Number of Soil Layers 7 = 3
Porosity 7 = 0.45 0.45 0.45
Pore Size Distribution 7 = 0.19 0.19 0.19
Bubbling Pressure 7 = 0.256 0.256 0.256
Field Capacity 7 = 0.3 0.3 0.3
Wilting Point 7 = 0.15 0.15 0.15
Bulk Density 7 = 1250 1250 1250
Vertical Conductivity 7 = 6.79E-06 6.79E-07 6.79E-07
Thermal Conductivity 7 = 0.65 0.65 0.65
Thermal Capacity 7 = 2.28E+06 2.28E+06 2.28E+06
Capillary Drive 7 = 0.41
Mannings n 7 = 0.25

Soil Description 8 = Haplic Nitisols (C-SiL-C)
Lateral Conductivity 8 = 9.56E-06
Exponential Decrease 8 = 1.10
Maximum Infiltration 8 = 3.01E-06
Surface Albedo 8 = 0.17
Number of Soil Layers 8 = 3
Porosity 8 = 0.45 0.45 0.45
Pore Size Distribution 8 = 0.131 0.211 0.131
Bubbling Pressure 8 = 0.373 0.208 0.373
Field Capacity 8 = 0.3 0.3 0.3
Wilting Point 8 = 0.22 0.17 0.25
Bulk Density 8 = 1250 1250 1250
Vertical Conductivity 8 = 9.56E-06 3.97E-07 3.18E-07
Thermal Conductivity 8 = 0.61 0.7 0.61
Thermal Capacity 8 = 2.25E+06 2.31E+06 2.25E+06
Capillary Drive 8 = 0.41
Mannings n 8 = 0.25

Soil Description 9 = Eutric Regosols (C-C-C)
Lateral Conductivity 9 = 6.37E-06
Exponential Decrease 9 = 1.10
Maximum Infiltration 9 = 8.46E-06
Surface Albedo 9 = 0.17
Number of Soil Layers 9 = 3
Porosity 9 = 0.45 0.45 0.45
Pore Size Distribution 9 = 0.131 0.131 0.131
Bubbling Pressure 9 = 0.373 0.373 0.373
Field Capacity 9 = 0.3 0.3 0.3
Wilting Point 9 = 0.15 0.15 0.15
Bulk Density 9 = 1250 1250 1250
Vertical Conductivity 9 = 4.45E-07 1.85E-07 1.48E-07
Thermal Conductivity 9 = 0.61 0.61 0.61
Thermal Capacity 9 = 2.25E+06 2.25E+06 2.25E+06
Capillary Drive 9 = 0.41
Mannings n 9 = 0.25

Soil Description 10 = Eutric Cambisols (CL-C-C)
Lateral Conductivity 10 = 6.79E-06
Exponential Decrease 10 = 1.10
Maximum Infiltration 10 = 7.08E-06
Surface Albedo 10 = 0.17
Number of Soil Layers 10 = 3
Porosity 10 = 0.45 0.45 0.45
Pore Size Distribution 10 = 0.194 0.131 0.131
Bubbling Pressure 10 = 0.256 0.373 0.373
Field Capacity 10 = 0.3 0.3 0.3
Wilting Point 10 = 0.19 0.2 0.25
Bulk Density 10 = 1250 1250 1250
Vertical Conductivity 10 = 6.79E-06 2.82E-07 2.26E-07
Thermal Conductivity 10 = 0.65 0.61 0.61
Thermal Capacity 10 = 2.28E+06 2.25E+06 2.25E+06
Capillary Drive 10 = 0.41
Mannings n 10 = 0.25

############################## VEGETATION INFORMATION SECTION ##########################
[VEGETATION]

Vegetation Map File = ./Input_data/Vegetation/Rib_vegetation.bin
Number of Vegetation Types = 10

Vegetation Description 1 = Cropland
Overstory Present 1 = FALSE
Understory Present 1 = TRUE
Fractional Coverage 1 =
Trunk Space 1 =
Aerodynamic Attenuation 1 =
Radiation Attenuation 1 =
Hemi Fract Coverage 1 =
Clumping Factor 1 =
Leaf Angle A 1 =
Leaf Abgle B 1 =
Scattering Parameter 1 =

Max Snow int Capacity 1 =
Mass Release Drip Ratio 1 =
Snow Interception Eff 1 =
Impervious Fraction 1 = 0.0
Height 1 = 1.0
Maximum Resistance 1 = 600
Minimum Resistance 1 = 120
Moisture Threshold 1 = 0.33
Vapor Pressure Deficit 1 = 4000
Rpc 1 = 0.50
Number of Root Zones 1 = 3
Root Zone Depths 1 = 0.06 0.16 0.18
Overstory Root Fraction 1 =
Understory Root Fraction 1 = 0.3 0.5 0.2
Overstory Monthly LAI 1 =
Understory Monthly LAI 1 = 0.40 0.40 0.40 0.30 0.30 0.30 1.00 2.00 2.50 1.60 0.80 0.50
Overstory Monthly Alb 1 =
Understory Monthly Alb 1 = 0.2 0.2 0.2 0.2 0.2 0.2 0.2 0.2 0.2 0.2 0.2 0.2

Vegetation Description 2 = Cropland/Grassland mosaic
Overstory Present 2 = FALSE
Understory Present 2 = TRUE
Fractional Coverage 2 =
Trunk Space 2 =
Aerodynamic Attenuation 2 =
Radiation Attenuation 2 =
Hemi Fract Coverage 2 =
Clumping Factor 2 =
Leaf Angle A 2 =
Leaf Abgle B 2 =
Scattering Parameter 2 =
Max Snow int Capacity 2 =
Mass Release Drip Ratio 2 =
Snow Interception Eff 2 =
Impervious Fraction 2 = 0.0
Height 2 = 1.0
Maximum Resistance 2 = 600
Minimum Resistance 2 = 200
Moisture Threshold 2 = 0.33
Vapor Pressure Deficit 2 = 4000
Rpc 2 = 0.50
Number of Root Zones 2 = 3
Root Zone Depths 2 = 0.045 0.120 0.135
Overstory Root Fraction 2 =
Understory Root Fraction 2 = 0.4 0.6 0
Overstory Monthly LAI 2 =
Understory Monthly LAI 2 = 0.40 0.40 0.40 0.30 0.30 0.30 1.00 2.00 2.50 1.60 0.80 0.50
Overstory Monthly Alb 2 =
Understory Monthly Alb 2 = 0.2 0.2 0.2 0.2 0.2 0.2 0.2 0.2 0.2 0.2 0.2 0.2

Vegetation Description 3 = Cropland/Shrubland mosaic
Overstory Present 3 = FALSE
Understory Present 3 = TRUE
Fractional Coverage 3 =
Trunk Space 3 =
Aerodynamic Attenuation 3 =
Radiation Attenuation 3 =

Hemi Fract Coverage 3 =
Clumping Factor 3 =
Leaf Angle A 3 =
Leaf Abgle B 3 =
Scattering Parameter 3 =
Max Snow int Capacity 3 =
Mass Release Drip Ratio 3 =
Snow Interception Eff 3 =
Impervious Fraction 3 = 0.0
Height 3 = 1.5
Maximum Resistance 3 = 600
Minimum Resistance 3 = 200
Moisture Threshold 3 = 0.33
Vapor Pressure Deficit 3 = 4000
Rpc 3 = 0.60
Number of Root Zones 3 = 3
Root Zone Depths 3 = 0.045 0.120 0.135
Overstory Root Fraction 3 =
Understory Root Fraction 3 = 0.4 0.6 0
Overstory Monthly LAI 3 =
Understory Monthly LAI 3 = 0.40 0.40 0.40 0.30 0.30 0.30 1.00 2.00 2.50 1.60 0.80 0.50
Overstory Monthly Alb 3 =
Understory Monthly Alb 3 = 0.2 0.2 0.2 0.2 0.2 0.2 0.2 0.2 0.2 0.2 0.2 0.2

Vegetation Description 4 = Cropland/Woodland mosaic
Overstory Present 4 = TRUE
Understory Present 4 = TRUE
Fractional Coverage 4 = 0.5
Trunk Space 4 = 0.45
Aerodynamic Attenuation 4 = 1.2
Radiation Attenuation 4 = 0.15
Hemi Fract Coverage 4 =
Clumping Factor 4 =
Leaf Angle A 4 =
Leaf Abgle B 4 =
Scattering Parameter 4 =
Max Snow int Capacity 4 = 0.003
Mass Release Drip Ratio 4 = 0.4
Snow Interception Eff 4 = 0.6
Impervious Fraction 4 = 0.0
Height 4 = 15.0 2.0
Maximum Resistance 4 = 4500. 2300.
Minimum Resistance 4 = 300. 150.
Moisture Threshold 4 = 0.33 0.13
Vapor Pressure Deficit 4 = 4000. 4000.
Rpc 4 = 0.60 0.50
Number of Root Zones 4 = 3
Root Zone Depths 4 = 0.105 0.280 0.315
Overstory Root Fraction 4 = 0.20 0.40 0.40
Understory Root Fraction 4 = 0.50 0.50 0.0
Overstory Monthly LAI 4 = 1.00 1.00 0.80 0.80 0.90 0.90 1.60 2.30 2.70 2.10 1.30 1.00
Understory Monthly LAI 4 = 0.40 0.40 0.40 0.30 0.30 0.30 1.00 2.00 2.50 1.60 0.80 0.50
Overstory Monthly Alb 4 = 0.2 0.2 0.2 0.2 0.2 0.2 0.2 0.2 0.2 0.2 0.2 0.2
Understory Monthly Alb 4 = 0.2 0.2 0.2 0.2 0.2 0.2 0.2 0.2 0.2 0.2 0.2 0.2

```
Vegetation Description 5      =    Cropland/Woody savana mosaic
Overstory Present 5      =    TRUE
Understory Present 5          =    TRUE
Fractional Coverage 5         =    0.5
Trunk Space 5            =    0.45
Aerodynamic Attenuation 5     =    1.2
Radiation Attenuation 5       =    0.15
Hemi Fract Coverage 5         =
Clumping Factor 5        =
Leaf Angle A 5           =
Leaf Abgle B 5           =
Scattering Parameter 5        =
Max Snow int Capacity 5       =    0.003
Mass Release Drip Ratio 5     =    0.4
Snow Interception Eff 5       =    0.6
Impervious Fraction 5         =    0.0
Height 5                 =    15.0 2.0
Maximum Resistance 5          =    4500.      2300.
Minimum Resistance 5          =    300. 150.
Moisture Threshold 5          =    0.33 0.13
Vapor Pressure Deficit 5      =    4000.      4000.
Rpc 5                    =    0.50 0.50
Number of Root Zones 5        =    3
Root Zone Depths 5       =    0.090      0.240      0.270
Overstory Root Fraction 5     =    0.20 0.40 0.40
Understory Root Fraction 5    =    0.50 0.50 0.0
Overstory Monthly LAI 5       =    0.90 0.90 0.80 0.80 0.90 0.90 1.60 1.80 2.40 1.90 1.20 1.00
Understory Monthly LAI 5      =    0.40 0.40 0.40  0.30  0.30 0.30 1.00 2.00 2.50 1.60 0.80 0.50
Overstory Monthly Alb 5       =    0.2 0.2 0.2 0.2 0.2 0.2  0.2 0.2 0.2 0.2 0.2 0.2
Understory Monthly Alb 5      =    0.2 0.2 0.2 0.2 0.2 0.2  0.2 0.2 0.2 0.2 0.2 0.2

Vegetation Description 6      =    Grassland
Overstory Present 6      =    FALSE
Understory Present 6          =    TRUE
Fractional Coverage 6         =
Trunk Space 6            =
Aerodynamic Attenuation 6     =
Radiation Attenuation 6       =
Hemi Fract Coverage 6         =
Clumping Factor 6        =
Leaf Angle A 6           =
Leaf Abgle B 6           =
Scattering Parameter 6        =
Max Snow int Capacity 6       =
Mass Release Drip Ratio 6     =
Snow Interception Eff 6       =
Impervious Fraction 6         =    0.0
Height 6                 =    0.5
Maximum Resistance 6          =    600
Minimum Resistance 6          =    200
Moisture Threshold 6          =    0.33
Vapor Pressure Deficit 6      =    4000
Rpc 6                    =    0.40
Number of Root Zones 6        =    3
Root Zone Depths 6       =    0.030      0.080      0.090
Overstory Root Fraction 6     =
```

Understory Root Fraction 6 = 0.4 0.6 0
Overstory Monthly LAI 6 =
Understory Monthly LAI 6 = 0.40 0.40 0.40 0.30 0.30 0.30 1.00 2.00 2.50 1.60 0.80 0.50
Overstory Monthly Alb 6 =
Understory Monthly Alb 6 = 0.2 0.2 0.2 0.2 0.2 0.2 0.2 0.2 0.2 0.2 0.2 0.2

Vegetation Description 7 = Open Shrubland
Overstory Present 7 = FALSE
Understory Present 7 = TRUE
Fractional Coverage 7 =
Trunk Space 7 =
Aerodynamic Attenuation 7 =
Radiation Attenuation 7 =
Hemi Fract Coverage 7 =
Clumping Factor 7 =
Leaf Angle A 7 =
Leaf Abgle B 7 =
Scattering Parameter 7 =
Max Snow int Capacity 7 =
Mass Release Drip Ratio 7 =
Snow Interception Eff 7 =
Impervious Fraction 7 = 0.0
Height 7 = 1.5
Maximum Resistance 7 = 600
Minimum Resistance 7 = 200
Moisture Threshold 7 = 0.33
Vapor Pressure Deficit 7 = 4000
Rpc 7 = 0.60
Number of Root Zones 7 = 3
Root Zone Depths 7 = 0.030 0.080 0.090
Overstory Root Fraction 7 =
Understory Root Fraction 7 = 0.4 0.6 0
Overstory Monthly LAI 7 =
Understory Monthly LAI 7 = 0.40 0.40 0.40 0.30 0.30 0.30 1.00 2.00 2.50 1.60 0.80 0.50
Overstory Monthly Alb 7 =
Understory Monthly Alb 7 = 0.2 0.2 0.2 0.2 0.2 0.2 0.2 0.2 0.2 0.2 0.2 0.2

Vegetation Description 8 = Plantation
Overstory Present 8 = TRUE
Understory Present 8 = TRUE
Fractional Coverage 8 = 0.5
Trunk Space 8 = 0.45
Aerodynamic Attenuation 8 = 1.2
Radiation Attenuation 8 = 0.15
Hemi Fract Coverage 8 =
Clumping Factor 8 =
Leaf Angle A 8 =
Leaf Abgle B 8 =
Scattering Parameter 8 =
Max Snow int Capacity 8 = 0.003
Mass Release Drip Ratio 8 = 0.4
Snow Interception Eff 8 = 0.6
Impervious Fraction 8 = 0.0
Height 8 = 25.0 1.5
Maximum Resistance 8 = 4500. 2300.
Minimum Resistance 8 = 300. 150.
Moisture Threshold 8 = 0.33 0.13

Vapor Pressure Deficit 8 = 4000. 4000.
Rpc 8 = 0.70 0.60
Number of Root Zones 8 = 3
Root Zone Depths 8 = 0.150 0.400 0.450
Overstory Root Fraction 8 = 0.20 0.40 0.40
Understory Root Fraction 8 = 0.50 0.50 0.0
Overstory Monthly LAI 8 = 2.40 2.50 1.80 2.10 2.40 2.50 2.60 2.60 3.10 3.10 2.40 2.30
Understory Monthly LAI 8 = 0.36 0.30 0.30 0.30 0.20 0.30 1.00 1.00 2.00 1.20 0.70 0.50
Overstory Monthly Alb 8 = 0.2 0.2 0.2 0.2 0.2 0.2 0.2 0.2 0.2 0.2 0.2 0.2
Understory Monthly Alb 8 = 0.2 0.2 0.2 0.2 0.2 0.2 0.2 0.2 0.2 0.2 0.2 0.2

Vegetation Description 9 = Urban
Overstory Present 9 = TRUE
Understory Present 9 = TRUE
Fractional Coverage 9 = 0.5
Trunk Space 9 = 0.55
Aerodynamic Attenuation 9 = 1.2
Radiation Attenuation 9 = 0.15
Hemi Fract Coverage 9 =
Clumping Factor 9 =
Leaf Angle A 9 =
Leaf Abgle B 9 =
Scattering Parameter 9 =
Max Snow int Capacity 9 = 0.003
Mass Release Drip Ratio 9 = 0.5
Snow Interception Eff 9 = 0.6
Impervious Fraction 9 = 0.0
Height 9 = 25.0 1.5
Maximum Resistance 9 = 5500. 2300.
Minimum Resistance 9 = 300. 150.
Moisture Threshold 9 = 0.33 0.13
Vapor Pressure Deficit 9 = 5000. 5000.
Rpc 9 = 0.70 0.40
Number of Root Zones 9 = 3
Root Zone Depths 9 = 0.150 0.400 0.450
Overstory Root Fraction 9 = 0.20 0.4 0.4
Understory Root Fraction 9 = 0.50 0.50 0.0
Overstory Monthly LAI 9 = 2.40 2.50 1.80 2.10 2.40 2.50 2.60 2.60 3.10 3.10 2.40 2.30
Understory Monthly LAI 9 = 0.36 0.30 0.30 0.30 0.20 0.30 1.00 1.00 2.00 1.20 0.70 0.50
Overstory Monthly Alb 9 = 0.2 0.2 0.2 0.2 0.2 0.2 0.2 0.2 0.2 0.2 0.2 0.2
Understory Monthly Alb 89 = 0.2 0.2 0.2 0.2 0.2 0.2 0.2 0.2 0.2 0.2 0.2 0.2

Vegetation Description 10 = Water
Overstory Present 10 = FALSE
Understory Present 10 = FALSE
Fractional Coverage 10 =
Trunk Space 10 =
Aerodynamic Attenuation 10 =
Radiation Attenuation 10 =
Hemi Fract Coverage 10 =
Clumping Factor 10 =
Leaf Angle A 10 =
Leaf Abgle B 10 =
Scattering Parameter 10 =
Max Snow int Capacity 10 =
Mass Release Drip Ratio 10 =
Snow Interception Eff 10 =

```
Impervious Fraction 10          =     0.0
Height 10               =
Maximum Resistance 10       =
Minimum Resistance 10       =
Moisture Threshold 10       =
Vapor Pressure Deficit 10       =
Rpc 10                  =
Number of Root Zones 10       =     3
Root Zone Depths 10           =     0.015       0.04  0.045
Overstory Root Fraction 10    =
Understory Root Fraction 10   =
Overstory Monthly LAI 10      =
Understory Monthly LAI 10     =
Overstory Monthly Alb 10      =
Understory Monthly Alb 10     =

############################## MODEL OUTPUT SECTION#################################
 [OUTPUT]
Output Directory              =     ./Results/
Initial State Directory       =     ./ModelState/
Number of Model States        =     2
State Date 1            =     12/31/1993-21:00
State Date 2            =     12/31/2000-21:00
Number of Map Variables =     0
########################################################################################
[End]
```

Annex D: Equations used to calculate the various terms in the Penman equation

Saturation vapor pressure

The saturation vapor pressure in kPa at temperature T in °C was computed by Equation D-1.

$$e_s(T) = 0.611 \cdot \exp\left(\frac{17.27T}{T + 237.3}\right) \quad \textbf{Equation D-1}$$

Actual vapor pressure

The actual vapor pressure was then calculated from the saturated vapor pressure and observed relative humidity (RH in %) using Equation D-2.

$$e_a = e_s(T) \cdot \frac{RH}{100} \quad \textbf{Equation D-2}$$

Slope of saturation vapor pressure

Equation D-3 was used to determine the slope of the saturation vapor pressure curve.

$$\Delta = \frac{4098 \cdot e_s(T)}{(T + 237.3)^2} \quad \textbf{Equation D-3}$$

Psychrometric constant

The psychrometric constant was calculated by Equation D-4.

$$\gamma = \frac{c_p P}{0.622\lambda} \quad \textbf{Equation D-4}$$

Where, c_p is the specific heat of water at constant pressure (0.001013 kJ/kg/°C. The latent heat of vaporization (λ) and atmospheric pressure (P) were calculated from Equations D-5 and D-6, respectively.

$$\lambda = 2.501 - (2.361 \times 10^{-3}) \cdot T \quad \textbf{Equation D-5}$$

$$P = 101.3 \cdot \left(\frac{293 - 0.0065Z}{293}\right)^{5.26} \quad \textbf{Equation D-6}$$

T is temperature in °C and Z is altitude in meters above mean sea level.

Net radiation at the surface

The net radiation at the water surface was determined as the algebraic sum of the solar and longwave radiations (Equation D-7).

$$R_n = R_s(1-\alpha) + R_l \quad \textbf{Equation D-7}$$

α is albedo of the water surface; R_s is solar radiation reaching the ground surface, and in the absence of observed data it can be estimated from readily available measurements using empirical relations. In this study as availability of temperature data is relatively better, solar radiation was estimated using Equation D-8.

$$R_s = kR_o(T_{\max} - T_{\min})^{0.5} \quad \textbf{Equation D-8}$$

Where, k is a constant which is usually taken as 0.16; T_{max} and T_{min} are the daily minimum and maximum temperatures in °C; R_o is extraterrestrial solar radiation which is given by

$$Ro = 37.59 d_r\left[\omega_s \sin(\phi)\sin(\delta) + \sin(\omega_s)\cos(\delta)\right] \quad \textbf{Equation D-9}$$

Where ϕ is latitude (rad) and the other terms are functions of the position of the sun: d_r is the relative distance between the sun and the earth, ω_s sunset hour angle (rad), δ solar declination angle (rad); they could be calculated as follows:

$$d_r = 1 + 0.033\cos\left(\frac{2\pi}{365}J\right) \quad \textbf{Equation D-10}$$

Where, J is the Julian day number which starts on January 1.

$$\delta = 0.409\sin\left(\frac{2\pi}{365}J - 1.39\right) \quad \textbf{Equation D-11}$$

$$\omega_s = \arccos(-\tan(\phi)\tan(\delta)) \quad \textbf{Equation D-12}$$

The net longwave radiation was computed as the difference between the downward and outgoing longwave radiations. The downward longwave radiation was determined following the procedure presented in Chapter 5, Section 5.2.6. The outgoing longwave radiation was calculated by Equation D-13.

$$R_l \uparrow = \varepsilon\sigma T^4 \quad \textbf{Equation D-13}$$

Where is emissivity of water surface, taken as 0.97; σ is Stephan-Boltzman constant (5.67×10^{-8} $Wm^{-2}K^{-4}s^{-1}$); T is the water surface temperature (K), assumed to be the air temperature.